# The Structure and Transport of the Agulhas Return Current

**Isabelle Jane Ansorge**

Submitted in fulfillment of the requirements of
the Master of Science degree

Department of Oceanography
University of Cape Town

**1996**

# ABSTRACT

*The Agulhas Current flows along the eastern coast of southern Africa as one of the largest western boundary currents in the world's ocean. On overshooting the southern tip of Africa at approximately 20°E, a retroflection loop is formed that causes the current to double back on itself and to form the easterly flowing Agulhas Return Current. No focussed investigation to establish the hydrography of this important component of global ocean circulation has to date been carried out.*

*To trace the Agulhas Return Current's passage eastwards into the South Indian Ocean, data collected from six CTD hydrographic cruises; AJAX, ARC, SCARC, Marathon, Discovery 164 and SUZIL, as well as from three XBT temperature cruises; Marion 83, Gallieni 72 and FIBEX, have been analysed.*

*It is shown that the Agulhas Return Current initially flows zonally from 20°-25°E at a latitude approximately 39°30'-40°30'S before forming a planetary wave over the Agulhas Plateau between 25°-28°E. This wave results in a northward shift of the Current to 37°S. Further eastward the Current continues it's zonal flow more or less at 40°S, except that over the Mozambique, Madagascar and Southwest Indian Ridges similar waves are evident.*

*Geostrophic speeds (referenced to the bottom) of the Agulhas Return Current show a gradual decrease from an average of 65 cm/s in the retroflection region to 17 cm/s at 76°E. Volume transports at the same depth, are similarly reduced from an average of 60 Sv in the retroflection region, to 23 Sv at 76°E.*

*Temperature-salinity properties show water masses characteristic of the Agulhas Current, $>16°C$ and $>35,4$ psu, to extend as far east as 61°E. East of this longitude, at approximately 66°E, Subantarctic Surface Water is shown to "cap" the surface waters, as the Agulhas Return Current weakens beyond recognition.*

*Based on these hydrographic results, it is clear that the Agulhas Return Current may be considered to extend across the width of the Southwest Indian Ocean, terminating between 66°E and 76°E. I therefore propose that the name "South Indian Ocean Current", given by Lutjeharms and Van Ballegooyen (1984) and later by Stramma (1992) for the flow just north of the Subtropical Convergence in the Indian Ocean, be retained for the flow east of 70°E only.*

# ACKNOWLEDGEMENTS

I would like to thank Professor J. R. E. Lutjeharms and Mr Henry Valentine for their constructive criticism, guidance and support. A special thank you is extended to Mr Roy van Ballegooyen for his invaluable advice. I thank my fellow students Stefan Kohrs, Craig Matthysen and Andrew Lee-Thorp for their office antics and the many jokes we shared. I also thank Mrs Lesley Staegemann for help and patience with my administrative problems.

The financial support of the Foundation for Research and Development and the Department of Environmental Affairs is gratefully acknowledged.

# CONTENTS

# LIST OF FIGURES

# Chapter 1
# INTRODUCTION

Flowing along the eastern coast of Southern Africa between 25°S and 37°S, the Agulhas Current (figure 1.1) is the major western boundary ocean current of the Southern Hemisphere. Originating in the tropics, in the South Equatorial Current, and in the subtropics, in a Southwest Indian Ocean subgyre, the current is found to have both tropical and subtropical characteristics with high surface temperatures (>24°C) and high salinity values (>35,4 psu).

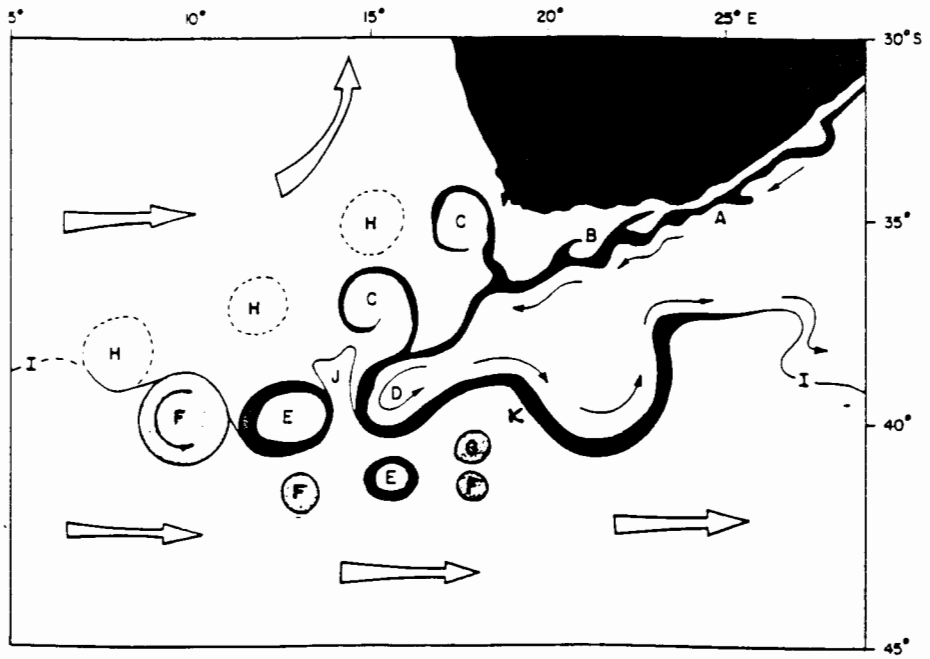


Figure 1.1: A conceptual diagram based on seven years of satellite imagery showing various mesoscale elements of the southern Agulhas Current System. Broad arrows indicate mean drift patterns, while solid arrows show the current direction in the southern regions of the Agulhas Current. Lettered features are described in the text (after Lutjeharms and van Ballegooyen 1988a).

The Agulhas Current, as can be seen from figure 1.1 (feature A), flows along the western coastline of South Africa reaching velocities in excess of 2,5 m/s (Gründlingh, 1977). The current follows the 200 m isobath of the narrow shelf, often as close as 12 km to the coastline (Lutjeharms, 1994). Downstream of Port Elizabeth large instabilities inshore of the current are formed due to the widening of the Agulhas Bank, leading to the formation of large (120 km) meanders, their amplitudes increasing with distance south (Lutjeharms 1981). These give rise to shear edge eddies and plumes (feature B) at the south-east shelf-break of the Agulhas Bank. Warm water plumes (feature C) formed further downstream close to the southern most tip of the Agulhas Bank, have been shown to advect into the Southern Atlantic Ocean as Agulhas filaments.

On overshooting the southern tip of the Agulhas Bank a significant turnabout or Retroflection of the current occurs (feature D), a phenomena first observed and described by Bang (1970). The retroflection loop is unstable (Lutjeharms 1989) and from time to time it will coalesce and pinch off (feature J) an independently circulating ring (feature E) (Lutjeharms 1981 and Lutjeharms and Gordon 1987). A number of warm eddies or rings (features F and G and E) lie south of the Sub-Tropical Convergence (feature I) and these may carry large amounts of heat southward into the Southern Ocean (Lutjeharms and Gordon 1987) and consequently play an important role in meridional heat flux of the world ocean. Agulhas rings (H) carry warm saline Indian Ocean water into the Atlantic (Gordon 1985 and Gordon et al. 1987). Older rings which with time have slowly decayed and lost their surface expressions are portrayed by feature F.

As a result of the retroflection the Agulhas Current flows back, north of the Sub-tropical Convergence (STC), into the South Indian Ocean as the Agulhas Return Current (feature K). During it's initial passage eastwards, between 20°-35°E, the Agulhas Return Current is shown to exhibit strong meridional excursions as it is deflected around topographical features; the Agulhas Plateau and the Mozambique Ridge. East of 35°E, the Agulhas Return Current

continues it's zonal flow at approximately 40°S as far east as between 72°-76°E (Park et al. 1993 and Belkin and Gordon 1994), gradually weakening as a result of interaction with surrounding water masses and through northward recirculation (Wyrtki 1971, Gordon et al. 1986 and Webb et al. 1991) at approximately 42°E, 50°E and 67°E.

The southern boundary of the Agulhas Return Current is known as the Agulhas Front and has been shown by (Park et al. 1993) to have a temperature/salinity range of 12-16°C and 35,1-35,5 psu at 200 m, with their axial values at 14°C and 35,3 psu. Belkin and Gordon (1994) use the depth range of the 10°C isotherm as criteria for the identification of the front. Analysis of numerous sections have shown that the 10°C, embedded into the AF, has the maximum depth range across the front, from $<300$ m (at the southern edge) to $>800$ m (northern edge) between 16°-27°E. Further eastwards this range decreases to ˜350-700m north of the Crozet Plateau and to ˜400-650m in the Kerguelan-Amsterdam Passage, reflecting a gradual weakening of the Agulhas Return Current and it's front.

Criteria for identifying the STC have been given by Belkin and Gordon (1994). Temperature and salinity ranges at 200 m are 8-12°C and 34,6-35,0 psu with axial values at 10°C and 34,8 psu.

Despite the recognised importance of the Agulhas Return Current in advecting subtropical, saline water eastwards across the South Indian Ocean, it would seem that very few studies on the Agulhas Return Current have been carried out to date. A thorough perusal of the available literature is therefore required to piece together all the existing knowledge on the Agulhas Return Current.

# Chapter 2

# PRESENT KNOWLEDGE OF THE AGULHAS RETURN CURRENT

No research paper has ever been written exclusively on the Agulhas Return Current as such, but in discussing the effects of topography on current flow in the region, the path taken by a sub-surface buoy or a disabled steamer and by using satellite imagery, oceanographers have made a great deal of reference to it.

## *The Age of Discovery - Early Oceanographers.*

One of the first publications of a chart depicting an eastward flowing current in the South Indian Ocean was made by Kerhallet's 1851 chart (figure 2.1) which shows two streams, the Mozambique and the Equatorial currents, merging near East London, forming the Agulhas Current. The current then subdivides; into a branch rounding the Cape and merging with an eastward flowing current at 16°E, the other flows eastwards into the South Indian Ocean at 20°E before merging with the Antarctic Circumpolar Current at 22°E 40°S.

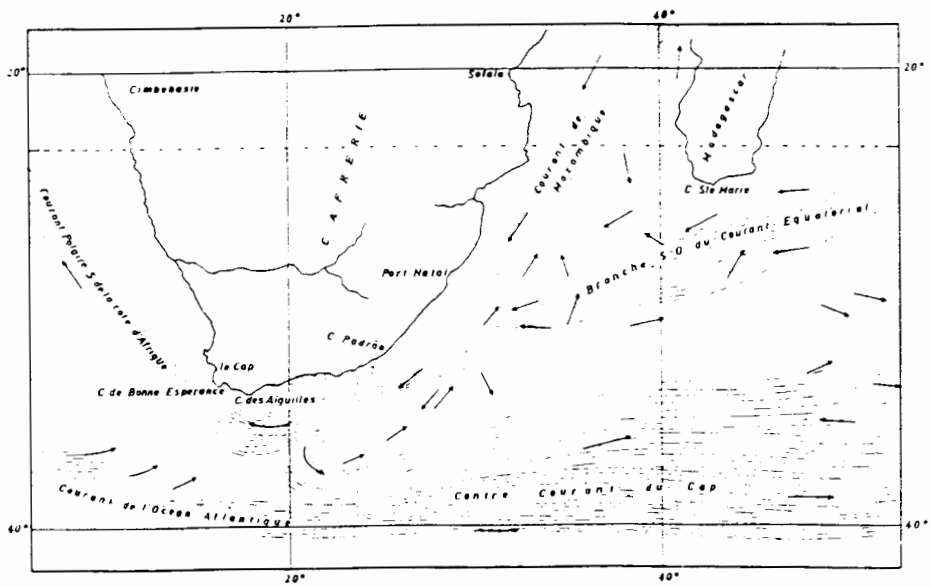


Figure 2.1: Kerhallet's 1851 chart showing the Agulhas Current branching at 20°E and forming the Agulhas Return Current, (taken from Pearce 1980).

Petermann's 1865 chart (figure 2.2), shows the Agulhas Current flowing closely along the coast of Africa and turning east in a series of retroflections between 15° and 45°E and again merging with the Antarctic Circumpolar Current.

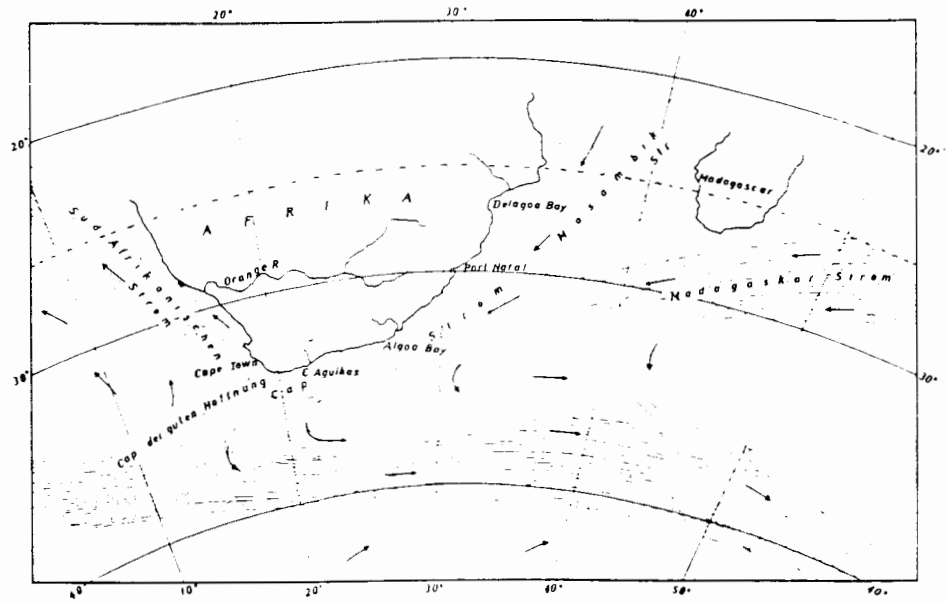


Figure 2.2: Petermann's 1865 chart of the Agulhas Current system, showing a series of retroflections and the Agulhas Return Current (taken from Pearce 1980).

Although these 19th century charts were accurate, considering the data available, the knowledge of the oceans was still severely limited since only limited aspects of the surface flow were known. Cruises were planned to correct this and samples from all depths were collected.

***Early Oceanographic Cruises.***

Lutjeharms (1972) has given a detailed account of early research cruises from 1857, when the *Novarra* sailed along 40°S from Cape Town, to 1932 when the *Discovery II* completed it's 1 year voyage to establish the hydrology of the Southern Ocean. In that

period over seven intensive (Germany, Britain and Austrian) research cruises were carried out in the Southern Indian Ocean and surrounding areas.

In 1925, Merz used data obtained from the German *Meteor* cruise to draw streamline charts of part of the South Indian Ocean. From his chart (figure 2.3) the Agulhas Return Current appears to be extremely convoluted forming eddies at 20°E, 26°E and 32°E. The current appears to divide at 36°S 26°E and 36°S 20°E and thereby forming the eastward flowing Return Current and the Benguela Current in the Atlantic Ocean.

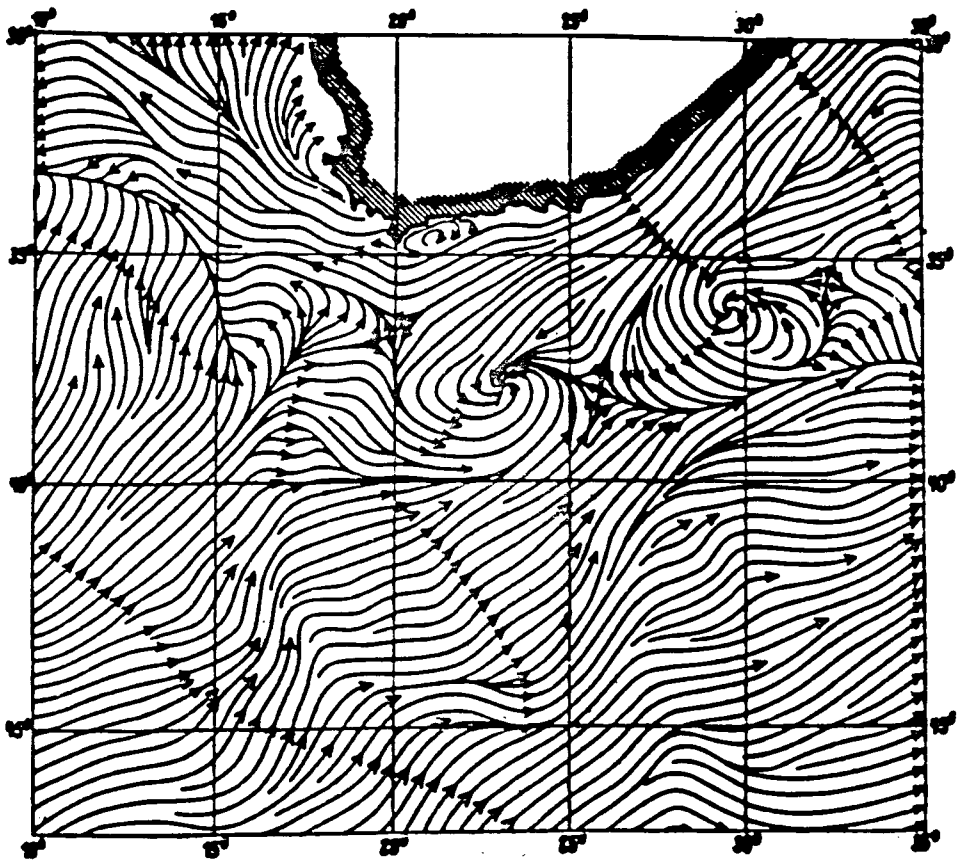

Figure 2.3: Merz's 1925 streamline chart (after Van Foreest, 1977).

The first study of the circulation in the southern part of the Agulhas Current, using the accumulated hydrographic data, was carried out by Dietrich (1935), using data obtained from eleven deep sea cruises, onboard the vessels *Gazelle* (1874), *Valdivia* (1898),

*Gauss* (1901, 1903), *Planet* (1906), *Möwe* (1912, 1913), *Meteor* (1925, 1926), *Discovery I* (1925) and *Discovery II* (1930). His chart (figure 2.4), based on datasets, shows the dynamic topography using the 1 000 db level as a reference. It clearly shows the strong Agulhas Return Current forming at 22°E and also a large meander between 20°-33°E over the Agulhas Plateau (approximately 40°S 27°E) and Mozambique Ridge (running between 26°S 45°E and 42°S 40°E) His investigation was the first to use the geostrophic concept as an analytical tool in the study of the Agulhas Current.

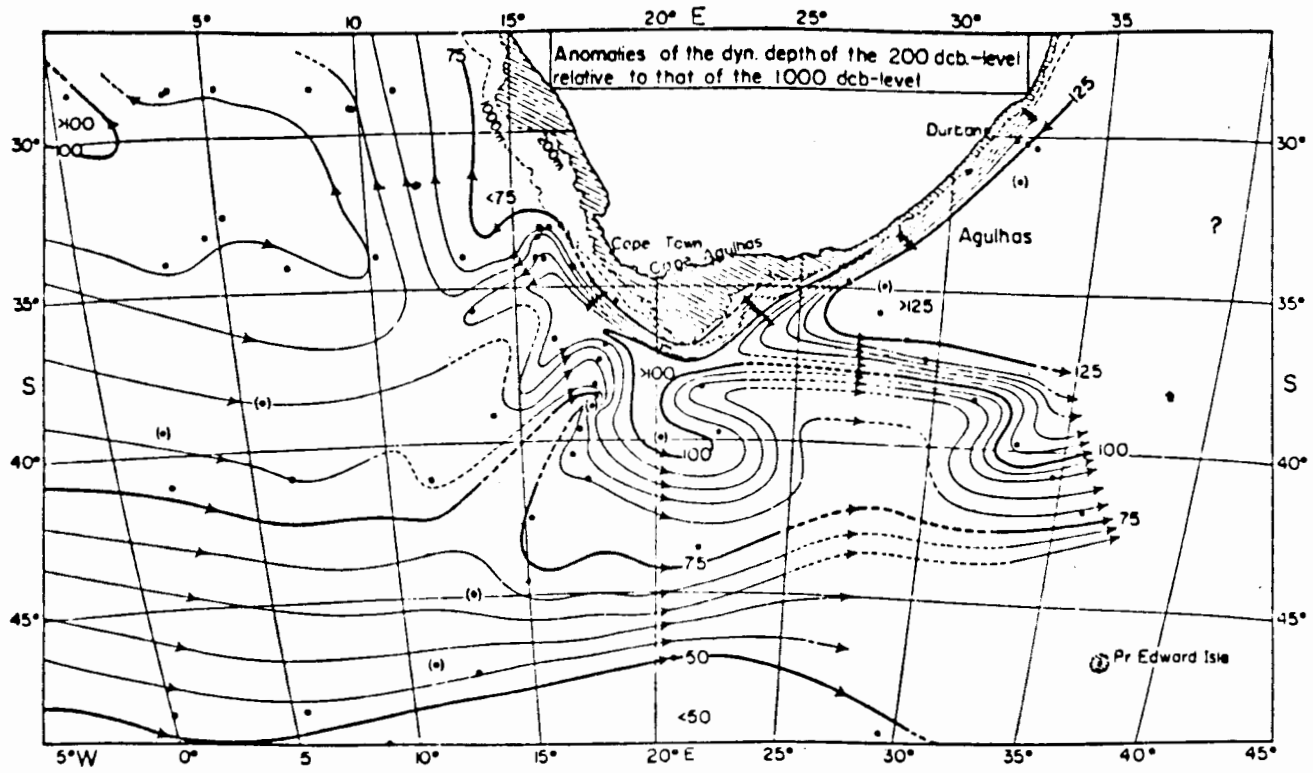


Figure 2.4: Dietrich's chart showing the topography of the 200 db surface relative to that of the 1 000 db surface. Isobaths marking 200 m and 1 000 m clearly show the underwater topography of this area (from Dietrich 1935).

Despite the great number of cruises a detailed study of the area was difficult owing to the wide station spacing. This was recognized by Dietrich (1935) who wrote "A few observations establish without a doubt that deep disturbances can be present in the

system. Because of the fact that the measurements are random nothing can be said about their cause, dimension or time dependency". Deacon (1937), using data collected onboard *Discovery* identified the Agulhas Return Current, "the temperature and salinity distribution also suggests that some of the subtropical water...is possibly deflected southwards near the Cape of Good Hope to mix with water which turns back from the Agulhas Current in an easterly movement across the Indian Ocean". Deacon believed that not only was the Agulhas Return Current an eastward flowing current but that it also had a southerly component at 42-44°S.

Detailed oceanographic research, with close station spacing of the Agulhas system, only came into it's own in 1960 after plans for the first International Indian Ocean Experiment had been made (Darbyshire 1964). This gave rise to an increase in interest in the Agulhas circulation and another expedition, the Agulhas Current Project was planned for March 1969, during which 3 ships were used simultaneously (Bang, 1969). These cruises succeeded in extending the hydrographic knowledge of the surface and deep layers and for the first time closely-spaced, accurate hydrographic data, other than ships drift, was available. Since then the amount of research carried out in the South Indian Ocean has increased substantially, with South African, British, French and American research vessels carrying out extensive research cruises in the region.

***Recent investigations into the path of the Agulhas Return Current***

The Agulhas Return Current is formed after the retroflection of the Agulhas Current. It then flows eastwards into the South Indian Ocean, where, Agulhas water may be lost by mixing. In it's journey eastwards, the current exhibits strong meridional meanders between 20° and 35°E, at the Agulhas Plateau and Mozambique Ridge.

The earliest reference to an anomalous flow in the area of the Agulhas Plateau was made by Dietrich in 1935. He showed from a non-synoptic, widely spaced dataset, a large meander extending from 20° to 32°E (figure 2.4). The poor quality dataset is possibly the reason why only one wave, over both Plateau and Ridge was identified. In later years Clowes (1950), Le Pichon (1960), Orren (1963), Darbyshire (1964) and Visser and Van Niekerk (1965), identified a meander from dynamic topography charts over both the Agulhas Plateau and Mozambique Ridge. However, the causes of these waves were still unknown, as can be seen from Darbyshire (1964), who, although they are clearly evident in his charts, has made no reference to them other than "a strong swirling motion .. leads to the easterly return flow".

With time, an increase in the interest of these waves led to the development of theories regarding their formation and Bang (1970), using data collected during the Agulhas Current Project in 1969, confirmed their presence at 27°E, hinting that they may be topographically induced. Further evidence for their formation was made through the deployment of drifting buoys (Stavropoulos and Duncan 1974, Gründlingh 1978, Luyten 1985).

One such deployment was that of buoy 1210 (figure 2.5), it's subsequent path clearly showing the distinctive features associated within the South West Indian Ocean. The

buoy travelled south west in the core of the Agulhas Current until it retroflected at 38°S 14°E, where it then meandered in an eastward direction along 40°S, before becoming deflected around the Agulhas Plateau, Mozambique Ridge. A series of cyclonic and anticyclonic eddies are shown to have existed, created as a result of the lateral shear between the northward and southward current flow. At 35°E the buoy continued to meander eastwards until contact was lost at 62°E.

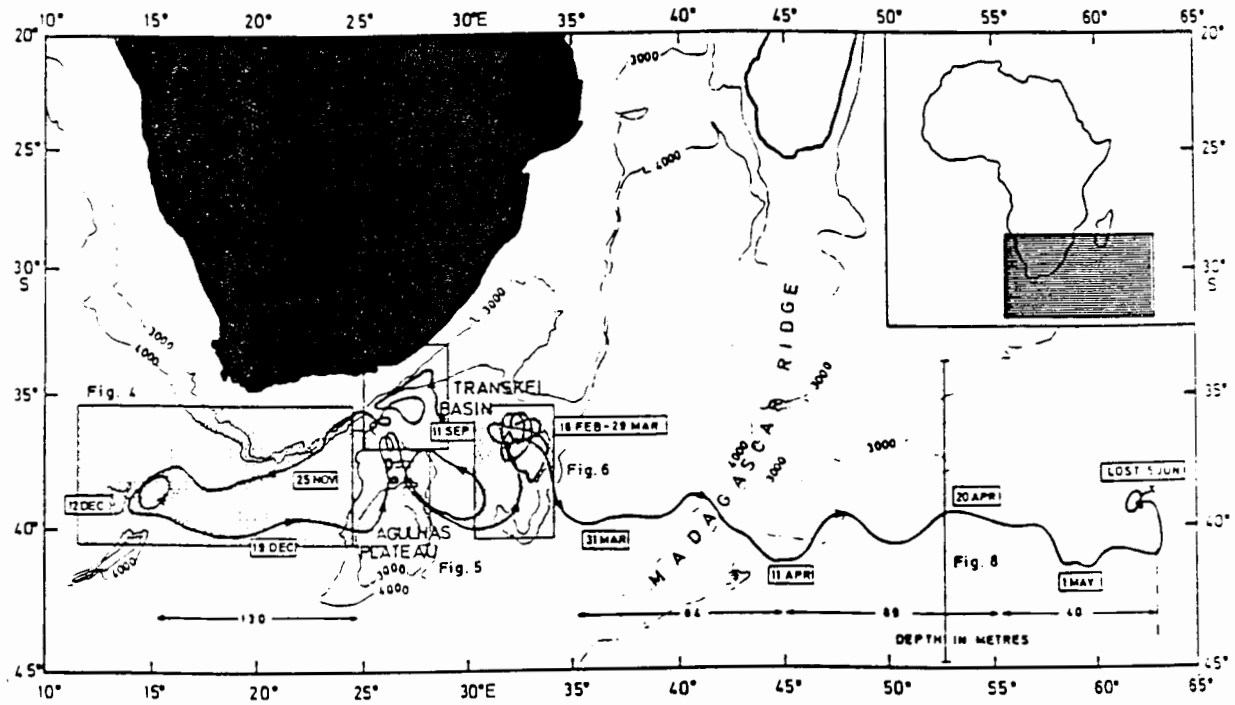


Figure 2.5: Track showing the path taken by Buoy 1210 from it's release over the Transkei Basin to 62°E. Several cyclonic and anticyclonic eddies were observed as the buoy moved with the Agulhas Current and Agulhas Return Current. Isobaths marking the 3 000 m and 4 000 m clearly show the underwater topography of this area (from Gründlingh, 1978).

Other examples of direct measurements of associated features within the Agulhas Return Current have been described by Pearce (1983). He has compared the similarity between the track taken by the disabled vessel *Waikato* in 1899 to that of Gründlingh's buoy 1210 (1978). Both tracks confirm the presence of topographically induced eddies

and meanders in the Agulhas Return Current. Luyten (1985) has compared the track taken by a torpedo shaped buoy deployed 300 miles south of Cape Point to onboard ship measurements taken while following the buoy's trajectory (figure 2.6). Readings were taken to establish where the 15°C isotherm intersects the 200 m depth level, as it is commonly thought that this intersection represents the edge of the Agulhas Return Current. Both the buoy track and the isotherm intersection were deflected to the north at the approach of the Agulhas Plateau. Results show the track and the isotherm location to have been similar with a northward deflection on approaching the Agulhas Plateau. The buoy continued to move with the Agulhas Return Current in an eastward direction, meandering continuously, while onboard operations following the 15°C isotherm were terminated.

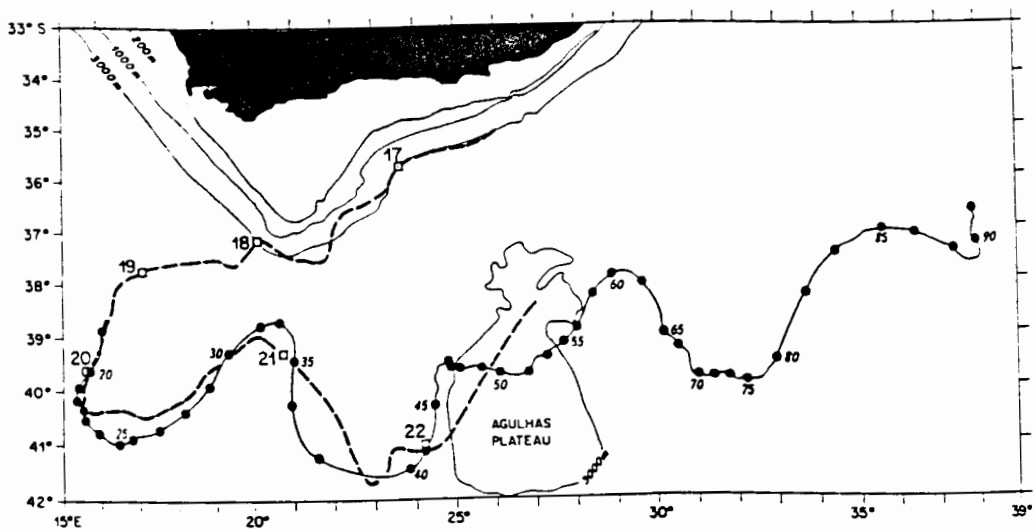


Figure 2.6: The 15°C isotherm as located by a research vessel (dashed line) and the track of the torpedo-shaped drifter (solid line). Isobaths marking the 200 m, 1 000 m and 3 000 m clearly show the underwater topography of this area (from Luyten 1985).

With the advent of satellite images, oceanographers were able to show for the first time, in detail, the meandering flow of the Agulhas Return Current. Gründlingh (1978) has shown from buoy 1210's track superimposed onto weekly GOSSTCOMP (Global Sea Surface Temperature Computation) satellite images, meridional disruptions in the STC at 17° and 32°E (figure 2.7) which coincide with the topographically induced deflections of the Agulhas Return Current.

The GOSSTCOMP charts shows the path and flow of the Return Current to be extremely erratic and unstable, with equatorward deflections at the Agulhas Plateau and Mozambique Ridge to be temporary features. This differs from Stavropoulos and Duncan's (1974) belief that the meanders in the Agulhas Return Current are a permanent feature.

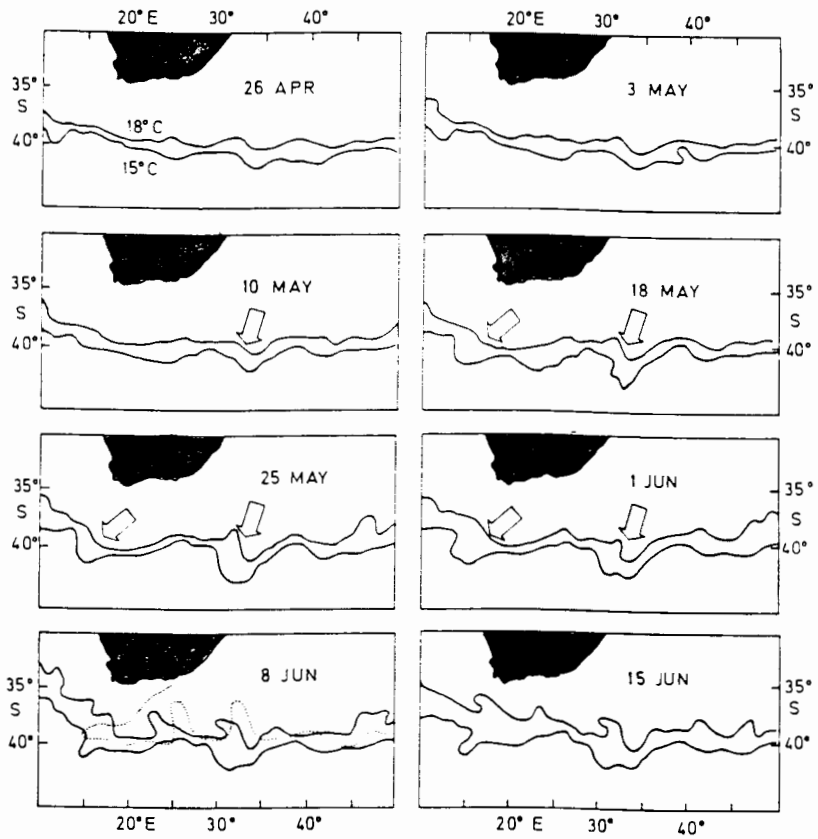


Figure 2.7: 1976 GOSSTCOMP charts representing the position of the Sub-Tropical Convergence. Two disruptions of the convergence due to warm water impinging from the north are indicated. The buoy track superimposed on chart 8 June shows the similarity in the excursions (from Gründlingh 1978).

Harris et al. (1978) have used satellite images to show how temperature contrasts of the sea surface can reveal various oceanographic phenomena. They used thermal infrared images to identify the formation of planetary waves at various topographical features. Harris noticed that the meandering wave caused by the Agulhas Plateau was unstable in it's pattern. The tops of the waves appear to slew westwards, suggesting a break-up of the wave into warm core eddies, over a period of 16 days.

Lutjeharms (1981), has used satellite images to calculate the dimensions of a wave at the Agulhas Plateau. He has found it to measure 450 km from east to west and 300 km from north to south. A wave was identified in each "useable" image and Lutjeharms concluded that "the influence of the Agulhas Plateau is not such as to cause a solitary standing deflection, but that it may trigger a train of waves", a possibility that has been implied by Harris (1970). Lutjeharms (1981) has confirmed this belief with Meteosat images, showing the waves to be "by no means dynamically stable, stationary features". Weeks (1992) has also, through the analysis of CZCS NIMBUS-7 data, identified from chlorophyll concentrations a rossby wave over the Agulhas Plateau.

The Agulhas Return Current has always been considered an easterly current, flowing across the South Indian Ocean and merging with the Antarctic Circumpolar Current near the Crozet Basin (Park et al. 1993). Charts (figures 2.1 and 2.2) dating back as far as 1851 and 1865 by Kerhallet and Petermann depict this. However, it was only in later years that the above mentioned meandering waves set up by topographical features, were shown to also extend over two thirds of the South Indian Ocean.

*East of 35°E*

A great advance on knowledge of the circulation of the South Indian Ocean was made by Stramma (1992), who identified an eastward flowing current at 40°S, which he named the South Indian Ocean Current. This current is shown, through historical hydrographic data, to be an extension of the Agulhas Return Current, marking the northern boundary of the Sub-Tropical Convergence (STC). Using geostrophic velocity profiles, Stramma has been able to prove that a strong (40 Sv) eastward current core reaching depths of over 1 000 m and extending the entire breadth of the South Indian Ocean (figure 2.8), exists only on the northern side of the STC. Stramma has been able to confirm the existence of northward recirculation branches (figure 2.8) as the volume transport reduces from 60 Sv at 50°E, 40 Sv at 65°E to 10 Sv at 92°E.

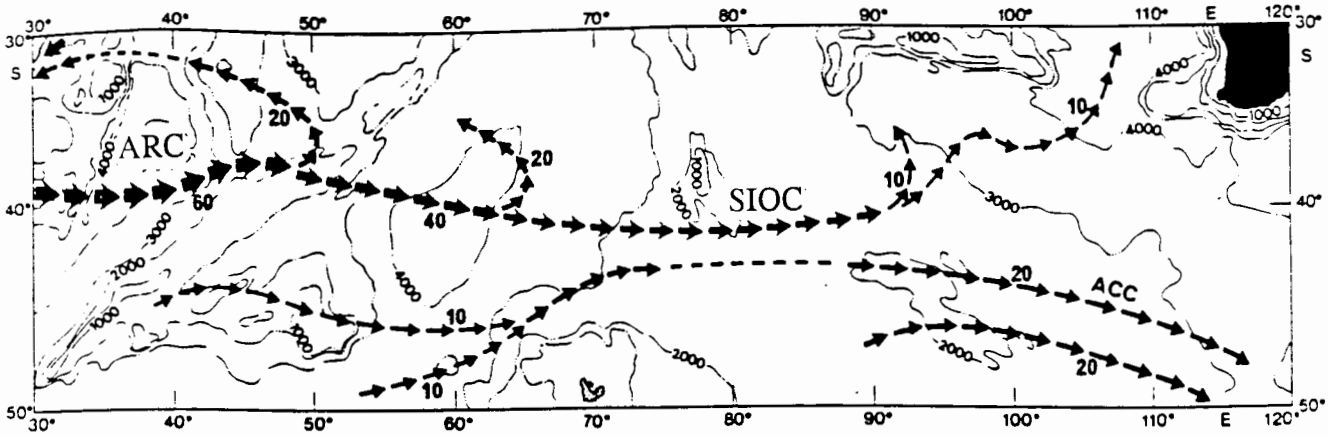


Figure 2.8: Schematic illustration of the flow field in the South Indian Ocean. The flow of the Agulhas Return Current (ARC) South Indian Ocean Current (SIOC) and the Antarctic Circumpolar Current (ACC), are shown by arrows. Transport values (Sv) for the upper 1 000 m are given in numbers. Isobaths ranging from 1 000 m to 4 000 m clearly show the underwater topography (from Stramma 1992).

One of the most recent hydrographic investigations to study the structure and transport of the Agulhas Return Current east of 35°E was carried out by Read and Pollard (1993). Using data collected onboard the *Discovery 164*, the existence of the Agulhas Return Current was confirmed at 40°E, forming a separate front north of the STC.

Other investigations further downstream have been made by Park et al. (1993) during their *SUZIL* cruise. In studying the confluence and topographical steering of the Antarctic Circumpolar Current in the Crozet Plateau, the Agulhas Return Current was identified to extend as far east as 70°E. Eddy like features centered at 42°S and 39°S and between 61°30'E - 62°E appear to have been formed from planetary waves generated by the flow of the Current over the Southwest Indian Ridge (Daniault 1984, Park and Saint-Guily 1992).

The Agulhas Return Current continues it's easterly flow at approximately 40°S as far east as 72°E (Belkin and Gordon 1994), gradually weakening as topographically induced recirculation branches occur at 41°E, 44°E-60°E and 60°E-64°E (Le Pichon 1960, Visser and Van Niekerk 1965, Harris 1970, Wytrki 1971, Van Foreest 1977, Gründlingh 1979 and Stramma 1992). Van Foreest (1977) has described how tongues of colder water spreading northwards to 30°S from the Agulhas Return Current, between 44°E and 60°E, can be seen from sea surface temperature charts.

These branches occur over the SW Indian Ridge and the Crozet Basin and are shown to meander as a result of topographical influences and the generation of eddies. It must be noted that energetic meanders and eddies have been commonly observed in the central part of the basin, from satellite-tracked surface buoys (Projet MARISONDE 1979, Daniault 1984) satellite altimetry-derived sea-level variability (Cheney et al. 1983, and Daniault and Ménard 1985) and a number of historical hydrographic sections

(Gambéroni et al. 1982, Park et al. 1989, 1991, 1993). Planetary waves generated by the flow over the shallow topography of the SW Indian Ridge are responsible for the frequent occurrence of these mesoscale features (Daniault 1984, Park and Saint-Guily 1992).

Gründlingh's (1978) buoy 1210 was the first direct measurement of the Agulhas Return Current east of 35°E. As can be seen from figure 2.5, the buoy, believed to be in the core of the Agulhas Return Current, meandered eastwards at approximately 40°-41°S, before drifting northwards at 63°E. This meridional excursion is not explainable in terms of topography, the deflection occurring over the deep (>5 000 m) Crozet Basin nor in terms of weather conditions, as stable westerlies prevailed. The abrupt northward movement of the *Waikato* (Pearce 1983) coincides with the location of a similar movement by buoy 1210, in an area indicated by Veronis (1973) to mark the eastern boundary of the Agulhas Return Current and supports views held by Harris (1970) as well as Stramma and Lutjeharms (1995) of a recirculating South Indian subtropical gyre between 60° and 70°E. Further evidence regarding this northward flow is given from dynamic topography charts produced by NASA (1992) that, using 10 days of TOPEX/POSEIDON data, reveals a northward flowing current at between 60°E and 64°E.

However, these observations have been dismissed by Belkin and Gordon (1994) who state "If it is really necessary to close the (South Indian Ocean) gyre with a northward branch of the Agulhas Return Current, it must occur **east** of the Amsterdam Plateau", located between 76°E - 79°E. Evidence for this statement is given from the dataset of the *Cruise 50/JASUS*, which has shown the Amsterdam Plateau to be flooded with typical sub-tropical Agulhas water during winter months, northward branching **west** of the Plateau would result in cooler sub-antarctic water being present.

As is evident from the existing literature, actual knowledge on the formation and passage of the Agulhas Return Current is somewhat eclectic. No work has to date been focussed exclusively on the characteristics and modifications occurring to the Agulhas Return Current as it flows from it's source; the retroflection, to 70°E.

# Chapter 3
# KNOWLEDGE GAPS ON THE AGULHAS RETURN CURRENT

It is clearly evident from the existing literature, discussed in the last chapter (**Present Knowledge of the Agulhas Return Current**, chapter 2) that a number of aspects of the Agulhas Return Current are already well documented. Past experiments using buoy trajectories (Stravopoulos and Duncan 1974, Gründlingh 1978 and Luyten 1985), satellite imagery (Harris et al. 1978, Lutjeharms 1981, Lutjeharms and Valentine 1988, Lutjeharms 1989 and Meeuwis 1991) and subsurface hydrographic measurements (Luyten 1985), have all revealed certain specific elements of the flow of the Agulhas Return Current, from the point of retroflection to as far east as 63°E. A number of modern research cruises (*AJAX, ARC, Marathon, SCARC, Discovery 164, SUZIL*; described in detail in **Data and Methodology**, chapter 4) that were dedicated to improving the understanding of the transport and hydrographic structure of regions overlapping the Agulhas Return Current have fortuitously enhanced existing knowledge on this Current. However, none of these cruises were aimed at improving our understanding specifically of the Agulhas Return Current, so that this new information on this Current has been mostly marginal to the main aim of these particular research cruises.

No comparison has ever been made between these modern datasets and they have never been combined to study the Agulhas Return Current as an entity. Consequently changes of the physical properties of the current as it flows downstream have not been accurately documented and as a result, confusion even exists in deciding what is the exact geographical extent of the Agulhas Return Current.

The object of this present investigation is therefore to partially fill this knowledge gap by establishing a reliable hydrographic profile of the Agulhas Return Current along it's full extent, from the above mentioned datasets. The following key research questions are

addressed, thereby providing the first accurate characterisation of the full Agulhas Return Current;

***What is the geographic location of the Agulhas Return Current?***

The Retroflection zone, south of South Africa, has been intensely investigated. Direct comparisons with buoy trajectories, satellite imagery and subsurface hydrographic measurements have clearly revealed the geographic location of the Agulhas Return Current and it's relationship with the STC during it's initial passage through the retroflection to approximately 30°E.

Further downstream, as a result of poorer cruise coverage, less is known of the Agulhas Return Current's position, despite the identification of an easterly current at specific longitudes. Park et al. (1991), Read and Pollard (1993), Park et al. (1993) and Belkin and Gordon (1994), have identified this flow and it's associated front to be the eastern extension of the Agulhas Return Current and Agulhas Front. However, the same easterly current has been identified by Stramma (1992) and Stramma and Lutjeharms (*submitted* 1995) to extend across the entire South Indian Ocean as the *South Indian Ocean Current* in accordance with a previous investigation (Stramma and Peterson 1990).

Consequently, before it is possible unequivocally to show the geographic extent of the Agulhas Return Current and it's relationship with the STC, it is essential first to establish whether there is some generic hydrographic characteristic one can use to determine where the exact eastern termination of the Agulhas Return Current lies and where the South Indian Ocean Current begins. Otherwise the differentiation between these two currents will remain entirely arbitrary.

***What is the geostrophic velocity characteristics and the volume transported by the Agulhas Return Current and how do these change with distance downstream?***

It has been shown by Stramma and Lutjeharms (1995), that during the Agulhas Return Current's passage eastwards, incremental weakening in the geostrophic velocities and volume transported by the Current occurs, as a result of recirculation concentrated at specific longitudes. However, the dataset used in this investigation covers the period 1935-1977 and is largely composed of bottle data with poor station spacing, often $>3°$ latitude apart. This increases chances of inaccuracy and misinterpretation of the results. To date very little has been mentioned on the heat fluxes associated with the Agulhas Return Current.

Consequently, using the modern hydrographic data obtained during recent cruises the geostrophic velocities and the volume transport of the Agulhas Return Current can be calculated to show the possible downstream modification in Current strength with considerably greater accuracy and reliability.

***What are the characteristic water properties of the Agulhas Return Current and how do these become modified with distance downstream?***

During the Agulhas Return Current's passage eastwards it interacts with surrounding water masses and is believed to gradually weaken. Observations have been made by Gordon et al. (1987), Bennett (1988), Read and Pollard (1993), Park et al. (1993) and Rigg (1995) of the physical properties associated with the Agulhas Return Current from individual cruise datasets at different locations. However, in order to show the rate at which the Agulhas Return Current becomes modified during it's passage east, it is important that the T/S and $T/O_2$ results obtained from the analysis of the most modern datasets are compared, not only with each other but also against selected stations within the source of the Agulhas Return Current; the Agulhas Current. This will give a much more reliable estimate of downstream hydrographic modifications in the physical properties of the Agulhas Return Current than any available to date.

***What do all the above tell us about the full geographic extent of what we may call the Agulhas Return Current?***

Confusion exists as to the eastern termination of the Agulhas Return Current. East of 30°E Stramma (1992) regards the easterly flow along the STC as the South Indian Ocean Current, whereas Read and Pollard (1993) and Park et al. (1993) show clearly from hydrographic studies the current and it's associated front extending between longitudes 44°E and 52-66°E respectively, to be the Agulhas Return Current. This confusion may exist as a result of Lutjeharms and van Ballegooyen (1984) suggesting that the term "Agulhas Return Current" only be used in the Agulhas Retroflection region west of the Agulhas Plateau (26°E) and east of this plateau the term "South Indian Ocean Current" be used. By comparing and combining all the answers to the questions outlined above, it will be possible to establish the exact eastern extent of the Agulhas Return Current.

In order to address the hydrographic nature of the full extent of the Agulhas Return Current in this way, datasets of a very specific quality and geographic distribution are needed.

# Chapter 4
# DATA AND METHODOLOGY

In order to address the research questions posed, the CTD data sets collected from 6 modern cruise projects; *AJAX, SCARC, ARC, Thomas Washington Marathon Cruise, Discovery 164 and SUZIL* have been analysed, see figure 4.1. During each cruise closely spaced station pairs (between 20-75 km apart over the frontal zone) that span the Agulhas Return Current were undertaken, thus enabling the geostrophic velocity and volume transport to be accurately calculated. Several XBT lines; *Marion 83 and 86, FIBEX, Gallieni 72,* are also included as they fill geographic gaps between the CTD cruise tracks (figure 4.1). However, it is important to remember that the two datasets when combined, cover a period of 19 years during which research is carried out between the calender months October to May. Consequently the datasets are not synoptic, but include possible seasonal as well as inter-annual variations of the Agulhas Return Current. Bearing this in mind, the two datasets nonetheless provide a coverage of the Agulhas Return Current of over 76° in longitude.

Trajectories and surface speeds obtained from several buoys deployed during experiments between 1974-1987 have also been studied and compared to results obtained from cruise datasets.

### *Hydrographic Data*

The cruises of main interest are the *SCARC, Marathon* and *ARC* as they cover both the Agulhas Retroflection and the Agulhas Return Current extensively. The similarities in geographical location means that salt and volume fluxes of the Agulhas Return Current during this period can be compared. The *Discovery 164* and *SUZIL* data sets are included as they may show the possible physical changes in the Agulhas Return Current as it becomes modified during it's passage further east. The dataset from the *AJAX*, although

upstream of the Agulhas Return Current, provides excellent baseline values from upstream for comparing with those from the other datasets located further downstream.

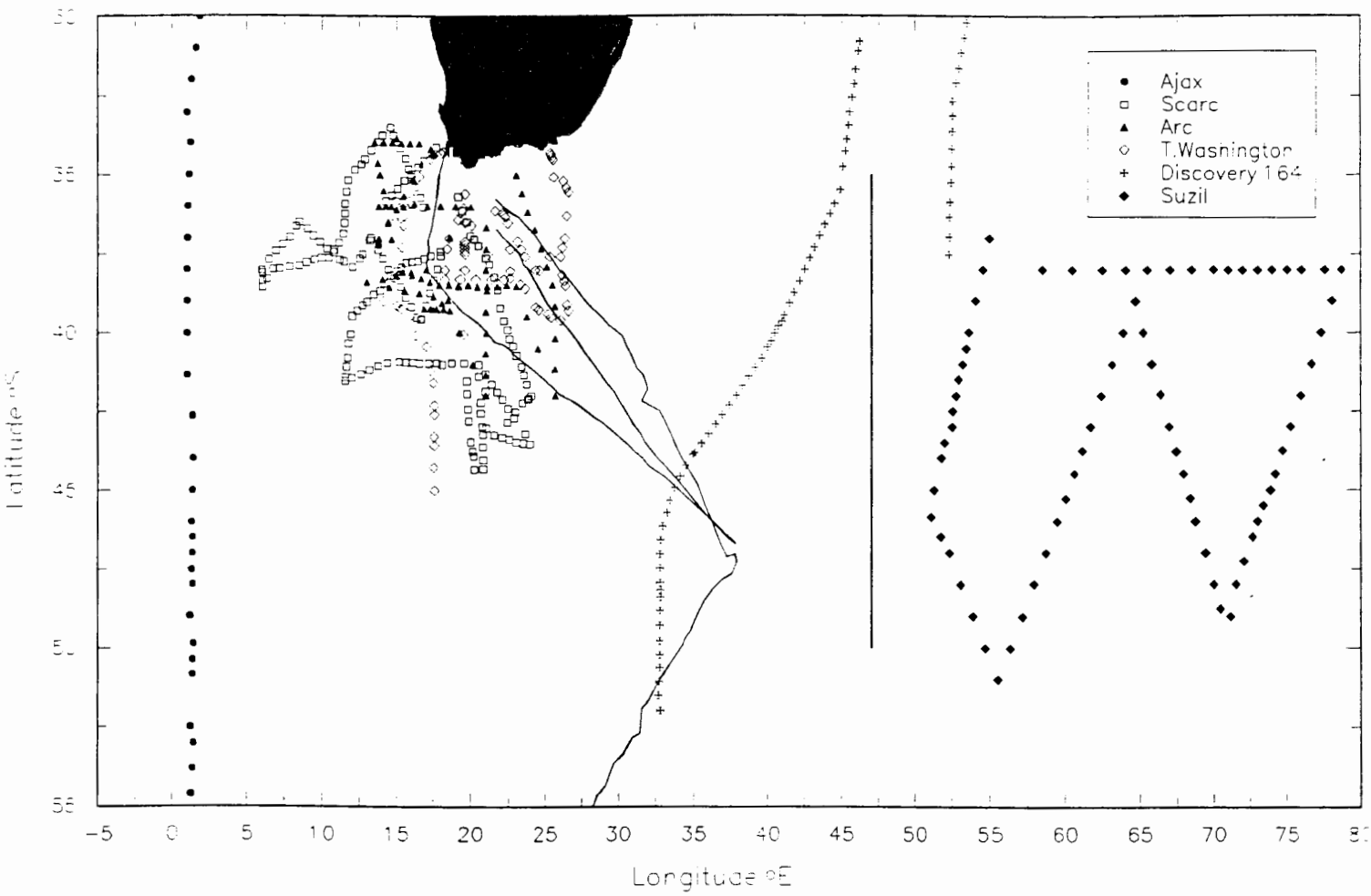


Figure 4.1: The distribution of all CTD (symbols) and XBT (solid line) stations occupied during the cruises shown in the inset. Select stations from each cruise have been analysed to show modifications occurring on the Agulhas Return Current with distance downstream.

*CTD Datasets*

*(a) AJAX Legl: October 1983 - January 1984*

The data was collected during *AJAX* legl (Whitworth and Nowlin 1987) onboard the *Knorr* during 7 October - 13 January 1984. Sampling occurred at 52 full depth CTD stations enroute from Abidjan, Ivory Coast, at 5°N down to 45°S, along the Greenwich meridian and also at 12 CTD stations during a diagonal line from CTD 52 to Cape Town, as can be seen from figure 4.2. Caution must be maintained about the lack of synopticity during interpretation of results of the diagonal transect between CTD stations 52-60, as a gap spanning 400 km between CTD stations 59-60 (37°S-34°S) was only filled a month later by CTD station 61-63, see figure 4.2. The objective of the cruise program was to fill in gaps in hydrographic data coverage of long transoceanic sections, with stationing on average 80 - 85 km.

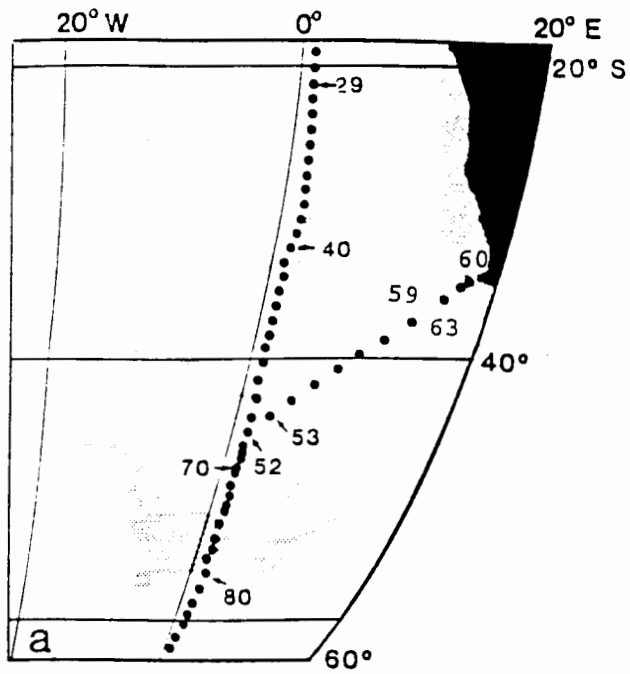


Figure 4.2: Distribution of CTD stations occupied during the *Ajax Legl* cruise. The coloured regions indicate areas shallower than 1 000 m (from Whitworth and Nowlin 1987).

***(b) The Subtropical Convergence and Agulhas Retroflection Cruise (SCARC): February - March 1987***

The *SCARC* (Valentine et al. 1988, Rigg 1995) cruise was undertaken between 12 February and 4 March 1987 and during that period a total of 56 CTD stations and 121 XBT stations were occupied. In order to achieve the primary aim of resolving the interbasin fluxes of eddies, infra-red satellite remote sensing was used to identify mesoscale features such as eddies and rings. It was from these images that the cruise's seemingly random track was determined, seen in figure 4.3.

The main objectives of the cruise were:

(a) to study the general circulation and thermohaline structure of the Agulhas retroflection area and it's associated eddy field.

(b) to investigate eddy shedding at the Retroflection and the STC;

(c) to study the biology at the fronts, Retroflection and in and around the various eddies encountered.

Stations were only sampled to a common depth of 1 500 m, thus limiting the analysis of water masses to the upper water column. A further limitation of the *SCARC* data set is that the cruise was designed to concentrate on eddy and ring shedding and therefore little direct attention was given to the Agulhas Return Current. Consequently only one station, CTD 53 seen in figure 4.3, is located directly within the current. Station spacing was 60 km.

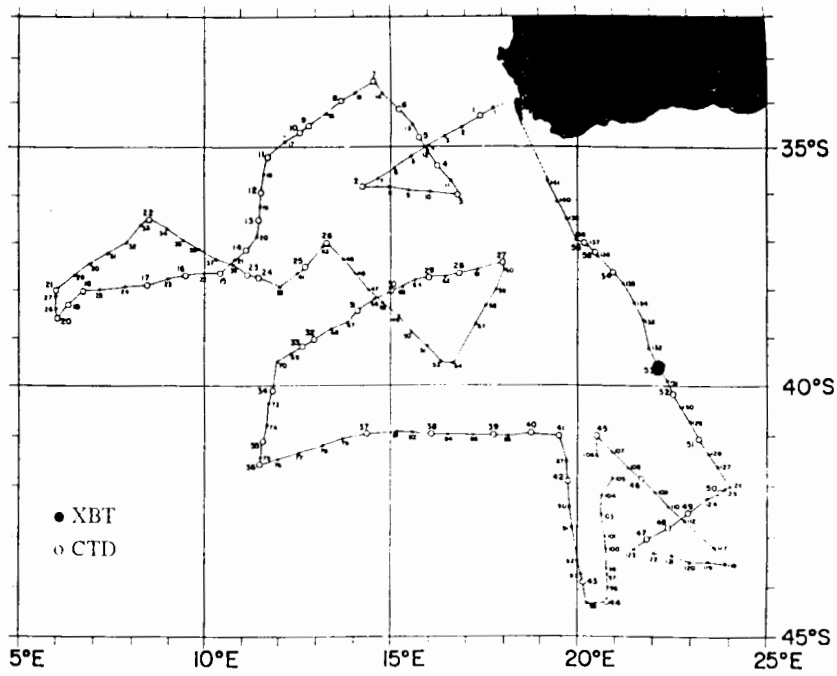


Figure 4.3: Distribution of CTD and XBT stations occupied during the *SCARC* cruise (from Valentine et al. 1988).

CTD stations were sampled to a maximum of 1 500 db, (except stations 1, 10 and 55) and XBT stations to a depth of 760 m. Stations 1 and 55 were located on the continental shelf and were therefore only carried out to 1 000 db.

A full account of the data collected, it's processing, accuracy and corrections has been given by Valentine et al. (1988). Rigg (1995) has described the results of the *SCARC* in detail with particular reference to the hydrography and dynamics of rings and eddies formed in the Agulhas Retroflection region.

***(c) Agulhas Retroflection Cruise (ARC): November - December 1983***

During 13 November to 10 December 1983 an intensive study of the Agulhas Current and the surrounding oceanic environment, between 12°30'E - 25°30'E and 34°S - 42°S was carried out on board the *Knorr* during the Agulhas Retroflection Cruise (Camp et al. 1986, Chapman et al. 1987, Gordon et al. 1987). Close to this period two lines with a total of 26 XBT stations, were carried out as part of this endeavor from the *SA Agulhas* enroute to Marion Island and back. Data obtained from this particular cruise provide a further two

cross sections of the Agulhas Return Current. The cruise tracks (*ARC* and *SA Agulhas*) are shown in figure 4.4, with the positions of the 85 deep CTD stations which were occupied in a program designed to carry out the following objectives:

(a) to resolve the thermohaline structure at the Agulhas retroflection;
(b) to investigate possible eddy shedding;
(c) to determine if there is significant "leakage" of Indian Ocean water into the South Atlantic Ocean; and
(d) to observe the characteristics of the winter cooled Indian Ocean water within the Agulhas extension and associated ventilation of the Indian Ocean Thermocline.

As a result the *ARC* was the first modern, detailed investigation of the chemical and physical oceanography and production potential of the Agulhas Retroflection region (Chapman et al. 1987).

CTD spacing for most transects was on average 75 km, however, between CTD stations 61-58 spacing increased to approximately 125 km, presenting difficulties in accurately resolving the frontal resolution.

A full account of the data processing, accuracy and the corrections made has been given by Camp et al. (1986).

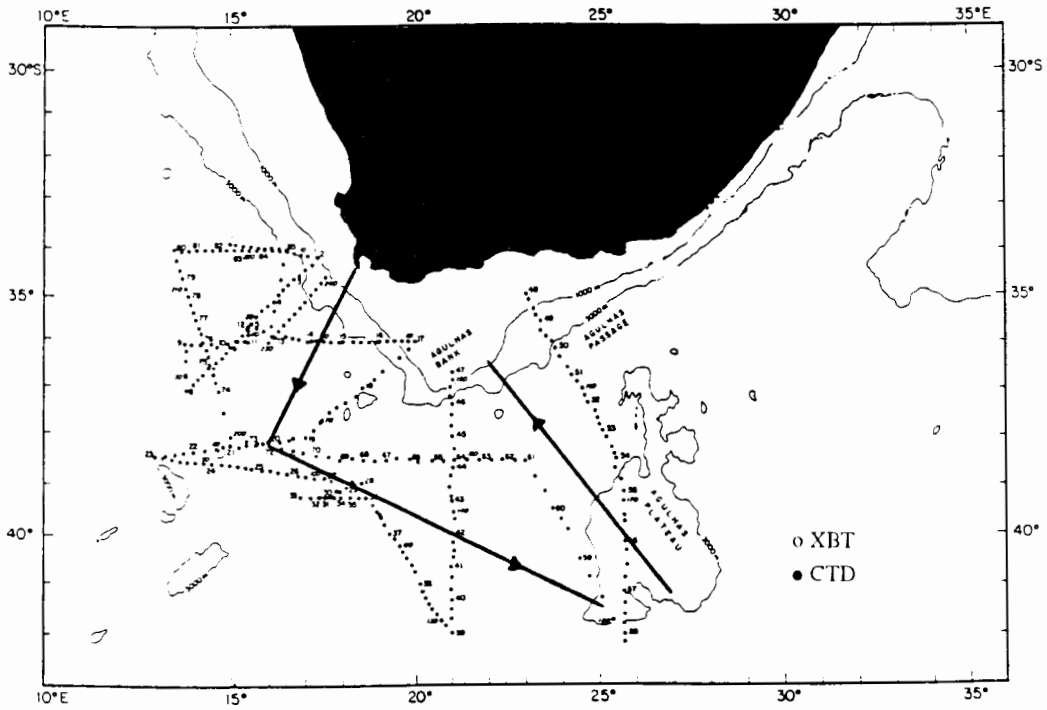


Figure 4.4: Distribution of CTD and XBT stations occupied during the *ARC* cruise (from Gordon et al. 1987). Superimposed onto this figure as a solid line, is the track taken by the *SA Agulhas* during it's voyage to Marion Island in 1983. Lines mark the 1 000 m and 3 000 m isobaths.

### *(d) Thomas Washington Marathon Cruise: February - March 1985*

Data was collected between 20 February and 26 March 1985 (Bennett 1988). The survey consisted of 92 CTD stations forming a complicated grid as shown by figure 4.5. Station spacing was on average between 20 - 60 km apart, with 71 stations reaching to within 200 m of the bottom. Four transects of the Agulhas Current, two of the Agulhas Return Current, a transect of a cold eddy within the Retroflection and a warm ring off Cape Town were carried out (Bennett 1988).

The main objective of the cruise was to provide information about current transport, recirculation and the overall Retroflection transport pattern from mass transport balances obtained from 4 closed grid boxes.

A continuous survey (2 500 km) of the Agulhas Current, it's Retroflection and the Agulhas Return current was carried out at the end of the cruise (16 -22 March) (figure 4.5). The current path was surveyed by following the intersection of the 15°C isotherm and the 200 m depth. The survey was accomplished by navigating the ship downstream according to temperature profiles obtained from XBTs deployed every 15-20 minutes (Bennett 1988).

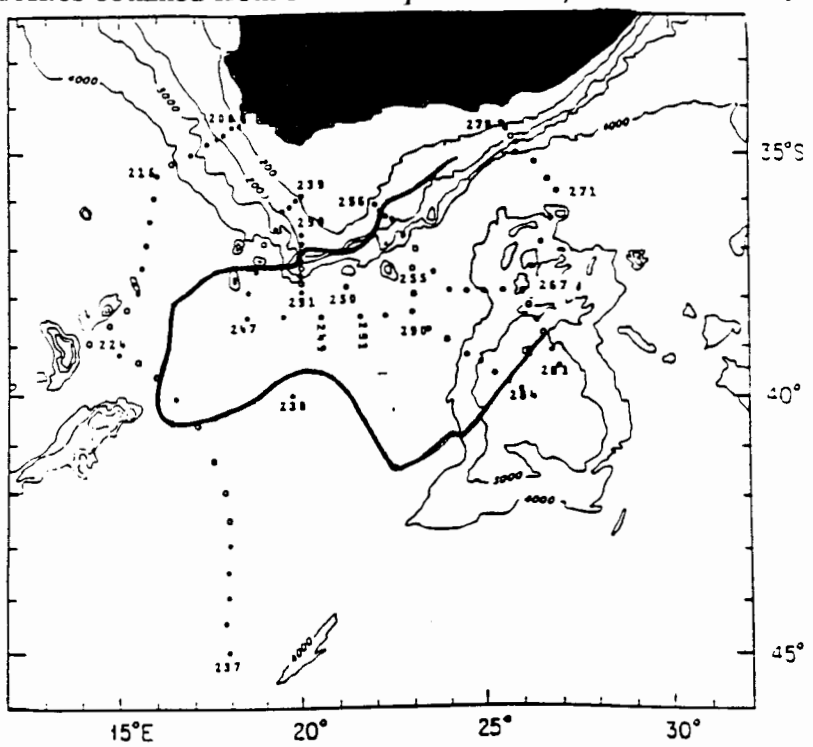


Figure 4.5: Distribution of CTD stations occupied during *Marathon*. The solid line represents the continuous survey of the current, produced by navigating along the intersection of the 15°C isotherm and the 200 m depth. Lines mark the 100 m, 200 m, 3 000 m and 4 000 m isobaths (taken from Bennett 1988).

A detailed study of the cruise results has been given by Bennett (1988).

***(e) Discovery Cruise 164: December 1986 - January 1987***

The data was collected onboard the *Discovery 164* (Pollard et al. 1987, Read and Pollard 1993) between 20 December 1986 and 6 January 1987. As can be seen from figure 4.6 the cruise ran southwest from Mauritius to the Madagascar Ridge, south along the ridge at 45°E to 35°S, then along the Atlantic side of the Atlantic-Indian Ridge to 33°E and 45°S before crossing the ridge at 47°30'S and terminating at 52°S, 32°45'E. Stations were

widely spaced (300 km) directly south of Mauritius, reduced to 100 km across the Madagascar Basin to 39°S and then down to between 50-33 km across the AF/STC/SAF/PF frontal zone.

The track crossed several fronts; Agulhas, Sub-Tropical Convergence, Sub-Antarctic and Polar Front. The cruise consisted of 52 CTD stations, all of them to full depth (1 200 - 5 500 m). This was made possible by the presence of an echosounder mounted to the CTD cage, enabling the CTD to stop as close to the bottom as possible, generally within 10 - 30 m. Nineteen XBT T-7 stations were also occupied.

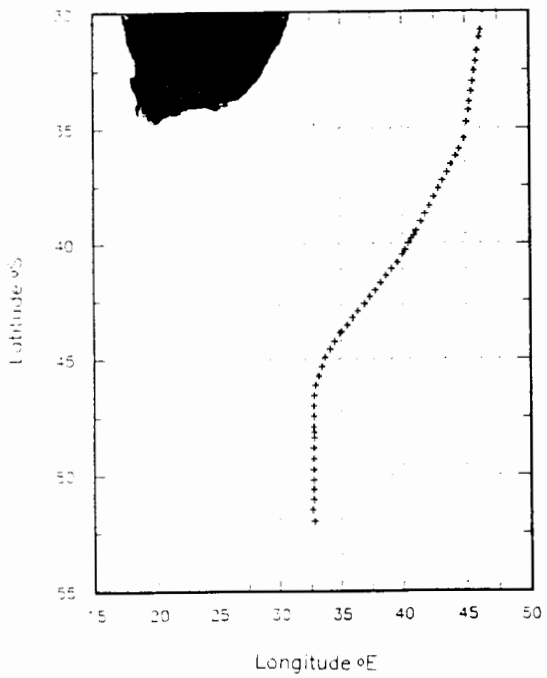


Figure 4.6: Distribution of CTD stations occupied during the Discovery Cruise 164 (from Read and Pollard 1993).

Details of the CTD recordings and profile plots have been reported in Pollard et al. (1987).

*(f) SUZIL: April - May 1991*

The main objective of *SUZIL* (Park et al. 1993) was to study the dynamics of the Antarctic Circumpolar Current as it flows around the Crozet and Kerguelen Plateaus. The survey was carried out between 12 April to 20 May 1991, consisted of 73 full depth CTD casts along four near-meridional sections as well as a zonal section along 38°S, between 51°-79°E and 37°-51°S, as can be seen from figure 4.7. Station spacing was between 50-80 km in the frontal zone and over 100 km outside, thus constituting the most densely spaced, quasi-synoptic dataset ever obtained in this sector of the Southern Ocean.

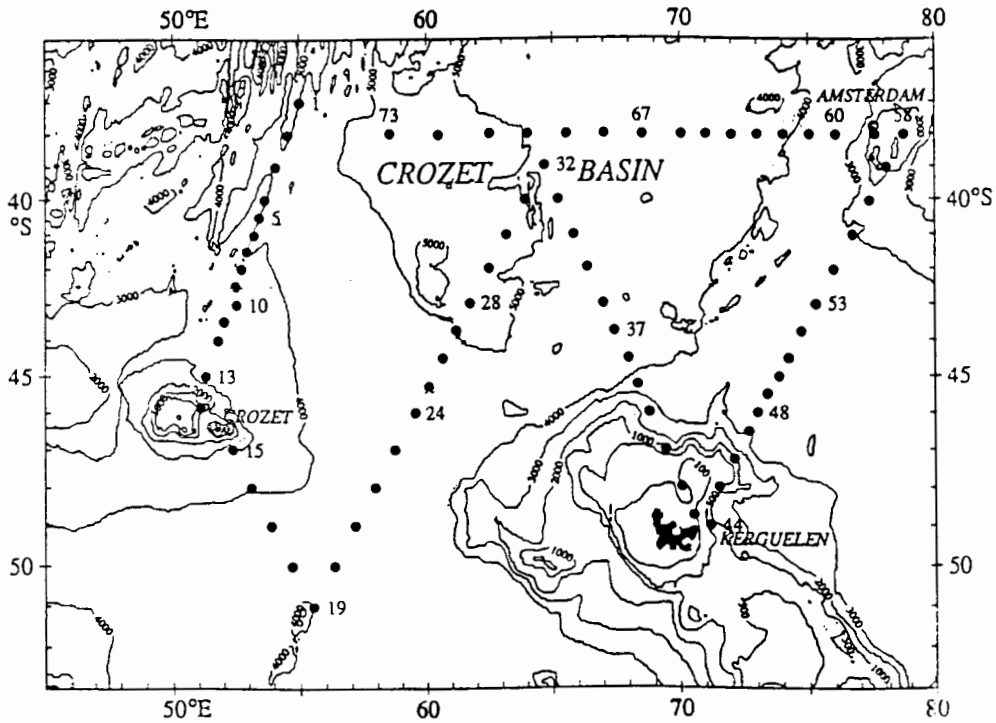


Figure 4.7: Showing the distribution of CTD stations occupied during the *SUZIL* cruise (from Park et al. 1993). Isobaths ranging between 100 m - 4 000 m show clearly the underwater topography of this area.

Further information has been given by Park et al. (1993).

*XBT Datasets*

Four additional XBT cruise lines (figure 4.1) have been used in this investigation in conjunction with the CTD datasets. During the *Marion 83* (8-21 November 1983) cruise over 26 XBTs were deployed on average 2 hours, or 30 nautical miles apart. Occurring at the same time and region as the *ARC*, it provides a good comparative dataset, with two crossings of the Agulhas Return Current (Figure 4.4). During 9-14 May 1986 the *Marion 86* cruise carried out 3 transects of the Agulhas Return Current during a north south zigzag course. Approximately 66 T7 XBTs were deployed every 2 hours or 30 nautical miles apart. *FIBEX* (First International Biomass Experiment) in 11 February-19 March 1981, deployed 187 XBTs every 2 hours or 30 nautical miles. During the *Gallieni 1972* cruise 25 T7 XBTs were deployed along 47°E between latitudes ~37°S-50°S.

Combined, the XBT and CTD datasets described above provide an extensive coverage of the Agulhas Return Current, from the point of Retroflection to approximately 76°E. Stations of the CTD datasets are spaced sufficiently close to one another to demonstrate clearly the gradual modification and attenuation of the Current as it flows east, away from the retroflection, if this exists. XBT data slotted between CTD lines can further confirm the location and width of the Agulhas Return Current.

This modern dataset is therefore entirely appropriately located and of sufficiently high quality to be used in addressing the key questions of this investigation, namely;

(1) What is the general hydrography of the Agulhas Return Current and how is this modified downstream?
(2) What is the geostrophic velocity characteristics and the volume transport of the Agulhas Return Current and how do these change with distance downstream?
(3) What are the characteristic water properties of the Agulhas Return Current and how do these become modified with distance downstream?

(4) What do all of the above tell us about the full geographic extent of what we may call the Agulhas Return Current?

In order to achieve the correct answers to these questions the correct methodology in the analysis of the data has to be employed.

## *Methodology*

### *Vertical Sections*

Sections for temperature, salinity, and oxygen have been drawn up for all cruises using a gridding and contouring software package called SACLANT on the UNIX mainframe computer at the University of Cape Town. Vertical sections of geostrophic velocities as well as the total volume transport between station pairs were calculated and drawn using AXUM, a graphics package.

### *Vertical Profiles*

Hydrographic profiles showing the potential temperature-salinity (T/S) and potential temperature-dissolved oxygen ($T/O_2$) relationships for individual and groups of stations have been drawn using a graphics package called AXUM. These profiles have been used to identify and characterize the various water masses associated with the Agulhas Current, it's retroflection and the Agulhas Return Current according to definitions based on previous investigations (Gordon et al. 1987, Valentine 1990). Boundaries between the various water masses are then defined by divisions based on a change in the slope on the T/S plot.

*Calculations: Great Circle Distances*

Distances between station pairs were calculated according to the formula;

(1) $\mathbf{dx} = R.\arctan\sqrt{(1/\alpha^2)-1}$

where;

**dx** is the great circle distance in kilometres

$\alpha = \cos(lat1).\cos(lat2).\cos(lon1-lon2)+\sin(lat1).\sin(lat2)$

$R$ is the radius of the earth = 6371 km.

The latitudes and longitudes are given in radians

*Calculations: Geostrophic flow*

Geostrophic flow (with reference to the sea floor) between two depths were calculated for each station pair at every 20 db pressure level in the upper layer (500 m) and either every 50 db or 100 db below 500 m.

Equations (2) and (3) are used in calculating geostrophic flow between a station pair;

(2) $\Phi = \int_{\text{level of no motion}}^{P} \delta.dp$

where;

$\Phi$ (J $kg^{-1}$) is the geopotential anomaly calculated for each level relative to a common reference.

$\delta$ ($m^3$ $Kg^{-1}$) is the specific volume anomaly calculated using the UNESCO (1983) algorithm.

**dp** (db) is the difference between the pressure levels.

(3) $\mathbf{vAB}=(1/f.\mathbf{dx})[\Phi\mathbf{B}-\Phi\mathbf{A}]$

where;

**vAB** the geostrophic flow measured in m/s between station pairs.

$f$ the Coriolis force at an average latitude for the two stations.

**dx** (m) is the distance between two stations, which is calculated using the above great circle equation (1).

*Calculations: Volume Fluxes*

Volume fluxes between station pairs have been calculated using the below equation (4), at the pressure levels outlined for the geostrophic calculations.

(4) **Volume flux= $\Sigma 1/2(vAB).dx.dp$**

where;

**dp = $-10^4.dz$** the difference in pressure between 2 levels which is equilivant to the difference in height (dz) between levels.

**volume flux** is measured in $m^3s^{-1}$.

# Chapter 5
# THE GEOGRAPHIC LOCATION AND GENERAL HYDROGRAPHY OF THE AGULHAS RETURN CURRENT

The geographic location and general hydrography of the Agulhas Return Current will be discussed in this chapter. For the purpose of this particular analysis the datasets for each of the six CTD cruises: *AJAX, ARC, SCARC, Marathon, Discovery 164* and *SUZIL* and three XBT lines *Gallieni 72, Marion 83* and *FIBEX*, have been analyzed and temperature and salinity sections to 1 500 db are discussed, while the temperature and salinity sections to 5 000 db and oxygen sections can be found in the addenda. Comparing the results from each cruise will show the degree of zonal modification that occurs during the Agulhas Return Current's passage eastwards.

## *The passage of the Agulhas Return Current 0°E-35°E*

The *AJAX* cruise was a detailed hydrographic survey along the Greenwich Meridian, as shown by figure 5.1 (Whitworth and Nowlin 1987). Although this meridional cruise is too far west of the retroflection to represent the Agulhas Return Current, it does provide an excellent baseline for the transects further downstream, where the influence of the Agulhas and the Agulhas Return Current becomes evident.

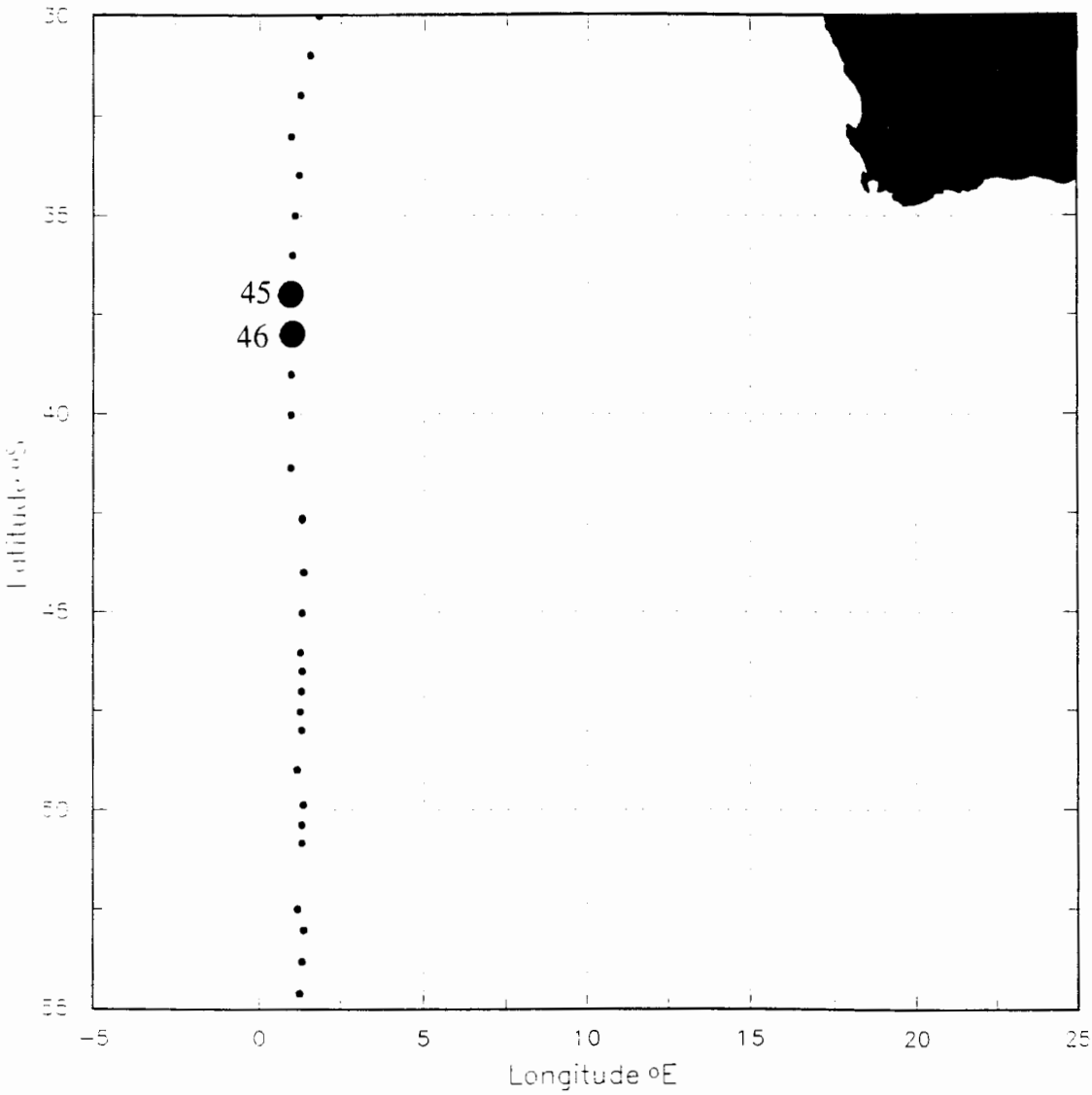


Figure 5.1: The location of the *AJAX* transect. The position of the STC lies between CTD stations 45-46, which are marked by solid dots.

Analysing figures 5.2a to 5.2b it can be seen, that as a result of the transect located so far upstream of the retroflection region only the STC is present between CTD stations 45 (37°S) - 46 (38°S).

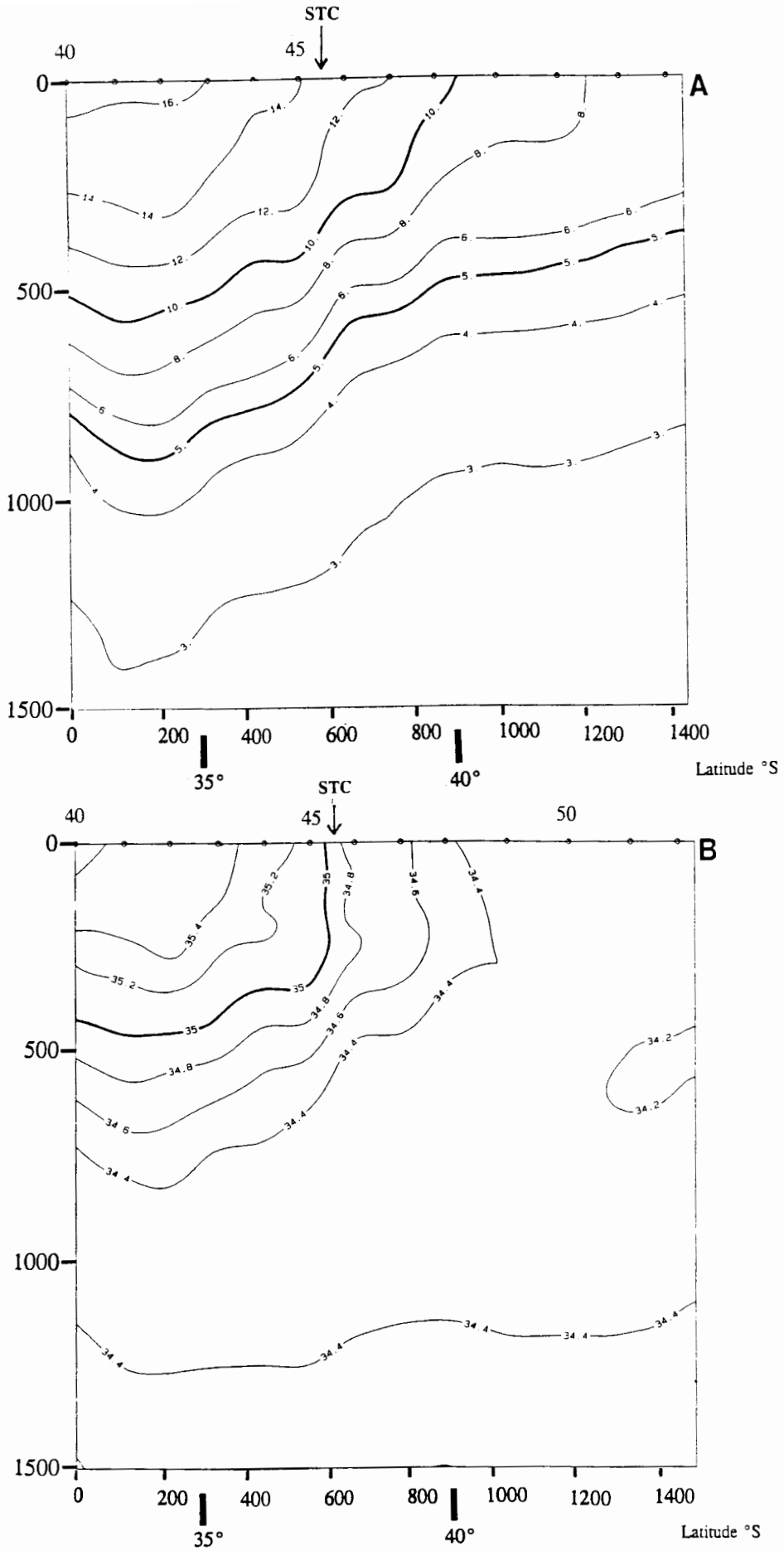


Figures 5.2a and b: Potential temperature and salinity sections between CTD stations 40-52 for a total depth of 1 500 db. The Agulhas Return Current and it's associated Agulhas Front are absent as a result of the cruise being west of the retroflection region. The location of the STC between CTD stations 45-46 can be seen from figure 5.1.

Between these two stations it forms a front with surface temperature values ranging from 14,3°C at CTD stations 45 to 12,07°C at CTD station 46 and surface salinity values from 35,17 psu to 34,63 psu. The surface temperature gradient in this meridional section (figures 5.2a) is fairly weak in comparison to those observed elsewhere (Stramma and Peterson 1992) with a middle temperature of 13°C (Lutjeharms et al. 1993), a value lower than those observed by Lutjeharms and Valentine (1984).

Further downstream, east of 10°E, the Agulhas Return Current forms in the retroflection region and flows eastwards into the South Indian Ocean, where, during it's initial passage, strong meridional excursions in the form of S-shaped meanders are executed. Located between 20°-35°E these planetary waves are a direct result of the current's deflection around topographical features, such as the Agulhas Plateau and the Mozambique Ridge. Analysing the hydrographic data obtained within the retroflection region, CTD cruises *SCARC, ARC* and *Marathon* and XBT lines *Marion 83* and *FIBEX*, it can be seen that the Agulhas Return Current and it's associated front (AF) are crossed on a number occasions, either, as a zonal current immediately following the retroflection, or during it's strong meridional deflection around the Agulhas Plateau.

During the first two transects at 21°E (CTD stations 47-37) and 24°E (CTD stations 61-58) of *ARC* the Agulhas Return Current and Agulhas Front are crossed as can be seen from figure 5.3. The geographic location of the Current and it's front is also clearly shown by the dynamic height anomaly of the sea surface relative to the 1 500 db surface (figure 5.4). The potential temperature and salinity structure of each transect section (figures 5.5a and 5.5b and 5.6a and 5.6b) show the Agulhas Return Current to lie zonally between CTD stations 43-41 at 39°20'S and CTD stations 60-59 at 40°40'S.

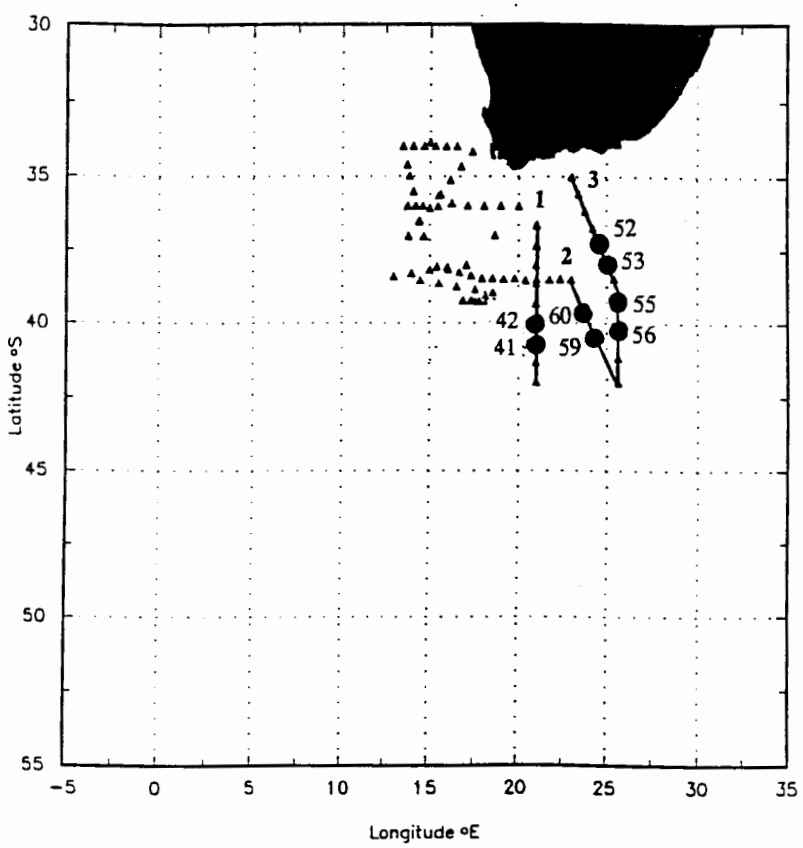


Figure 5.3: The location of the three transects during *ARC*. The position of the Agulhas Return Current, as interpreted from the figures 5.4a-d to 5.5a-d, lies between CTD stations 41-42 (transect 1), 59-60 (transect 2), 55-56, 55-54 and 53-52 (transect 3) as can be seen from the solid dots.

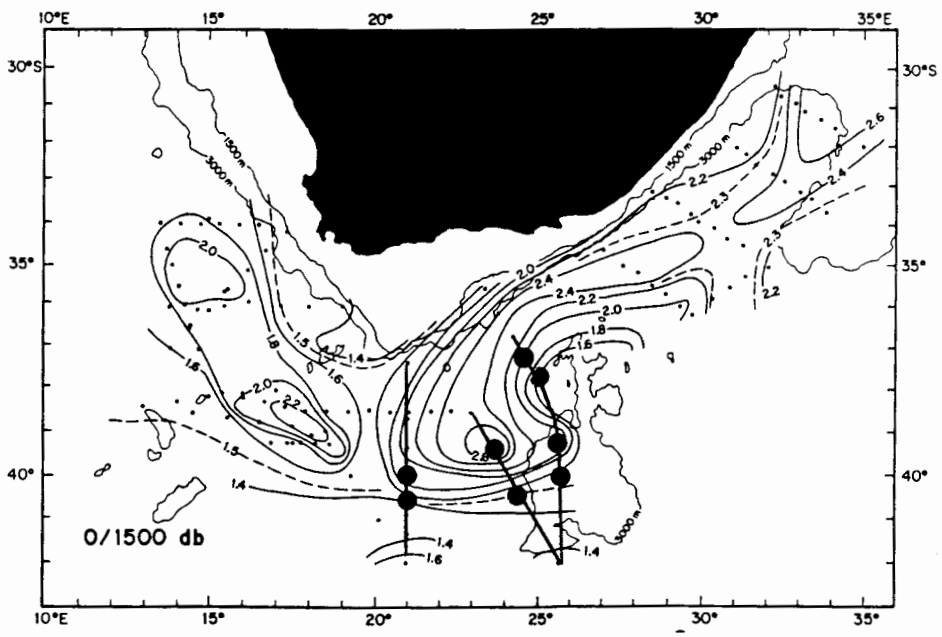


Figure 5.4: Dynamic height anomaly of the sea surface relative to 1 500 db. Transects are marked showing the position of the Agulhas Return Current in relation to station position. Values are given in meters. Isobaths show the 3 000 m depth.

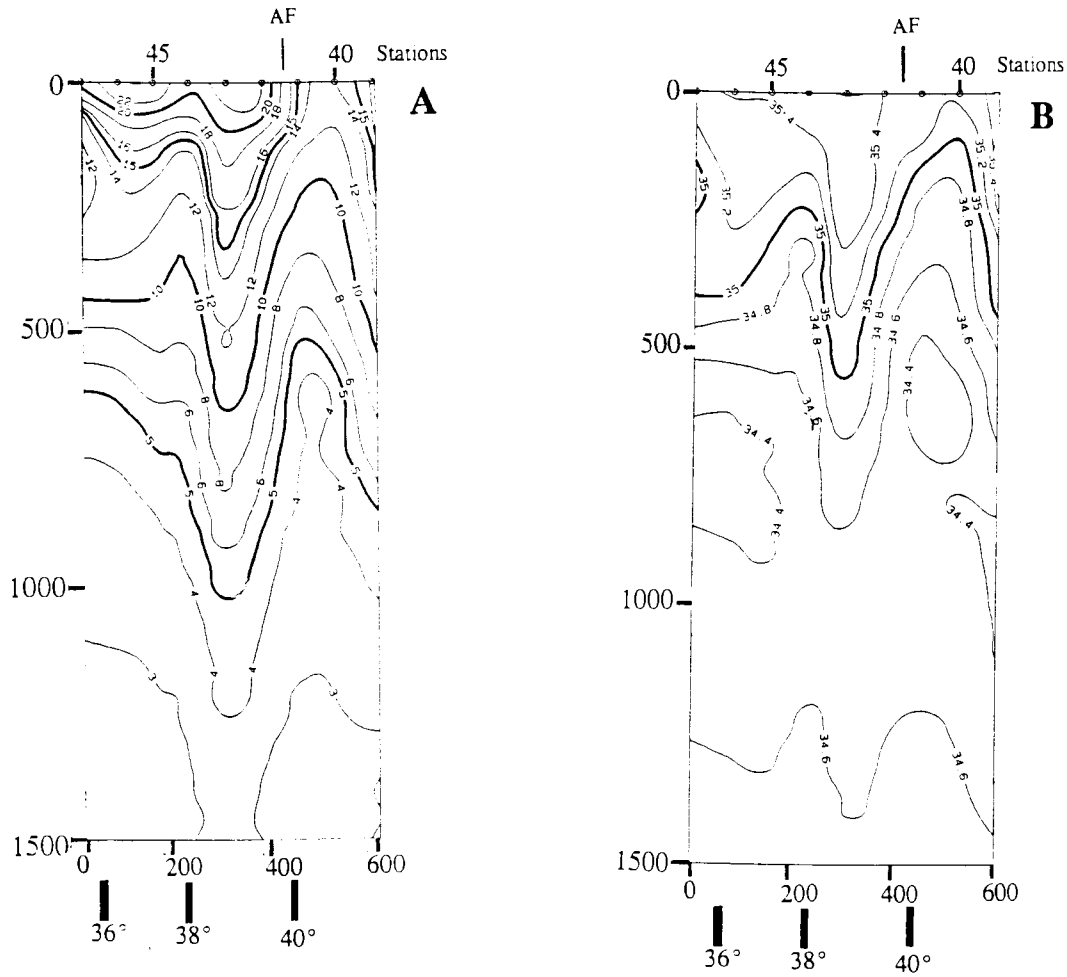


Figures 5.5a and 5.5b: ***ARC* Transect 1** Potential temperature and salinity sections between CTD stations 47-39 for a total depth of 1 500 db. The position of the Agulhas Front; the southern boundary of the Agulhas Return Current is evident between CTD stations 41-42.

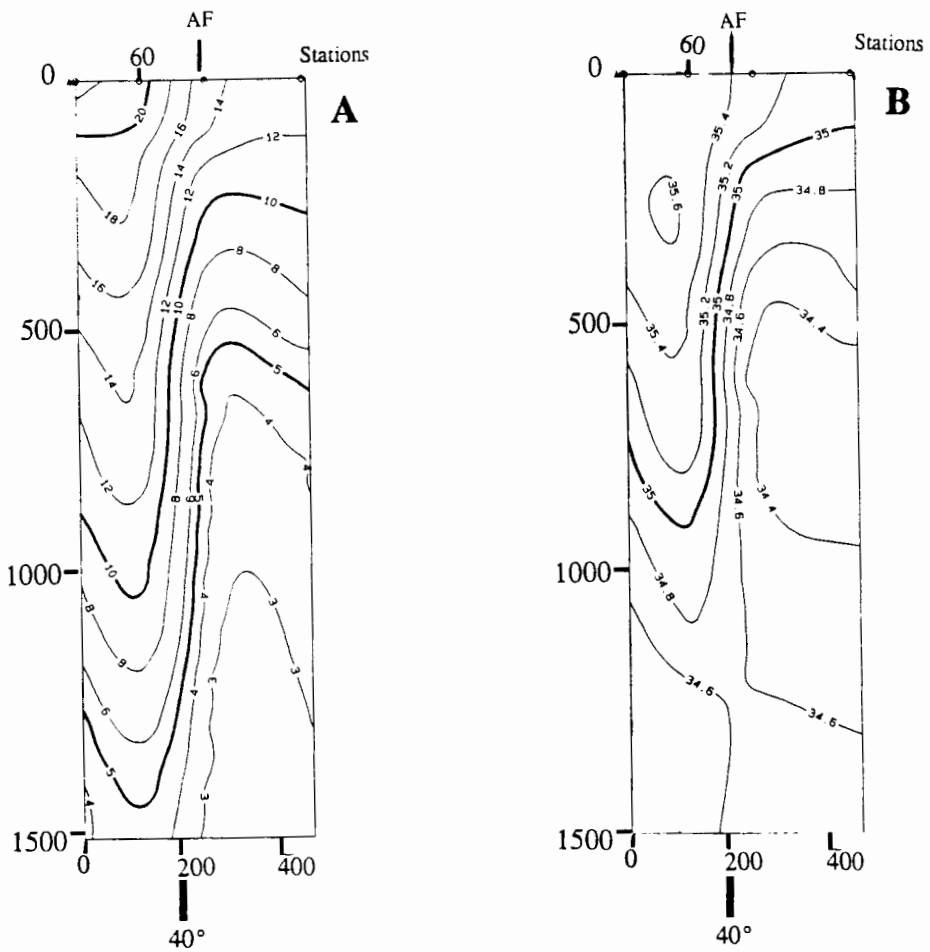


Figures 5.6a and 5.6b: ***ARC* Transect 2** Potential temperature and salinity sections between CTD stations 61-58 for a total depth of 1 500 db. The position of the Agulhas Front; the southern boundary of the Agulhas Return Current is evident between CTD stations 60-59.

Values at the 200 db level, a depth thought best to represent the core of the Agulhas Return Current show the Agulhas Front to exhibit a temperature range of approximately 7°C, from 18°C to 11°C, salinity values range from 35,57 psu to 34,80 psu and oxygen values range from 5,1 to 5,3 ml/l.

The location of the Agulhas Return Current and Agulhas Front at transect 1 is comparable to results obtained during the outward bound XBT leg of *Marion 83*, where the Agulhas Return Current, as can be seen from figure 5.7, was crossed at a similar longitude (21°E). During *Marion 83*, the Agulhas Return Current and STC (as in *ARC* transect 1) merge to form a single front, however it appears to be less intense with temperature from 19°C to 15°C compared to 21°C to 14°C of the *ARC*.

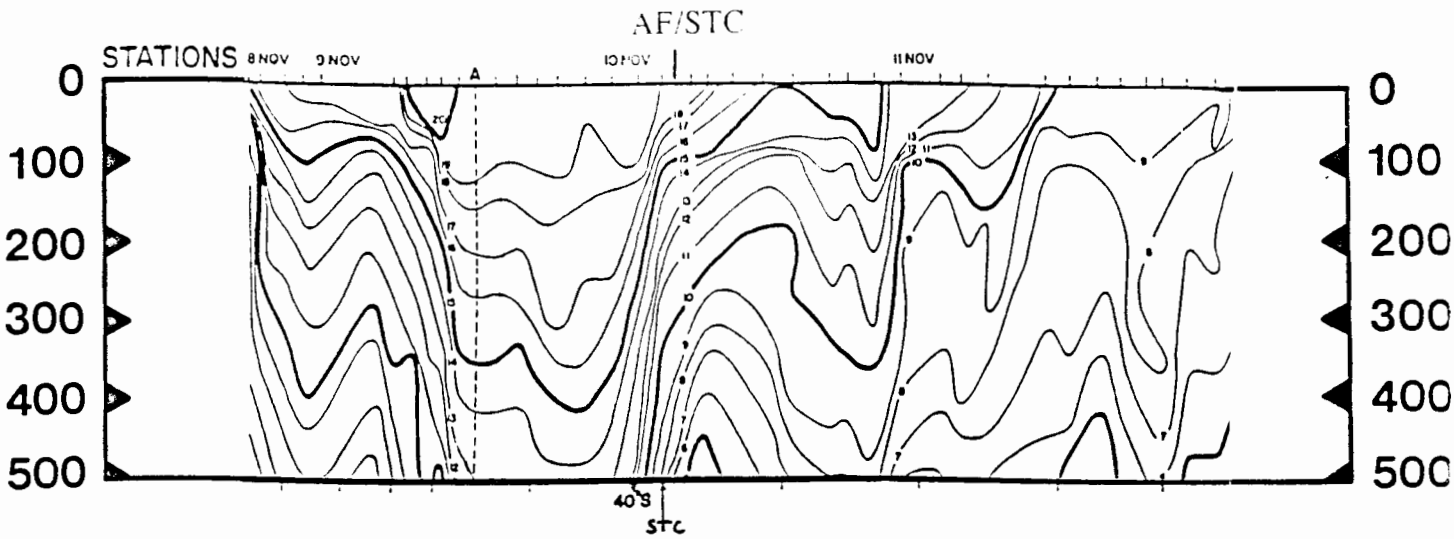


Figure 5.7: Temperature section occupied during the outward bound XBT leg of *Marion 83*. The Agulhas Front; the southern boundary of the Agulhas Return Current, appears to have merged with the STC to form a single front.

Further downstream at approximately 25°E, at the easternmost section of the *ARC* hydrographic grid between CTD stations 48-58, the Agulhas Return Current is shown from figures 5.8a and 5.8b, to execute an S-shaped meander between 36°33'S and 40°S (CTD station 55 and XBT 169-172, CTD station 54 and XBT 165-167, CTD station 51-52 and XBT 159-164). XBT 170 defines the center of the anticyclonic turn and XBT 165-166 defining the cyclonic turn, which directs the flow through the Agulhas Passage. This planetary wave is brought on by subjecting the Agulhas Return Current to firstly increasing anticyclonic relative vorticity as the depth decreases to 2 000 m (XBT 170) and secondly cyclonic vorticity as the northern flank is crossed and the depth once again increases (XBT 165-166). This deflection occurs over depths between 1 500 m to 2 000 m, confirming that the Agulhas Return Current extends to such depths.

From these figures (5.8a to 5.8b) the location of the westward flowing Agulhas Current is evident north of the Agulhas Return Current, between CTD station 50 and XBT 152-153.

The AF is located between XBT 172 and CTD station 56, 39°46'S-40°10'S, as a combined front with the STC with temperatures decreasing from approximately 15,5°C to 11,5°C at the 200 db pressure level. Surface salinity values at the two stations are 35,44 psu (XBT 172) and 35,23 psu (CTD station 56).

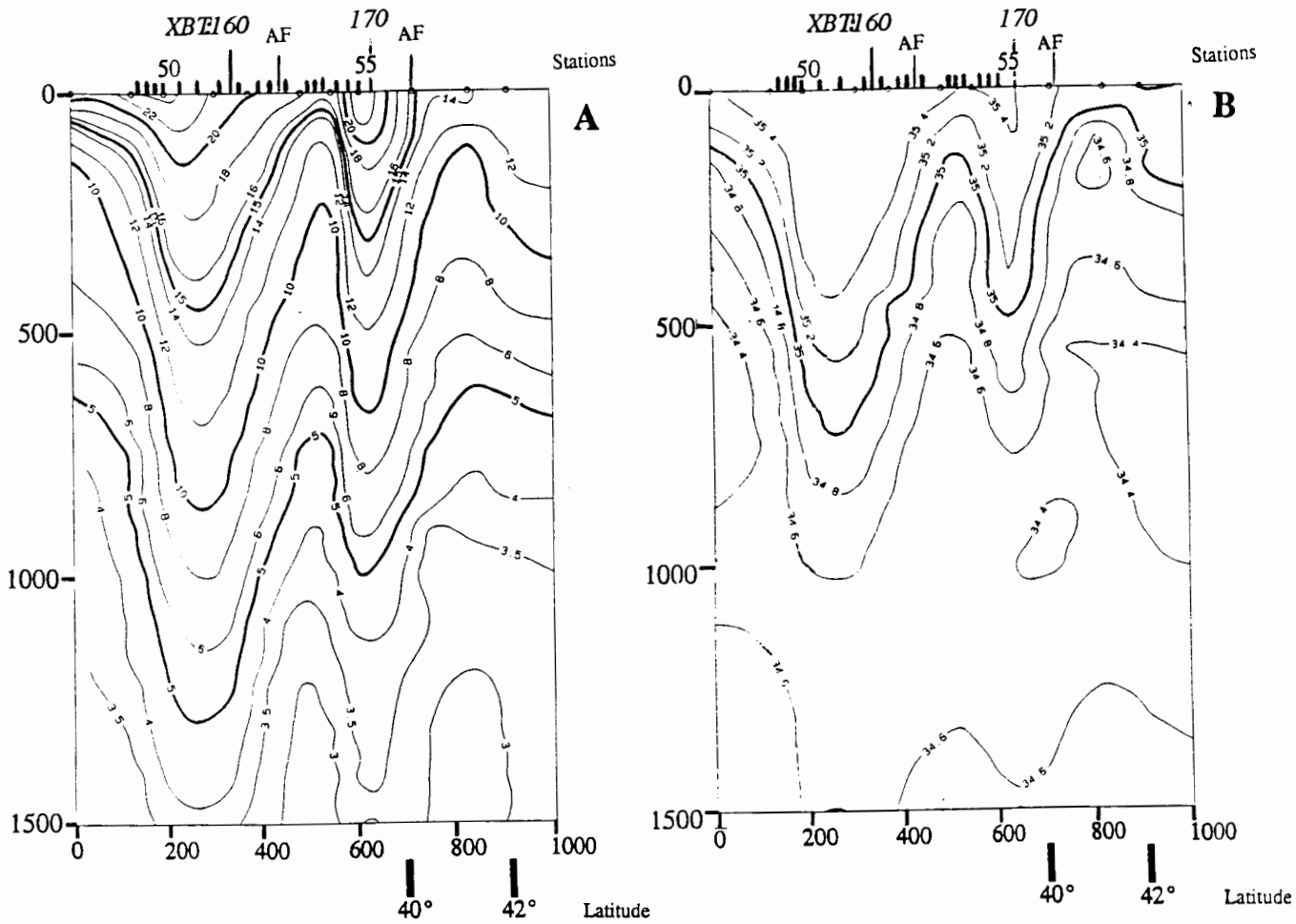


Figures 5.8a and 5.8b: ***ARC* Transect 3** Potential temperature and salinity sections between CTD stations 48-58 for a total depth of 1 500 db. The position of the Agulhas Front; the southern boundary of the Agulhas Return Current is evident between CTD stations 55-56 and CTD stations 52-53.

South of the front it becomes difficult to identify features as this area is "messy", but it is believed by Gordon et al. (1987) that the slight tilt of the isotherms downwards on proceeding southwards south of CTD station 57 marks the position of an eastward drifting old Agulhas warm eddy. Further north between XBT 161-167, 37°09'S-38°23'S a separate AF is seen, formed by the Agulhas Return Current passing over the northern flank of the Agulhas Plateau. Temperature and salinity values range from 17°C to 10°C at 200 db and 35,51 psu to 35,24 psu. It is thought that cooler Subantarctic water is advected northwards over the central Agulhas Plateau as a result of the Agulhas Return Current's northward divergence (Gordon et al. 1987).

During the *SCARC* cruise the Agulhas Return Current was crossed during a single transect, however station spatial resolution during this line was extremely poor with the closest station CTD 53 located only at the southern edge of the Current at 39°37'S and 22°10'E. The position of the Agulhas Return Current can be clearly seen from figure 5.9 below which shows the dynamic height (in metres) relative to the 1 500 db.

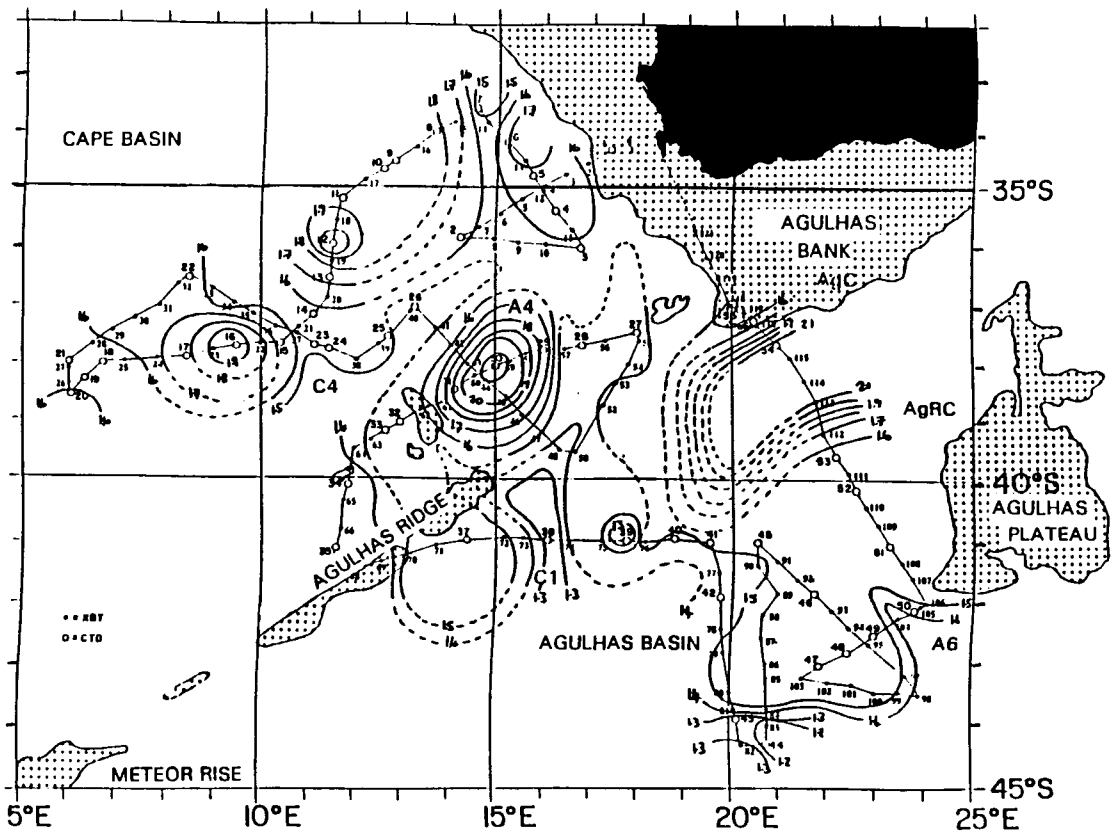


Figure 5.9: Dynamic height anomaly of the sea surface relative to 1 500 db (after Rigg 1995). The transect between CTD station 53 to 55 showing the position of the Agulhas Return Current in relation to station position is marked. Values are given in metres. The main bathymetry $< 3\,000$ db is shaded.

During the *Marathon* cruise, the Return Current was identified during two transects between approximately 22°E and 26°E as can be seen from figure 5.10.

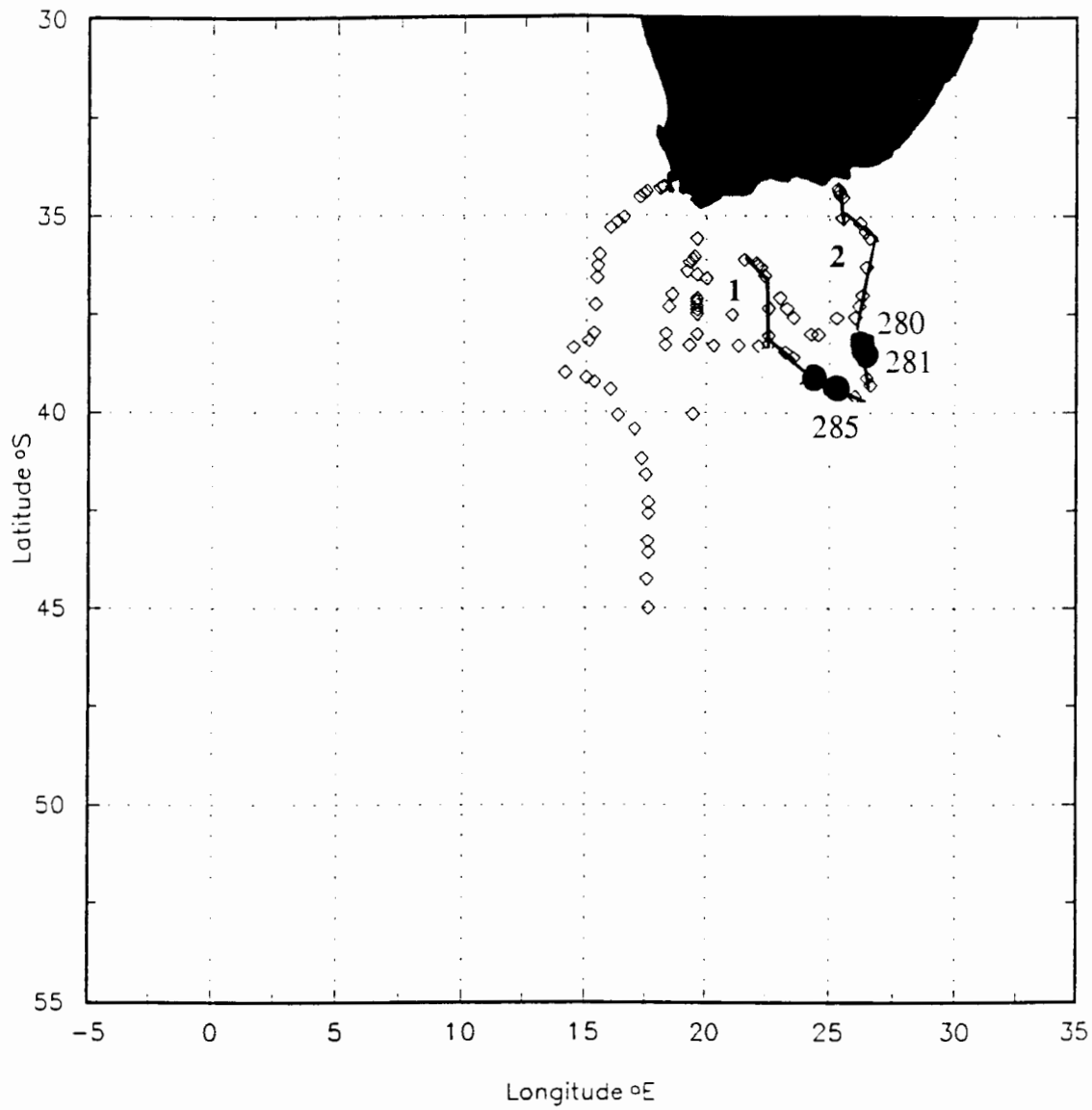


Figure 5.10: The location of the two *Marathon* transects. The position of the Agulhas Return Current and Agulhas Front, as interpreted from figures 5.11a and b and 5.12a and b, lies between CTD stations 285-287 (transect 1) and CTD stations 280-281 (transect 2), as shown by the solid dots.

The transects were made over the western and northern flank of the Agulhas Plateau and the thermal characteristics are clear from figures 5.11a to 5.11b and 5.12a to 5.12b. The temperature ranges between the two transects is approximately 5°C between 17,5° to 12,5°C and salinity values range from 35,39 psu to 34,98 psu. At CTD station 281 there appears to be a narrow thermal front 72 km wide, marking the southern boundary of the Agulhas Return Current.

During this transect it is thought that there has been a large displacement polewards of approximately 300 km in the path of the Agulhas Return Current as it crosses over the Agulhas Plateau (Bennett 1988). This can be seen from the 15°C/200m depth contour which lies over the 2 700 db level while in previous surveys (Harris van Foreest 1978 and Gordon et al. 1987) this contour has been identified at 4 200 db.

A planetary wave can also be observed between 25°-28°E from the inward bound XBT legs occupied during *Marion 83* and *FIBEX* (figure 5.11). During the return legs from Marion Island to Cape Town, the *FIBEX* and *Marion 83* cruises pass over the Agulhas Plateau. As can be seen from figures 5.13 and 5.14, the Agulhas Return Current and the Agulhas Front are clearly noticeable between 38°S and 38°30'S during *FIBEX* and between 37°S and 39°20'S during *Marion 83*. On both occasions the Current is seen to flow around the Agulhas Plateau forming a planetary wave. Temperature values range from 21°C at the northern boundary to 17°C at the south. The sharp temperature gradient of 5°C (19°C to 14°C) at 40°S (*FIBEX*) and 4°C (17°C to 13°C) at 39°40'S (*Marion 83*) marks the location of the STC.

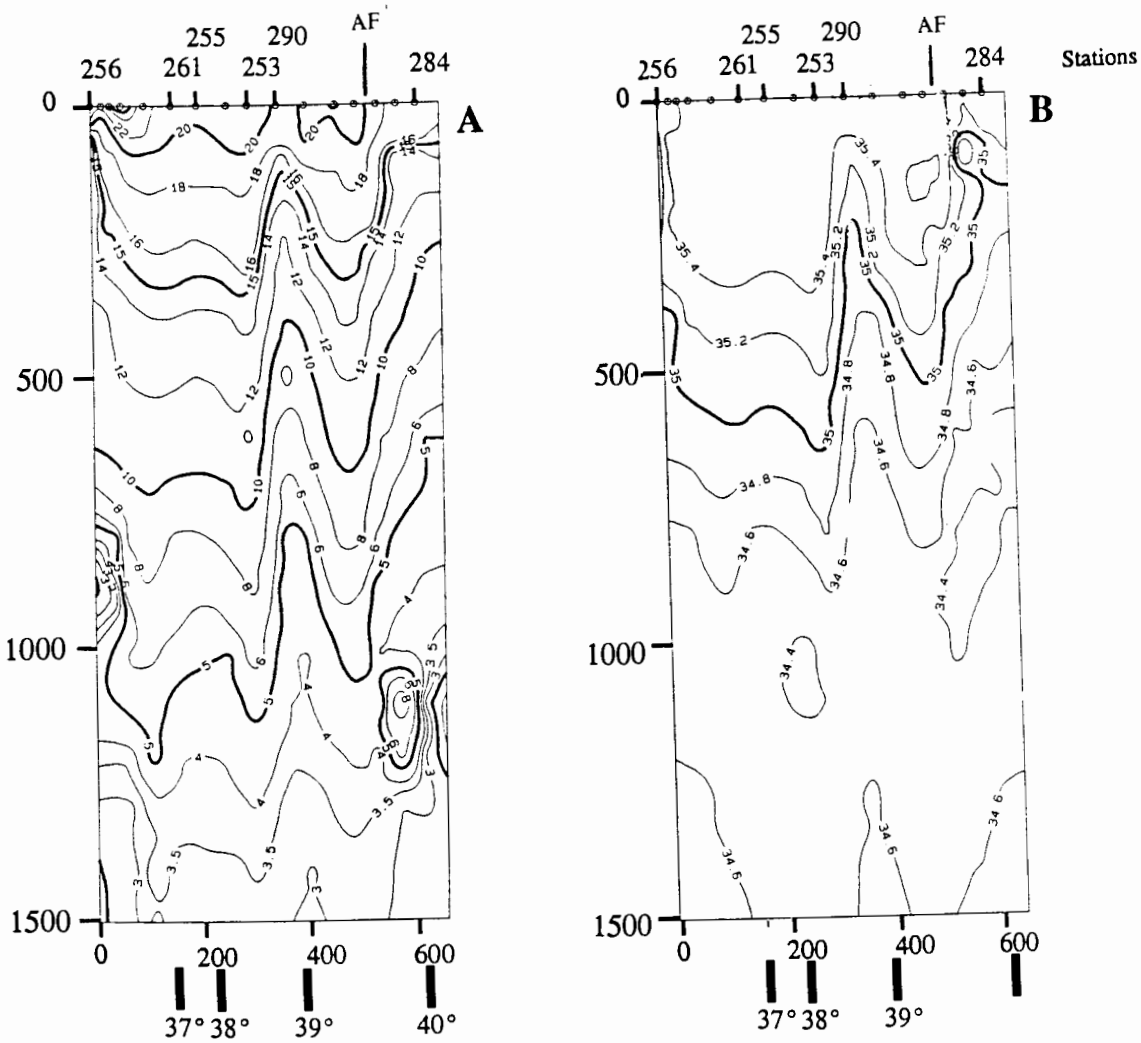


Figures 5.11a and 5.11b: ***Marathon*** **Transect 1** Potential temperature and salinity sections between CTD stations 256-284 for the total depth of 1 500 db. The position of the Agulhas Front, the southern boundary of the Agulhas Return Current, is evident between CTD 285-287.

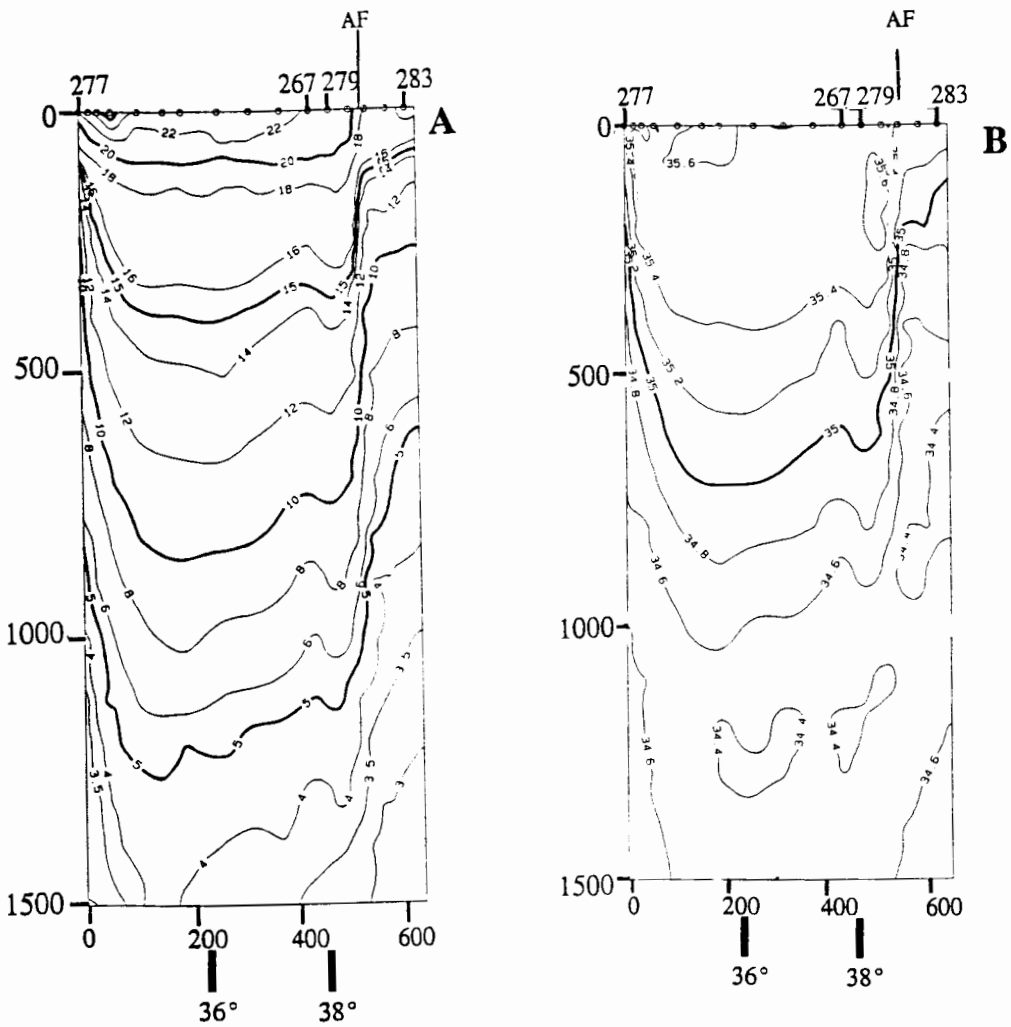


Figures 5.12a and 5.12b: ***Marathon*** **Transect 2** Potential temperature and salinity sections between CTD stations 277-283 for the total depth of 1 500 db. The position of the Agulhas Front, the southern boundary of the Agulhas Return Current, is evident between CTD 280-281.

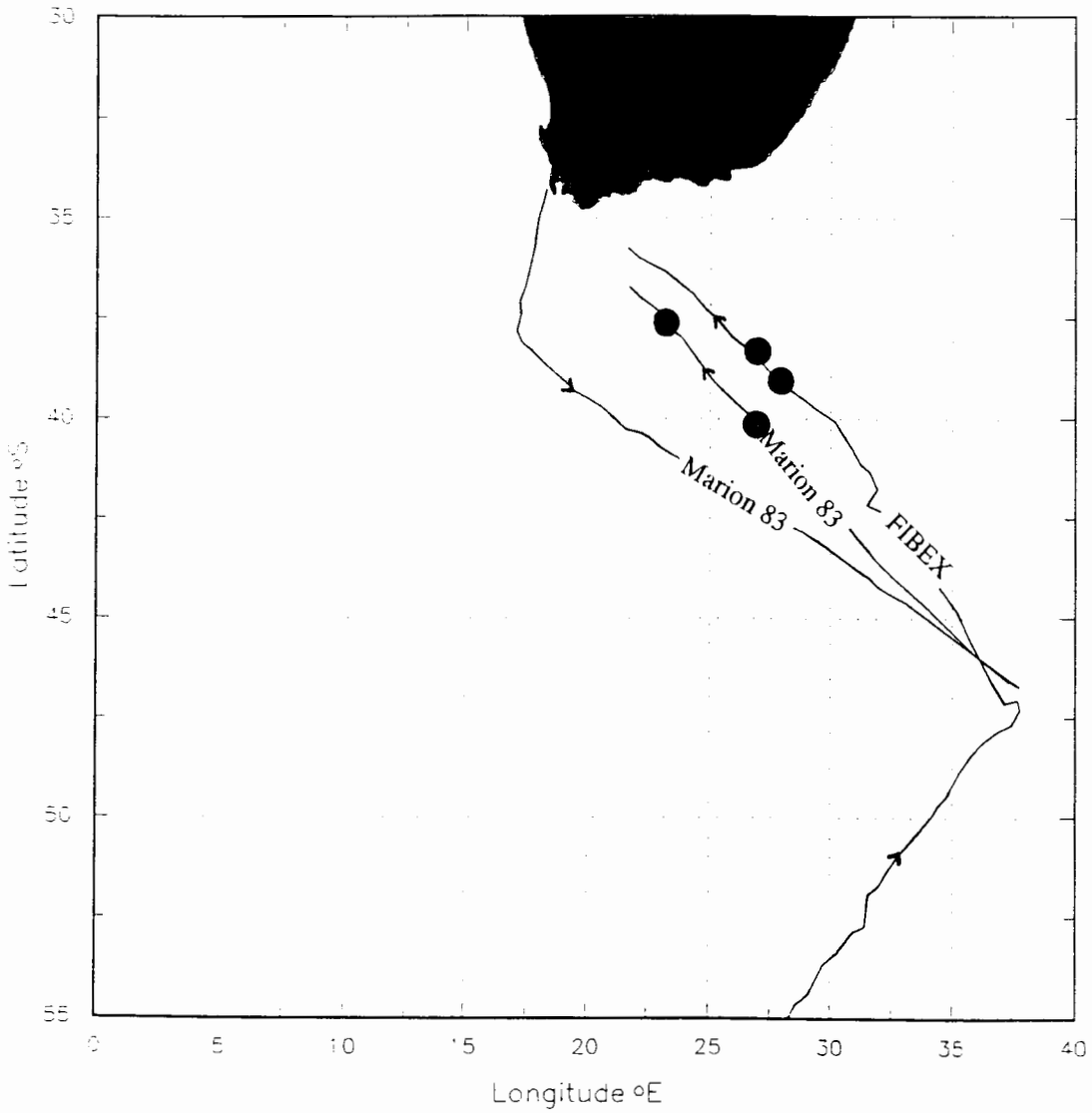


Figure 5.13: The location of the *Marion 83* and *FIBEX* XBT cruise tracks. The position of the Agulhas Return Current and Agulhas Front, as interpreted from XBT figures 5.14 and 5.15 is shown by a solid dot.

This meandering pattern over the Agulhas Plateau should be considered as quasi-stationary, having been identified so frequently, that it now appears in all schematic representations (Lutjeharms 1981).

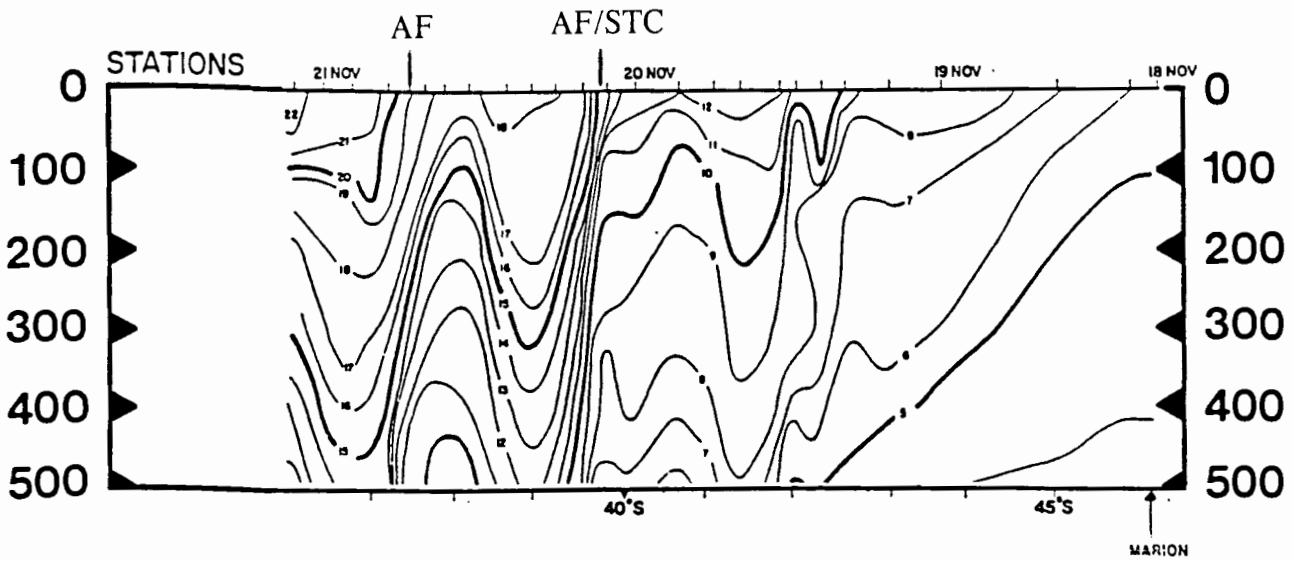


Figure 5.14: Temperature section occupied during the inward bound XBT leg of *Marion 83*. The Agulhas Front, the southern boundary of the Agulhas Return Current, appears to flow around the Agulhas Plateau as a planetary wave.

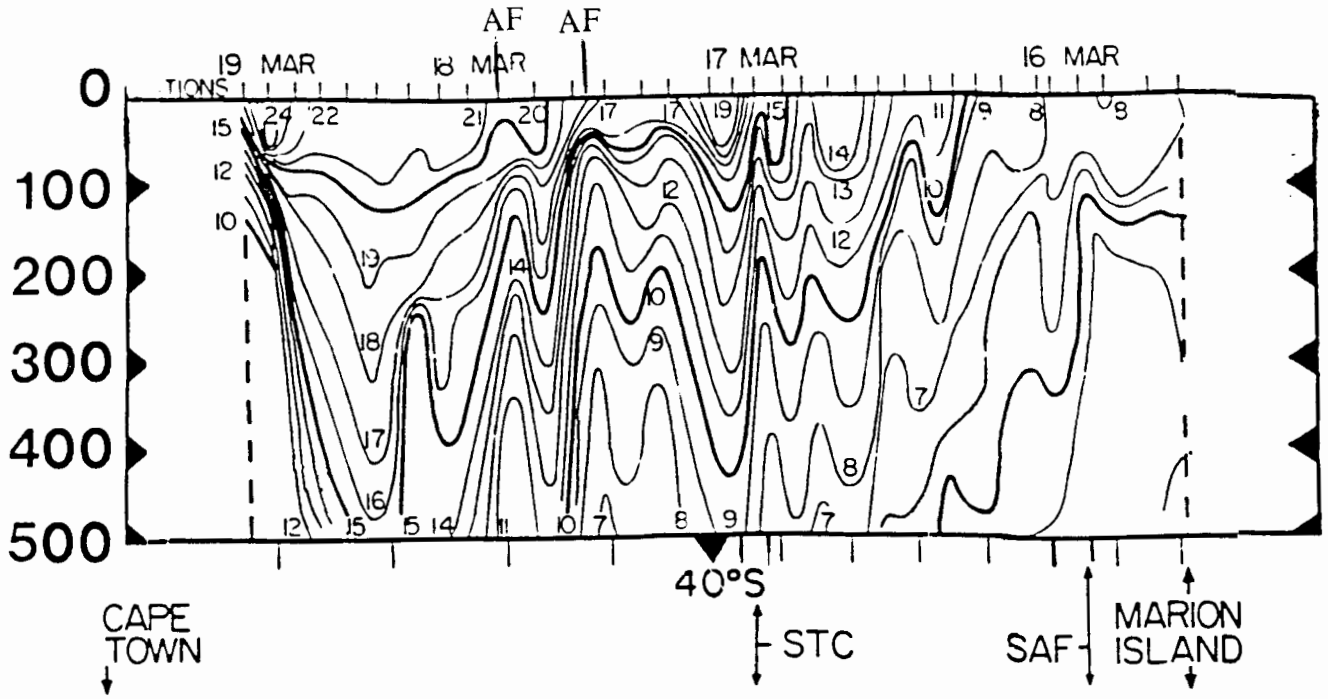


Figure 5.15: Temperature section occupied during the inward bound XBT leg of *FIBEX*. The Agulhas Front, the southern boundary of the Agulhas Return Current, appears to flow around the Agulhas Plateau as a planetary wave.

### *The passage of the Agulhas Return Current east of the retroflection region: East of 35°E*

East of 35°E, the Agulhas Return Current continues it's zonal flow at approximately 40°S as far east as 72°-76°E (Park et al. 1993, Belkin and Gordon 1994), gradually weakening as Agulhas water is recirculated northwards. Planetary waves generated by the flow over the shallow topography of the SW Indian Ridge are responsible for the frequent occurrence of these meandering recirculation branches and eddies (Daniault 1984, Park and Saint-Guily 1992). All of these mesoscale features have been commonly observed in the central part of the Crozet Basin, by satellite-tracked surface buoys (Projet MARISONDE 1979, Daniault 1984), satellite altimetry-derived sea-level variability (Cheney et al. 1983 and Daniault and Ménard 1985) and a number of historical hydrographic sections (Gambéroni et al. 1982, Park et al. 1989, 1991, 1993). Maps of dynamic topography (Wyrtki 1971, Gordon et al. 1986) and results of the fine resolution Antarctic model (Webb et al. 1991) show the geostrophic flow of the Agulhas Return Current and confirm the presence of the recirculating branches at approximately 42°E, and 50°E and 67°E, which can be also seen in the property distributions at 200 m (Figure 5,16).

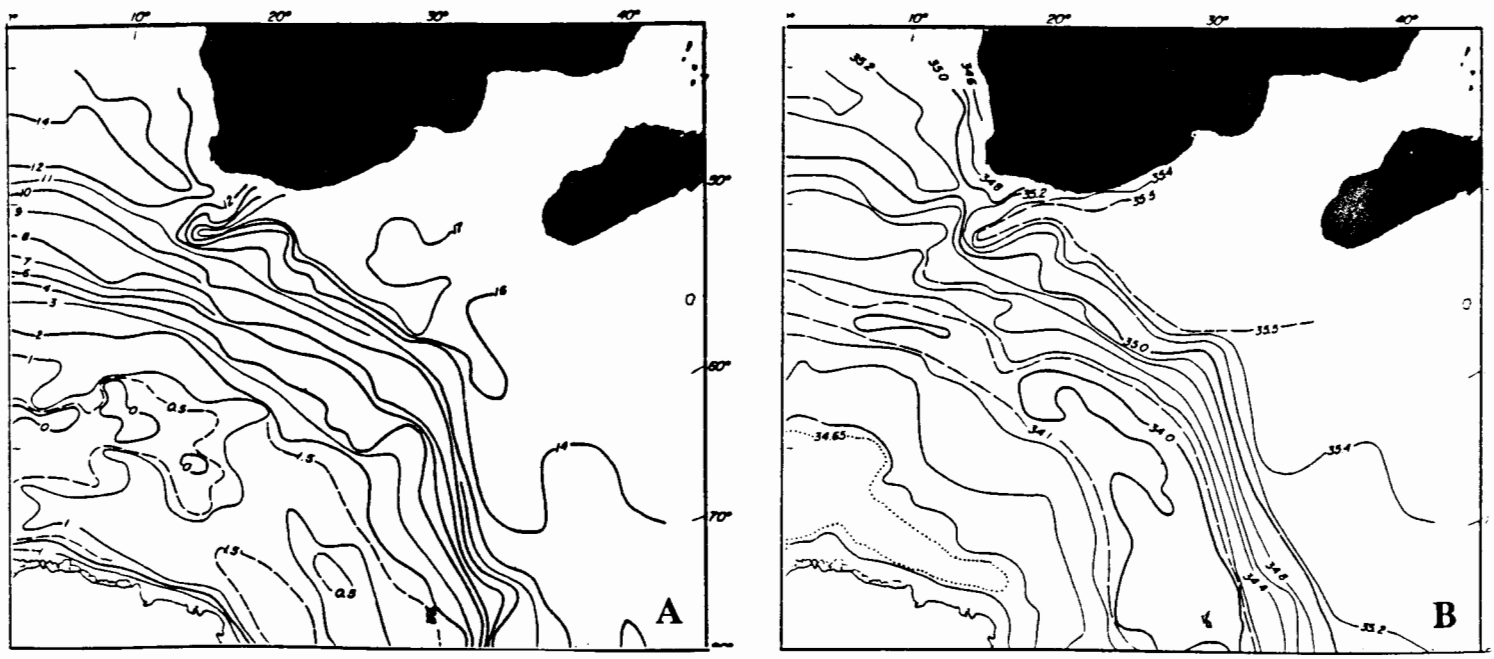


Figures 5.16a and 5.16b: Horizontal distributions of (a) temperature and (b) salinity at 200 m, modified from Gordon et a. (1986). The general location and passage of the Agulhas Return Current, including it's northward recirculation branches, can be determined by the range of 17° to 13°C isotherms (a) and the 35,5 psu to 35,0 psu isohalines (b).

Analysing hydrographic data obtained during the *Discovery 164* and *SUZIL* cruises, it is possible to identify and follow the course of the Agulhas Return Current and the Agulhas Front from 40°E across the South Indian Ocean.

During the *Discovery 164*, the Agulhas Return Current and it's associated front were identified as being entirely separate from the STC, as can be clearly seen from figures 5.18a to 5.18b.

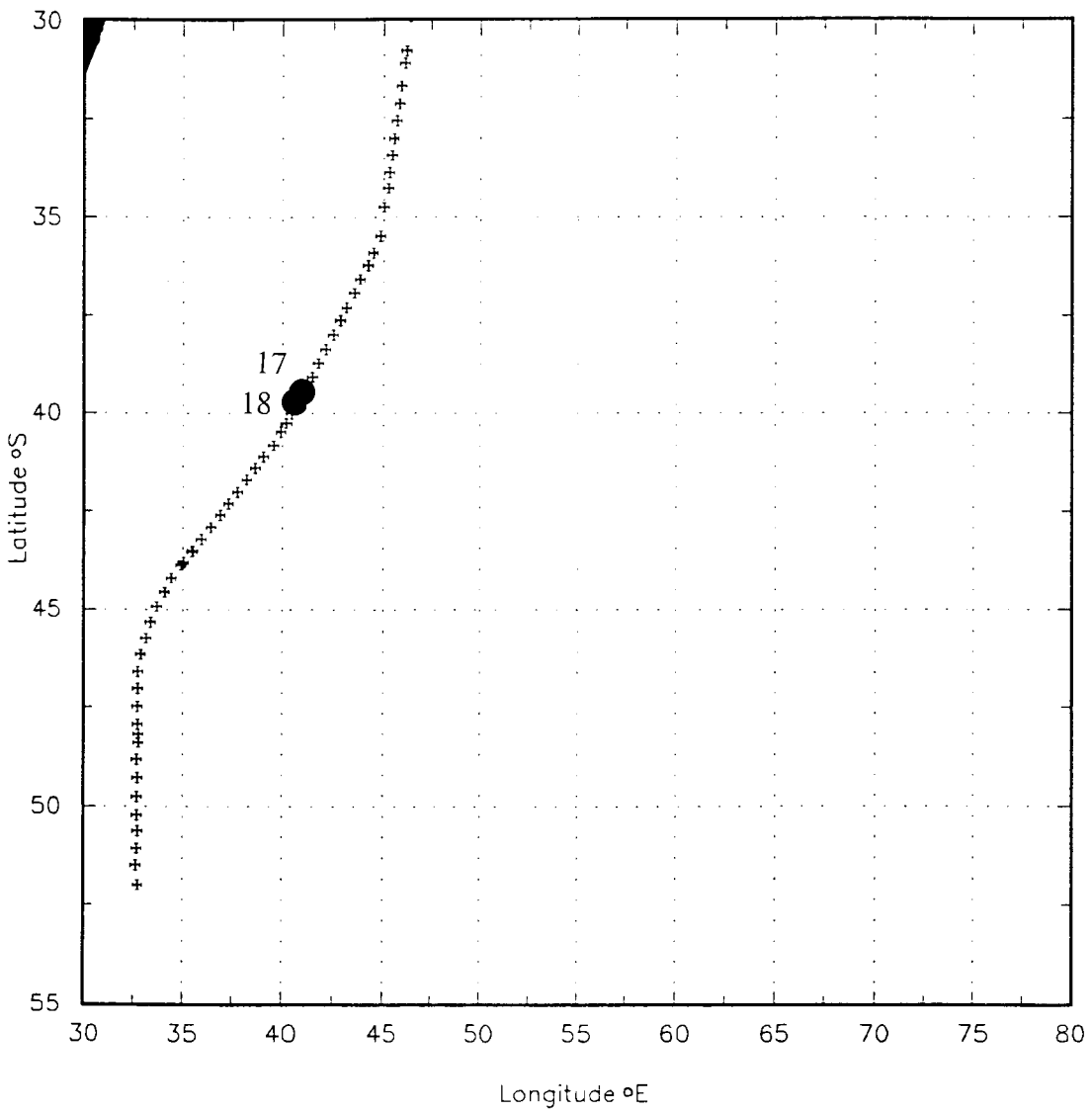


Figure 5.17: The location of the *Discovery 164* transect. The Agulhas Return Current and the Agulhas Front, as interpreted from the sections figures 5.18a and 5.18b, lies between CTD stations 17-18 as can be seen from the solid dots.

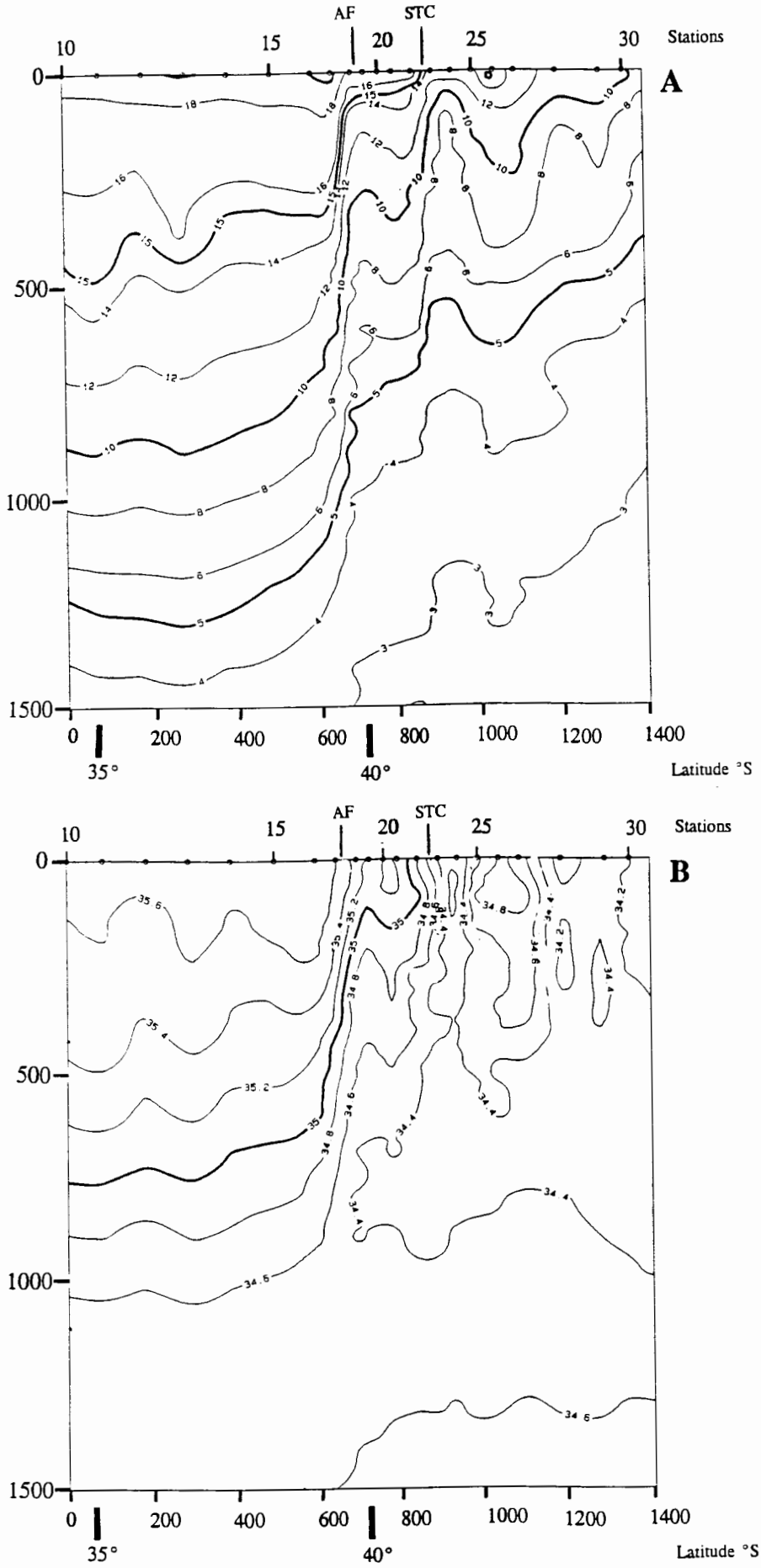


Figures 5.18a and b: Potential temperature and salinity sections between CTD stations 10-30 for a total depth of 1 500 db. The position of the Agulhas Front, the southern boundary of the Agulhas Return Current, is clearly visible as a separate front from the STC between CTD stations 17-18.

In analysing the *Discovery 164* section (figures 5.18a and 5.18b), the Agulhas Front (AF) is completely separate from the STC at 40°E between CTD stations 17 and 18 (39°27'S and 39°48'S). The AF forms a narrow band (50 km wide) of strong horizontal gradients extending from the surface downwards to depths greater than 3 000 m.

Temperatures and salinities across the front from 16°C to 12°C and 35,48 psu to 34,97 psu at 200 db. Crossing the AF it can also be seen from *Addenda figure* A7.c, that the water masses become oxygenated from 4,73 ml/l at CTD station 17 to 5,68 ml/l at CTD station 18 at 200 db. Further south between CTD 18 and 21, (figures 5.18a and 5.18b), a cyclonic eddy consisting of modified Agulhas water exists and with values ranging between 12°C to 11,8°C and 34,97 psu to 34,91 psu. This feature is believed by Read and Pollard (1993) to have propagated from the retroflection zone 1 800 km upstream. Further confirmation is given from the geostrophic calculations, in the following chapter, which show both easterly and westerly velocity components between these two CTD stations. Further south, centered at 42°S, another cyclonic warm eddy exists, consisting of further modified subtropical Agulhas water with surface temperatures and salinity values at approximately 10°C and approximately 34,7 psu.

The STC was found at 41°S between CTD stations 22 and 23. Described by Whitworth and Nowlin (1987) as a surface feature that can be defined by the horizontal surface temperatures at 200 db of between 11°C and 8,5°C and salinity values of between 34.8 psu and 34.4 psu. Comparing these values with those measured during *AJAX*, 40° upstream (figure 5.1), it can be seen that the STC is located 3° further south in the Indian Ocean. The physical ranges encountered during *Discovery 164* where found by Read and Pollard (1993) to be comparable to those reported by Jacobs and Georgi (1977) who encountered the STC at the same latitude in 1974 during the *CONRAD 17* cruise.

In between the intensive hydrographic cruises of *Discovery 164* and *SUZIL*, a meridional XBT line was carried out at 47°E, the *Gallieni*, (see figure 5.19). During the transect a

triple front consisting of the AF/STC and SAF was shown to exist between 40°30'-43°S (figure 5.20). The sharp subsurface temperature gradients associated with the AF between 40°30'-41°S, forms the northern boundary of the front separating warm >16°C (at 200 db), saline >35,30 psu (surface) subtropical water from cooler 4°C subantarctic water.

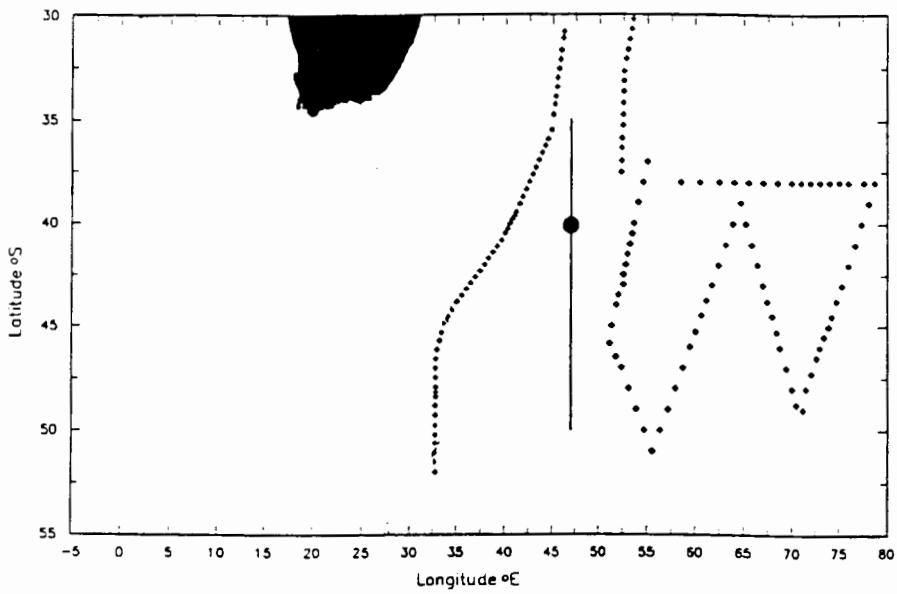


Figure 5.19: The location of the XBT line at 47°E, in between *Discovery 164* and *SUZIL*, occupied by *Gallieni* XBT cruise. The location of the Agulhas Front, the southern boundary of the Agulhas Return Current, can be seen as a solid dot.

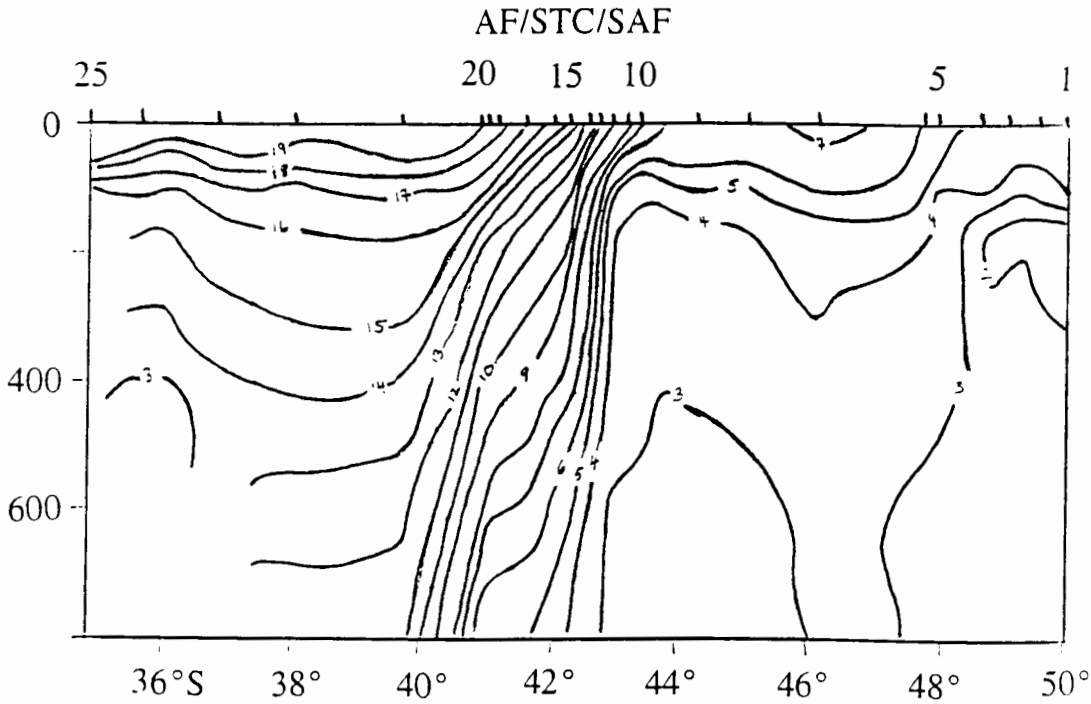


Figure 5.20: Temperature section between XBT 1-25 for a total depth of 800 m. The position of the Agulhas Front, the southern boundary of the Agulhas Return Current, is evident between XBT stations 17-20. The Agulhas Front forms a merged intensive front with the STC and SAF.

Further downstream four north/south transects were carried out as part of the *SUZIL* project between 51°E-79°E, see figure 5.21.

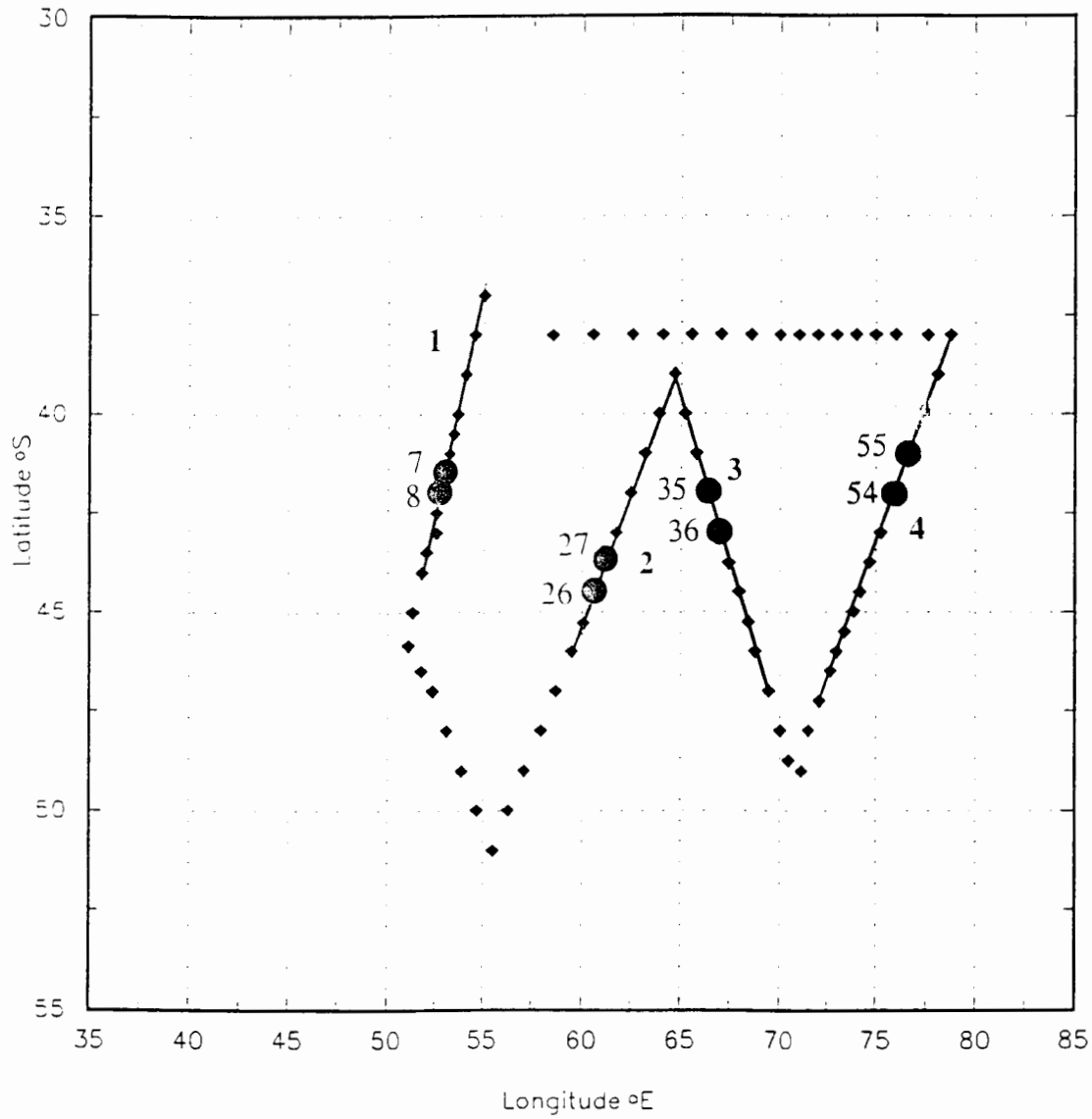


Figure 5.21: The location of the four transects occupied during *SUZIL*. The position of the Agulhas Front, the southern boundary of the Agulhas Return Current, as interpreted from figures 5.22a and b to 5.25a and b is marked by solid dots between CTD stations 7-8 (transect 1), 26-27 (transect 2), 35-36 (transect 3) and 54-55 (transect 4).

During the first two transects (figures 5.22a and b and 5.23a and b), the Agulhas Return Current was shown to have merged with the ACC at 53°E and 61°E, as a result of the Antarctic Circumpolar Current (ACC) shifting northwards around the Crozet Plateau. A narrow (150 km) intense AF/STC/SAF frontal zone, with strong bottom reaching horizontal gradients between 41°30'S to 43°S is clearly visible in figures 5.22a and b to 5.23a and b. This frontal zone separates abruptly warm saline oxygen-poor subtropical Agulhas water from cold, fresh oxygen-rich subantarctic water.

From the first two sections, occupied during *SUZIL*, it can be seen that the AF forms the northern boundary of the ACC between CTD stations 7-8 at 52°45'E and CTD stations 26-27 at approximately 61°E, where it is between 60 km and 90 km wide. During the first section, figures 5.22a and b, (CTD 7-8) the Agulhas Return Current lies between 41°30'S and 42°S further downstream at transect 2 figures 5.23a and b, as a result of the southward shift of the ACC around the Crozet Plateau, the Agulhas Return Current lies between 43°45'S and 44°30'S. Temperature and salinity values at 200 db range from 15,8°C to 12,04°C and 35,53 psu to 35,04 psu. It is noticeable that in comparing these sections (transect 1 and 2), the Agulhas Return Current has become significantly cooler (at 200 db) by 1°C, less saline by 0,1 psu and more oxygenated by 0,3 ml/l (addenda figures A.8a/b/c and A.9a/b/c) with distance downstream, suggesting a substantial downstream decrease in the strength of the Agulhas Return Current (Park et al. 1993). This can be attributed to the gradual weakening of the Agulhas Return Current brought on by topographically induced meanders or eddies "peeling" Agulhas water off from the main current body and recirculating equatorwards. Such subtropical meanders or eddy like features, are centered at 42°S and 39°S and can be seen from figures 5.23a and b, to perturbate the water column stratification and constitute the most intensified mesoscale activities observed during *SUZIL* (Park et al. 1993).

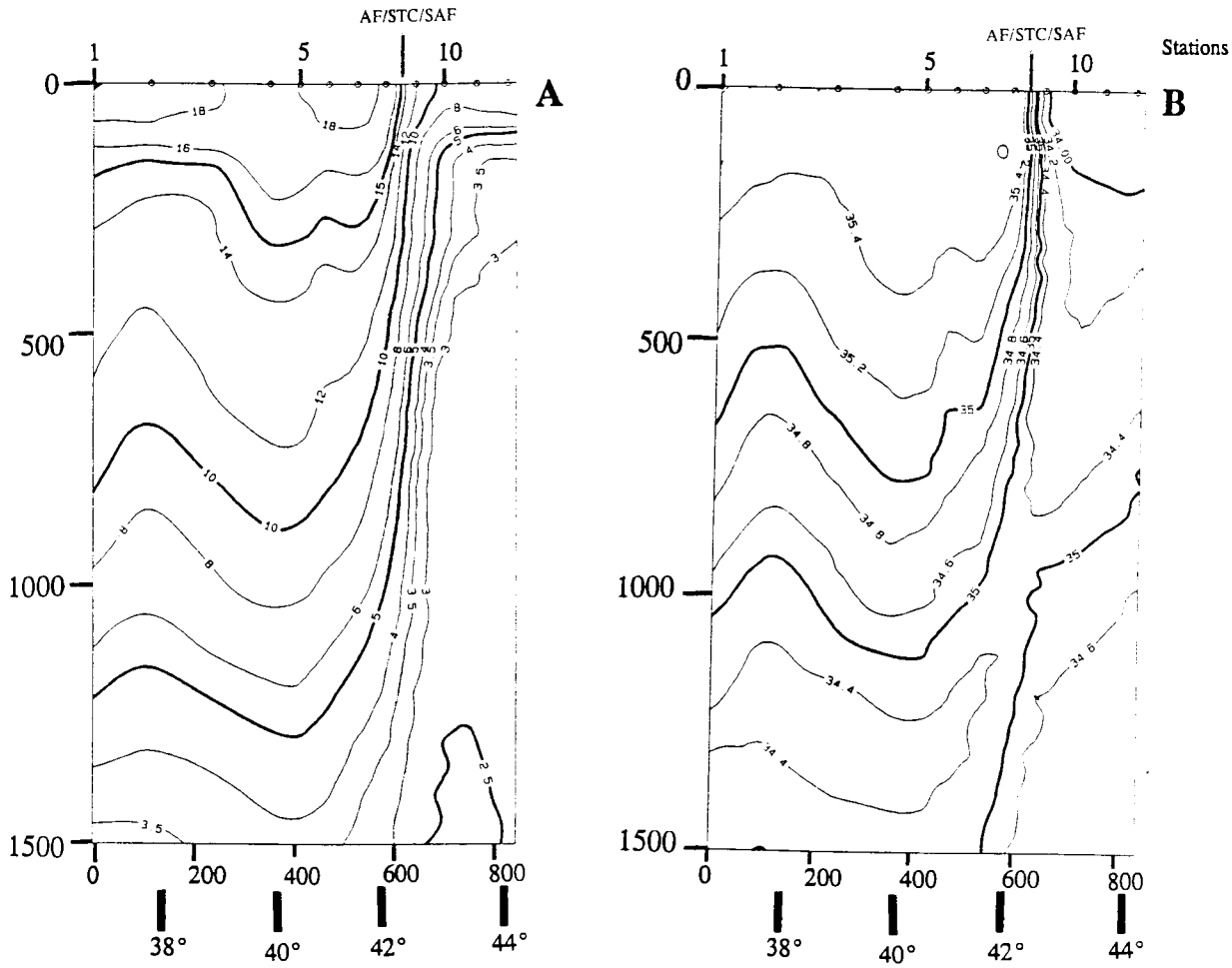


Figures 5.22a and 5.22b: ***SUZIL* Transect 1** Potential temperature and salinity sections between CTD stations 1-12 for a total depth of 1 5000 db. The position of the Agulhas Front, the southern boundary of the Agulhas Return Current, is evident between CTD stations 7-8.

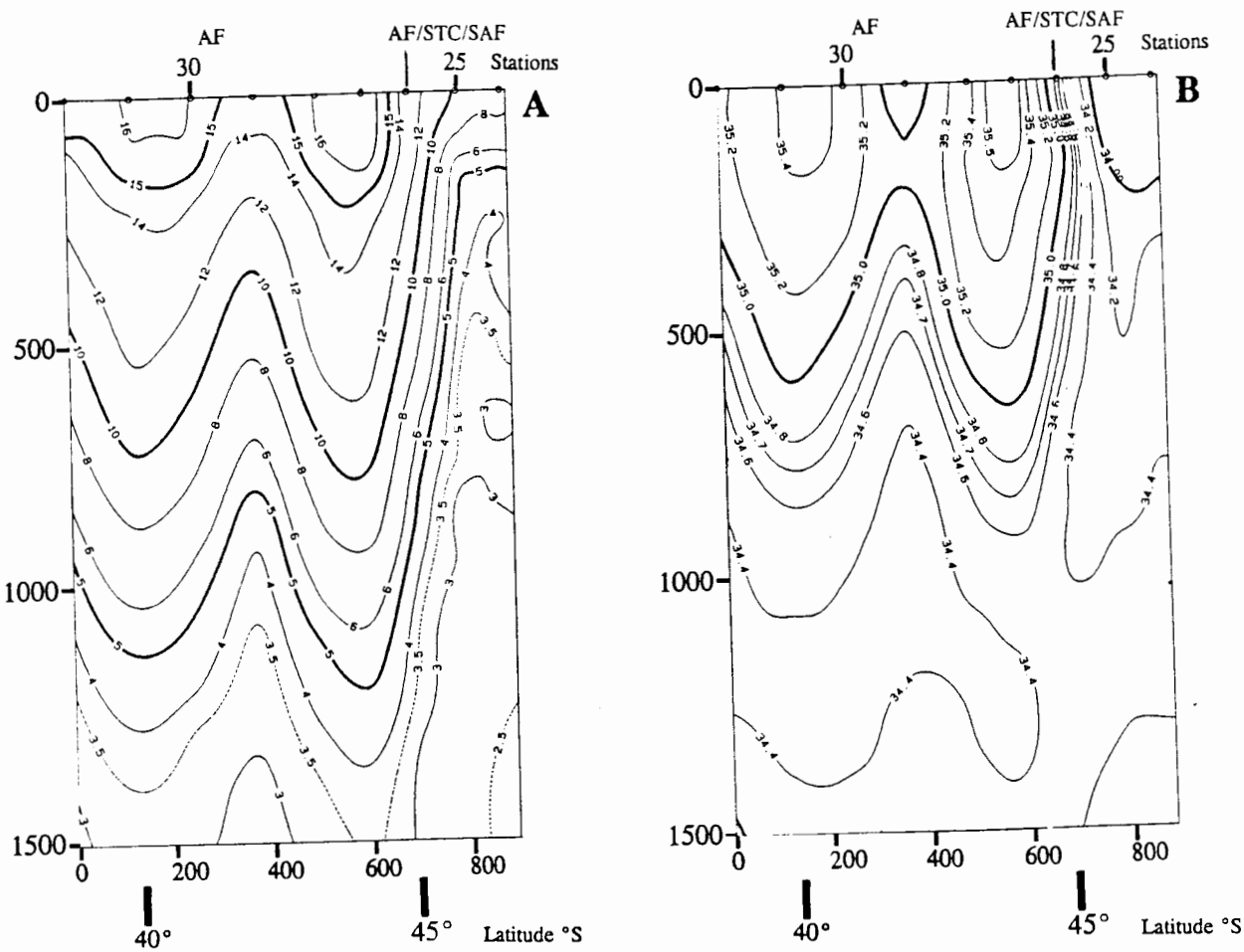


Figures 5.23a and 5.23b: ***SUZIL* Transect 2** Potential temperature and salinity sections between CTD stations 24-32 for a total depth of 1 500 db. The position of the Agulhas Front, the southern boundary of the Agulhas Return Current, is evident between CTD stations 26-27.

This northward recirculation pattern of subtropical water is consistent with the anticyclonic circulation in the South Indian subtropical gyre seen in Wyrtki's (1971) maps of dynamic topography.

Further downstream at transect 3 (see figures 5.24a and b), at 66°E, the subsurface characteristics at the northern boundary of the frontal zone are significantly cooler and fresher by 2°C (14°C) and 0,15 psu (35,35 psu). Lying between 42°S and 43°S the AF appears to no longer be merged with the SAF and STC, but has become separated from the STC and SAF frontal zone. From figures 5.24a and b, the Agulhas Return Current is shown to flow between CTD stations 35-36, approximately 2° further north. This separation has been observed in the past (Belkin and Gordon 1994) during the *Ak.Shirshov Cruise #5* at 70°E (*addenda figures* A.12a/b), *Yu. M. Schokalskii Cruise #33* at 65°E (*addenda figures* A.13a/b), and the *Vitayaz II Cruise #4* between 67° and 73°E (*addenda figures* A.14a/b). The salinity section shows low salinity surface water <35psu overlaying higher salinities, indicating an equatorward advection of fresher surface water (Park et al. 1993).

At 76°E along the transect 4 despite the STC and SAF continuing to form a single front, the presence of the AF north of the frontal zone is almost beyond recognition as can be seen from figures 5.25a and b, as a result of the progressive weakening of the current downstream from the Crozet Plateau. Temperature and salinity values (at 200 db) between CTD stations 55-54 are between 12,82°C and 13,00°C and 35,17 psu and 35,09 psu. Low salinity surface water (0,1psu) again overlies higher salinity suggesting the advection of Subantarctic water masses equatorwards.

Despite the physical properties between CTD stations 55-54 no longer representing Agulhas water, a weak geostrophic current over 120 km wide is however observed (see **Geostrophic Velocities and the Volume Transport of the Agulhas Return Current,** chapter 6).

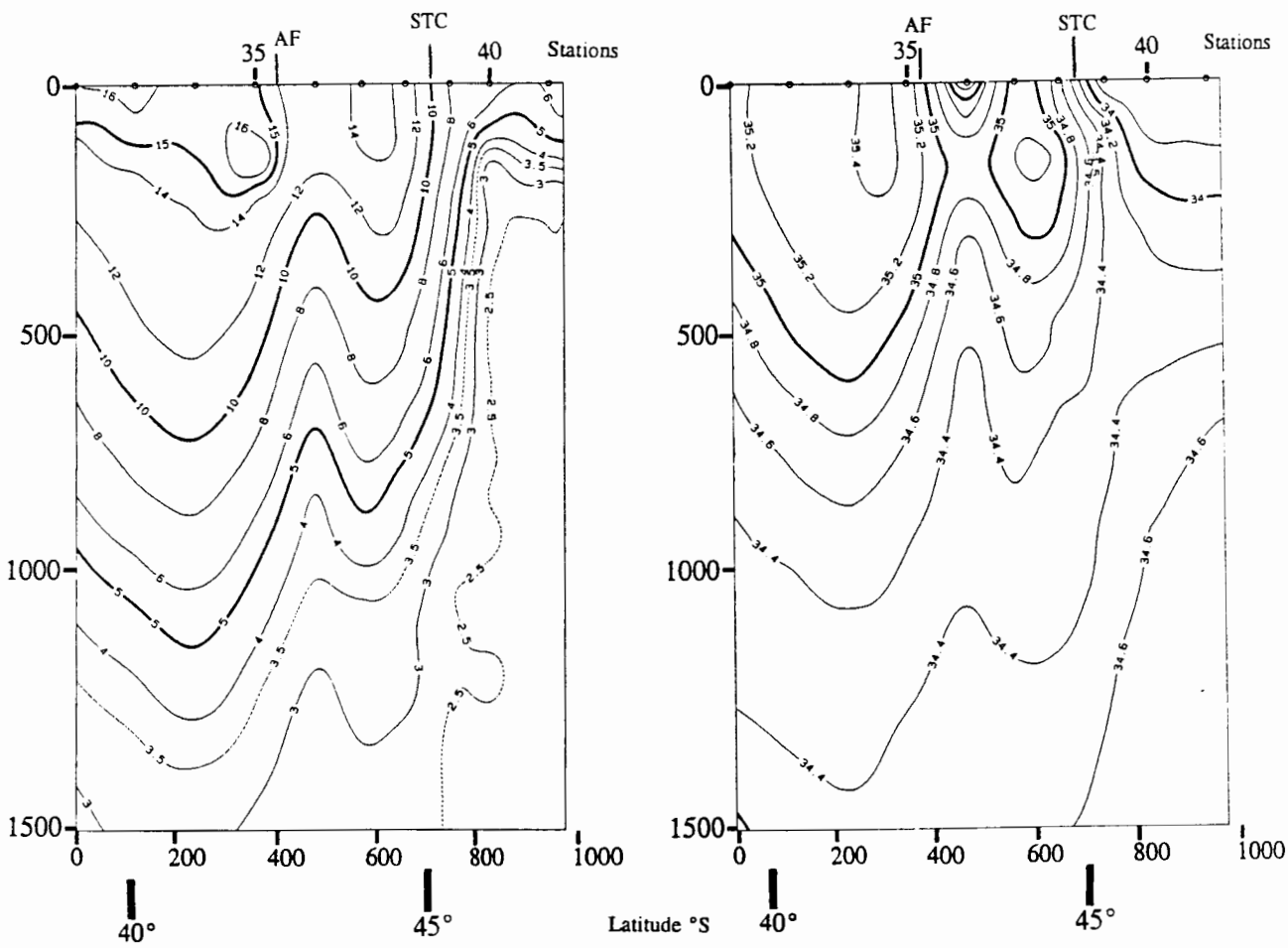


Figures 5.24a and 5.24b: ***SUZIL* Transect 3** Potential temperature and salinity sections between CTD stations 32-41 for a total depth of 1 500 db. The position of the Agulhas Front, the southern boundary of the Agulhas Return Current, is evident between CTD stations 35-36.

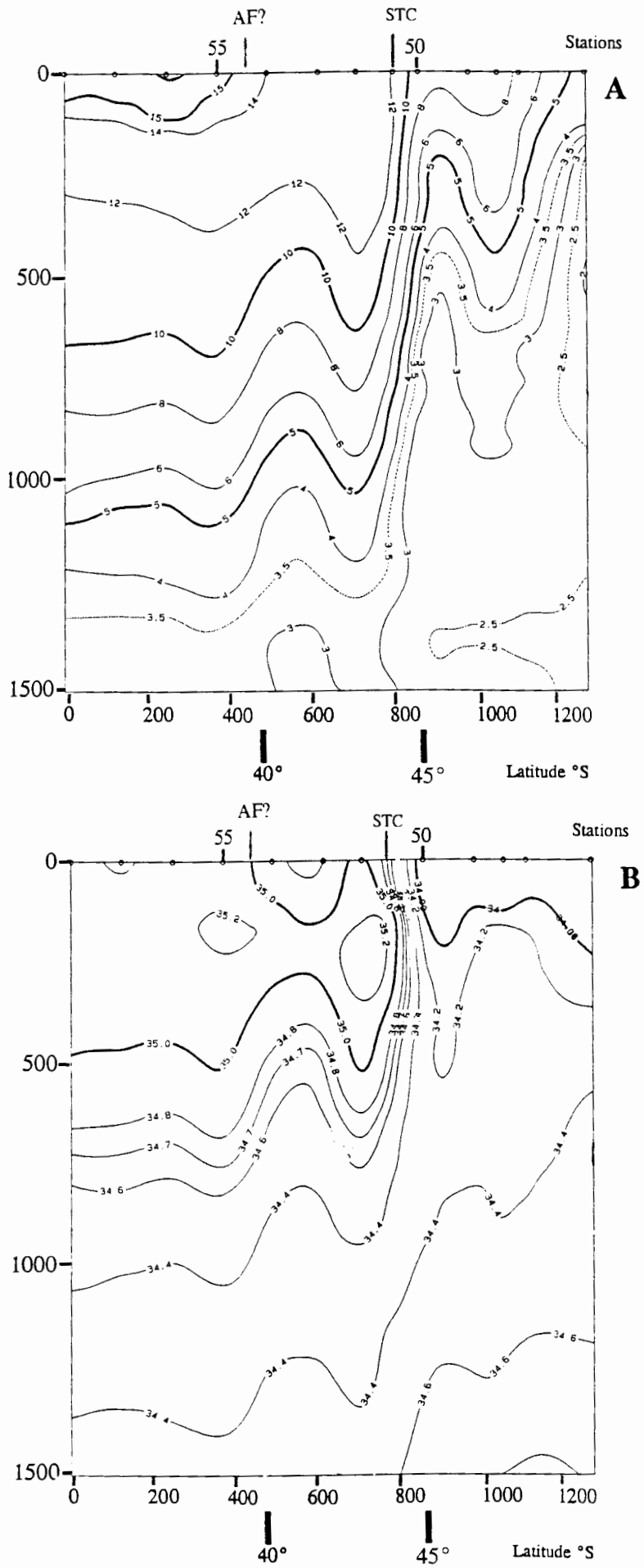


Figures 5.25a and 5.25b: ***SUZIL* Transect 4** Potential temperature and salinity sections between CTD stations 46-58 for a total depth of 1 500 db. A front exists between CTD stations 54-55, it is possible that this may be a highly modified Agulhas Front, the southern boundary of the Agulhas Return Current.

In order to examine the meridional circulation a zonal transect along 38°S was occupied during *SUZIL*. No fronts appear on the section CTD stations 58-73 (see Park et al. 1993), however, a gradual upward tilt towards the east in the upper level properties west of 72°E is evident, suggest a slow northward flow. Upper level water properties show great zonal anomalies from 67°E with saline, warm oxygen poor water on the western side and vice versa. This indicates that most of the Agulhas water is advected into the Crozet Basin recirculates northwards between 53°E and 67°E. Geostrophic calculations (chapter 6) confirm this theory with northward transports between CTD stations 67-69 (67°E), 70-71 (64°E) and 72-72 (59°E).

Previous studies by Stramma (1992) and Stramma and Lutjeharms (1995) have shown that the Agulhas Return Current extends only as far east as 30°E, where it becomes the South Indian Ocean Current. However, analysing the hydrographic data from cruises east of this longitude; *Discovery* and *SUZIL*, it can be seen that water characteristics, typical of warm >14°C, saline >35,30psu, subtropical Agulhas water are present at 40°E (*Discovery*) and between 53°E-66°E (*SUZIL*). East of 76°E, (section 4 of *SUZIL*), these properties are no longer present, however, a weak geostrophic flow north of the STC, between 41°S-42°S is evident and it is my proposal that this is now the start of the South Indian Ocean Current.

Thus it can be said that following the Agulhas Return Current's formation at the retroflection zone it flows eastwards, gradually cooling from 18°C at 22°E (*ARC*), 16°C at 40°E (*Discovery*) to 14°C at 66°E (*SUZIL*) (200 db) as interaction with surrounding water masses occurs. Comparing sections east and west of the retroflection zone, the effect this warm, saline current has, is clearly seen by comparing temperature and salinity values obtained at 200 db across the frontal zone. These are shown to vary from 13,3°C and 8,8°C, 35,2 psu and 34,5 psu at ~1°E during *AJAX* to 15,9°C and 12,2°C 35,5 psu and 35,0 psu over 3 000 km downstream at 40°E during *Discovery*.

It can be seen that during the Agulhas Return Current's passage eastwards into the south Indian Ocean, gradual weakening in the Current's chemical properties and strength occurs as interaction with surrounding water masses takes place. A further cause of this gradual weakening is due to the formation of planetary waves, brought on by the current's passage over shallow topographical features. Large mesoscale features, such as meandering branches and eddies are formed, resulting in the "peeling off" of Agulhas water from the main current body and recirculation northwards across the frontal zone.

In order to show this gradual weakening it is essential that the geostrophic velocity and the volume transport of the Agulhas Return Current are calculated for each transect and then compared in order to show the modifications occurring to the current during it's passage downstream.

# Chapter 6
# GEOSTROPHIC VELOCITIES AND THE VOLUME TRANSPORT OF THE AGULHAS RETURN CURRENT

The geostrophic velocities and the volume transported by the Agulhas Return Current for each transect of *AJAX, ARC, Marathon, Discovery 164* and *SUZIL* along the course of the Agulhas Return Current are discussed in this chapter. The *SCARC* dataset however, is not discussed as only a single mid depth (1 500 db) CTD station falls within the Agulhas Return Current.

Geostrophic velocity profiles have been calculated (using methods outlined in **Data and Methodology** chapter 4), relative to the ocean floor between station pairs along all 11 transects. Using the bottom as a level of no motion provides a fair indication of the relative strengths and direction of baroclinic flow through the water column. It is important to bear in mind that these are only estimated velocities based on the assumption that the "bottom" velocities are zero and may differ from the real values.

In each case, the geostrophic current velocities and the volume transported between station pairs are presented and comparisons are made between transects crossing the Agulhas Return Current.

In all, 11 transects cover the length of the Agulhas Return Current and it's eastern extension; {Agulhas Return Current Extension after Park et al. (1993) or South Indian Ocean Current after Stramma (1992)}, and by comparing results it will be possible to show the gradual decrease in velocity and volume transport of the Agulhas Return Current from the point of retroflecting to 76°E.

The results are analysed per cruise and then discussed to show (a) the velocities and volume transport of the Agulhas Return Current within the Retroflection zone (0°E-35°E) and (b) it's eastern extension across the South Indian Ocean (35°E-76°E).

***The Agulhas Return Current between 0°E-76°E***

Following the Retroflection, the Agulhas Return Current begins it's passage eastwards, where several strong meridional meanders between 20° and 76°E, at the Agulhas Plateau, Mozambique Ridge, South West Indian Ocean Ridge, Crozet Plateau and Crozet Basin are formed. Graphs showing the course taken and the geostrophic velocities and volume transport of the Agulhas Return Current have been drawn from selected sections during the *AJAX, ARC, Marathon, Discovery 164* and *SUZIL* cruises. Using these results, calculated from formulae described in **Data and Methodology** (chapter 4), it will be possible to also show what degree of deceleration/volume lost has occurred during the retroflection i.e. compare the inflow (Agulhas Current) to the outflow (Agulhas Return Current).

However, it must be remembered that combined the cruises do not resemble a "snapshot" of the Agulhas Return Current, but cover a period of over 8 years.

***0°E-35°E: AJAX***

During this cruise, (described in more detail in **Data and Methodology**, chapter 4), a north-south transect along 0°E-1°E, was carried out (see figure 5.1, **Geographic Location and General Hydrography of the Agulhas Return Current**, chapter 5). A diagonal line from CTD station 52 to Cape Town was surveyed, however this transect will not be analysed as stations were not carried out in sequence and a gap of over 400 km (37°S to 34°S) was filled a month later (Whitworth and Nowlin 1987).

Being too far upstream of the retroflection zone and the Agulhas Return Current, only low geostrophic velocities, volume transports associated with the STC are encountered during this transect. However, it is still worth including as it provides an excellent baseline for the

transects further downstream, where the influence of the Agulhas and Agulhas Return Current become evident.

***CTD stations 41-52:*** Meridional line between 0°E and 1°E

*Geostrophic Velocities*

The STC is one of the major oceanic fronts in the world ocean and forms the generic boundary to the Southern Ocean which surrounds the Antarctic Continent (Lutjeharms and Van Ballegooyen 1993). In the proximity of the continents in the southern hemisphere - Africa, Australia and South America - the meridional gradients of the STC are intensified, whereas in the middle of the ocean basins these gradients are much weaker. This intensification is due to the southward advection of warm salty water by the Brazil and Agulhas Currents along the eastern shores of the continents. Consequently, geostrophic velocities encountered in the middle of ocean basins, such as the South Atlantic, are greatly reduced.

The geographic location of the STC is shown by figure 5.1 and from the hydrographic sections figures 5.2a and b, in the previous chapter, to lie between CTD stations 44 (36°S) and 48 (40°S) and centering between CTD 45 (37°S) and 46 (48°S). This broad frontal zone compares well with previous studies carried out by Shannon et al. (1989) and Lutjeharms et al. (1993), which identify a single STC forming a wide frontal zone Sub Tropical Convergence Zone (STCZ) between 4-5° in latitude. Analysing four hydrographic datasets including *AJAX*, Lutjeharms et al. (1993) have suggested that the thermal expression of the STC in the south-east Atlantic Ocean is intermittent rather than weak, consisting of several fronts interspersed by zones of relatively homogeneous waters and as a result the average STC surface expression is diffuse.

The maximum geostrophic surface speed (referenced to the bottom) can be seen from figure 6.1 (vertical structure) and 6.2b (surface values) to be approximately 13.20 cm/s this compares well to Whitworth and Nowlin's (1987) estimate of 13 cm/s between CTD

station 45-46. These results are more or less identical to the mean zonal 13 cm/s velocity obtained by drifter #776 launched at 10°W in the STCZ in 1976 (Harris and Stavropoulos 1978).

However, these velocities are substantially lower than the average 26 cm/s velocity observed by Hoffman (1985) from 35 drifters in the STC. The averaged data encompasses drifters spanning the entire breadth of the STC including areas where speeds accelerate i.e. western boundary currents, resulting in large differences between averaged speeds and speeds encountered at particular locations.

Analysing South Atlantic archive data, Belkin and Gordon (1994) have been able to distinguish a North and South STC boundary extending from the Brazil Current to the Agulhas-Benguela area. Stramma and Peterson (1990) analysed historic data and showed the presence of a current, which they called the *South Atlantic Current* (SAC), corresponding with the North STC and closing the circulation of the South Atlantic subtropical gyre. Results have shown that the SAC eventually turns northwestward separating from the STC and commences it's northward flow into the Benguela Current. Further evidence supporting this are given by trajectories of surface drifters north of 40°S which show a northward turn, whereas drifters south of 40°S continued east into the South Indian Ocean (Piola et al. 1987). Investigations during the SAVE-4 (South Atlantic Ventilation Experiment) into the T/S properties in the South Atlantic although support views held by Stramma and Peterson (1990) that the South Atlantic Current folds northwestwards into the Benguela Current, oxygen and CFM patterns obtained are not consistent with this picture (Gordon et al. 1992). The high CFM concentrations in the South Atlantic Current relative to the Benguela Current clearly reveals that, during SAVE-4, approximately 50% of the thermocline water of the South Atlantic Current does not fold into the Benguela but continues eastwards into the Indian Ocean. This is further supported by the Meteor 11/5 section along 5°-18°E as well as the atlases of Wyrtki (1971) and

Gordon et al. (1982) which show water south of the Agulhas Return Current with characteristics similar to those found in the South Atlantic Current (Gordon et al. 1992).

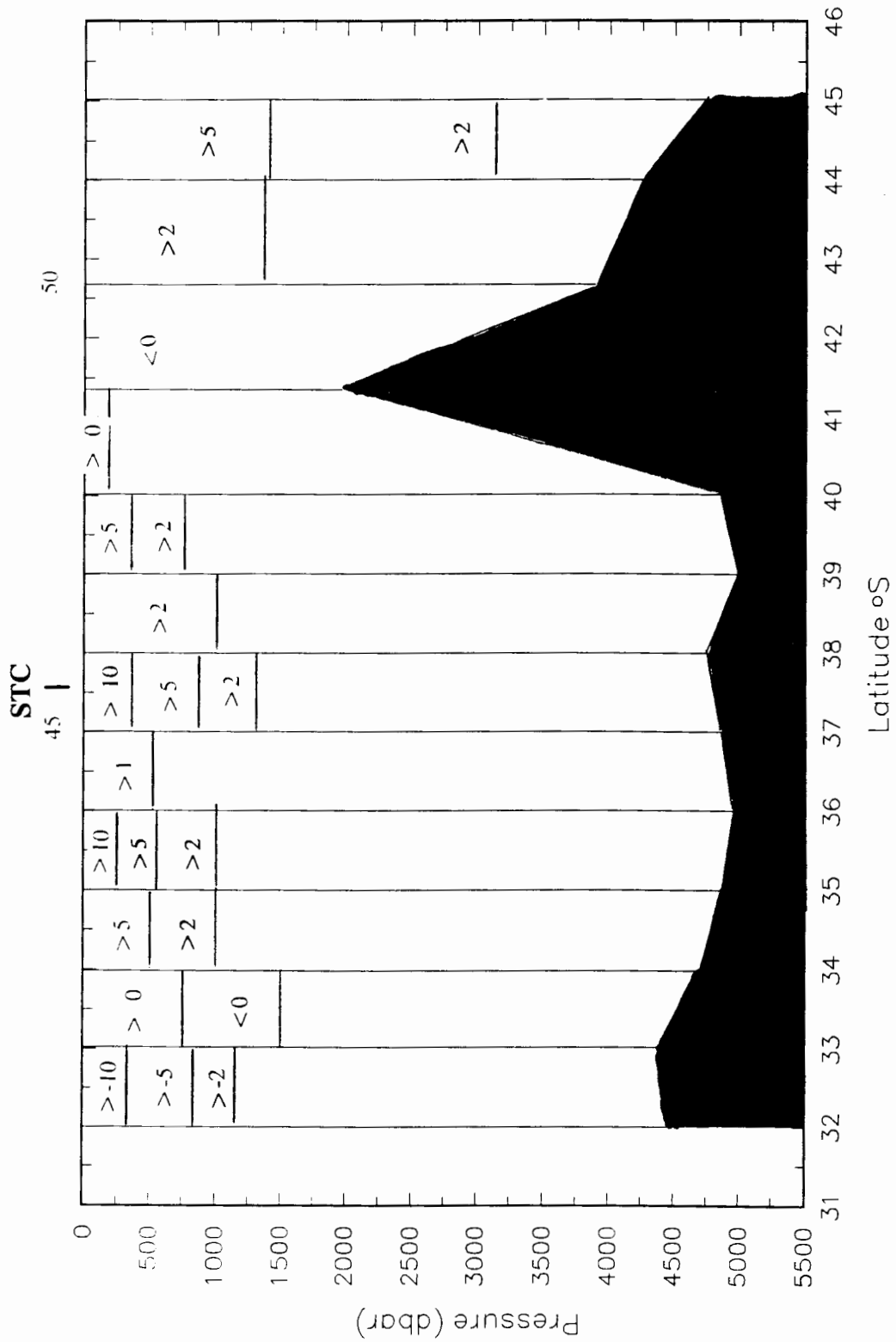


Figure 6.1: Geostrophic velocities calculated between station pairs with reference to the bottom, during *AJAX*.

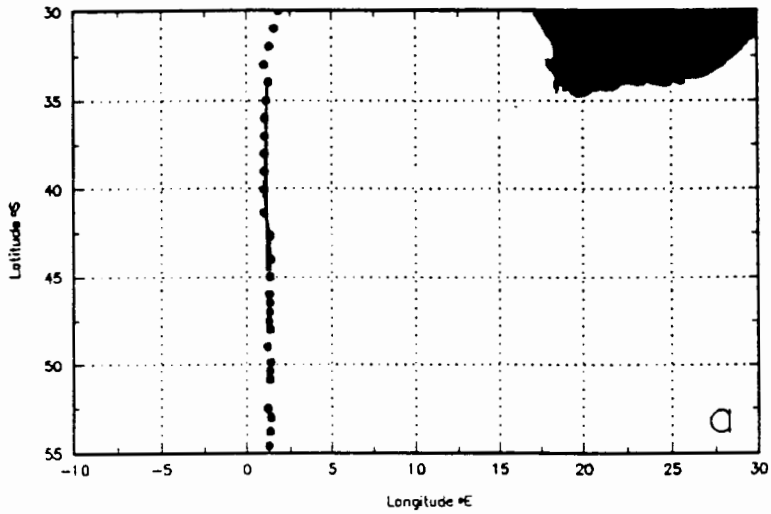


Surface geostrophic velocities (cm/s) referenced to the bottom

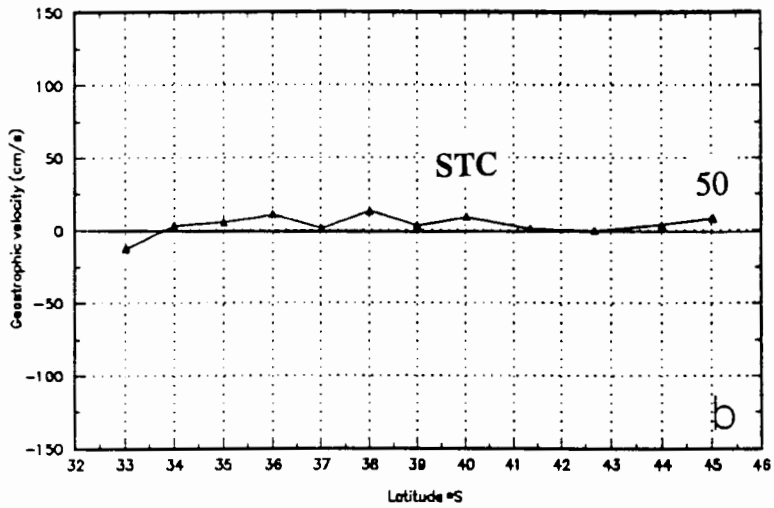


Volume transports (Sv) referenced to the bottom

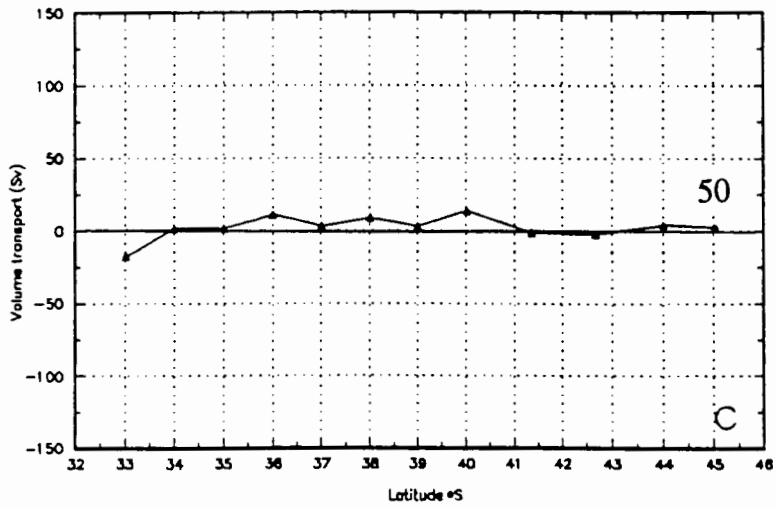


Figures 6.2a,b,c: The solid line in the upper panel (a) shows CTD stations 41 to 52 of *AJAX*. The calculated geostrophic velocities (b) and the volume transport (c) referenced to the bottom, between each station along the line. East coordinate is marked by + and west is marked by -.

*Volume Transport*

Volume transport (referenced to the bottom) associated with the STCZ between CTD station 44-48 is approximately 24 Sv (figure 6.2c).

## *ARC*

This cruise, described in more detail in **Data and Methodology**, chapter 4, was undertaken to investigate the chemical and physical oceanography and production potential in the Agulhas Retroflection Zone (Chapman et al. 1987). Station spacing is such that the geostrophic velocities and volume transport within the Agulhas Current and at three locations along the Agulhas Return Current CTD stations 47-39, 61-58 and 48-58 (mentioned in order of longitude east) can be compared to show modifications between the inflow and outflow and with distance east.

*The Agulhas Current*

The calculations show that maximum geostrophic velocity of 110 cm/s occurs between CTD stations 49-50 spanning the Agulhas inflow, as can be seen from figure 6.3 (vertical structure) and 6.4b (surface values). This compares favorably to drifter velocities ranging between 90-119 cm/s (Gründlingh 1978) as well as ADCP data, 100-130 cm/s in the upper 30 m, collected off Port Alfred (Rouault et al. 1995). Easterly surface velocities of 10 cm/s are measured at the southern boundary of the Agulhas Current, between CTD stations 50-51, but below 100 db the flow reverses producing a maximum westerly speed of 9 cm/s. This has also been noted by Gründlingh (1980) during direct current observations offshore Durban, where reverse shear was observed from the surface to the maximum flow near 100-200 m.

*Volume Transport*

Calculations (referenced to the bottom) yield a total of 61 Sv to the east between CTD stations 49-50 and CTD stations 50-51. However from the thermal sections in the previous chapter (**Geographic Location and General Hydrography of the Agulhas Return**

chapter 5) figures 5.8a and b, it can be seen that the Agulhas Current extends another 20 km landward of CTD station 49. Gordon et al. (1987) have extrapolated the transport function between CTD stations 49-50 and estimate a further 21 Sv, bringing the total volume transported by the Agulhas Current into the Retroflection to 70 Sv, a value approximately 14 Sv greater than *SCARC* (Rigg 1995). This difference is highlighted by Holford (1990) who does not regard the Agulhas Current as a steady stream with constant volume fluxes, but it must also be remembered that the cruises (*SCARC* and *ARC*) occurred during different months and over 5 years apart.

*The Agulhas Return Current*

***Transect 1: CTD stations 39-47***

This transect passes meridionally through the Retroflection (see Gordon et al. 1987) and is the first line (in order of longitude) occupied during *ARC* to traverse the Agulhas Return Current at 21°E, approximately 550 km downstream from the Agulhas Current inflow at CTD stations 49-50. The Agulhas Return Current exhibits a maximum geostrophic velocity of 75 cm/s between CTD stations 42-41, as shown by figures 6.3 and 6.4b. When compared to the inflow velocity of 110 cm/s it can be seen that a large deceleration of approximately 35 cm/s has occurred.

*Volume Transport*

Total volume transports over the Agulhas Return Current are 47 Sv between station pairs CTD stations 43-42 and CTD stations 42-41 (see figure 6.4c), 23 Sv less than the Agulhas inflow. These stations do not pass through the entire Agulhas Return Current, as can be seen from the hydrography figures 5.4 and 5.5a and b (chapter 5), but cross the south western boundary at the turning point of the Retroflection/Agulhas Return Current (see Gordon et al. 1987) and therefore the volume transport is under estimated.

*Transect 2: CTD stations 58-61*

These stations are carried out as part of a long zonal transect (stations 80-58) through the Retroflection and Agulhas Return Current. Between CTD stations 60-59 the Agulhas Return Current is traversed and a maximum surface velocity of 98 cm/s is encountered, see figures 6.5 and 6.6b. This value appears to be high in comparison to the previous result of 75,4 cm/s, nearly 300 km downstream, and may be due to wide spacing 129 km, between CTD stations 60-59 and therefore the possibility of the transect extending over the STC. This would result in a significant contribution in the overall easterly speeds obtained. Surface geostrophic velocities over the STC have been calculated by Gordon et al. (1987) to be 17 cm/s between CTD stations 56-57 at ~25°E and therefore, assuming this value to hold true at this transect corrected velocities for the Agulhas Return Current are 81 cm/s.

Comparing this velocity to those associated with the Agulhas Current it can be seen that there has been a 29 cm/s deceleration in flow between the Agulhas inflow (CTD stations 49-50) and CTD stations 60-59, approximately 850 km downstream.

*Volume Transport*

The volume transport of the Agulhas Return Current between CTD 60-59 is 84 Sv as can be seen from figure 6.6c. This large value is possibly an over estimation as station spacing is wide, as mentioned previously, it is possible that a significant eastward contribution from the STC occurs. Gordon et al. (1987) have calculated the STC volume transport to be 11,5 Sv between CTD stations 56-57, correcting the Agulhas Return Current value by this produces a volume transport of 72,5 Sv. This is still considerably high, Gordon et al. (1987) estimates the transport of the Agulhas Return Current to be in the region of 60 Sv.

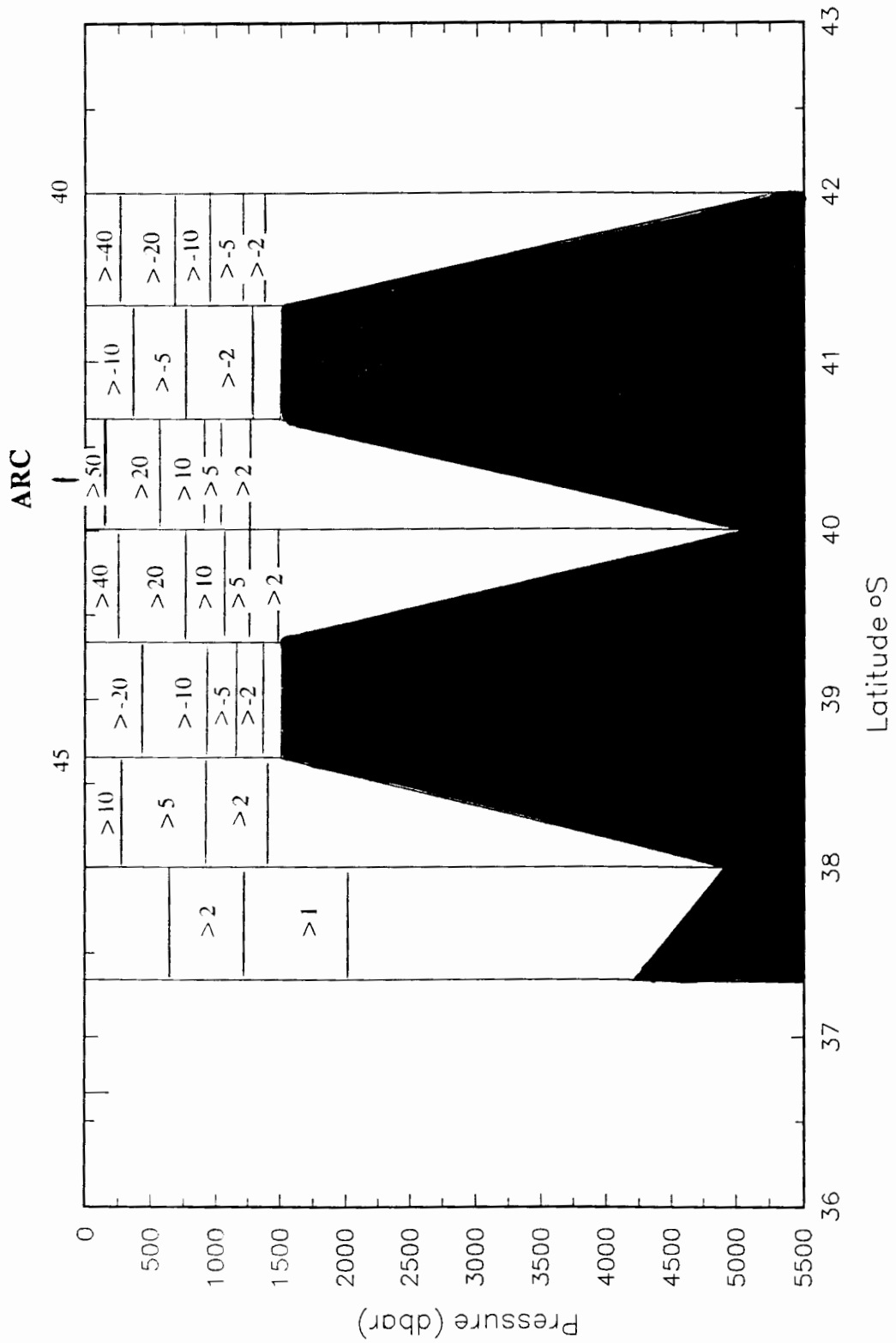


Figure 6.3 ***ARC* Transect 1:** Geostrophic velocities calculated between CTD stations 39-47 with reference to the bottom.

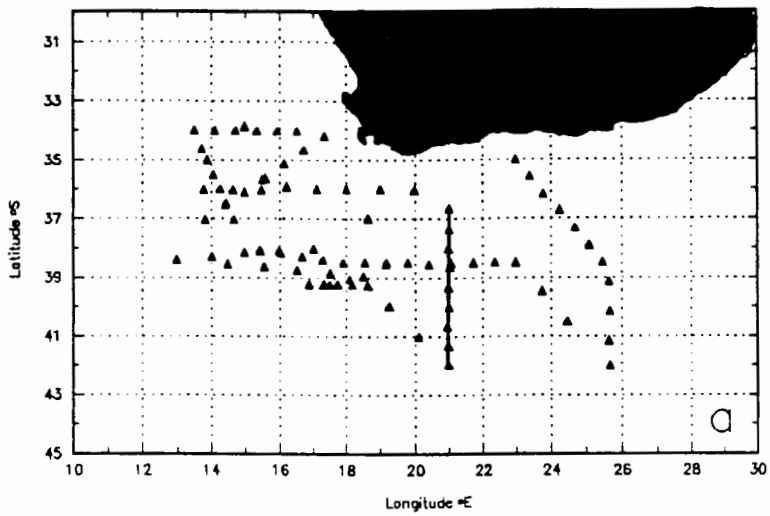


Surface geostrophic velocities (cm/s) referenced to the bottom

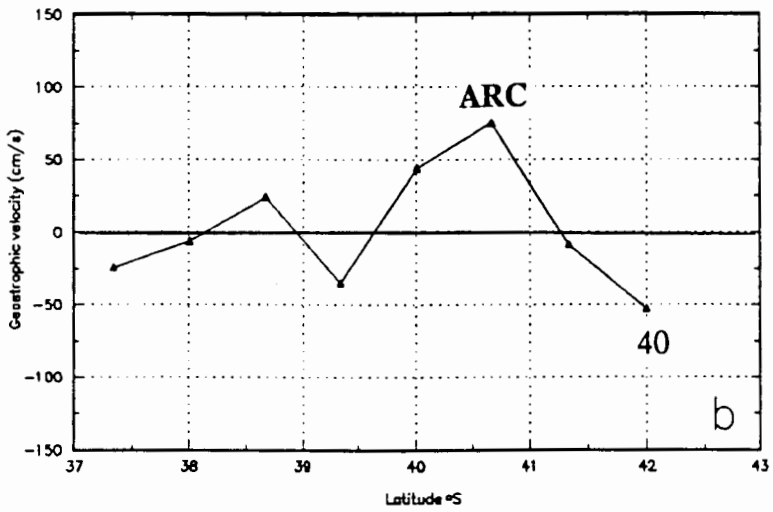


Volume transports (Sv) referenced to the bottom

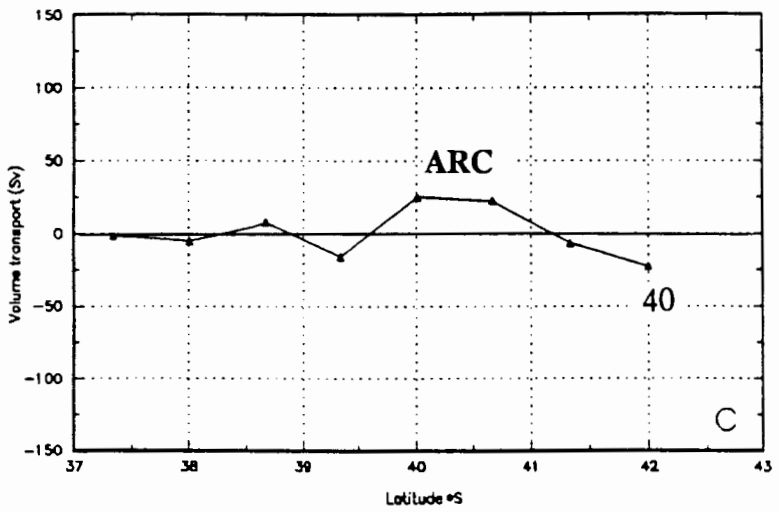


Figures 6.4a,b,c: The solid line in the upper panel (a) shows CTD stations 39 to 47 of *ARC*. The calculated geostrophic velocities (b) and the volume transport (c) referenced to the bottom, between each station along the line. East co-ordinate is marked by + and west is marked by -.

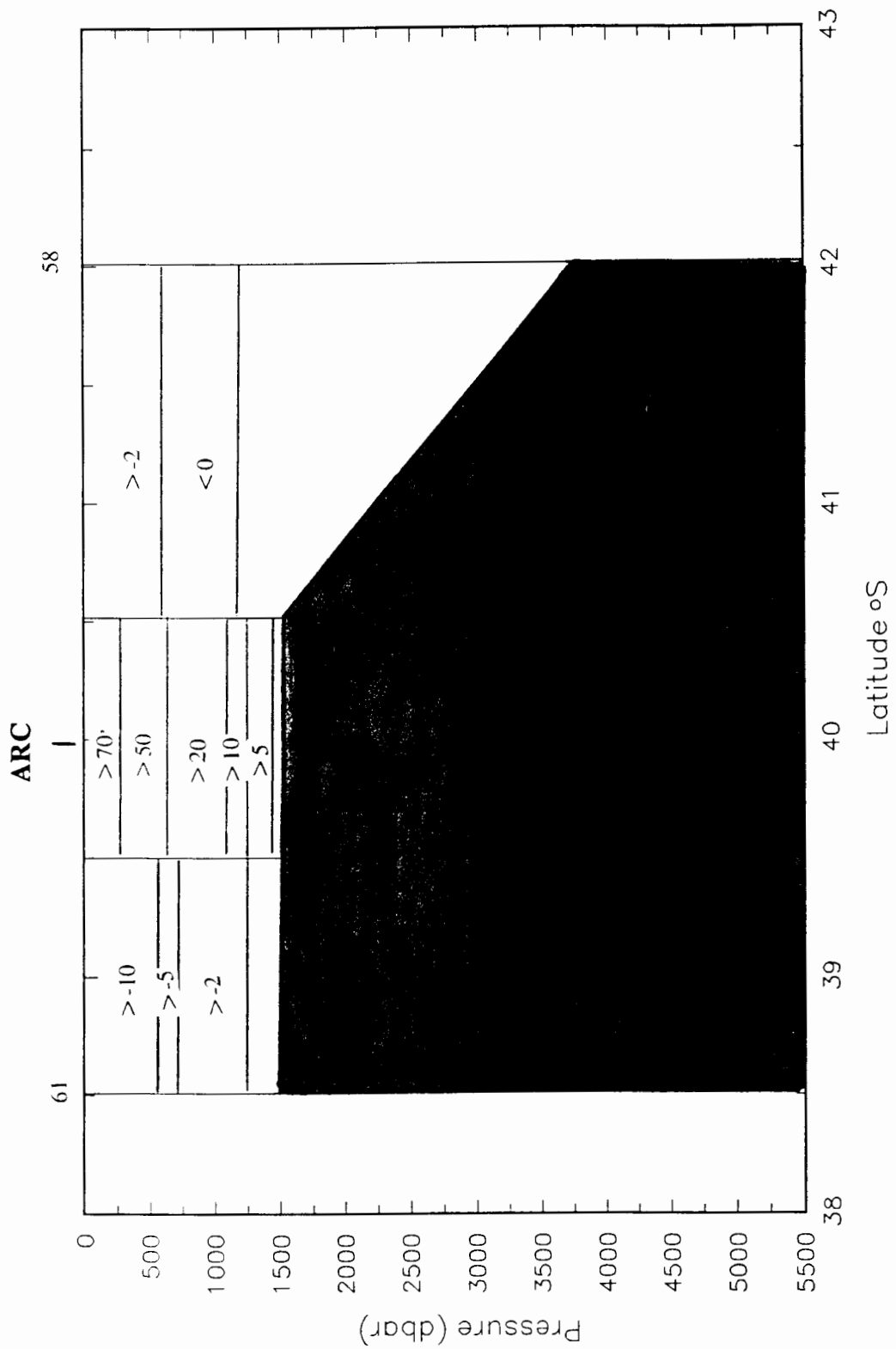


Figure 6.5 ***ARC* Transect 2:** Geostrophic velocities calculated between CTD stations 58-61 with reference to the bottom.

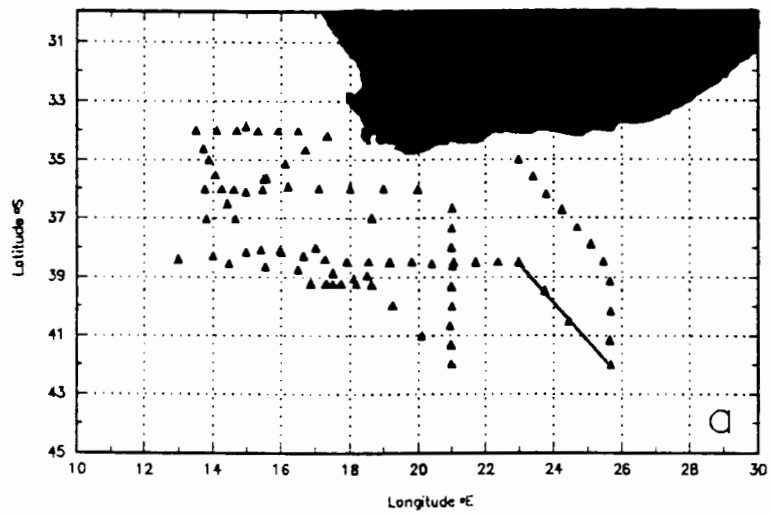


Surface geostrophic velocities (cm/s) referenced to the bottom

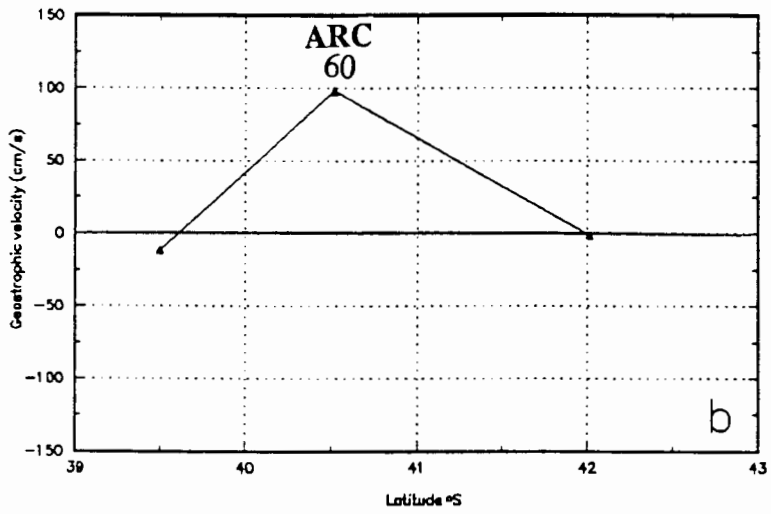


Volume transports (Sv) referenced to the bottom

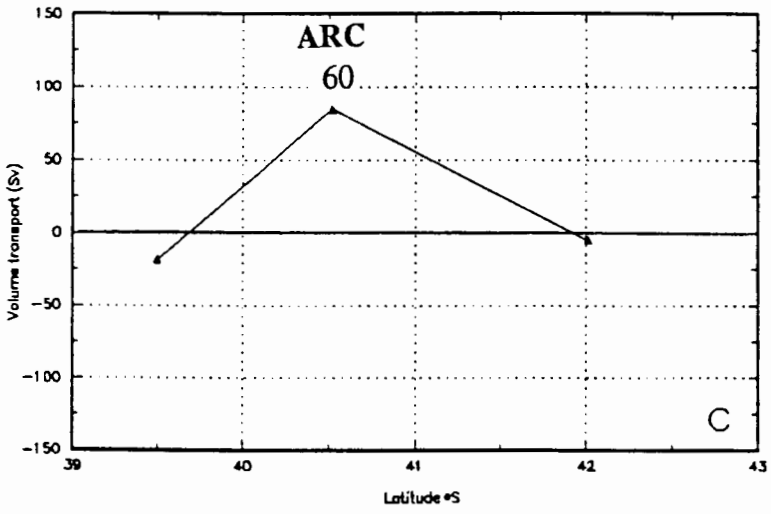


Figures 6.6a,b,c: The solid line in the upper panel (a) shows CTD stations 58 to 61 of *ARC*. The calculated geostrophic velocities (b) and the volume transport (c) referenced to the bottom, between each station along the line. East co-ordinate is marked by + and west is marked by -.

*Transect 3: Stations 48-58*

During this transect, as can be clearly seen by the hydrographic sections 5.8a and b in the previous chapter (chapter 5), the Agulhas Return Current is traversed three times as it becomes deflected around the Agulhas Plateau, forming an S-shaped meander. The geostrophic velocities of the Agulhas Return Current are discussed in order downstream.

Of great interest is the reversal in flow between the two CTD station pairs CTD stations 54-56 and CTD stations 51-53 caused by the Agulhas Return Current executing a sharp anti-cyclonic turn during it's initial encounter with the Agulhas Plateau. The first traverse of the current occurs between CTD stations 56-54 see figures 6.7 (vertical structure) and 6.8b (surface values), surface velocities calculated are 56 cm/s (east) between CTD stations 55-56, a deceleration of 54 cm/s from the Agulhas inflow and 87 cm/s (west) between CTD stations 54-55, a deceleration of 23 cm/s from the inflow. The higher surface geostrophic velocity calculated between CTD stations 54-55 may be caused by a velocity contribution from the cyclonic eddy formed as a result of the planetary wave over the Agulhas Plateau, a topographic feature shown by Lutjeharms and Valentine (1988) to be an area of particularly potent eddy generation.

After the initial deflection between CTD stations 54-56, the Agulhas Return Current flows along the western edge of the AgulhasPlateau before turning east on the northern flank at CTD stations 51-52 and CTD stations 52-53. Geostrophic velocities between these two CTD pairs are between 73 cm/s and 74 cm/s, a deceleration of 37 cm/s and 36 cm/s from the Agulhas Current inflow between CTD 49-50.

*Volume Transport*

Volume transports over the Agulhas Return Current are 63 Sv between CTD stations 56-54 and CTD stations 54-53 and 60 Sv between CTD stations 51-53, see figure 6.8c. This results in a mismatch of between 7 and 10 Sv between the Agulhas Current inflow (70 Sv) and the outflow.

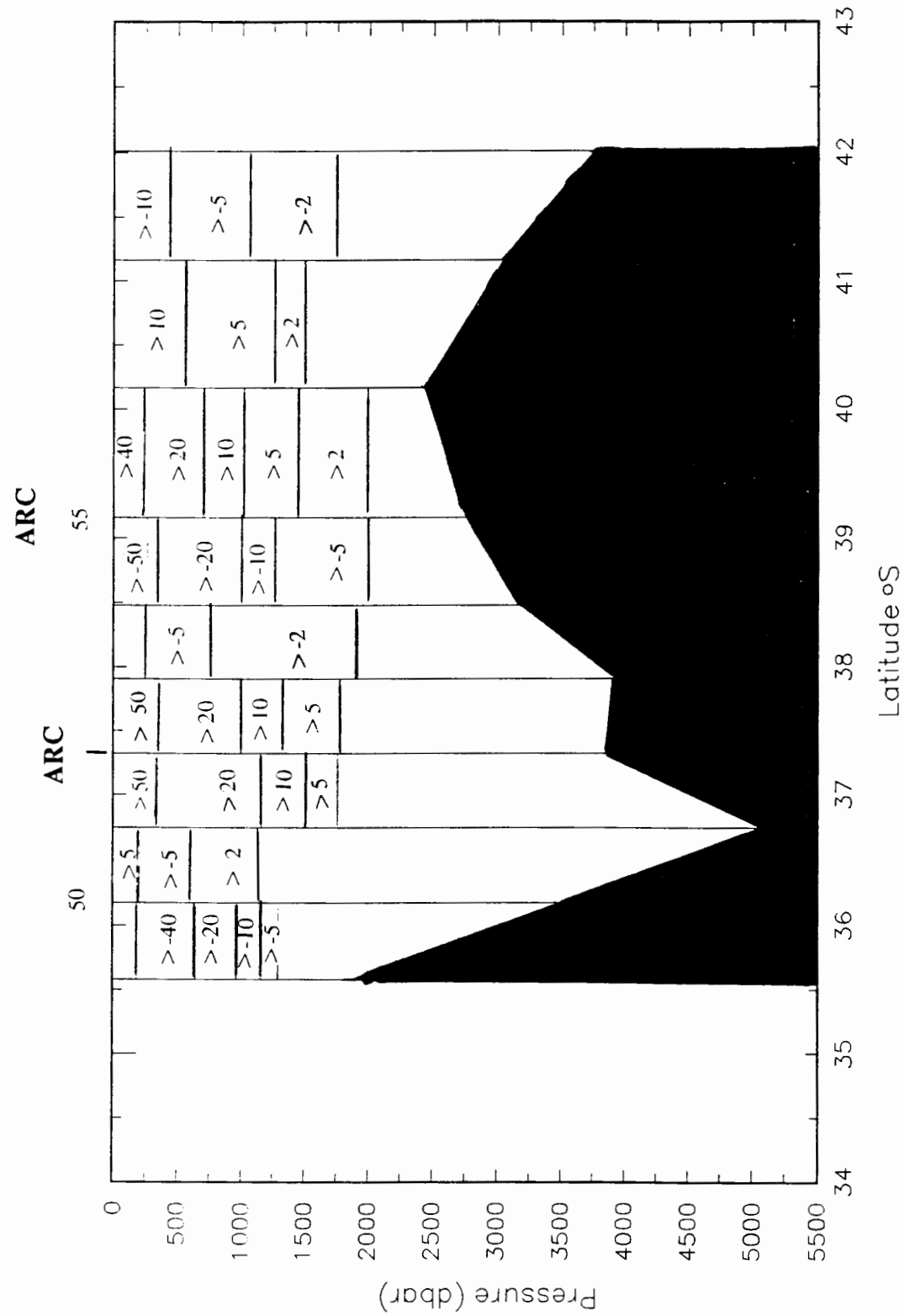


Figure 6.7 ***ARC* Transect 3:** Geostrophic velocities calculated between CTD stations 48-58 with reference to the bottom.

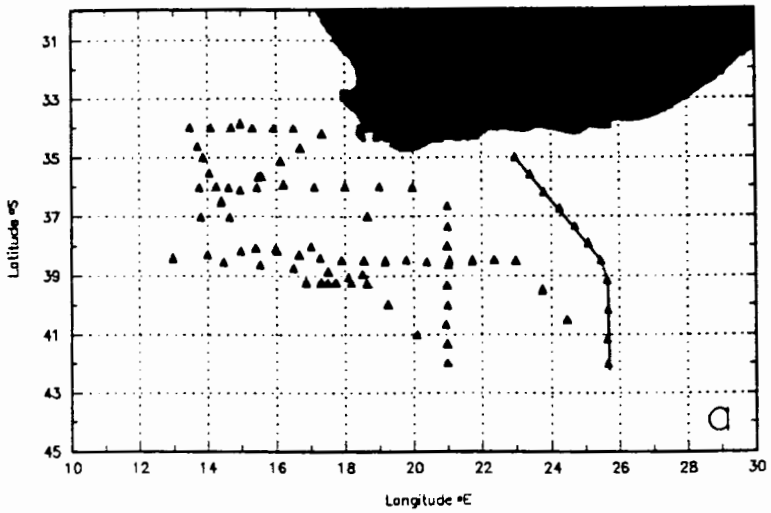


Surface geostrophic velocities (cm/s) referenced to the bottom

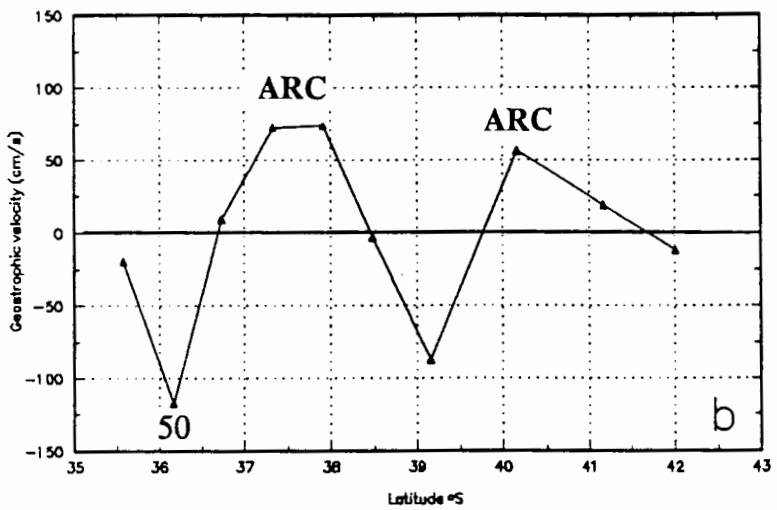


Volume transports (Sv) referenced to the bottom

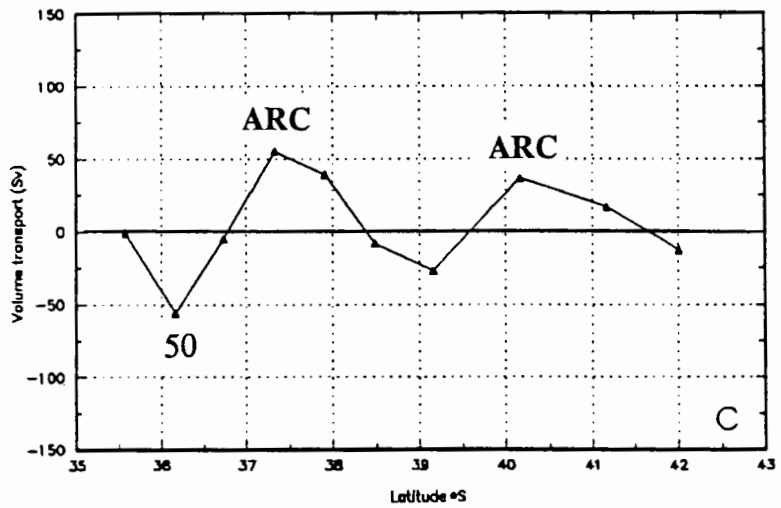


Figures 6.8a,b,c: The solid line in the upper panel (a) shows CTD stations 48 to 58 of *ARC*. The calculated geostrophic velocities (b) and the volume transport (c) referenced to the bottom, between each station along the line. East co-ordinate is marked by + and west is marked by -.

The imbalance can possibly be attributed to a loss of 10 Sv which splits from the retroflection and continues west into the Atlantic Ocean, where it contributes two thirds to the Cape Town Eddy (Gordon et al. 1987).

*MARATHON*

The Marathon cruise was carried out to provide more information into the overall transport of the Retroflection region (see **Data and Methodology**, chapter 4). During this cruise four transects of the Agulhas current and two of the Agulhas Return Current were made. All six transects are nearly perpendicular (90 $\pm$20°) to the axis of the flow. A continuous survey was also carried out in which the intersection between the 15°C isotherm and the 200 m depth were followed.

During the survey the Agulhas Current appeared to form a double retroflection with branches at 26°E and 17°E. A phenomenon previously observed by Lutjeharms and Van Ballegooyen (1988a), in which eleven years of satellite imagery and the drift of a buoy were scrutinized. Their findings showed that 2 to 3 times per year a total retroflection, lasting between 3 to 6 weeks, occurred at approximately 25°E. It is believed that this is induced by large meanders in the Agulhas Current, known as "Natal Pulses" (Lutjeharms and Connell 1989) which progress downstream, while the Agulhas Return Current, forced to lie landward of it's mean position, as a result of topographical steering, causes a high horizontal shear between it and the meander, resulting in it's amalgamation and a partial upstream retroflection (Bennett 1988).

During this passage several meanders occurred however it must be noted that the drifter was shown to flow over the central Agulhas Plateau and only execute a meander further to the east.

*The Agulhas Current*

The Agulhas Current can be identified from the hydrographic sections seen in the previous chapter (chapter 5) figures 5.12a and b, between CTD stations 277-272 with maximum geostrophic velocities of 181 cm/s between CTD stations 277-276, see figures 6.11 (vertical structure) and 6.12b (surface values).

*Volume Transport*

Total volume transport of the Agulhas Current (CTD stations 277-272) is 99 Sv, see figure 6.12c.

*The Agulhas Return Current*

***Transect 1: Stations 253-256 and 284-290***

During this transect maximum geostrophic velocities of 66 cm/s to the east between CTD stations 287-286 were encountered. To the north between CTD 289-287, there is a reversal in flow with a maximum 58 cm/s (west), see figure 6.9 (vertical structure) and 6.10b (surface values). This flow constitutes the secondary southward flowing retroflection branch at 24°E and it's cause has been discussed previously (Lutjeharms and Van Ballegooyen 1988b). A free inertial jet model was used by Lutjeharms and Van Ballegooyen (1984) to simulate the southern Agulhas Current and the effects varying surface and bottom velocities and velocity profile have on the flow. It was found that with varying velocity profiles the vertical velocity shear decreased resulting in an increased volume and momentum transport and consequently a reduced westward penetration of the Agulhas Current. This would result in an early retroflection at approximately 24°E, more or less the same longitude as between CTD stations 290-284. The Agulhas Return Current appears to flow through the heart of the Agulhas Plateau as a result of the double retroflection, unlike in the *ARC* dataset where the current executes an S-shaped meander around the plateau.

Between CTD stations 260-253 the transect crosses the southern boundary of a cold core ring centered near 38°S and 24°E on the northwest flank of the Agulhas Plateau. The ring is clearly seen in temperature charts 5.11a and b in the previous chapter (chapter 5). It is believed by Bennett (1988) to have been previously spawned as a result of instabilities set up in a meander in the Agulhas Return Current over the Agulhas Plateau.

*Volume Transport*

Volume Transports (referenced to the bottom) associated with the Agulhas Return Current are 43 Sv between CTD stations 288-284, see figure 6.10c. This relatively low value when compared to previous cruises is due to the Agulhas Return Current being formed from the weaker secondary retroflection loop. CTD stations 290-288 which span the retroflection branch exhibits a volume transport of 44 Sv this is comparable to the Agulhas Return Current transport along this section.

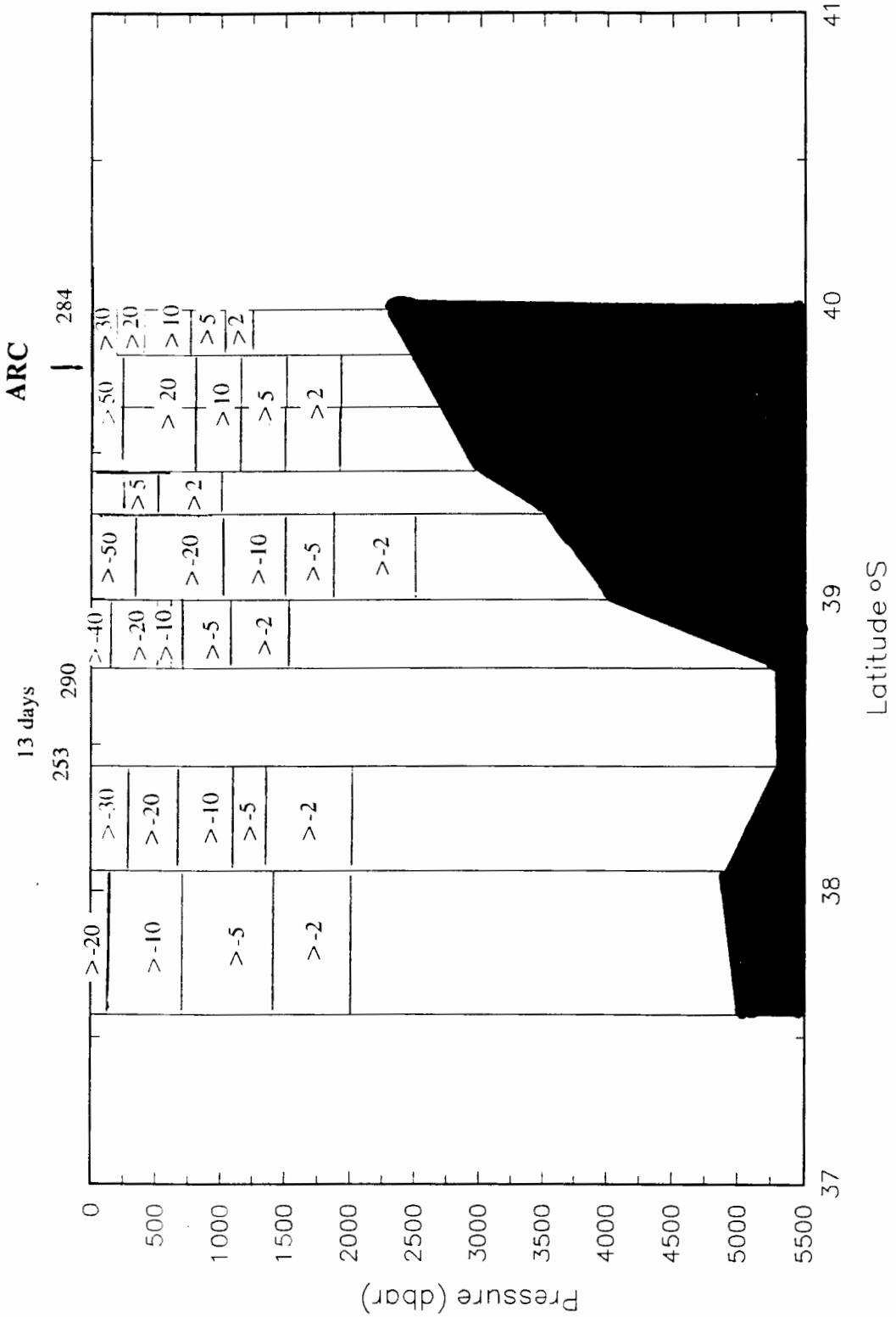


Figure 6.9 ***Marathon*** **Transect 1:** Geostrophic velocities calculated between CTD stations 253-256 and 284-290 with reference to to the bottom.

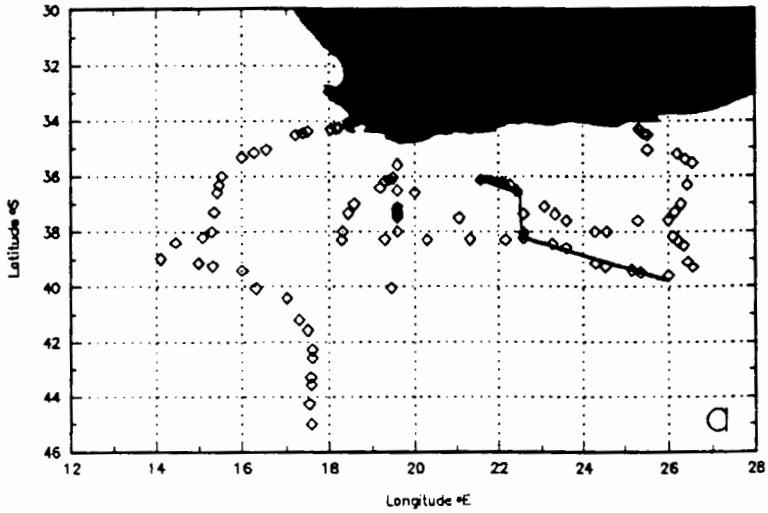


Surface geostrophic velocities (cm/s) referenced to the bottom

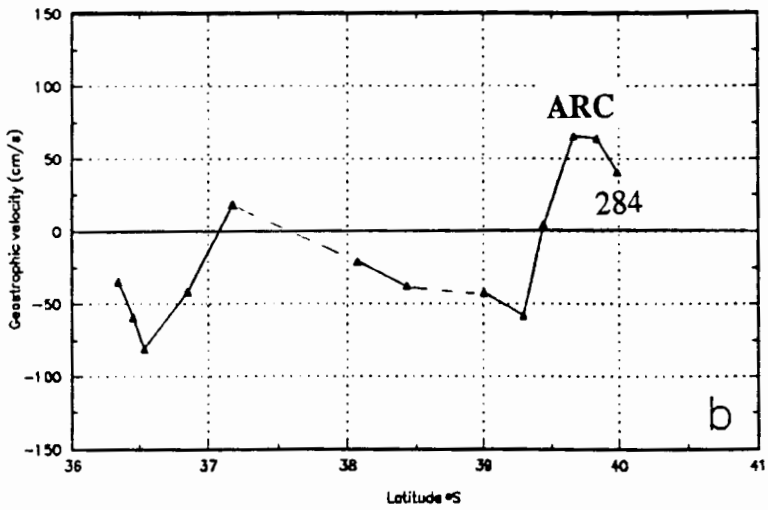


Volume transports (Sv) referenced to the bottom

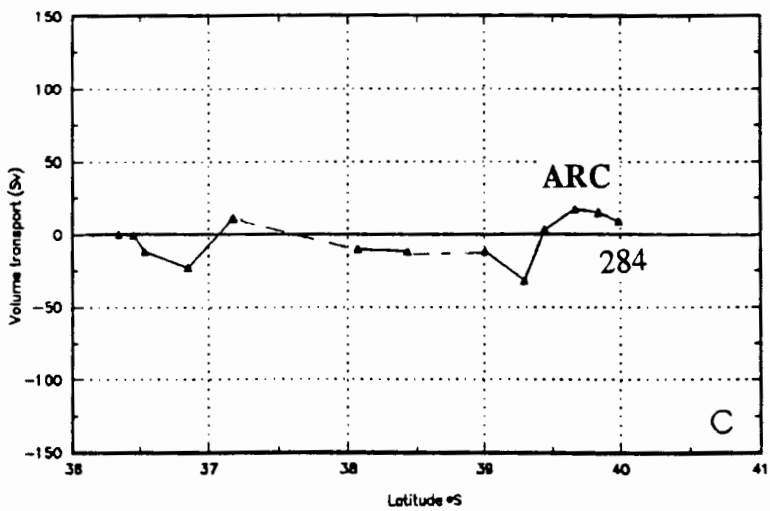


Figures 6.10a,b,c: The solid line in the upper panel (a) shows CTD stations 253 to 256 and 284 to 290 of *Marathon*. The calculated geostrophic velocities (b) and the volume transport (c) referenced to the bottom, between each station along the line. East co-ordinate is marked by + and west is marked by -. Dashed lines represent large time gaps (days) between stations.

*Transect 2: Stations 277-283*

As shown from the hydrographic sections, figures 5.12a and b, in the previous chapter, this transect crosses the Agulhas Return Current further upstream at approximately 26°E. High geostrophic velocities of 128 cm/s are encountered between CTD stations 280-281, see figures 6.11 (vertical structure) and 6.12b (surface values), these values appear to be exceptionally high in comparison to the previous section upstream. The reason for this is because it is approximately 1 1/2 times larger than section 290-284.

*Volume Transports*

Volume transport between CTD stations 280-282 is 49 Sv, see figure 6.12c.

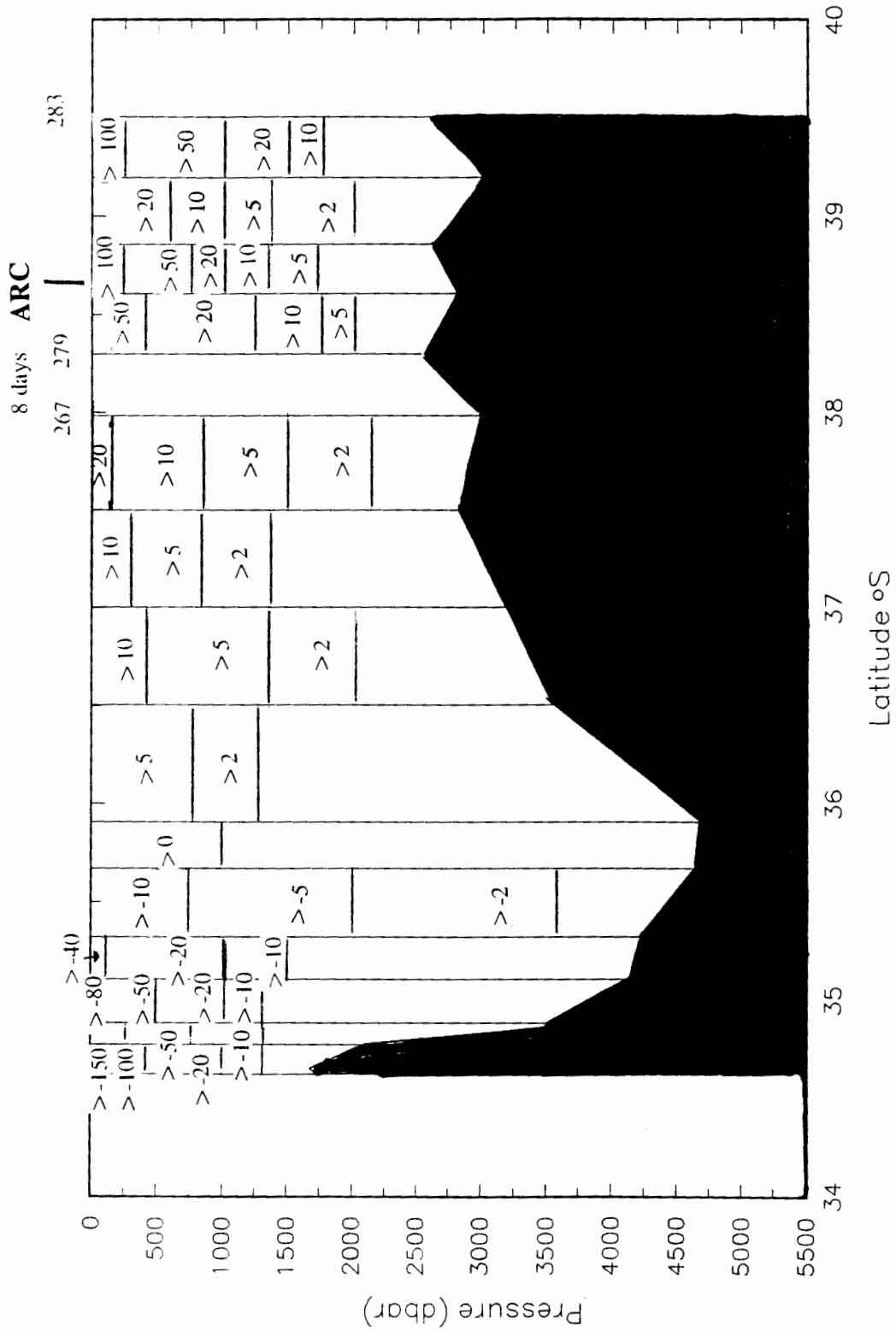


Figure 6.11 ***Marathon*** **Transect 2:** Geostrophic velocities calculated between CTD stations 277-283 with reference to to the bottom.

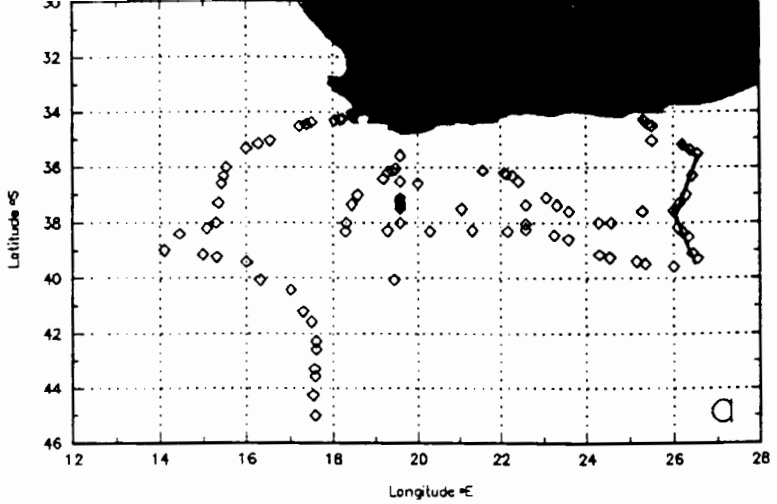


Surface geostrophic velocities (cm/s) referenced to the bottom

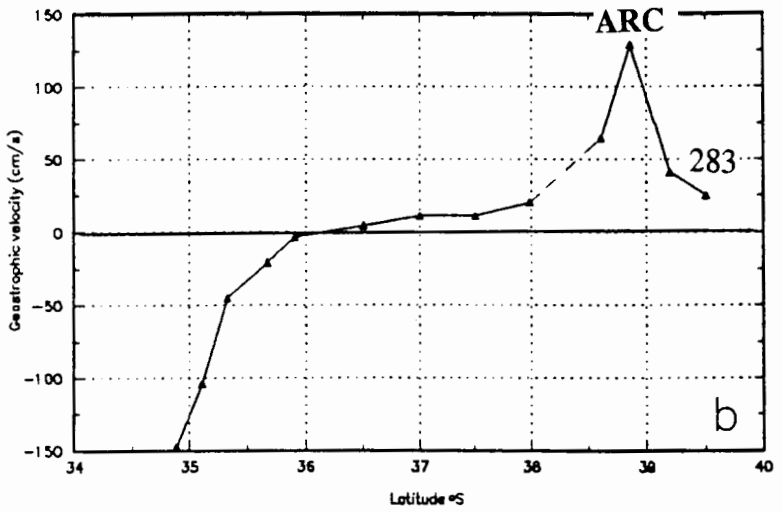


Volume transports (Sv) referenced to the bottom

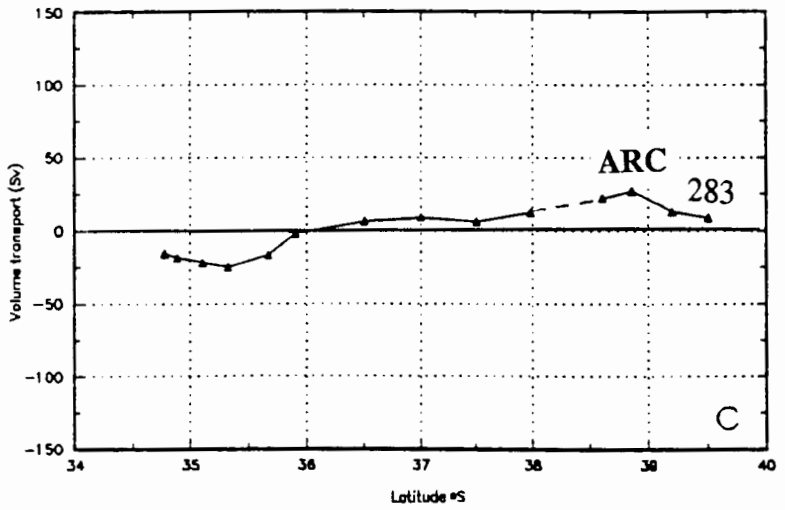


Figures 6.12a,b,c: The solid line in the upper panel (a) shows CTD stations 277-283 of *Marathon*. The calculated geostrophic velocities (b) and the volume transport (c) referenced to the bottom, between each station along the line. East co-ordinate is marked by + and west is marked by -. Dashed lines represent large time gaps (days) between stations.

*DISCOVERY 164*

During a single transect of the *Discovery 164* cruise, the Agulhas Return Current and it's associated front (AF) was identified as a separate front. This is the first time that a double front has been identified so far east and contradicts views held by Lutjeharms and Valentine (1984) that the AF exists only between 13,30'°E and 25°E.

Maximum geostrophic velocities calculated over the Agulhas Return Current are 82 cm/s between CTD stations 17-18 (referenced to the bottom), see figures 6.13 and 6.14b. These results compare well to the 73 cm/s velocities obtained at 39°E by a drifter deployed during the *Marathon* cruise and to the 84 cm/s velocity recorded by a drifting buoy, in the vicinity of the Madagascar Ridge (Gründlingh 1978).

Read and Pollard speculate the presence of an eddy centered at 42°E is due to it's downstream propagation from the Retroflection zone, over 1 700 km west. Although this explanation is feasible it is also possible for the eddy to have formed as a result of topographical influences in the vicinity of the South West Indian Ridge. This would be consistent with results obtained by Daniault and Ménard (1985), who have been able to show from Seasat altimetry data that maximum eddy generation is correlated with major ridges and plateaus.

The STC, as seen from previous figures 5.18a and b (in **Geographic Location and General Hydrography of the Agulhas Return Current**, chapter 5), lies between CTD stations 21-24 and has a maximum speed of 29 cm/s (figures 6.13 and 6.14b), this compares well with drifter velocities of 26 cm/s obtained by Hoffman (1985).


Figure 6.13 ***Discovery 164***: Geostrophic velocities over the frontal zone between CTD stations 14-26 with reference to the bottom.

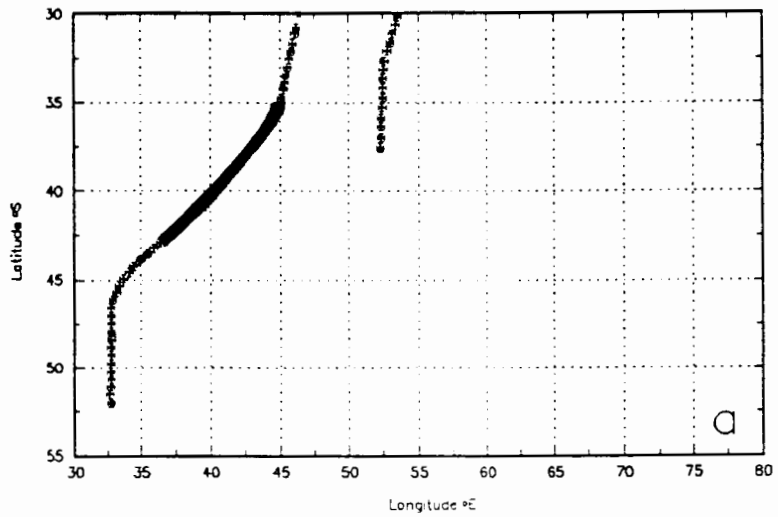


Surface geostrophic velocities (cm/s) referenced to the bottom

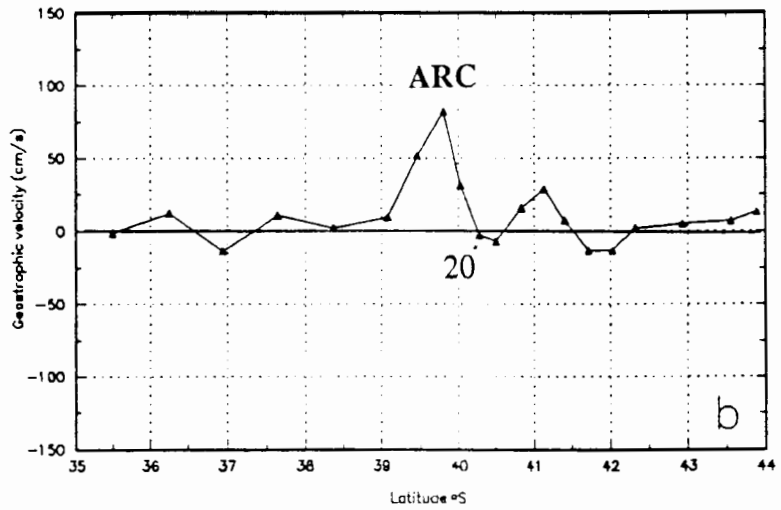


Volume transports (Sv) referenced to the bottom

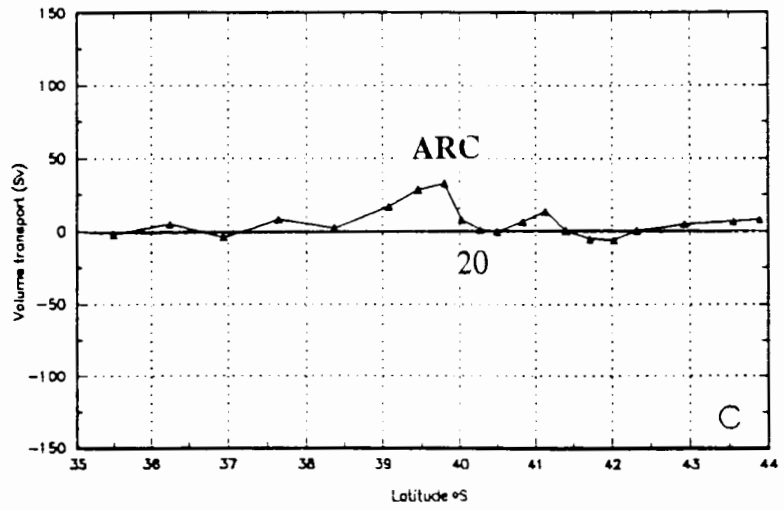


Figures 6.14a,b,c: The solid line in the upper panel (a) shows CTD stations 10 to 30 of *Discovery 164*. The calculated geostrophic velocities (b) and the volume transport (c) referenced to the bottom, between each station along the line. East co-ordinate is marked by + and west is marked by -.

*Volume Transport*

The hydrographic sections, figures 5.18a and b, discussed in the previous chapter (chapter 5) show the Agulhas Return Current to lie between CTD stations 17-19. Volume transports between these stations is 69 Sv (figures 6.13 and 6.14c).

Centered at 42°S CTD station 26 (CTD stations 25-27) is an anti-cyclonic eddy with a volume flux transport of 10 Sv (referenced to the bottom). The STC is situated between CTD stations 21-24 and has a volume transport of 20 Sv.

*SUZIL*

In order to study the frontal structure, water masses and transport associated with the Antarctic Circumpolar Current, a survey grid consisting of four near meridional sections between 51°E-80°E and a single zonal section at 38°E were carried out (see **Data and Methodology**, chapter 4) (Park et al. 1993).

*Transect 1: Stations 1-14*

During this section the Agulhas Return Current is shown to have merged with the STC and SAF as a result of the Antarctic Circumpolar Current's equatorward deflection around the Crozet Plateau, to form a strong frontal zone marking a sharp transition between subtropical and subantarctic waters, (see figures 5.22a and b of chapter 5) (Park et al 1993). However this confluence of the Agulhas Front, the southern boundary of the Agulhas Return Current, with the STC and SAF is believed by Belkin and Gordon (1994) to be transient, as the front was repeatedly observed separately from hydrographic data obtained during *Geroevka Cruise #6*. This front combining the AF/STC/SAF is referred by Belkin and Gordon (1994) as the *"Crozet Front"* due to it's location in the Crozet Basin and is believed to be one of the strongest fronts in the world ocean (Belkin 1988b, 1989 a,b).

The frontal zone exists between CTD stations 7-10 with speeds ranging from 41 cm/s-89 cm/s (referenced to the bottom) (figures 6.15 and 6.16b) between the northern and southern boundaries. The maximum geostrophic velocities between CTD stations 7-8 at approximately 52°45'E is 89 cm/s and is associated with the Agulhas Return Current and it's Front.

North of the frontal zone alternating east between CTD stations 2-3 (15-21 cm/s) and west between CTD 1-2 (14 cm/s) are a result of meandering or eddy activity (Park et al 1993). These observations are comparable to energetic meanders and eddies commonly observed in the central Crozet Basin, from satellite tracked surface buoys (Projet MARISONDE 1979, Daniault 1984), satellite altimetry-derived sea level variability (Cheney et al. 1983 and Daniault and Ménard 1985) and a number of historical hydrographic sections (Gambéroni et al. 1982, Park et al. 1989, 1991). Planetary waves generated by the flow over the shallow Southwest Indian Ridge seem to be responsible for the frequent occurrence of these mesoscale features (Daniault 1984, Park and Saint-Guily 1992). It is highly feasible that these alternating flows are meandering branches of the Agulhas Return Current being peeled off, resulting in the current's gradual weakening..

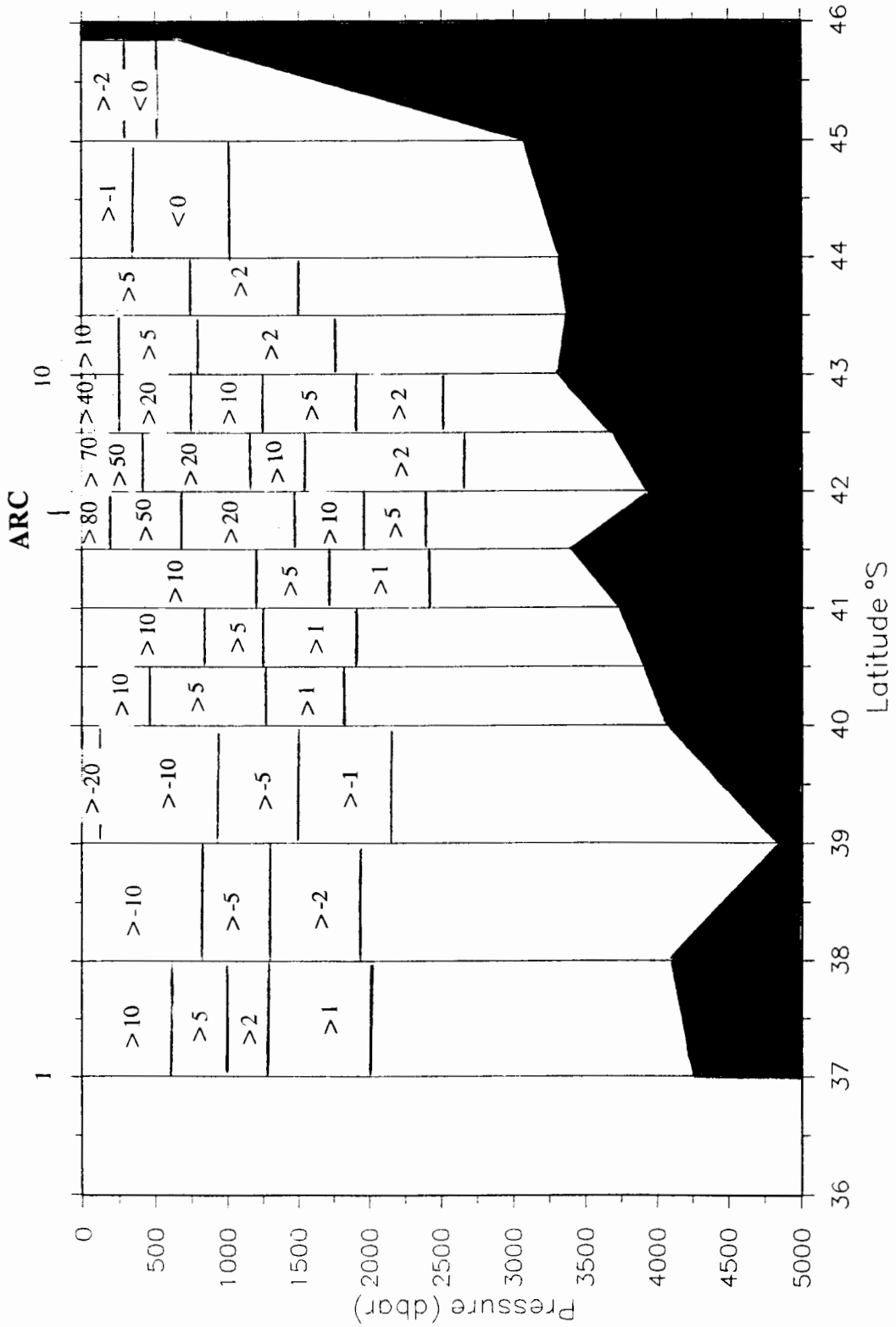


Figure 6.15 ***SUZIL* Transect 1:** Geostrophic velocities calculated between CTD stations 1-14 with reference to the bottom.

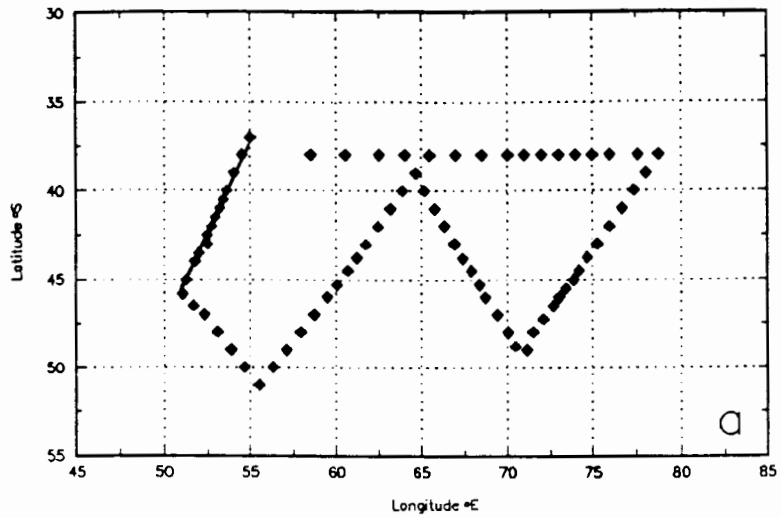


Surface geostrophic velocities (cm/s) referenced to the bottom

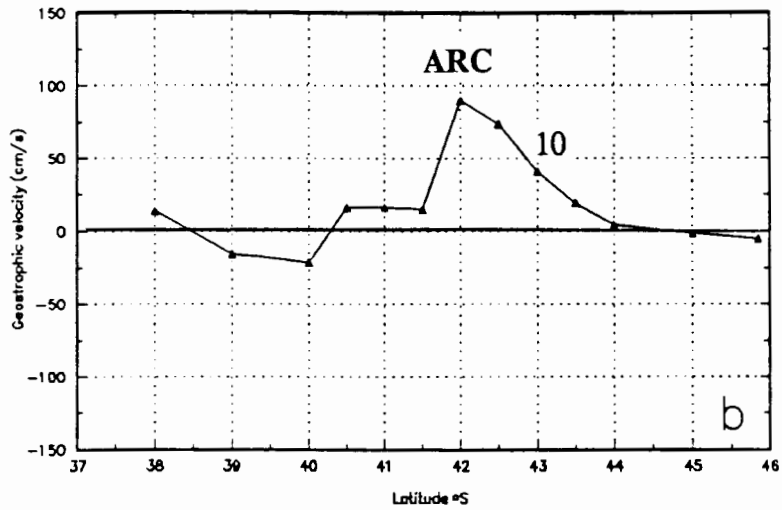


Volume transports (Sv) referenced to the bottom

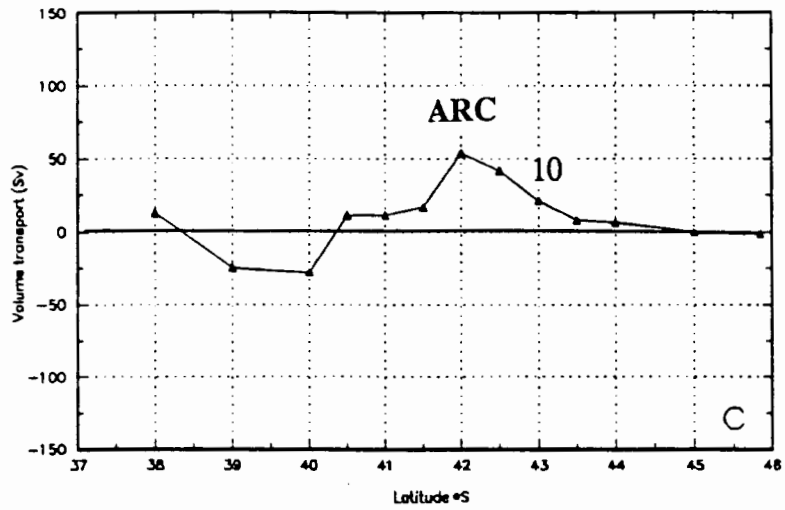


Figures 6.16a,b,c: The solid line in the upper panel (a) shows CTD stations 1 to 14 of *SUZIL*. The calculated geostrophic velocities (b) and the volume transport (c) referenced to the bottom, between each station along the line. East co-ordinate is marked by + and west is marked by -.

*Volume Transport*

Total volume transport over the frontal zone between CTD stations 7-10 is 68 Sv (figure 6.16c), with a volume transport of 53 Sv associated with the Agulhas Return Current. Comparison with the dataset of the *Discovery 164*, it can be seen that there has been a large reduction of 16 Sv in the volume transported by the Agulhas Return Current further upstream. This is possibly due to northward recirculation branches generally weakening the flow and compares with findings by Stramma and Lutjeharms (1995) of approximately 20 Sv which recirculated when crossing the Southwest Indian Ridge located 46°S 50°E, just northwest of the Crozet Islands.

***Transect 2: Stations 22-32***

Geostrophic surface velocity of 57 cm/s (figures 6.17 and 6.18b) is found at the northern boundary of the frontal zone between CTD stations 27-26 and represents the Agulhas Front. There is a sharp reduction in geostrophic speed of 32 cm/s between the previous transect. The AF continues to be merged with the STC and SAF forming a broad (>200 km) frontal zone between CTD stations 27-25. Surface speeds over the frontal zone range between 46 cm/s-57 cm/s (referenced to the bottom).

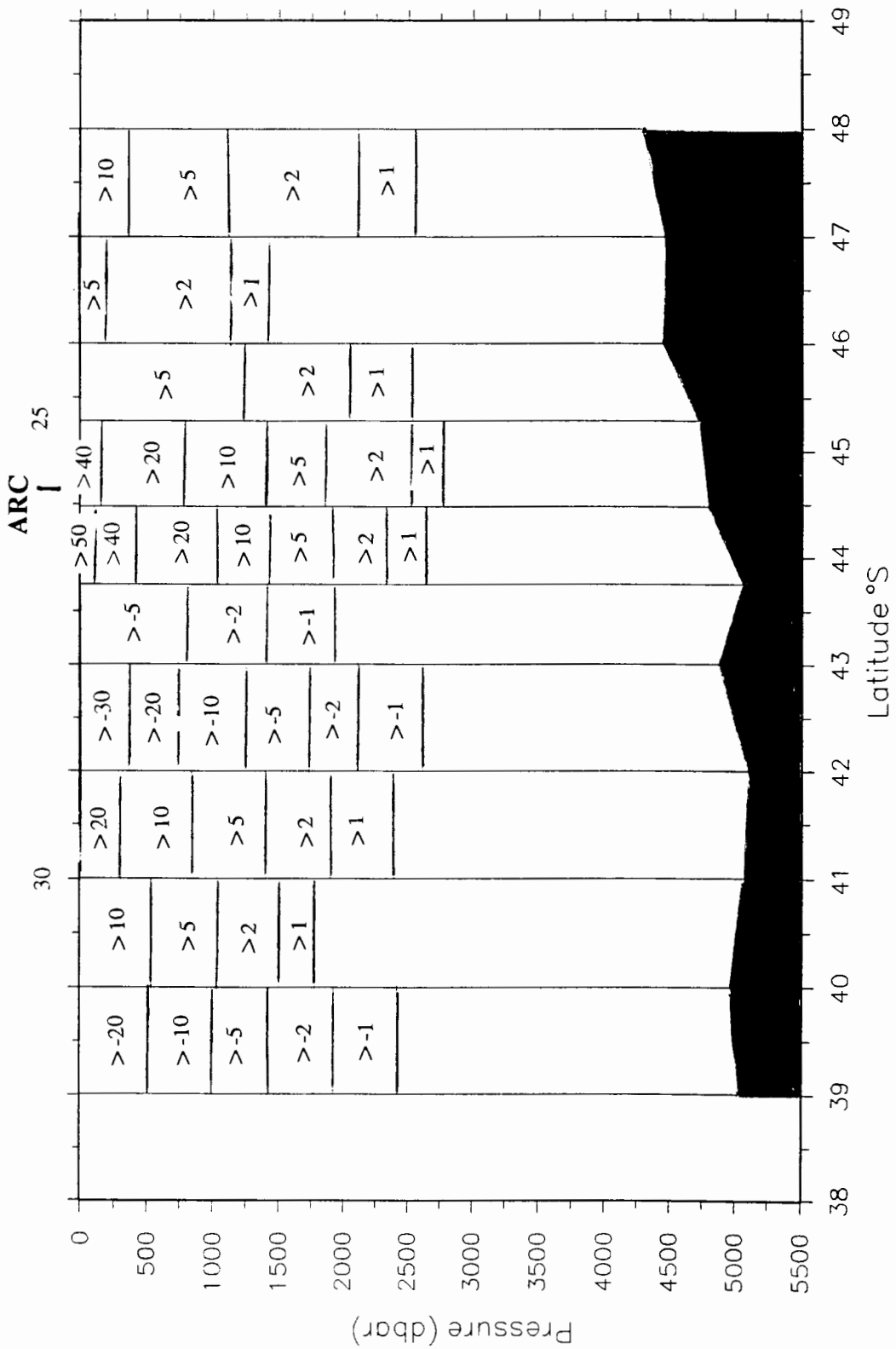


Figure 6.17 ***SUZIL* Transect 2:** Geostrophic velocities calculated between CTD stations 22-32 with reference to the bottom.

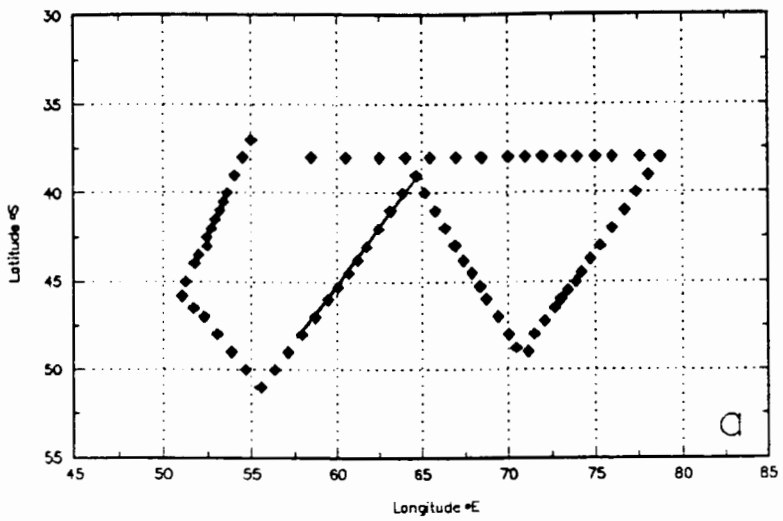


Surface geostrophic velocities (cm/s) referenced to the bottom

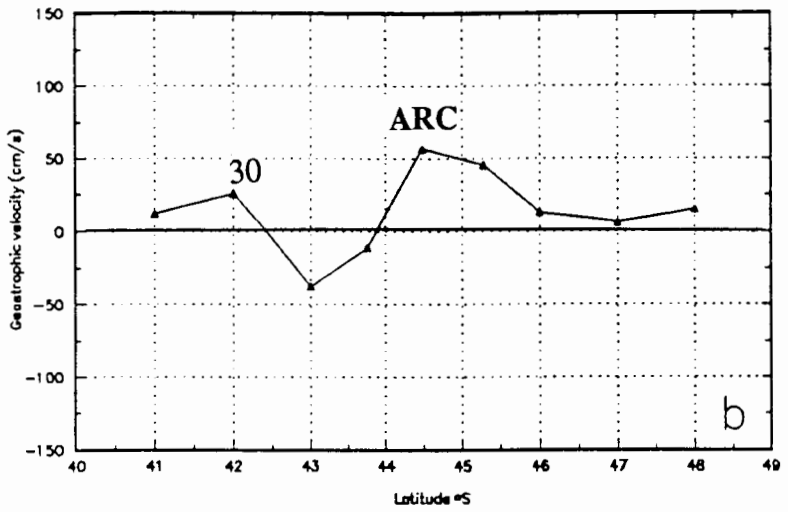


Volume transports (Sv) referenced to the bottom

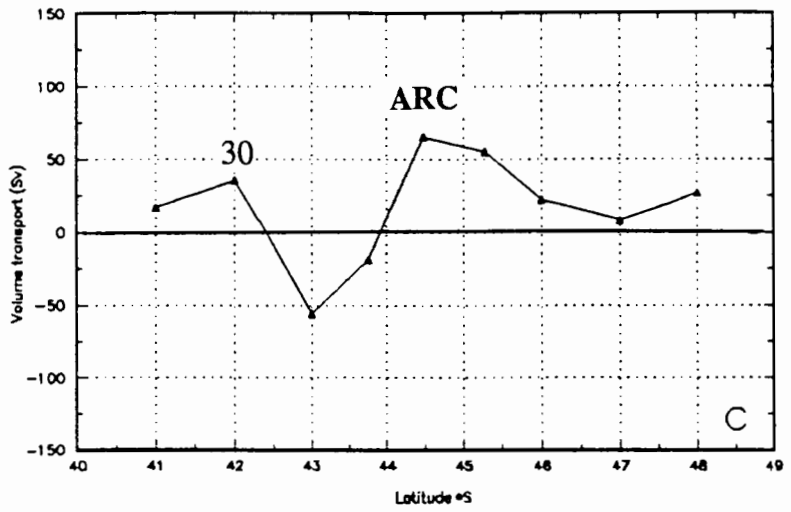


Figures 6.18a,b,c: The solid line in the upper panel (a) shows CTD stations 22 to 32 of *SUZIL*. The calculated geostrophic velocities (b) and the volume transport (c) referenced to the bottom, between each station along the line. East co-ordinate is marked by + and west is marked by -.

Eddy like features centered at 42°S, constitute the most intensified mesoscale eddy and energetic meander activities observed during the whole cruise and also compare well in position and characteristics to previous findings (Gambéroni et al. 1982, Cheney et al. 1983, Projet MARISONDE 1979, Daniault 1984, Daniault and Ménard 1985, Park et al. 1989 and Park 1991). Geostrophic speeds associated with these features (in both easterly and westerly directions) are 28 cm/s (see figures 6.17 and 6.18b). It is also possible that these alternating east-west components may be a meandering branch causing subtropical Agulhas water to be peeled away from the main Agulhas Return Current.

*Volume Transport*

Volume transports over the Agulhas Return Current, between CTD stations 27-26 are 51 Sv, a 2 Sv reduction from those obtained during the first transect lying approximately 7°E to the west.

***Transect 3: Stations 32-40***

This section extends southeast from the basin center to Kerguelan. During this transect the Agulhas Return Current appears to have separated from the frontal zone, flowing north between CTD stations 35-36. Belkin and Gordon (1994) also have shown a separate AF between 60° and 80°E.

Geostrophic velocities over the frontal zone between CTD stations 38-40, range 29 cm/s-54 cm/s (see figures 6.19 and 6.20b), with velocities of 28 cm/s encountered over the Agulhas Front between CTD stations 35-36. This flow pattern is consistent with dynamic charts in the area (Wyrtki 1971, Gordon et al. 1986) showing the Agulhas Return Current to diverge northwards away from the frontal zone.

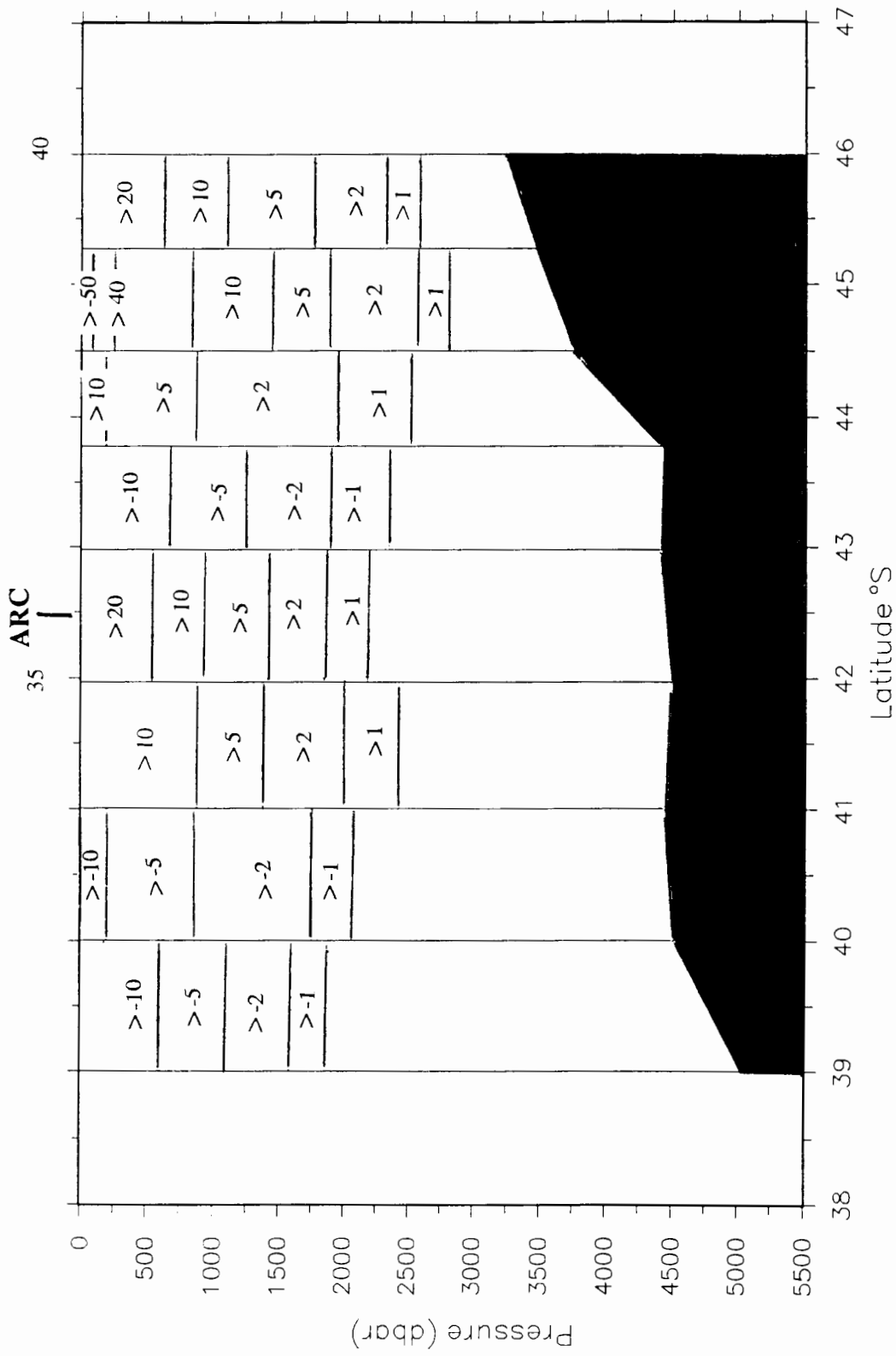


Figure 6.19 ***SUZIL* Transect 3:** Geostrophic velocities calculated between CTD stations 32-40 with reference to the bottom.

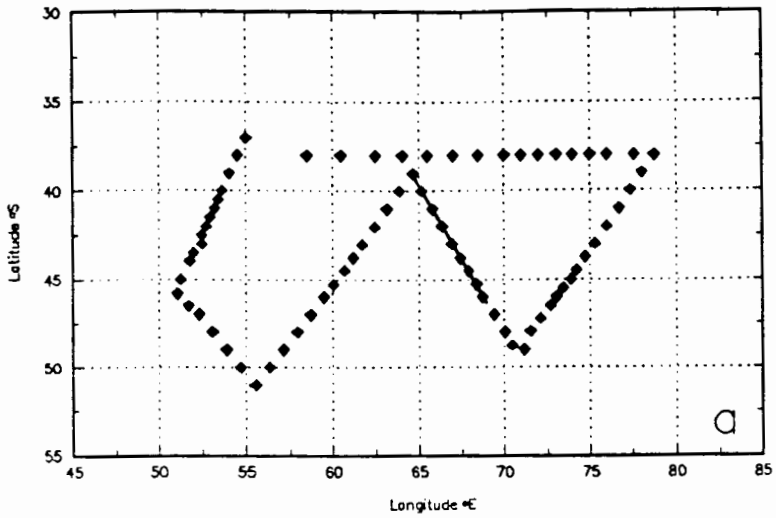


Surface geostrophic velocities (cm/s) referenced to the bottom

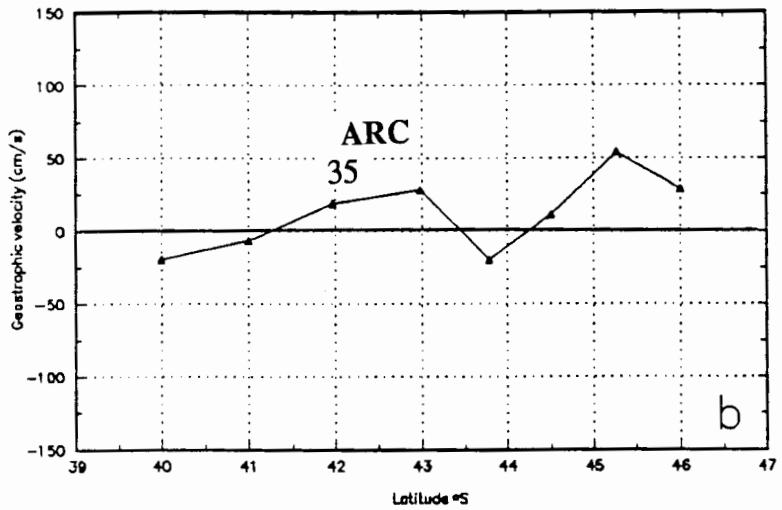


Volume transports (Sv) referenced to the bottom

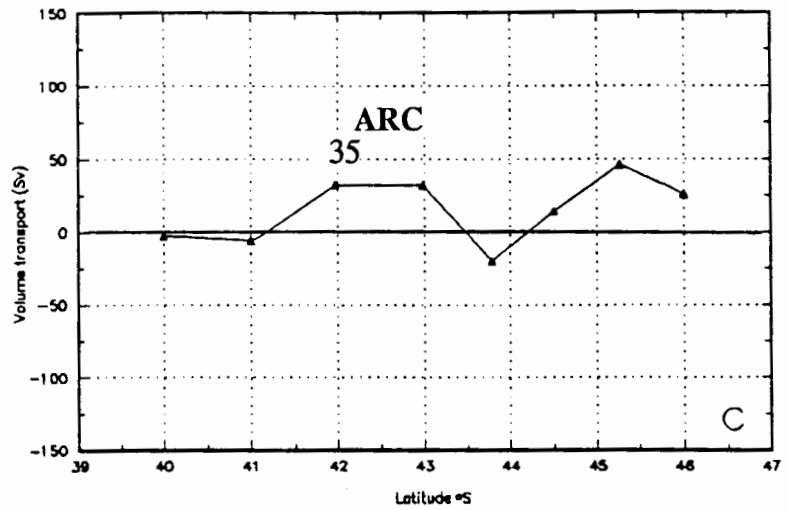


Figures 6.20a,b,c: The solid line in the upper panel (a) shows CTD stations 32 to 40 of *SUZIL*. The calculated geostrophic velocities (b) and the volume transport (c) referenced to the bottom, between each station along the line. East co-ordinate is marked by + and west is marked by -.

There is a reduction of 61 cm/s between transect 3 and transect 1 at ~52°E and 29 cm/s from transect 2 at ~60°E. These results are consistent with the belief that the Agulhas Return Current gradually weakens during it's passage east, as a result of branches peeling Agulhas water northwards (Stramma and Lutjeharms 1995).

*Volume Transport*

The volume transported by the Agulhas Return Current between CTD stations 35-36 provides further proof of the gradual weakening of the Agulhas Return Current during it's course eastwards. Volume transport between CTD stations 35-36 is 32 Sv (see figure 6.20c). When compared to the results obtained in the previous two transects, a 21 Sv reduction from transect 1 and a 19 Sv reduction from transect 2 is evident. These results compare well to the 30 Sv (referenced to 3 000 db) eastward transport at 72°E encountered during the *Vityaz II Cruise #4* when, as mentioned previously, a separate AF was observed (Belkin 1989a). Total volume transport over the frontal region, CTD stations 38-40, is 71 Sv.

***Transect 4: Stations 48-58***

This transect represents the easternmost line occupied during *SUZIL* and runs across the Kerguelan and Amsterdam passage. The frontal zone (STC and SAF) is between CTD stations 50-52 and has a maximum geostrophic velocity of 69 cm/s (see figures 6.21 and 6.22b). To the north of this zone are alternating east and west components associated with mesoscale features; either eddies or meanders. The easterly AF is situated between CTD stations 55-54 and has a maximum geostrophic speed of 17 cm/s. It's existence this far east has been previously observed during *JASUS* (David and Guerin-Ancey 1990). Results obtained during this cruise identified subtropical water typical of the Agulhas Return Current flooding the Amsterdam Plateau (Belkin and Gordon 1994).

*Volume Transport*

The volume transport associated with the weakened Agulhas Return Current between CTD stations 55-54 is 23 Sv (figure 6.22c), a loss of 9 Sv from the previous transect 3. This reduction in flow compares with Stramma and Lutjeharms (1995) which shows that at roughly 70°E a 10 Sv (referenced to the upper 1 000 m) northward recirculation branch occurs significantly reducing the volume transported east. The frontal zone between CTD stations 50-51 has a total geostrophic flow of 45 Sv.

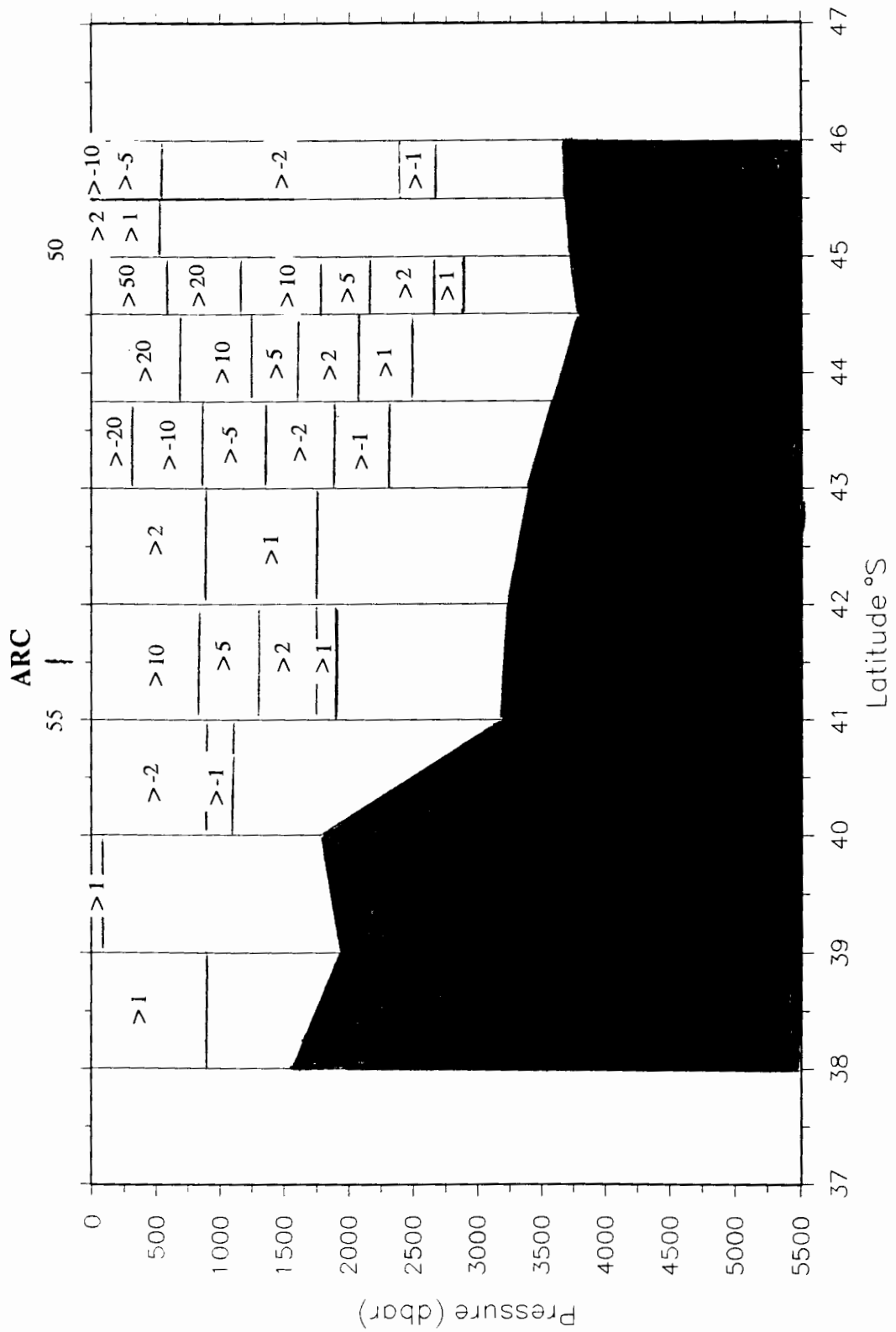


Figure 6.21 ***SUZIL* Transect 4:** Geostrophic velocities calculated between CTD stations 48-58 with reference to the bottom.

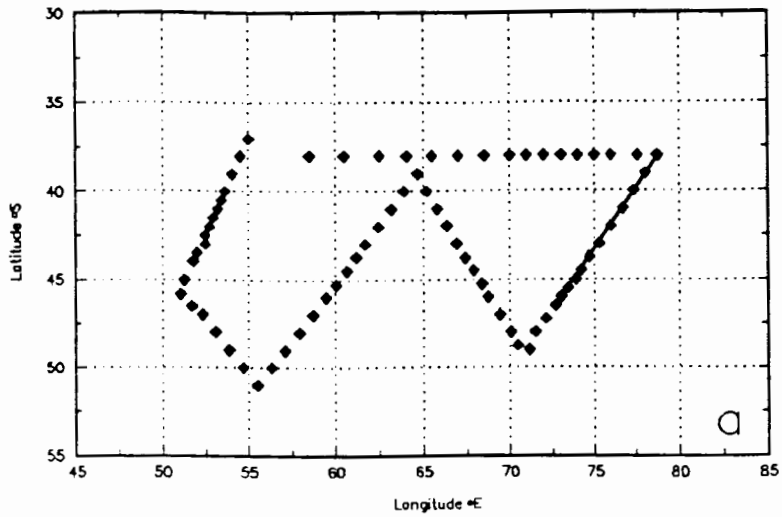


Surface geostrophic velocities (cm/s) referenced to the bottom

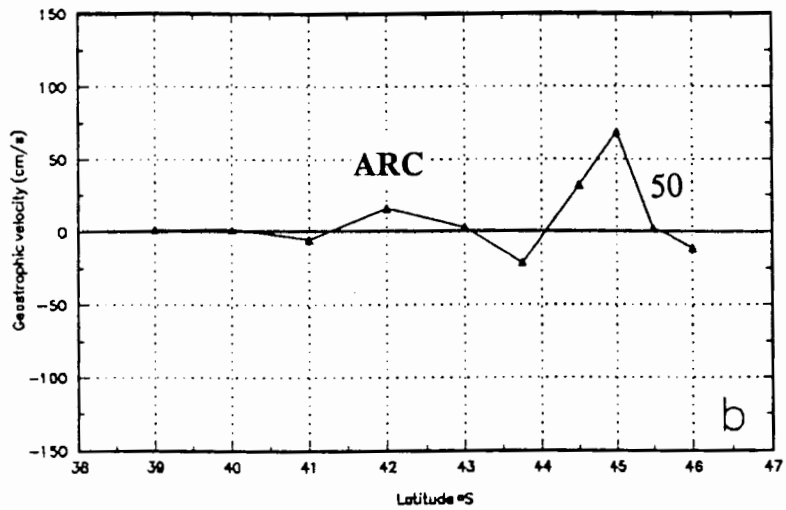


Volume transports (Sv) referenced to the bottom

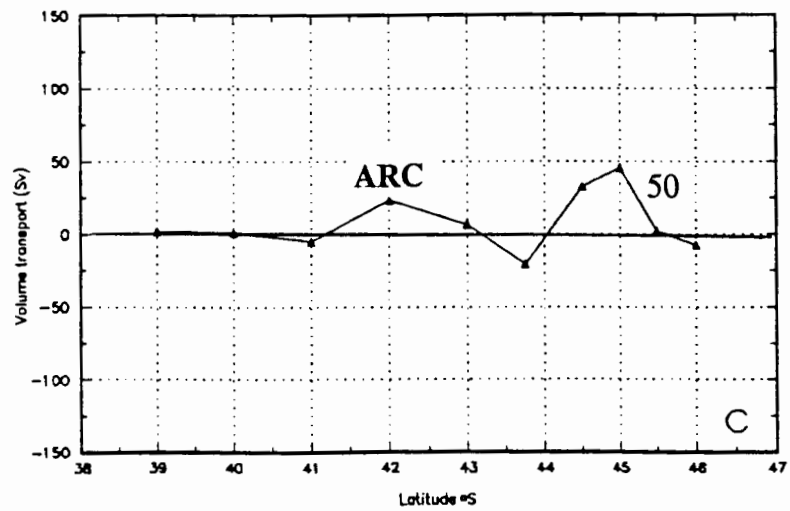


Figures 6.22a,b,c: The solid line in the upper panel (a) shows CTD stations 48 to 58 of *SUZIL*. The calculated geostrophic velocities (b) and the volume transport (c) referenced to the bottom, between each station along the line. East co-ordinate is marked by + and west is marked by -.

*Transect 5: Stations 58-73*

This transect runs back westwards at 38°E and investigates the meridional circulation in the Crozet Basin, including the northward leakages of the Agulhas Return Current. Maximum northward geostrophic speeds during this transect are >10 cm/s (see figures 6.23 and 6.24b) between CTD stations 65-64. Frequent north and southward components appear between CTD stations 66-64, (71°E), CTD stations 69-68 (67°E), CTD stations 71-70 (64°E) and CTD stations 73-72 (59°E), indicating a highly structured upper level flow system (Park et al. 1993). These northward components are indicative to recirculation branches gradually peeling Agulhas water away from the main current body, during it's passage over the Crozet Basin and are comparable to findings by Stramma and Lutjeharms (1995) at 60°E and 71°E.

*Volume Transport*

Significant northerly volume transports between 5 Sv-27 Sv exist between CTD stations 66-64, CTD stations 67-69, CTD stations 70-71 and CTD stations 72-73 and reflects the gradual weakening of the Agulhas Return Current from 28 Sv on entering the Crozet Basin at 52°E to 15 Sv at the Kerguelan-Amsterdam Passage at 76°E.

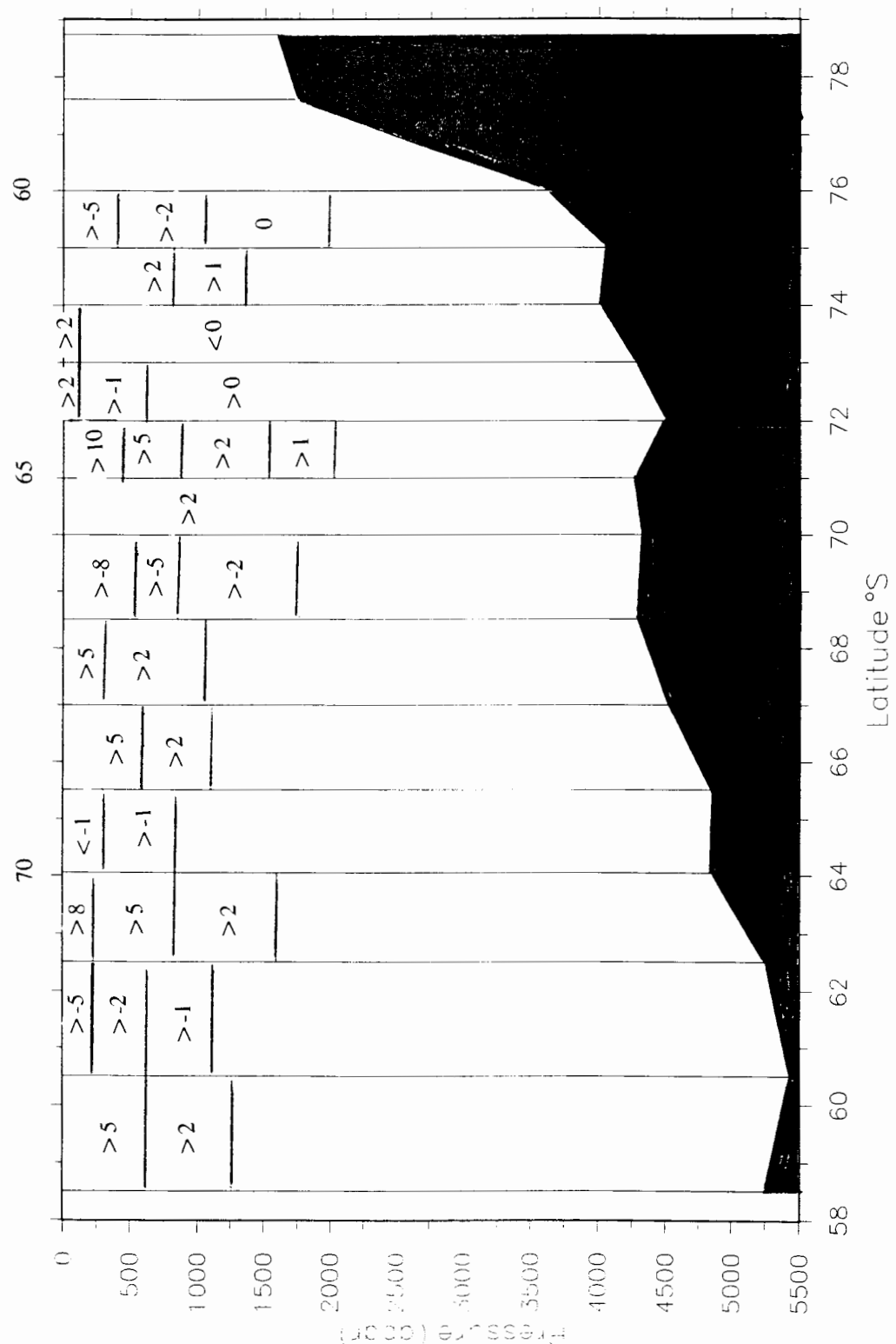


Figure 6.23 ***SUZIL* Transect 5:** Geostrophic velocities calculated between CTD stations 58-73 with reference to the bottom.

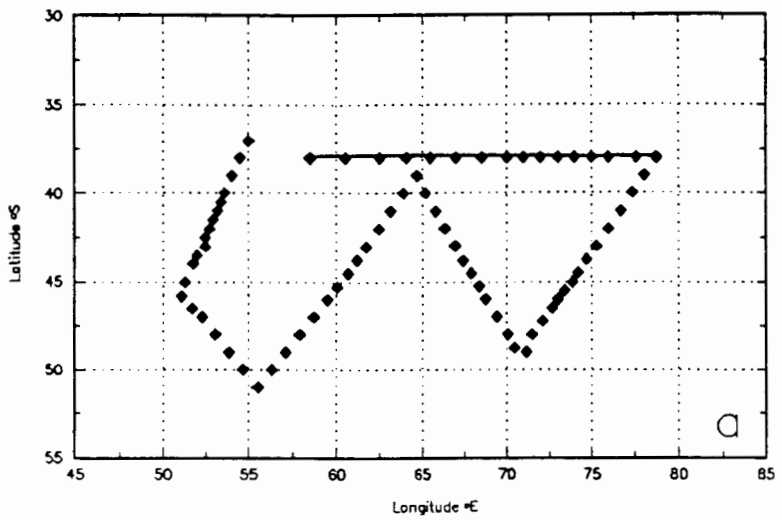


Surface geostrophic velocities (cm/s) referenced to the bottom

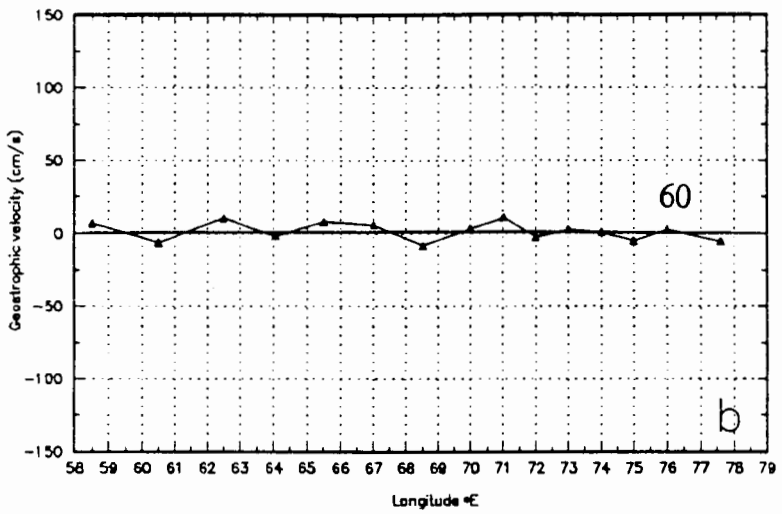


Volume transports (Sv) referenced to the bottom

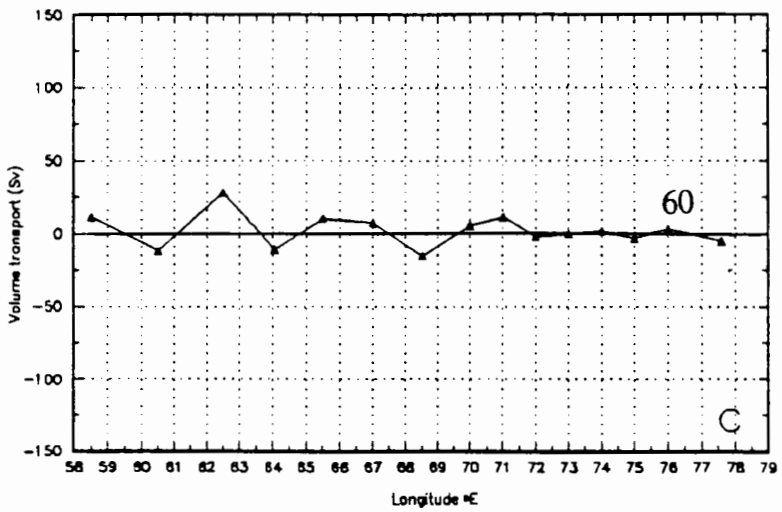


Figures 6.24a,b,c: The solid line in the upper panel (a) shows CTD stations 58 to 73 of *SUZIL*. The calculated geostrophic velocities (b) and the volume transport (c) referenced to the bottom, between each station along the line. East co-ordinate is marked by + and west is marked by -.

***Geostrophic Transport Pattern of the Agulhas Return Current:***

***(a) in the Retroflection Zone***

The *ARC* and *Marathon* datasets clearly show the course and varying geostrophic speeds and transport values associated with the Agulhas System as the Agulhas Current retroflects and forms the easterly flowing Agulhas Return Current. During it's initial passage the Agulhas Return Current is known to form several meanders as it is topographically steered around features such as the Agulhas Plateau and Mozambique Ridge.

Geostrophic velocities for *ARC* and *Marathon* cruises range from 47 cm/s to 128 cm/s in the retroflection region as can be seen from figure 6.25a. However, speeds obtained during transect 1 and 3 of *ARC* and transect 1 of *Marathon* range 47-87 cm/s and average 65 cm/s and consequently compare more realistically with drifter data deployed during *Marathon* which between 21°-32°E averaged 54 cm/s.

Volume transports range from 44 Sv to 98 Sv as can be seen from figure 6.25b. Again values obtained during the above mentioned transects are more realistic, averaging 60 Sv and compare with Stramma (1992) and Stramma and Lutjeharms (1995) estimated volume transports of 60 Sv at approximately 30°E.

However, it must be remembered that the datasets together do not resemble a "snapshot" of the Current but that the cruises are carried out over a period of 4 years (1983-1987) and therefore only show the characteristics of the Agulhas Return Current at the time of each cruise.

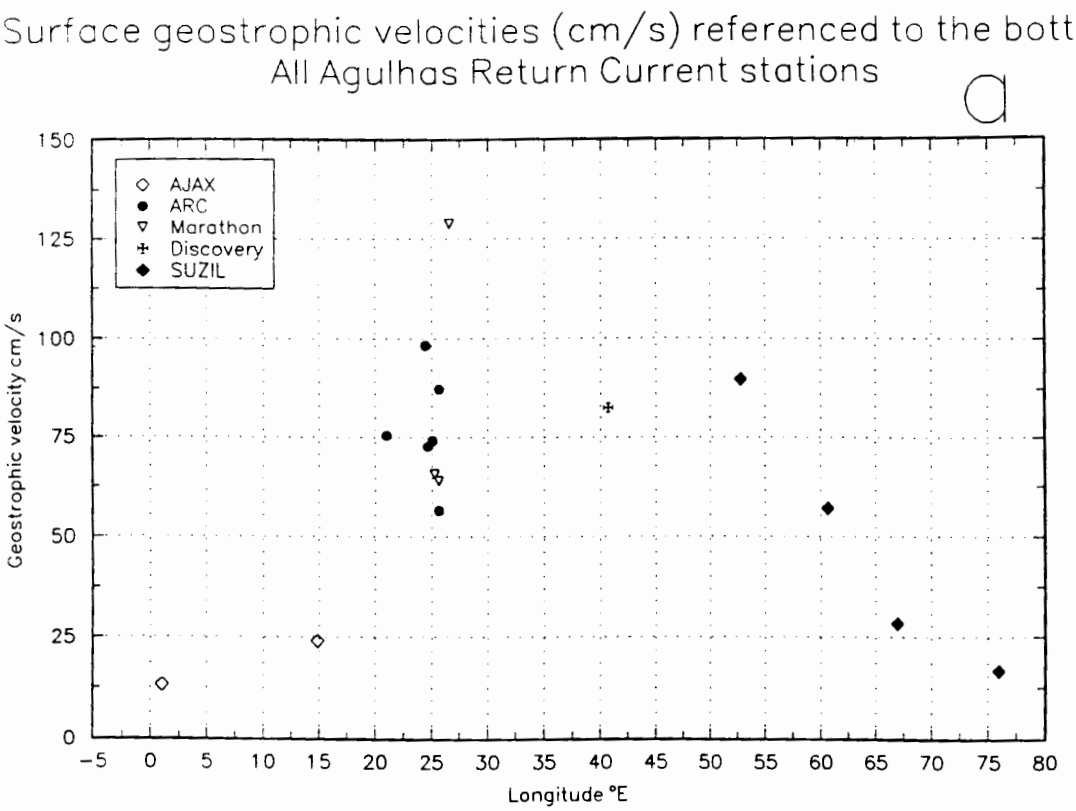


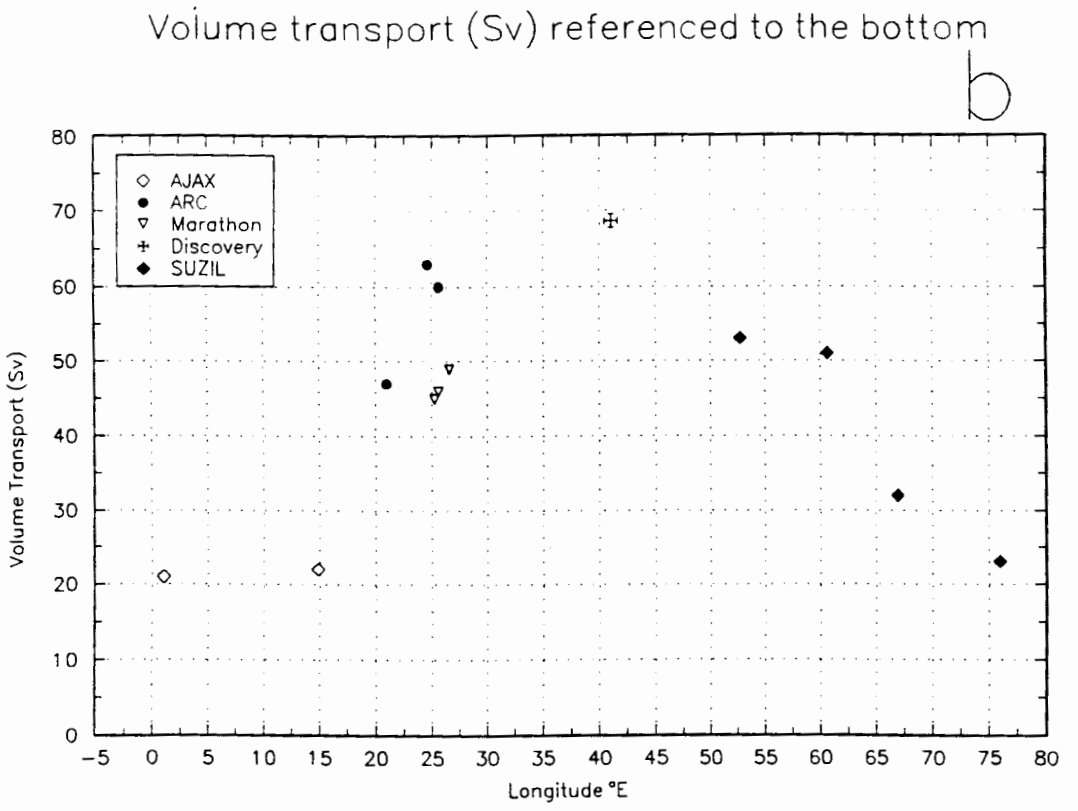


Figures 6.25a and b: The calculated surface geostrophic velocities (a) and volume transported (b), referenced to the bottom, for all stations located within the Agulhas Return Current, from 1°E to 76°E. cruises. East co-ordinate is marked by + and west is marked by -.

*(b) east of 35°E*

East of the retroflection region, the Agulhas Return Current continues it's flow at approximately 40°S (±1°) across the southern Indian Ocean to as far east as 76°E (Park et al. 1993, Belkin and Gordon 1994). During it's passage the Agulhas Return Current slowly weakens and loses it's surface thermal signature as shown from investigations by Meeuwis (1991). Geostrophic velocities calculated from the *Discovery* and *SUZIL* datasets confirm this gradual weakening from 82 cm/s (*Discovery*) at 40°E to 17 cm/s (*Leg4 SUZIL*) at 76°E, as can be seen from figure 3.25a. Velocities obtained during *Discovery* reasonably compare well to the 73 cm/s obtained at 39°E by a drifter deployed during *Marathon* and to the 84 cm/s velocity recorded in the vicinity of the Madagascar Ridge (Gründlingh 1978).

Total volume transports decrease rapidly with distance east from an average of 60 Sv encountered in the retroflection region, to 23 Sv at 76°E (*SUZIL*), as can be seen from figure 3.25b. This gradual loss is caused by topographically induced meanders and the generation of eddies seen at 40°E, 53°E, 59°E, 60°-67°E, 71°E and 76°E, during *Discovery* and *SUZIL* cruises, which result in the "peeling" away of Agulhas water from the main Agulhas Return Current. There appears to be significant leakage northwards, between the 40°E (*Discovery*) and 76°E (*Leg4 SUZIL*), possibly as a result from topographical influences such as the shallow Southwest Indian Ridge.

During *SUZIL* energetic eddies and meanders observed during transects results in the volume transported by the Agulhas Return Current decreasing from 53 Sv at the entrance of the Crozet Basin to 23 Sv at the Kerguelan-Amsterdam Passage. The location of these meanders (53°E, 59°E, 60°-67°E, 71°E and 76°E) compares well to the northward fluxes encountered during the 38°S zonal transect Leg 5 during *SUZIL*.

Analysis of the five datasets (*AJAX*, *ARC*, *Marathon*, *Discovery* and *SUZIL*) confirm that through the formation of mesoscale features; such as branches, meanders and eddies,

gradual weakening during the Agulhas Return Current's course eastwards across the South Indian Ocean occurs. This weakening is clearly evident in figure 6.26 below, which shows branches "peeling" off and recirculating Agulhas water northwards.

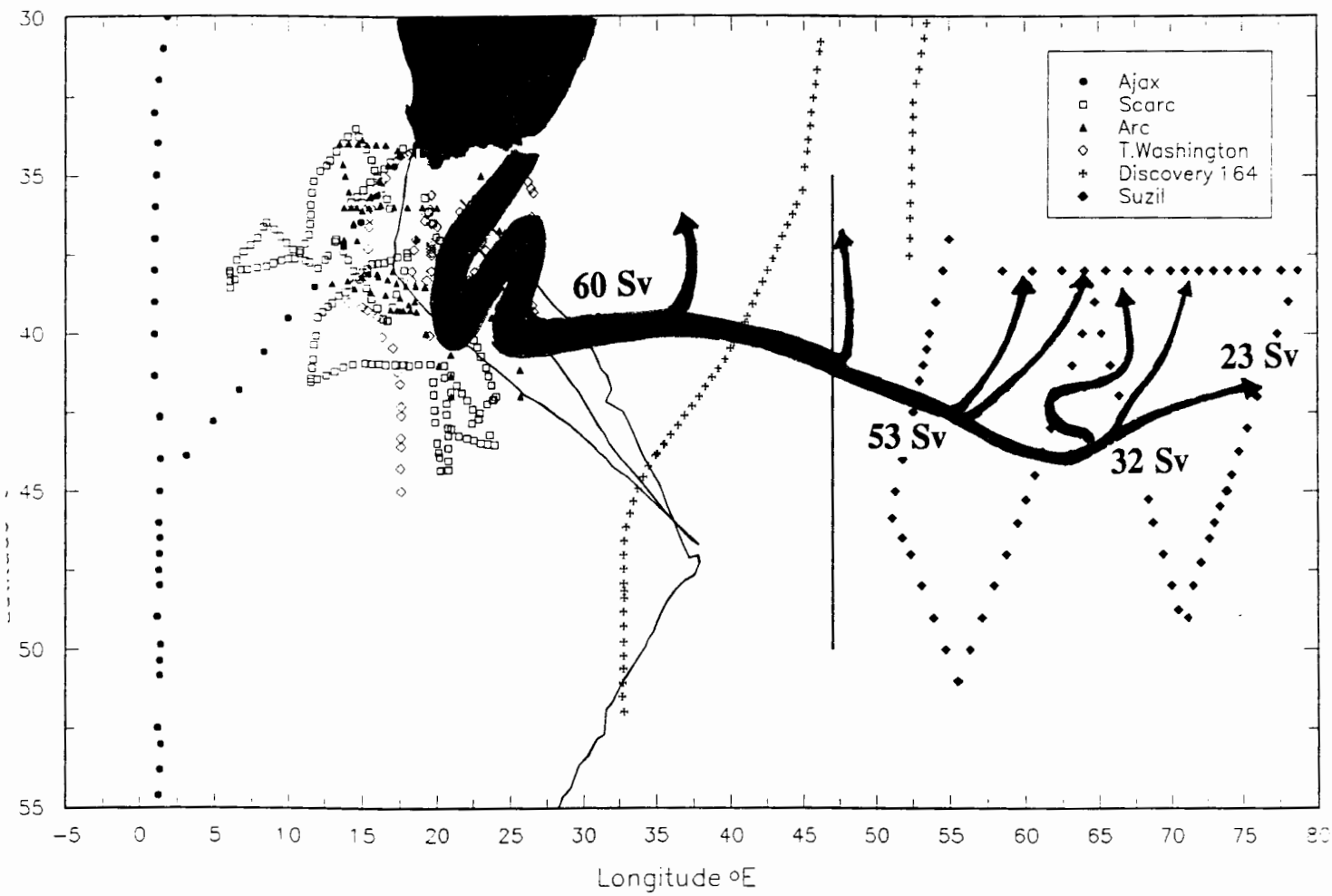


Figure 6.26: Volume transports for all the stations located within the Agulhas Return Current. Combined these results show the gradual weakening occurring during it's passage across the South Indian Ocean. Northward branches in which Agulhas water is "peeled" away from the Agulhas Return Current are evident.

The geostrophic calculations have successfully shown the incremental weakening in the speed and volume transported by the Agulhas Return Current. However, in order to fully understand this weakening it is also essential that the physical properties; such as temperature, salinity and oxygen, be analysed. This will enable one to examine the effects interaction with surrounding water masses and distance away from the source; Agulhas Current system, have on the overall strength and identity of the Agulhas Return Current.

# Chapter 7
# WATER MASS CHARACTERISTICS OF THE AGULHAS RETURN CURRENT

It has been shown in the previous chapters (5 and 6) that the Agulhas Return Current extends roughly two thirds across the Indian Ocean to approximately 76°E. During it's passage east the Agulhas Return Current gradually weakens as Agulhas water rapidly becomes modified by interacting with surrounding cooler and fresher water masses (Read and Pollard 1993 and Park et al. 1993).

To understand fully the mass composition and origin of the water masses found within the Agulhas Return Current and to show it's gradual modification it is necessary to first discuss the water masses present in the Agulhas Current the source of this current. Gordon et al. (1987) have used temperature, salinity and oxygen data collected during a selection of *GEOSECS* and *CONRAD 17* stations in the western Indian Ocean, to display the large range of water properties from which the Agulhas Current can draw. Figures 7.1 a and b represent typical characteristics of the western Indian Ocean.

The aim of this investigation is to identify the water masses that constitute the Agulhas Current (inflow) and to study the degree of modification by comparing them to the various profiles along the length of the Agulhas Return Current (outflow).

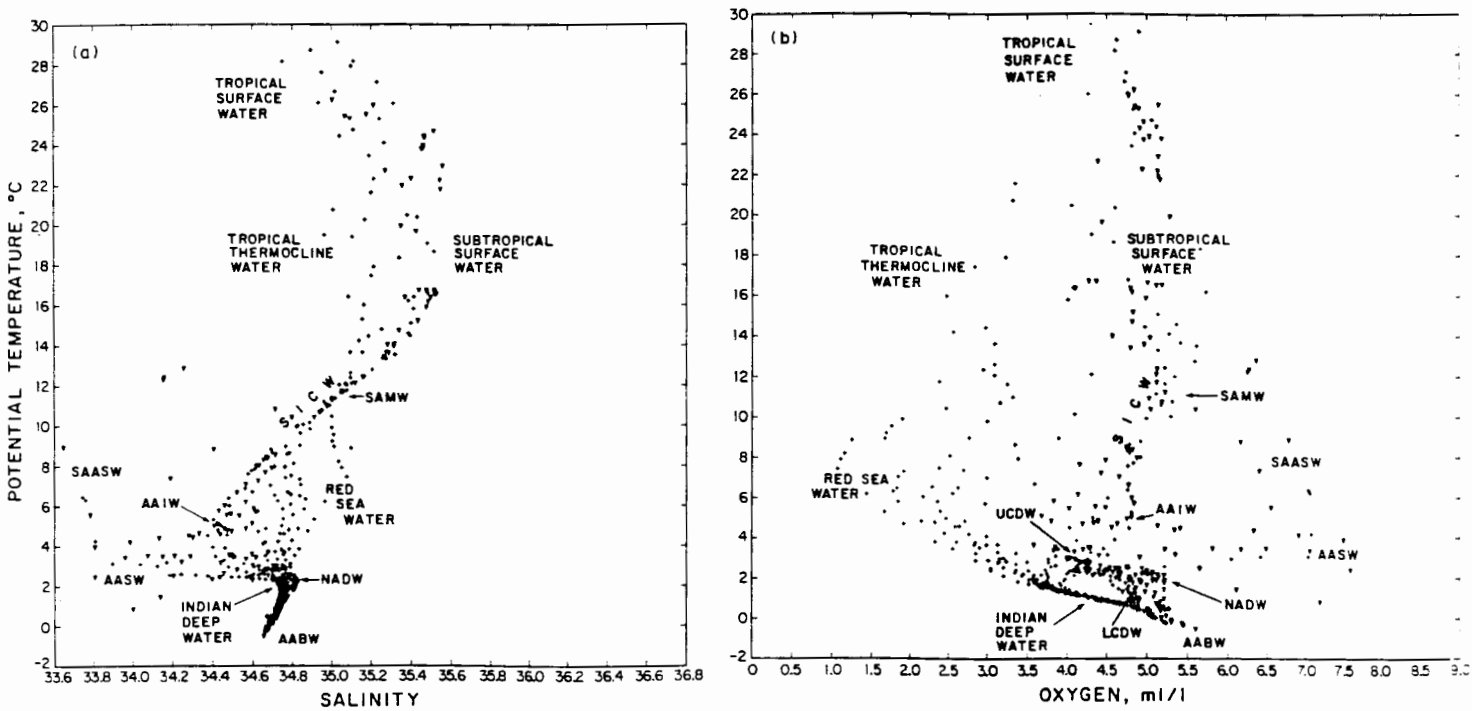


Figure 7.1a and b: T/S and T/O plots for the western Indian Ocean (Gordon et al. 1987).

*Surface water - Tropical Surface Water (TSW)*

The surface water in the low/tropical latitudes of the Indian Ocean is relatively fresh, as seen from figures 7.1a and b, between 34,8-35,1 psu, characterised by high temperatures >24°C and dissolved oxygen concentrations of 4,8-5,0 ml/l. These low salinities are due to the inflow of Pacific water through the Indonesian Archipelago and then westward by the South Equatorial Current (Warren, 1981), as well as through excess precipitation >200 cm at these latitudes. This low salinity water mass spreads southwards as a result of fluctuations in the South Equatorial Current (Warren, 1981).

*Subtropical Surface water (STSW)*

Beneath the TSW at 250 m a 300 m thick layer of high salinity >35,4 psu is centered at the 17°C isotherm. This salinity maximum known as Subtropical Surface Water (STSW) can be traced to latitudes 25°-35°S, where a high salinity surface water exists across the breadth of the Indian Ocean (Wyrtki, 1973). The high values >35.4 psu, are due to excess evaporation between 60-160 cm $y^{-1}$ occurring at these latitudes (Baumgartner and Reichel,

1975). The subtropical water sinks and forms the subsurface maximum at temperatures of 17°-18°C throughout the Indian Ocean.

*Tropical Thermocline Water (TTW)*

Water exhibiting TTW characteristics is the most common surface water encountered in the retroflection region, with over 67% of CTD stations occupied during *SCARC* consisting of TTW in it's surface layers (Rigg 1995). TTW can be found in figures 7.1a and b, at temperature $>17°C$ and at approximately 35,10 psu. It is thought that TTW is formed as a result of the contamination of STSW by cooler/fresher SAASW from the south. This invasion often occurs in the form of surface filaments entrained along the eastern perimeter of Agulhas rings and eddies (Rigg 1995).

Embedded in the STSW/TTW and diminishing southward is a sharp oxygen minimum $<3$ ml/l, recognizable at 200 m. It is associated with a nutrient maximum and is formed by the oxidation of sinking detritus. The oxygen minimum is better developed to the east and west of the ocean than at the center (Warren, 1981). This oxygen minimum is transported southwards by the Agulhas Current into the Retroflection zone where it is still recognizable (Gordon et al. 1987, Valentine et al. 1993, Rigg 1995) and may act as a tracer for Agulhas Water in the Atlantic Ocean (Chapman 1988).

*South Indian Central Water (SICW)*

Below the STSW lies the oxygen maximum of the South Indian Central Water (SICW). Central water is formed at the Sub-Tropical Convergence (STC) region by the sinking and northward spreading of mixed subtropical and subantarctic surface water masses (Orren 1963, 1966). Central water has been defined by Sverdrup et al. (1942) as the water in the Southwest Indian Ocean with a T/S range of 8°C-15°C and 34,6-35,5 psu and a $T/O_2$ range of 4,90 ml/l - 5,5 ml/l. This water is also carried south by the Agulhas Current.

Central water in the Southeast Atlantic Ocean (SACW) has very similar characteristics to that of the South Indian Central Water (Orren 1963, Shannon 1966). Gordon (1986) has pointed out that between 7° and 15°C the South Atlantic and South Indian thermoclines are similar in T/S properties, with SACW displaying a range of 6°-16°C and 34,5-35,5 psu. South Atlantic Water enters the Southern Agulhas region as a blend of thermocline water and Subantarctic Surface water from the south (Gordon 1981). The similar $O_2$/S curves of the South Atlantic and Indian thermoclines between 7°C and 15°C may be a consequence of exchange between these basins across the retroflection (Gordon 1985).

*Antarctic Intermediate Water (AAIW)*

This water mass is found at the base of the Central water and is traditionally thought to form near the Antarctic Polar Front between 50°-55°S, where water of 2,2°C and 33,87 psu sinks and spreads northwards in the Atlantic, Indian and Pacific Oceans (Sverdrup et al. 1942). McCartney (1977) however, has suggested that penetration of the Subantarctic Mode water into the Atlantic Ocean via the Drake Passage gives the AAIW in this region it's low salinity and potential temperature characteristics. The salinity minimum at depths 600-1000 m (Valentine et al. 1993) which marks the core of the AAIW, is gradually eroded with distance away from it's source. the salinity range of the AAIW in the Indian and Atlantic Ocean is 33,80-34,80 psu, while temperature between the 2 oceans ranges 2°-6°C and 2°-10°C respectively (Emery and Meincke 1986). It is possible for some AAIW to be advected from the Indian Ocean into the Atlantic around the Agulhas Bank (Clowes 1950, Shannon 1966).

The high salinity values within the AAIW is a result of influence from the highly saline Red Sea Water (RSW) (Piola and Geogi 1982, Jacobs and Georgi 1977). During the AAIW's northward spreading it encounters, at more or less the same depth, the southward penetration of the RSW at approximately 20°S off the east coast of Africa (Gründlingh 1985). Gordon et al. (1987) found from the *ARC* dataset RSW to be present between 4°-6°C in the southern Agulhas region.

*Deep Water (DW)*

Below the AAIW in the southern region of the Agulhas Region is the North Atlantic Deep Water (NADW) and the Circumpolar Deep Water (CDW). The NADW is formed in the North Atlantic Ocean and is found as far south as 56°S (Clowes 1950), dominating the deep water in the Atlantic as well as within the western Indian Ocean, where it is less saline. It is characterised by a deep salinity maximum of between 34,80-35,00 psu and a temperature range of 1,5°-1,0°C (figures 7.1a and b and Emery and Meincke 1986). The Indian Deep Water (IDW) is associated by lower oxygen levels than the North Atlantic Deep water and this results in the formation of two distinct modes in the potential temperature and oxygen plots.

In the Southern Ocean the NADW lies between two layers of CDW (upper and lower). In the southern Agulhas region, Gordon et al. (1987) from quasi-synoptic hydrographic data found very little CDW.

*Antarctic Bottom Water (ABW)*

The Deep Water overlies the Antarctic Bottom Water (ABW). This water has a a T/S range of -0,9°-1,7°C and 34,64-34,76 psu. Very little of this water can be found in the retroflection region.

*The Agulhas Current*

CTD stations 49, 50 of *ARC*, 56 of *SCARC* and 258, 259, 274, 275, 276 of *Marathon* have been selected, as combined they best represent the T/S and $T/O_2$ properties of the Agulhas Current inflow into the retroflection. There location can be seen below in figure 7.2. Comparing this dataset to stations within the Agulhas Return Current will enable the modifications during the current's passage eastwards to be examined. It is expected that water flowing within the Agulhas Return Current will become slightly fresher and cooler within and with distance away from the retroflection zone, as a result of interocean exchange of Indian and Atlantic water.

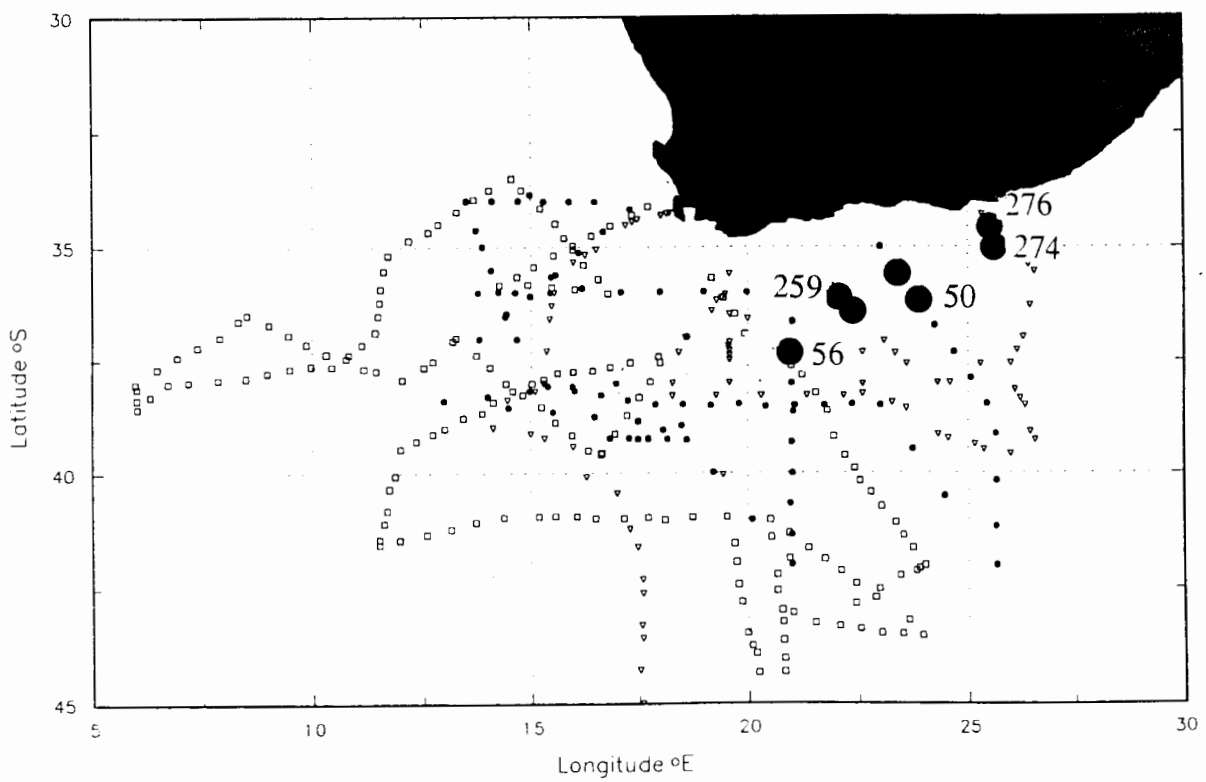


Figure 7.2: Distribution of Agulhas Current inflow CTD stations from *SCARC* (56), *ARC* (49, 50) and *Marathon* (259, 274 and 276).

Analysing T/S and T/$O_2$ properties (figures 7.3a and b) it can be seen that the dominant signal for the Agulhas Current are the **STSW, SICW** and **AAIW** water masses (Gordon et al. 1987).

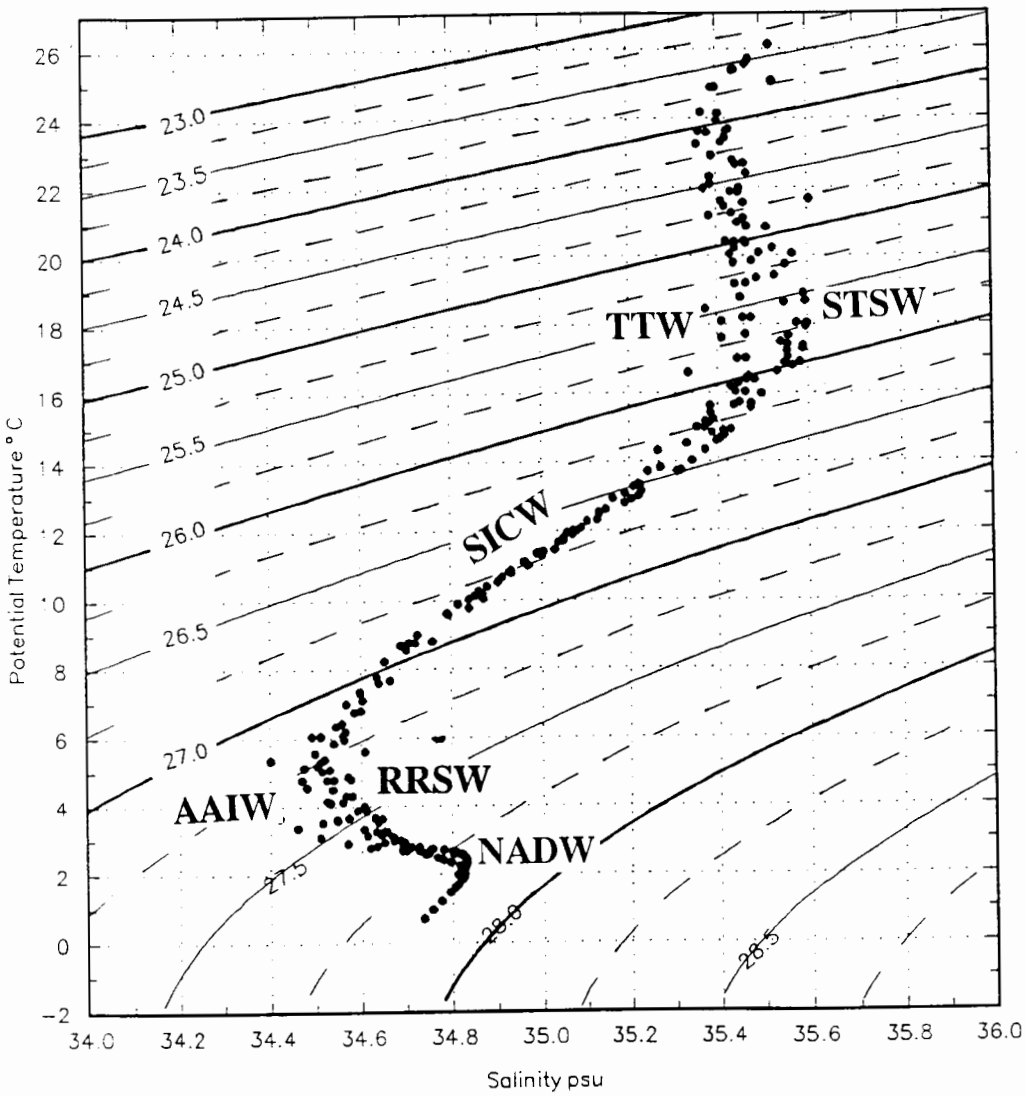


Figure 7.3a: T/S plot of the Agulhas Inflow CTD stations; *ARC* 49 and 50, *SCARC* 56 and *Marathon* 258, 259, 274 -276. Abbreviations are given for Sub-Tropical Surface Water (STSW), Tropical Thermocline Water (TTW), South Indian Central Water (SICW), Antarctic Intermediate Water (AAIW), Remnant Red Sea Water (RRSW) and North Atlantic Deep Water (NADW).

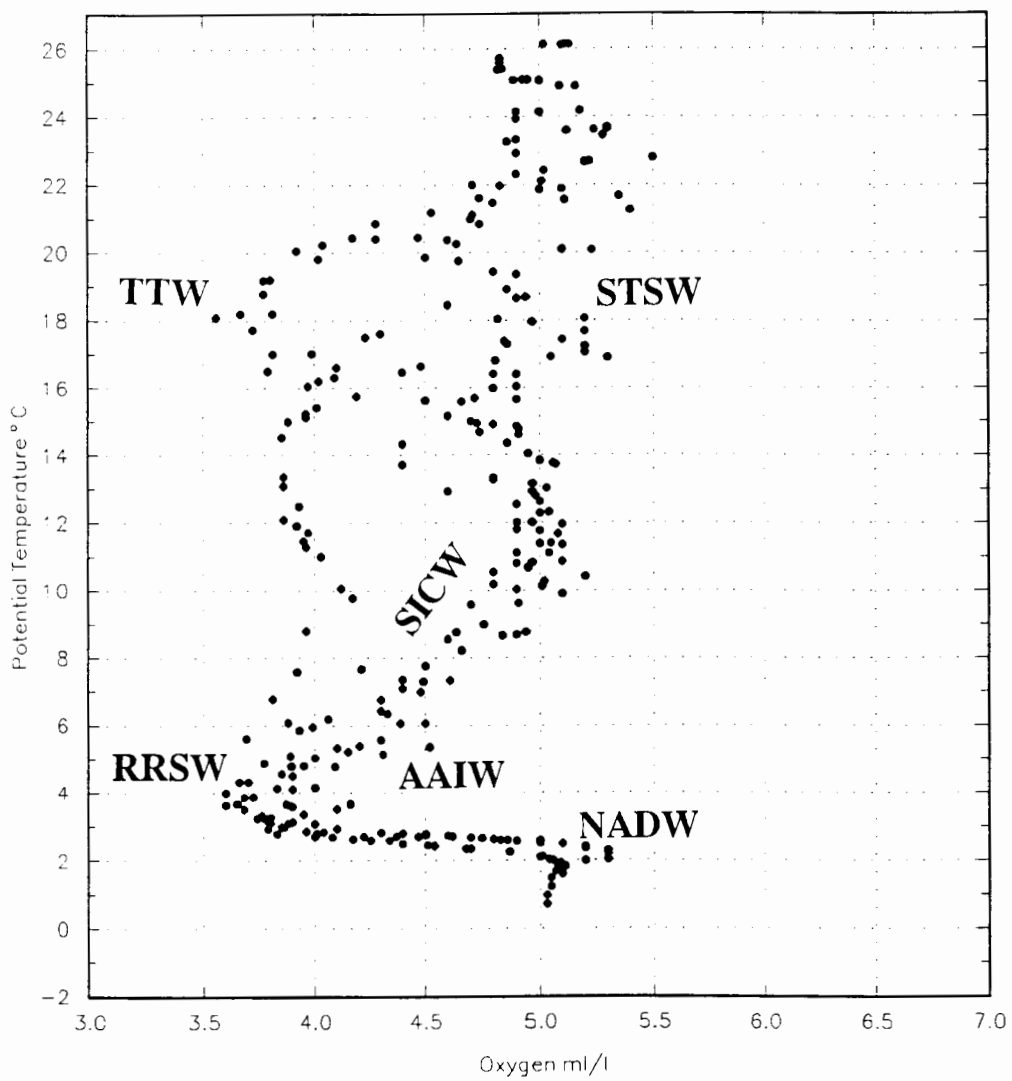


Figure 7.3b: $T/O_2$ plot of the Agulhas Inflow CTD stations; *ARC* 49 and 50, *SCARC* 56 and *Marathon* 258, 259, 274 -276. Abbreviations are given for Sub-Tropical Surface Water (STSW), Tropical Thermocline Water (TTW), South Indian Central Water (SICW), Antarctic Intermediate Water (AAIW), Remnant Red Sea Water (RRSW) and North Atlantic Deep Water (NADW).

Water temperatures in excess of 15°C and covering a salinity range of 35,3 psu-35,6 psu and densities 26,00 $\sigma$t-23,33 $\sigma$t,are associated with the surface layers; TSW, STSW and TTW water masses. Two strong characteristics of the Agulhas Current are;

(a) the presence of TSW in the inshore edges of the Current (Gordon et al. 1987, Rigg 1995). This water mass is identified by it's high temperatures (>24°C) and low salinities ~35,0 psu, as a result of it's formation in the tropical zone of the Indian Ocean.
(b) the presence of a shallow oxygen minimum associated with TTW (Chapman 1988, Rigg 1995).

Below the surface layers, the T/S profiles show that SICW lies between 14°C and 8°C, 34,6 and 35,25 psu and 26,35 $\sigma t$ and 27,0 $\sigma t$. The line is slightly curved and is better defined as a line of constant density ratio. Suggesting that double diffusive mixing takes place between the two end points; warm, saline STSW above and cool, fresh AAIW below (Read and Pollard 1993).

At the base of the SICW is the salinity minimum of the AAIW 34,37 psu at ~4°C and at density 27,28 $\sigma t$. The range of salinity values (34,27 psu-34,6 psu) indicates the remnants of the highly saline RSW. The RSW influences is very weak, as during it's progression the core salinity reduces from about 38,0 psu at the Red Sea exit to about 34,7 psu in the Mozambique Channel to 34,6 psu within the retroflection region (figures 7.3a and b). Thus only diluted remnants/traces of RSW (RRSW) can be seen from the profiles obtained by the above mentioned CTD stations. Below the AAIW and RRSW "trace" stratum is the NADW indicating that the Indian Deep Water does not enter the retroflection region. At the sea floor lies the AABW at approximately 0,6°C, 34,73 psu and at density 27,84 $\sigma t$.

Having identified water mass characteristics associated with the Agulhas Current inflow it will be possible, by comparing with selected stations, to examine the degree of modification that has occurred in the Agulhas Return Current within;
(a) west of the retroflection region
(b) the retroflection region
(c) east of the retroflection region.

*(a) West of the retroflection region: Intercomparisons with AJAX*

The *AJAX* dataset occupies a meridional southward line at the Greenwich meridian $\pm 1°$. Although this transect does not cross the Agulhas Return Current, being too far upstream, it is still included as it provides an excellent baseline with T/S and $T/O_2$ plots obtained during transects further downstream.

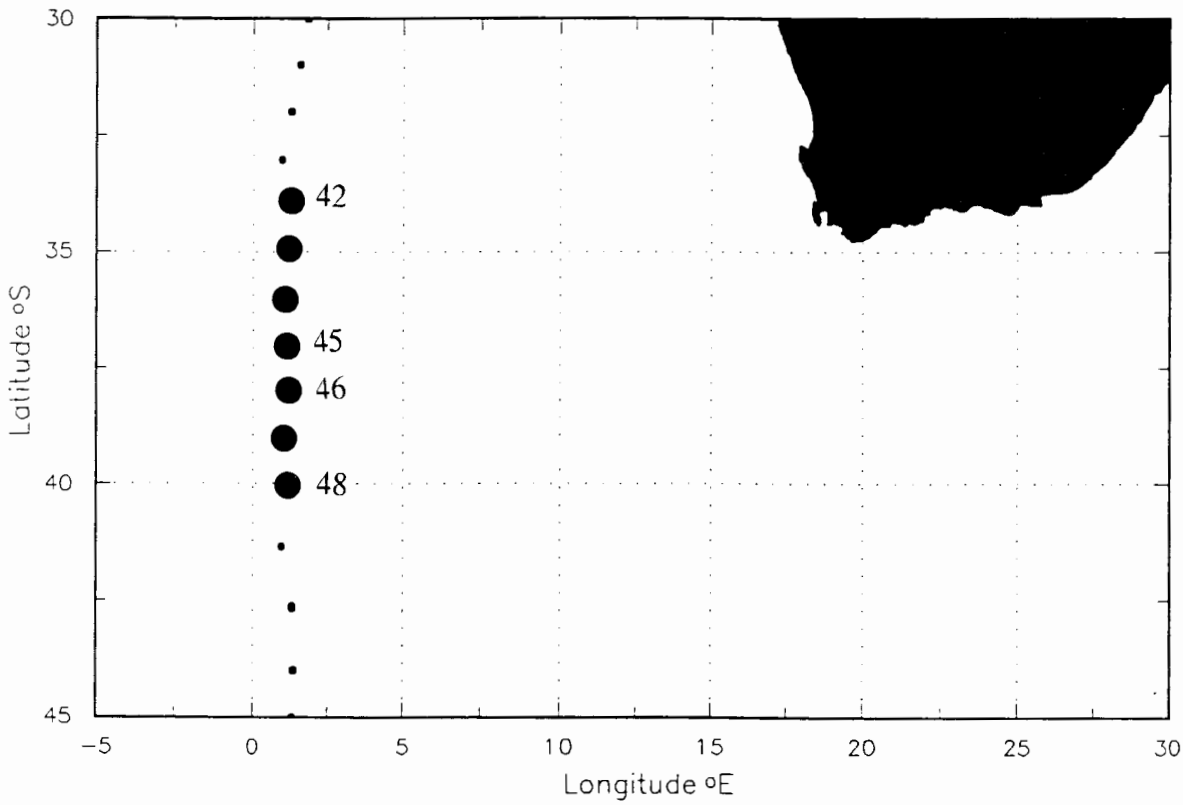


Figure 7.4: Distribution of the *AJAX* CTD stations

During the transect between CTD stations 40-52 the STC is shown from the steep salinity gradients in chapter 5 (figures 5.2a and b) and maximum geostrophic speeds in chapter 6 (figures 6.1 and 6.2b), to center between CTD stations 45-46 (37°S-38°S) (Whitworth and Nowlin 1987). North of the STC (CTD stations 43 at 35°S) and closing the circulation of the subtropical subgyre is a secondary front known as the Benguela-South Atlantic Current Front (BSAF) (Gordon et al. 1992). This compares well with results obtained by Gordon et al. (1992) during the SAVE-4 cruise, where the BSAF was identified between 33°S-34°S, and to analysis of archive data by Belkin (1993a, 1994) and Belkin and Gordon (1994).

The salinity structure of the Southern Atlantic Ocean is believed to be boosted by the intermittent shedding of eddies and injection of streams of Indian Ocean Central Water at the Agulhas Retroflection (Gordon et al. 1992). As confirmed during SAVE-4 when two Agulhas eddies were traversed at 2°E and 6°E and from the examination of GEOSAT altimetry (Gordon et al. 1987). Gordon and Haxby (1990), confirm that Agulhas eddies are capable of crossing most, if not all, of the South Atlantic Ocean. This is regarded importantly to the overall heat and salinity budgets of the South Atlantic and may play a role in the global thermocline circulation (Gordon 1985, 1986). In effect the Atlantic's salinity is increased by drawing salty Indian Ocean water. Estimates of this leakage range from 20 Sv (Whitworth and Nowlin 1987) to 2,8 Sv (Bennett 1988).

*AJAX vs Agulhas Inflow*

Comparing the two datasets it can be seen that substantial differences exist between the key stations located in the Agulhas Current and the stations spanning the STC frontal zone in the South Atlantic. Stations used in the T/S and $T/O_2$ plot span from 34°S to 40°S and cross the BSAF and STC.

Analysing property values centered along the 26,25 $\sigma t$ density line, it can be seen that there is a salinity "boost" in the modified subtropical surface layers of CTD stations 42 and 43 (north of the BSAF) of the *AJAX* data set. This boost of 0,07 psu in the top 100 m is assumed to be due to salinity enrichment as a result of evaporation. Rigg (1995) analysing *SCARC* data, has identified boosting in Agulhas rings and eddies shed at the retroflection and composed of a Modified type of Surface Water (MSSW). However, Rigg's (1995) "boosting" occurs between 17°C-20,5°C compared between 15,5°C-16,6°C, seen in the *AJAX* dataset. This reduction is undoubtedly due to heat lost in the surface waters. During SAVE-4 Agulhas eddies with stads consisting of slightly saltier remnant winter mixed layers modified by air-sea interaction were identified at 2°E and 6°E by Gordon et al. (1992).

South of the BSAF, water within the 9°C-14°C thermal layer has salinity well below the SACW thermocline curve. This modification is due to the gradual capping of low-salinity Sub-Antarctic Surface Water (SAASW) as stations move further south, as can be seen from the $T/O_2$ plot which shows a surface increase of approximately 1 ml/l between CTD stations 44-45. At colder temperatures ($>10$ °C and below density 26,75 $\sigma t$) the SACW becomes slightly fresher compared to the SICW in the Agulhas Current inflow. This is due to the presence of a greater concentration of low-salinity AAIW, which flows eastwards from it's formation at the Antarctic Polar Front and penetration into the Atlantic Ocean through the Drake Passage.

Comparing properties along the 27,25 $\sigma t$ density line it can be seen that a large modification in the Intermediate AAIW water mass occurs. Salinity and oxygen values range from 34,39 psu and 5 ml/l in the Agulhas Current to between 34,22-34,30 psu and 5,2-5,8 ml/l in the *AJAX* dataset. The AAIW stratum shows water to the south of the BSAF to be fresher and more oxygenated than to the north. This enrichment of low-salinity, high oxygen AAIW water mass south of the BSAF and west of the retroflection region is due to the direct supply of newly formed AAIW from it's formation region; the subantarctic zone in the southwest of the South Atlantic (Piola and Gordon 1989). There is no evidence of high saline RSW in the AJAX dataset confirming that remnant RSW is restricted to within the Agulhas Current inflow (Gründlingh 1985).

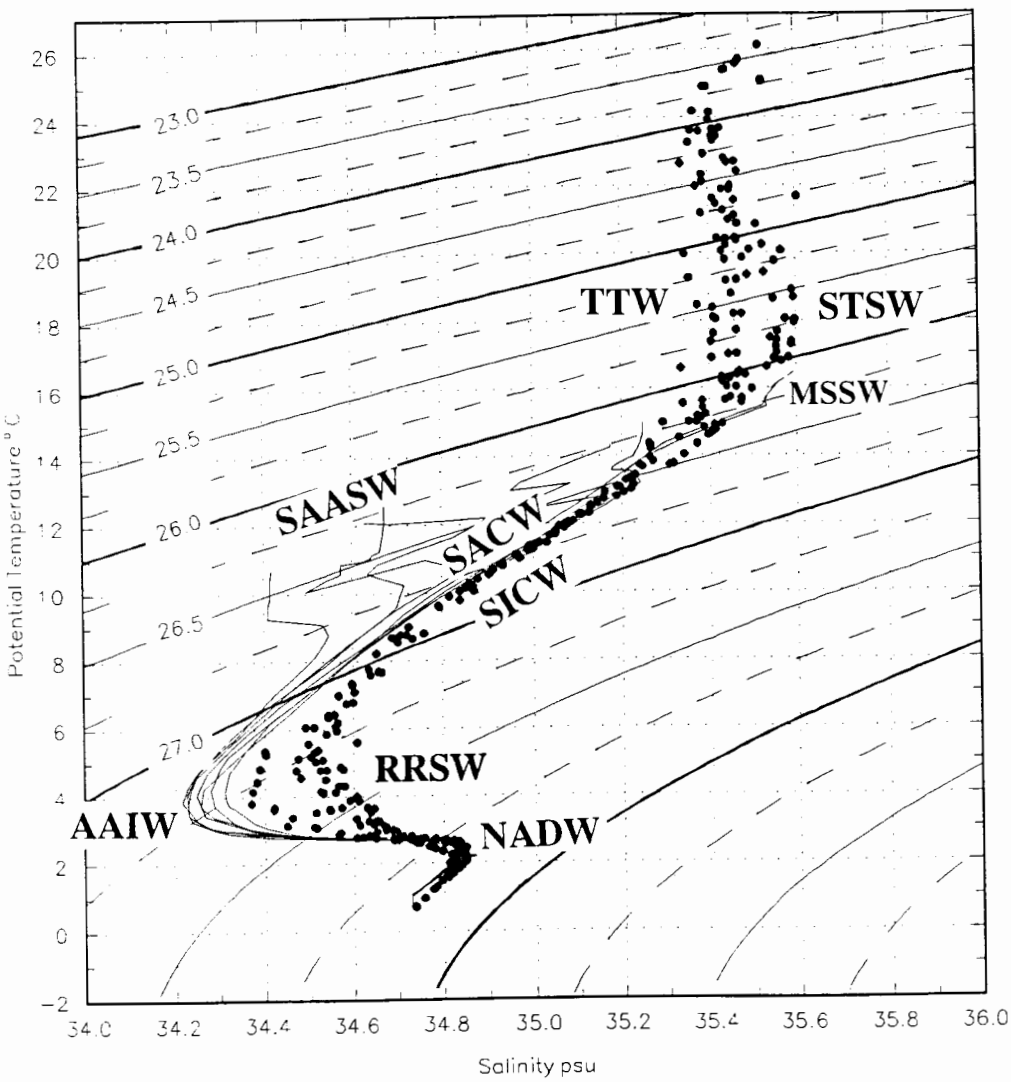


Figure 7.5a: T/S plot comparing the Agulhas Inflow CTD stations; *ARC* 49 and 50, *SCARC* 56 and *Marathon* 258, 259, 274-276 (black dots) to the *AJAX* CTD stations 42-48 (solid lines). Abbreviations are given for Sub-Tropical Surface Water (STSW), Tropical Thermocline Water (TTW), Modified Surface Water (MSSW), Sub-Antarctic Surface Water (SAASW), South Atlantic Central Water (SACW), South Indian Central Water (SICW), Remnant Red Sea Water (RRSW), Antarctic Intermediate Water (AAIW) and North Atlantic Deep Water (NADW).

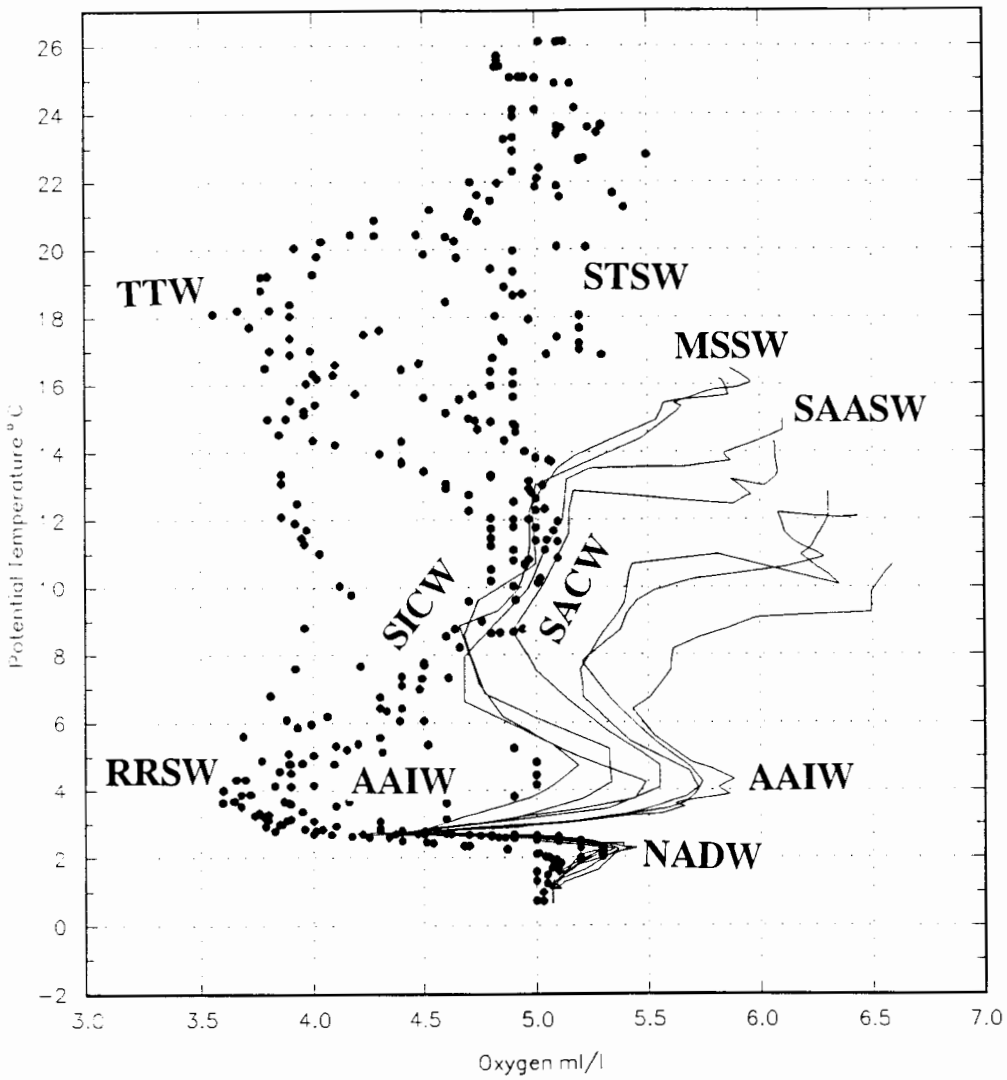


Figure 7.5b: $T/O_2$ plot comparing the Agulhas Inflow CTD stations; *ARC* 49 and 50, *SCARC* 56 and *Marathon* 258, 259, 274-276 (black dots) to the *AJAX* CTD stations 42-48 (solid lines). Abbreviations are given for Sub-Tropical Surface Water (STSW), Tropical Thermocline Water (TTW), Modified Surface Water (MSSW), Sub-Antarctic Surface Water (SAASW), South Atlantic Central Water (SACW), South Indian Central Water (SICW), Remnant Red Sea Water (RRSW), Antarctic Intermediate Water (AAIW) and North Atlantic Deep Water (NADW).

*(b) The Retroflection Region*

The retroflection region serves as a ventilation window for the southwestern Indian Ocean gyre, where mixing between South Indian and South Atlantic water masses occurs. It can be seen from figures 7.7a and b that in the surface layers above 26,50 $\sigma$t and in the intermediate layers below 26,75 $\sigma$t a slight modification in the water properties has occurred. Fine et al. (1988) in comparing CFC concentrations between inflow (Agulhas Current stations) and outflow stations, found the outflow stations to be fresher and colder as a result of the mixing and exchange of substantial amounts of South Atlantic water.

Differences between the Southwest Indian and Southeast Atlantic Central Waters (SACW, SICW), in the retroflection region, unlike water masses above 26,50$\sigma$t and below 26,75$\sigma$t, are difficult to determine because of their similar T/S characteristics. Indeed, Gordon (1985) and Fine et al. (1988) suggest that the similar T/S characteristics of the South Atlantic and South Indian thermoclines are a result of the active mixing/exchange across the Agulhas retroflection region. In agreement with Rigg (1995), for the purpose of this thesis then, no attempt has been made to resolve the identity of the Central waters in this region and have been labeled SICW, consistent with the results of Gordon et al. (1987) and Holford (1990). Both fresh (SACW) and saline (SICW) varieties of Central Water can be identified in the T/S plots. Rigg (1995) has therefore labeled this band of water mass as Modified Central water (MCW) in the Central/thermocline water layer due to the similarity in physical properties of the SACW and SICW

Although the Agulhas Return Current was crossed on a number of occasions during *ARC* and *Marathon* cruises, CTD stations 52 and 55 (*ARC*) and CTD stations 280 and 287 (*Marathon*) best represent the current, as can be seen from figures 5.8a and b d, 5.11a and b and 5.12a and b, in chapter 5. These stations are the closest to lying within the axis of the Agulhas Return Current. The location of these stations can be seen in figure 7.6.

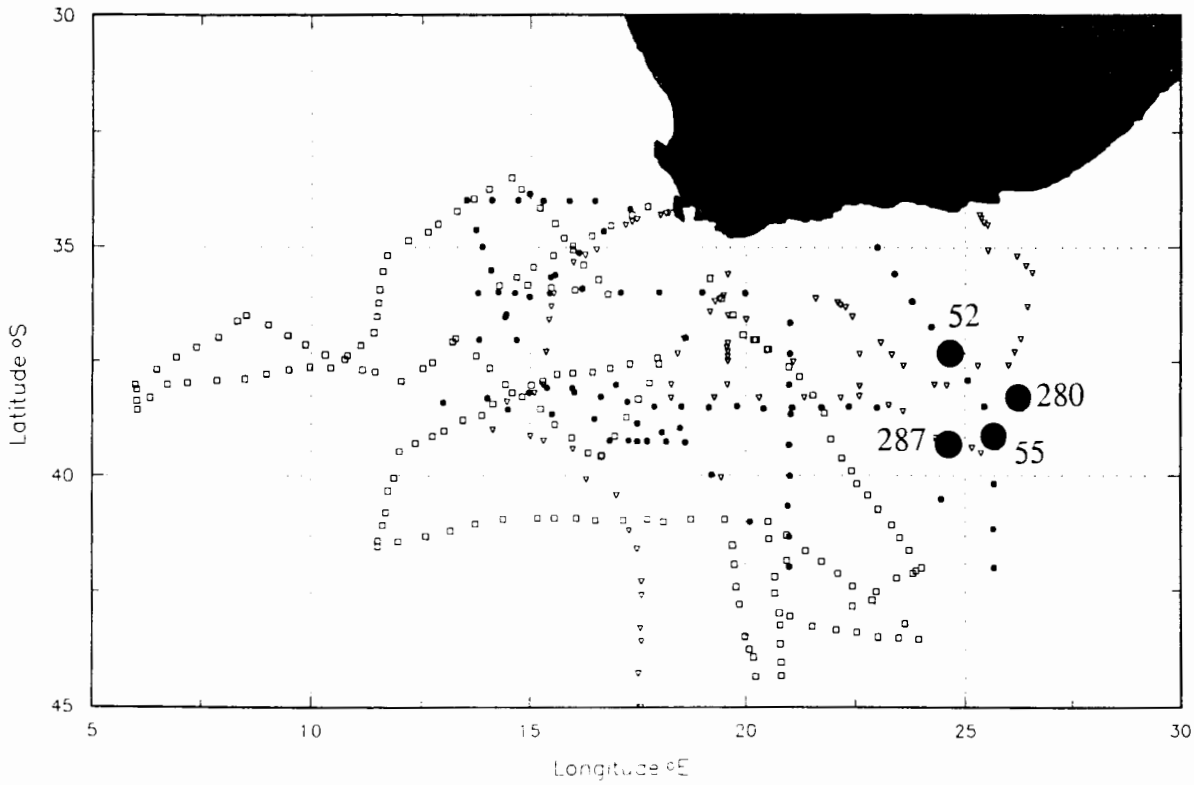


Figure 7.6: Distribution of Agulhas Return Current (outflow) CTD stations from *ARC* 52 and 55 and *Marathon* 280 and 287.

The stations occupied during *ARC* lie within the Agulhas Return Current as it executes a sharp S-shaped meander around the Agulhas Plateau. CTD station 52 (37°19'S) lies on the northern flank of the Agulhas Plateau as the Agulhas Return Current, having been deflected equatorwards, flows eastwards before turning poleward and completing it's meander, while CTD station 55 (39°09'S) is situated further south at the onset of this deflection. CTD stations 280 and 287 lie in similar positions, as can be seen from figure 7.6, to CTD stations 55 and 52, with CTD station 287 on the eastern flank of the Agulhas Plateau and CTD stations 280 more towards the northern edge.

***Intercomparison between Agulhas Current (inflow) stations and ARC/Marathon (outflow) stations***

*Surface water masses*

Comparing the T/S and $T/O_2$ plots of the Agulhas Current and Agulhas Return Current CTD stations it can be seen that TSW, which is present in the inshore edges of the Agulhas Current (Gordon et al. 1987) is no longer evident in CTD stations 52 and 55 of *ARC* and CTD stations 280 and 287 of *Marathon* as can be seen from the figures 7.7a and b. It is therefore tempting to surmise that it has been eroded along it's course through the retroflection. As a result the water masses remaining within the surface layers (above 26,5 $\sigma t$) of the Agulhas Return Current are Subtropical Surface Water (STSW) and Tropical Thermocline Water (TTW).

STSW found in the surface waters above 25,80$\sigma t$, between 17-20°C and between 35,50 psu-35,60 psu in the Agulhas Current inflow is also visible in CTD stations 52 (*ARC*) and TW 280, 287 (*Marathon*), but at a slightly reduced (approximately 0,015 psu) salinity value. This freshening has possibly occurred as a result gradual heat loss to the atmosphere of possibly by mixing with fresher South Atlantic water masses during the retroflection (Gordon 1985, Gordon et al. 1987, Fine et al. 1988). Using CFM 11 tracers, Fine et al.(1988) was able to confirm this showing that at the same density the Agulhas Return Current had larger CFM-11 values than the Agulhas Current (from 0,52 at CTD station 49 inflow to 0,82 CTD station 52), due to the admixture with recently ventilated water formed in the retroflection region.

Comparing *ARC* to *Marathon* data it can be seen that CTD stations 52, 280 and 287 display very similar surface characteristics, suggesting that these three represent typical Agulhas Return Current characteristics, while CTD station 55 south of the Plateau consists of TTW, which is believed by Rigg (1995) to be a mixture of the warm STSW and fresher SAASW. This mixture may possibly be due to possible "contamination" of SAASW as

large indentations in the STC, pulling this water mass equatorwards, occur as a result of the Agulhas Return Current's deflection around the Plateau (Lutjeharms and Valentine 1988).

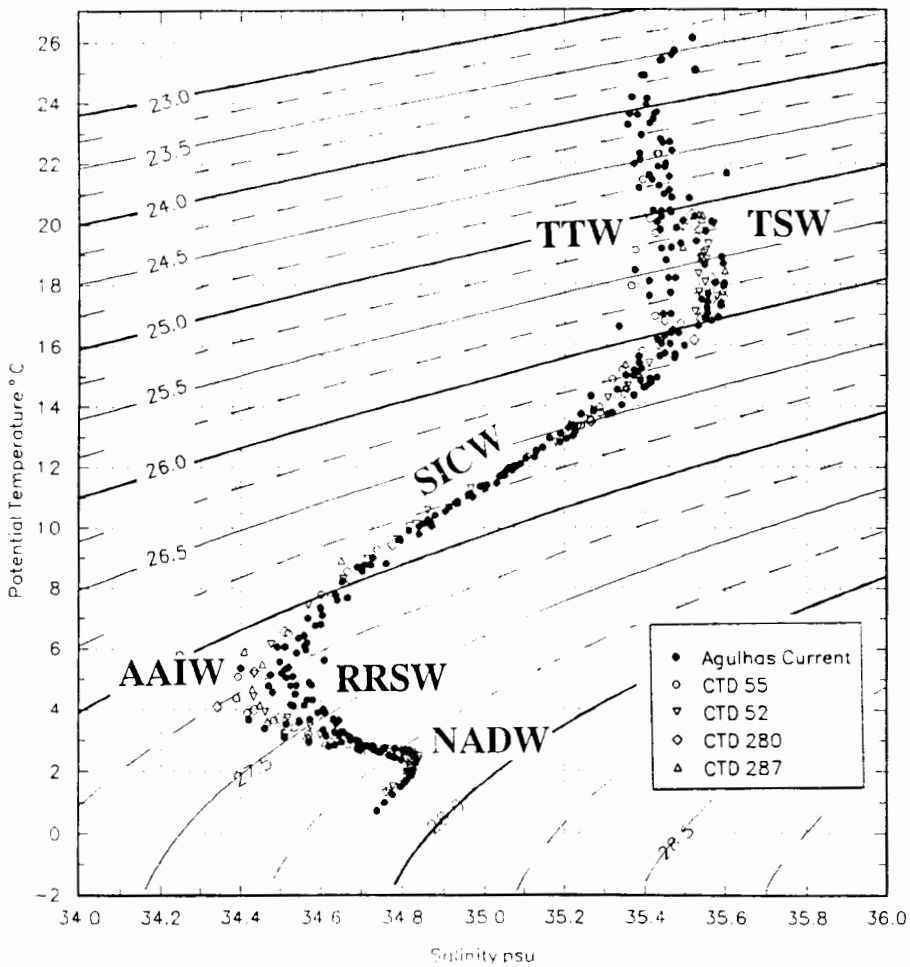


Figure 7.7a: T/S plot comparing the Agulhas Inflow CTD stations; *ARC* 49 and 50, *SCARC* 56 and *Marathon* 258, 259, 274-276 (black dots) to the *ARC* CTD stations 52 (upturned triangle) and 55 (circles) and *Marathon* CTD stations 280 (diamond) and 287 (triangle). Abbreviations are given for Sub-Tropical Surface Water (STSW), Tropical Thermocline Water (TTW), South Indian Central Water (SICW), Remnant Red Sea Water (RRSW), Antarctic Intermediate Water (AAIW) and North Atlantic Deep Water (NADW).

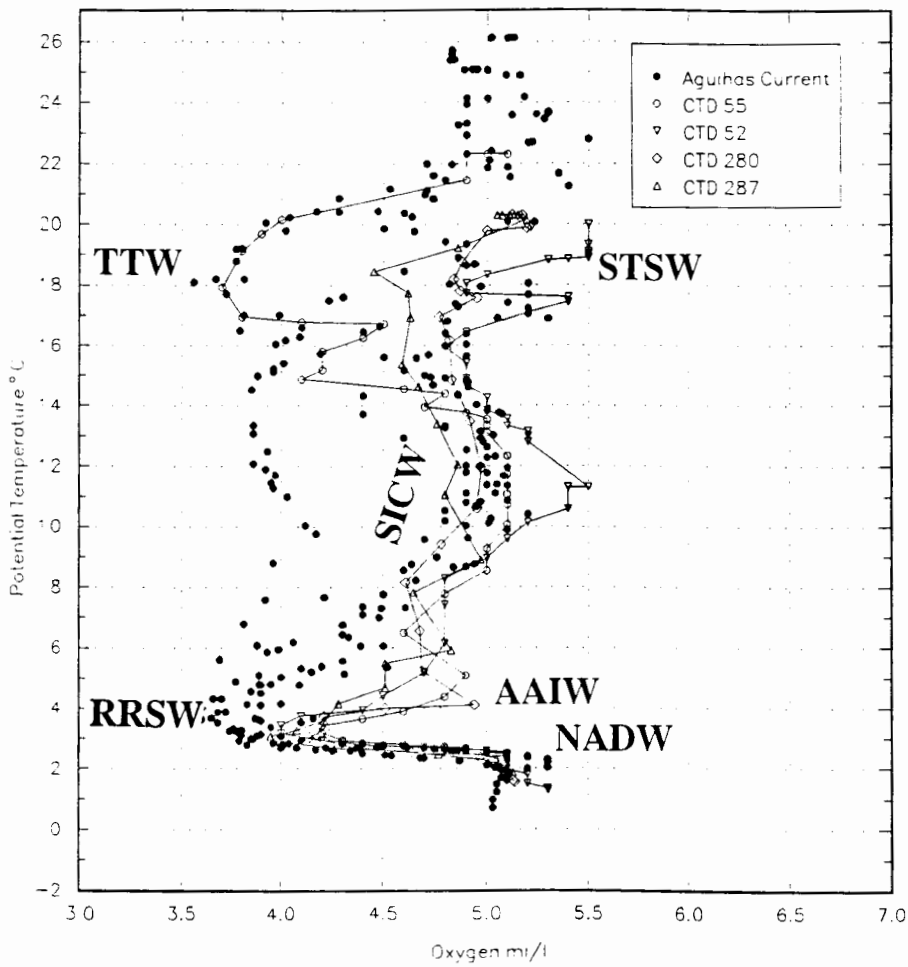


Figure 7.7b: $T/O_2$ plot comparing the Agulhas Inflow CTD stations; *ARC* 49 and 50, *SCARC* 56 and *Marathon* 258, 259, 274-276 (black dots) to the *ARC* CTD stations 52 (upturned triangle) and 55 (circles) and *Marathon* CTD stations 280 (diamond) and 287 (triangle). Abbreviations are given for Sub-Tropical Surface Water (STSW), Tropical Thermocline Water (TTW), South Indian Central Water (SICW), Remnant Red Sea Water (RRSW), Antarctic Intermediate Water (AAIW) and North Atlantic Deep Water (NADW).

A shallow oxygen minimum at approximately 18°C comparable, to the Agulhas inflow stations, can be identified in all four CTD stations. Comparing stations, it can be seen that there is a large difference in concentration values between the stations CTD 52, 280 and 287, 4,4 ml/l-4,8 ml/l, which consist of STSW in it's surface layers and CTD station 55 3,75 ml/l, consisting of TTW. This shallow oxygen minimum occurs predominantly in the

TTW and forms as a result of density changes that occur across the thermocline in tropical and subtropical waters (Chapman 1988). It is within these regions that organic matter tends to accumulate (Biggs and Wetzel 1968, Harder 1968). The density stratification tends to prevent oxygen diffusion through the water column resulting in oxygen depletion during the decay of this organic matter. Chapman (1988) suggests that this shallow oxygen minimum can be used as a possible trace of Agulhas Water.

Comparing *SCARC* and *Discovery 165A* datasets Rigg (1995) has shown that STSW dominates the interior of the retroflection loop and is a dominant signal at the northern edge of the Agulhas Return Current. Consequently it is more difficult to define the northern boundary of the Agulhas Return Current due to the similarities in T/S properties, than it is for the southern boundary where STSW lies adjacent to cooler fresher Sub-Antarctic surface water masses.

*Intermediate Water Masses*

Fine et al. (1988) has shown that the South Atlantic Intermediate waters were more recently ventilated than the South Indian thermocline and Intermediate waters. This is partially because South Atlantic waters, some originating in the subantarctic sector, are transported eastward via the Agulhas retroflection to the South Indian Ocean. The South Indian Ocean is further downstream from the source regions of the South Atlantic subantarctic sector

The Intermediate waters of the retroflection region are surprisingly diverse as a consequence of low-salinity AAIW mixing with high-salinity remnant RSW. Because these two Intermediate Water masses display contrasting properties, identification is relatively simple. At 27,25$\sigma$t a broad band of salinities 34,53 psu-34,39 psu and oxygen concentrations 3,6 ml/l- 5 ml/l, is encountered with AAIW lying close to the 34,40 psu 5 ml/l and RSW occupying 34,53 $\pm$0,01 psu 3,6 ml/l.

Jacobs and Georgi (1977) noted that in the retroflection region AAIW is strongly eroded by high salinity intrusions due to mixing with the highly saline remnant RSW (RRSW), resulting in AAIW within the Agulhas Return Current to be generally fresher and more oxygenated than in the Agulhas Current inflow. Between these two extremes (AAIW and RRSW) lies a host of AAIW/RRSW mixtures. AAIW found in CTD stations 52, 55 of *ARC* and CTD 280,287 of *Marathon* (figures 7.7a and b) has a salinity range of 34,4 at 27,25 $\pm$0,1 $\sigma$t. CTD station 55 appears to be slightly less saline than the other three stations and this is undoubtedly due to it's location on the southern flank of the Agulhas Plateau close to the STC and fresher Sub-Antarctic water masses.

*Deep water*

Distinctions between the deep waters of the retroflection region are difficult to make because if the mixing of the NADW (salinity-oxygen maximum) with the UCDW (oxygen minimum) above and LCDW (oxygen minimum) below. From the T/S plot the "knee" of the high saline NADW is clearly distinguishable in all CTD stations. Salinity within the deep salinity maximum core layer is closer to that of NADW than IDW and indicates that the latter is more prominent in the retroflection region (Gordon et al. 1987). Comparing to the LCDW masses in the Agulhas inflow it can be seen that there is evidence of this oxygen minimum layer, although CTD station 55 appears to be more oxygenated 4,3 ml/l than the other three stations, as a result of contamination with fresher sub-antarctic water masses.

***(b) East of the retroflection zone***

East of the retroflection zone, the Agulhas Return Current continues it's passage zonally across the South Indian Ocean at approximately 40°S, to as far east as 76°E (Belkin and Romanov 1990, Park et al. 1993 and Belkin and Gordon 1994). During it's passage, it gradually weakens through heat loss and interaction with cooler/fresher water masses as well through topographically induced northward branches "peeling" Agulhas water away from the main current body (Park et al. 1993 and Stramma and Lutjeharms 1995).

To investigate this gradual modification in the Agulhas Return Current during it's passage, T/S and $T/O_2$ plots associated with selected stations occupied during the *Discovery 164* and *SUZIL* cruises are analyzed. The positions of the selected stations can be seen below in figure 7.8.

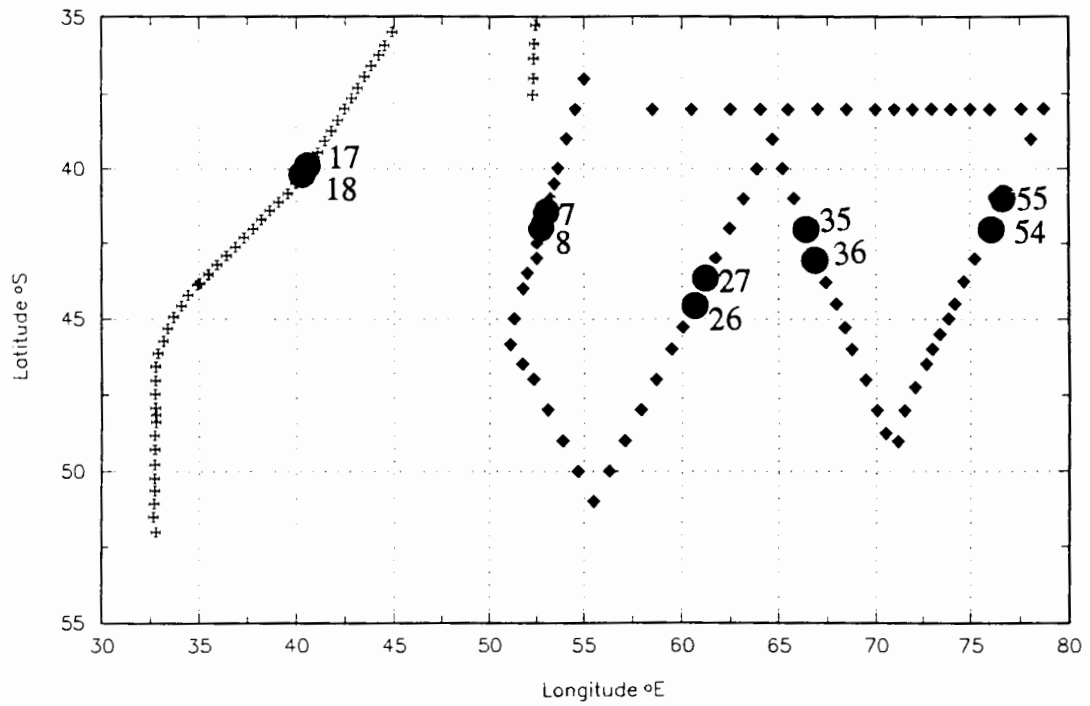


Figure 7.8: Distribution of *Discovery 164* CTD stations 17-18 and *SUZIL* CTD stations 7-8, 26-27, 35-36 and 55-56 located within the Agulhas Return Current.

*Intercomparisons between Discovery*

During *Discovery 164* the Agulhas Return Current was crossed at approximately 40°E. From the sections in chapter 5, figures 5.18a and b, it can be seen that a double front consisting of a separate AF and STC between CTD stations 17-23 is encountered. CTD stations 17-18 span the AF with water masses comparable to the Agulhas Return Current in the retroflection region (CTD 52, 280 and 287) lying in-between, as can be seen from

figures 7.9a and b. To the south of CTD station 18 lies a cyclonic eddy. Further proof of it's presence can be seen from previous geostrophic calculations (see **Geostrophic Velocities and Volume Transported by the Agulhas Return Current**, chapter 6), which show both east and west velocity and transport components between CTD stations 18-22. Read and Pollard (1993) suggest that this eddy could have propagated downstream from the Agulhas retroflection and is Agulhas water which has become modified through contamination with SAASW.

*Surface water masses*

As the AF is crossed a significant change in the surface water masses occurs. Marking the northern boundary of the Agulhas Return Current/AF, CTD station 17 consists of STSW in the surface layers. Values range between 18°C-20°C with a salinity maximum of between 35,60 psu-35,63 psu, this "boost" is caused by excessive evaporation. Marking the southern boundary of the AF and consisting of slightly cooler and fresher surface water masses, 16°C-18°C and ~35,35 psu, similar to TTW, is CTD station 18. This compares well with investigations by Darbyshire (1966) who identified water in excess of 14°C and between 35,30-35,35 psu as "Agulhas Water". In the $T/O_2$ plots (figure 7.9b) CTD station 17 displays a shallow oxygen minimum of 4,7 ml/l at 16°C, while at CTD station 18 this minimum seems to have been eroded away.

I therefore propose, that Agulhas water found between CTD stations 17 and 18 at 40°E, has become a mixture of STSW and TTW during it's passage eastwards. This compares well with stations lying in the retroflection area, as can be seen by figure 7.9a all stations other than CTD station 55 appear to "nestle" along the STSW line between 17°C-20°C and 35,5 psu-25,6 psu, while CTD station 55 is composed of TTW in it's surface layers.

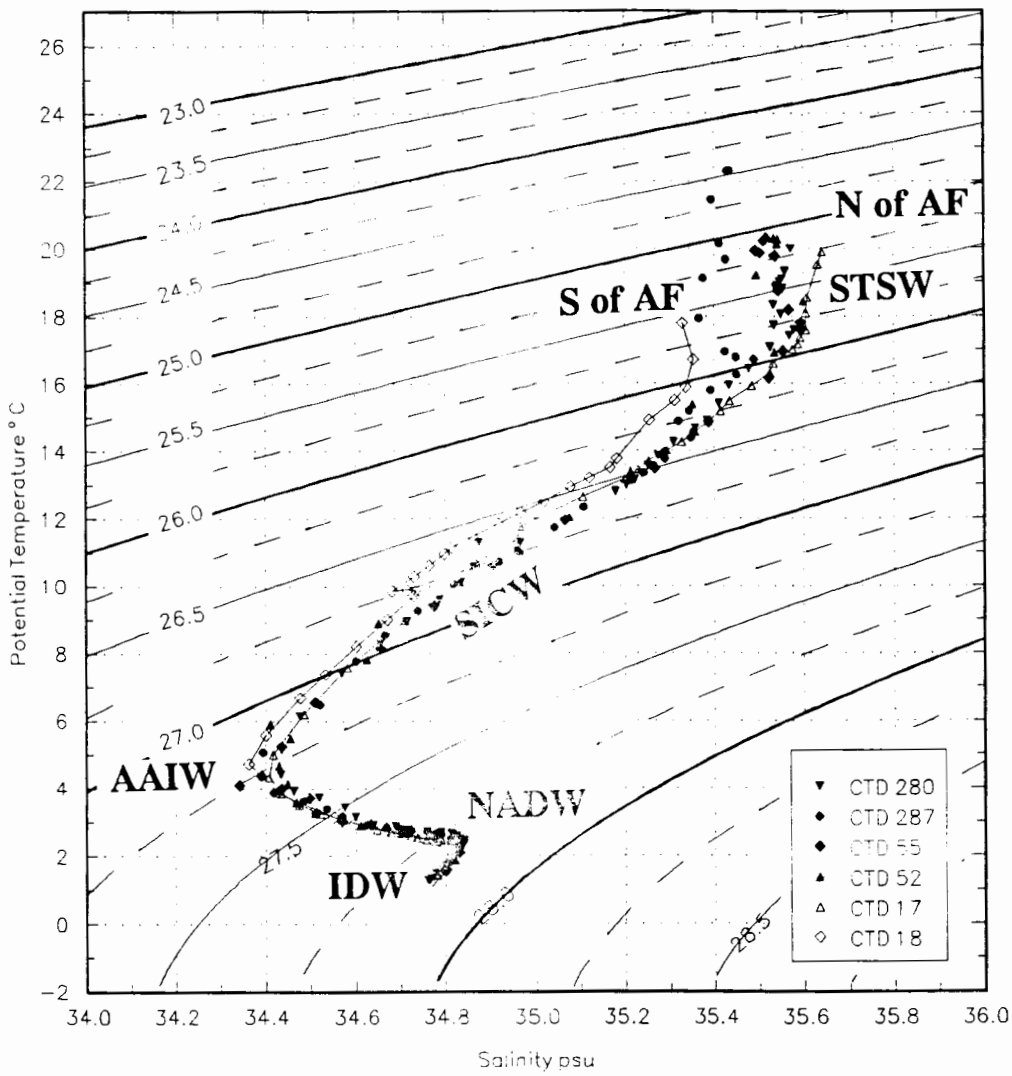


Figure 7.9a: T/S plot comparing the Agulhas Return Current CTD stations; *ARC* 52 and 55 and *Marathon* 280 and 287 to the *Discovery 164* CTD stations 17 and 18. Abbreviations are given for Sub-Tropical Surface Water (STSW), Agulhas Water (AW), Sub-Antarctic Surface Water (SAASW), South Indian Central Water (SICW), Antarctic Intermediate Water (AAIW) and Indian Deep Water (IDW).

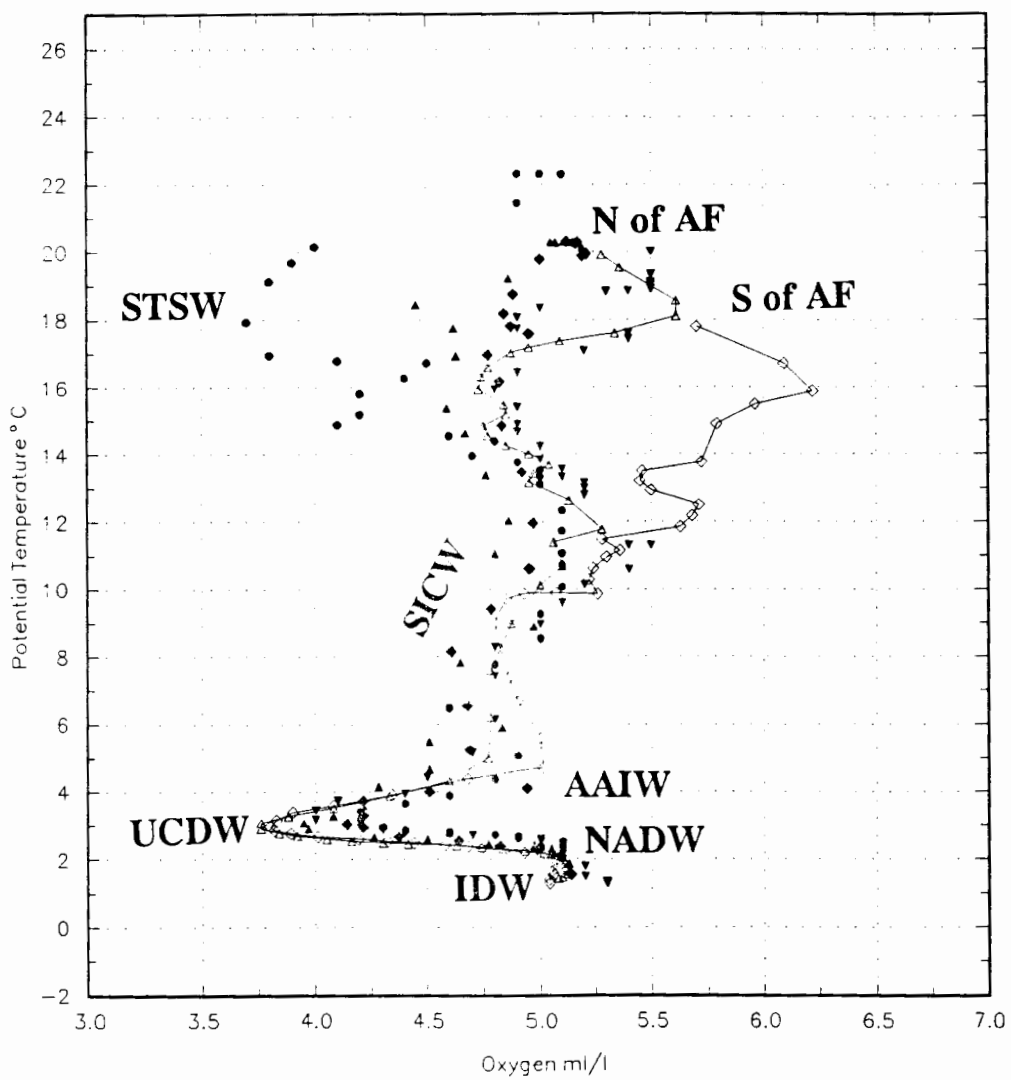


Figure 7.9b: $T/O_2$ plot comparing the Agulhas Return Current CTD stations; *ARC* 52 and 55 and *Marathon* 280 and 287 to the *Discovery 164* CTD stations 17 and 18. Abbreviations are given for Sub-Tropical Surface Water (STSW), Agulhas Water (AW), Sub-Antarctic Surface Water (SAASW), South Indian Central Water (SICW), Antarctic Intermediate Water (AAIW), Indian Deep Water (IDW) and Upper Circumpolar Deep Water (UCDW).

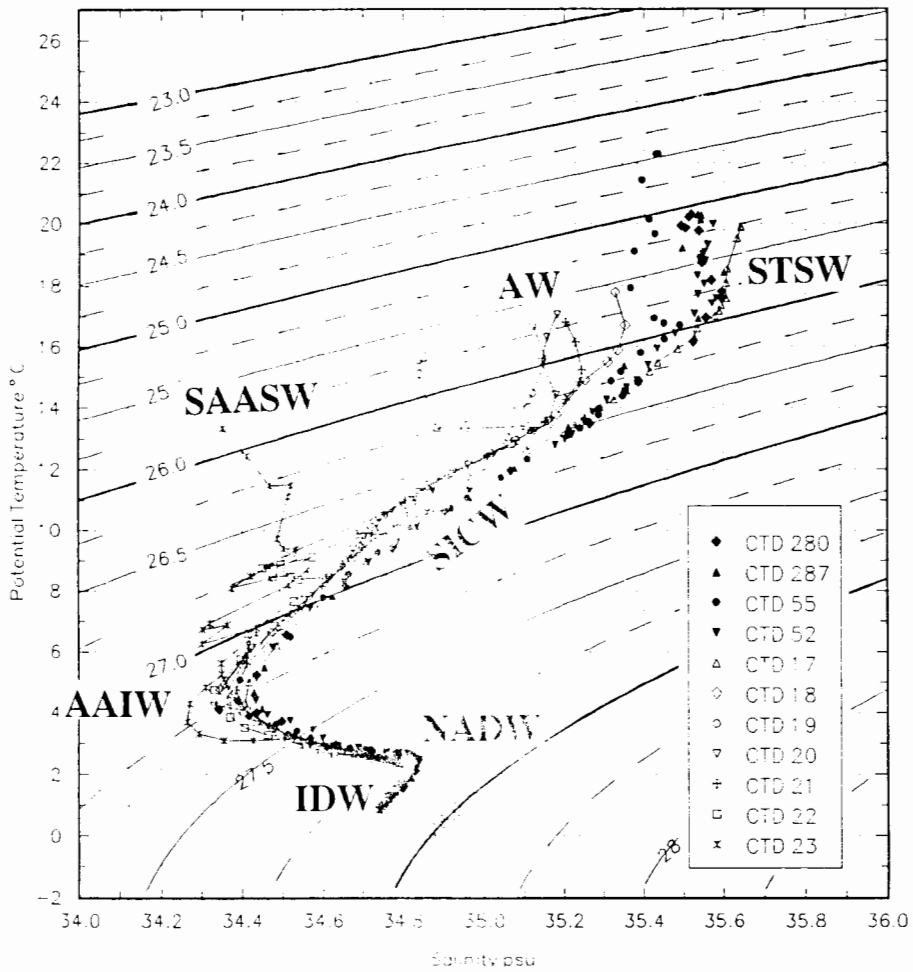


Figure 7.10a: T/S plot comparing the Agulhas Return Current CTD stations; *ARC* 52 and 55 and *Marathon* 280 and 287 to the *Discovery 164* CTD stations 17-21 spanning the frontal zone. Abbreviations are given for Sub-Tropical Surface Water (STSW), Agulhas Water (AW), Sub-Antarctic Surface Water (SAASW), South Indian Central Water (SICW), Antarctic Intermediate Water (AAIW) and Indian Deep Water (IDW).

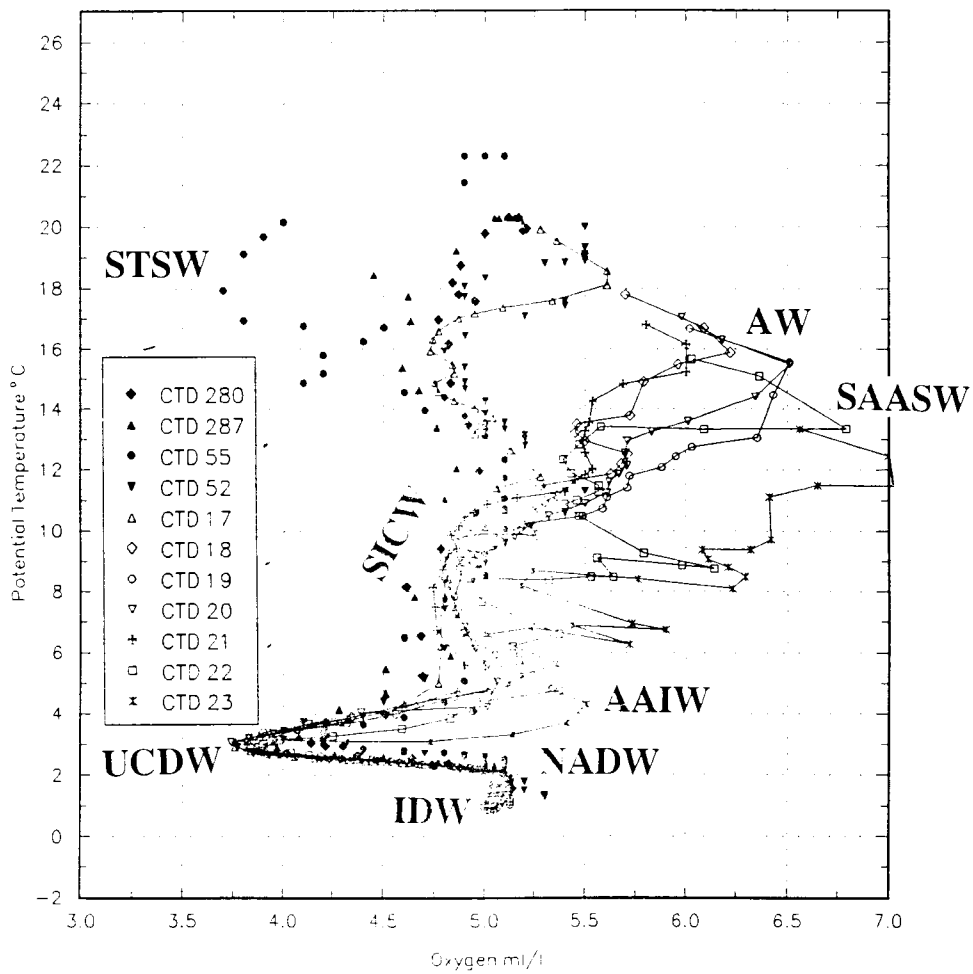


Figure 7.10b: $T/O_2$ plot comparing the Agulhas Return Current CTD stations; *ARC* 52 and 55 and *Marathon* 280 and 287 to the *Discovery 164* CTD stations 17-21 spanning the frontal zone. Abbreviations are given for Sub-Tropical Surface Water (STSW), Agulhas Water (AW), Sub-Antarctic Surface Water (SAASW), South Indian Central Water (SICW), Antarctic Intermediate Water (AAIW), Indian Deep Water (IDW) and Upper Circumpolar Deep Water (UCDW).

Between CTD stations 18-21 within the cyclonic eddy, surface waters ranging between 14-18°C and 35,1 psu-35,35 psu identify with a cyclonic eddy formed in the frontal zone and consisting of modified Agulhas Water, see figures 7.10a and b. In the surface layers (26,00$\sigma$t), temperatures change from 16,5°C and 35,5 psu at CTD 17 north of the AF to 15°C and 35,15 psu at CTD 21, the southern edge of the cyclonic eddy.

*Central Waters*

It appears that there is a gradual freshening of the Central waters as the Agulhas Return Current and frontal zone are crossed. CTD station 17 displays a tight Central thermocline comparable to the SICW found in the Agulhas Current inflow stations, as can be seen from figures 7.9a and b. Further south between CTD stations 18-21, a gradual decrease occurs from 11°C to 10°C and 34,88 psu to 34,7 psu along 26,75 $\sigma$t, as the water column becomes modified by surrounding water masses (figures 7.10a and b).

*Intermediate water masses.*

AAIW found between CTD 17-18 is far less saline (0,08 psu along 27,25$\sigma$t) than the AAIW associated with the Agulhas Return Current stations, as can be seen from figure 7.9a. Crossing the Agulhas Return Current, a decrease of 0,01 psu along 27,25 $\sigma$t occurs between CTD stations 17 and 18 (figure 7.9a). Temperatures decrease from 5°C to 4°C and 34,4 psu to 34,35 psu across the frontal zone CTD stations 17-21 (figure 7.10a). This gradual freshening occurs with stations becoming closer to the source region of the AAIW: the Subantarctic Zone. As the AAIW crosses the Subantarctic Zone the pronounced salinity minimum, associated with it, is gradually eroded and reduced by mixing (Read and Pollard 1993).

***Intercomparisons with SUZIL***

*SUZIL* was carried out in order to investigate the confluence and topographical steering of the Antarctic Circumpolar Current in the Crozet Basin. To accomplish this, four near meridional sections between 37°S-51°S and 50°E-80°E and a zonal line at 38°S were

occupied (see **Data and Methodology**, chapter 4). During the sections the AF was shown to initially merge with the STC and SAF, forming an intensive single-band frontal zone, separating warm saline Agulhas water from fresher Sub-Antarctic water masses. East of 67°E the Agulhas Return Current is shown to become separated again flowing north of the frontal zone. Current speeds decrease rapidly with distance east (see chapter 6) indicating the gradual weakening of the Agulhas Return Current as northward branches slowly "peel" Agulhas water away from the main body. Comparing T/S and $T/O_2$ plots from selected stations (CTD 7, 27, 35 and 55) within the Agulhas Return Current it can be seen that the current becomes significantly cooler and fresher (Park et al. 1993).

*Surface waters*

Above the 26$\sigma$t, surface waters associated with CTD station 7 (~53°E) consist of STSW characterised by high temperature and salinity values, 16°C-18,5°C and 35,57 psu and is comparable to the Agulhas Return Current stations (CTD 52, 280 and 287) within the retroflection region. Further downstream at CTD station 27 (61°11'E), the surface waters still consist of STSW but have become cooler by 2°C and fresher by 0,02 psu, indicating a substantial downstream decrease in the Agulhas Return Current's strength as a result of northward branching and interaction with surrounding water masses (Park et al. 1993). Comparing to T/S plots located upstream in the retroflection region (CTD stations 52, 280 and 287), it can be seen that above 26,50$\sigma$t, CTD stations 7 and 27 in the Crozet Basin are more saline (0,09 psu).

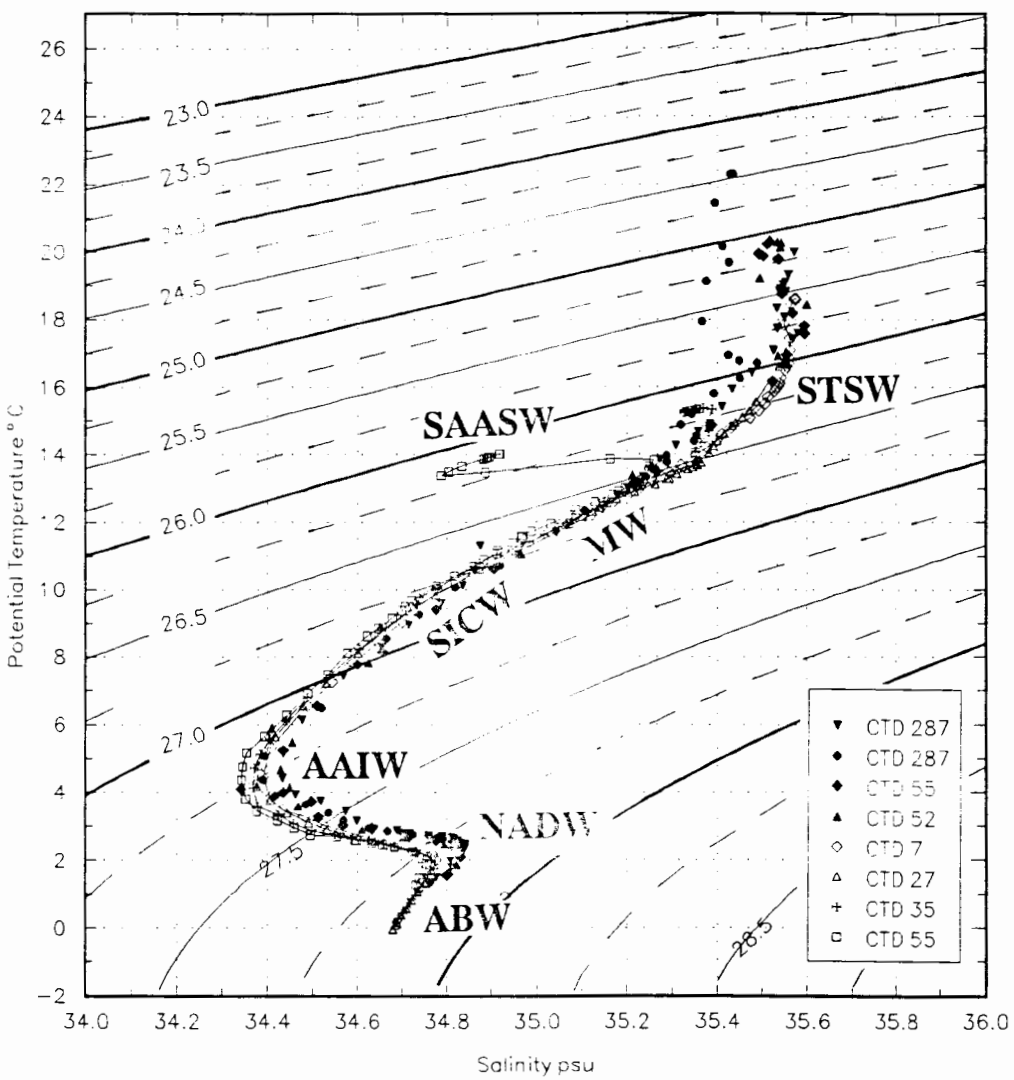


Figure 7.11a: T/S plot comparing the Agulhas Return Current CTD stations; *ARC* 52 and 55 and *Marathon* 280 and 287 to the *SUZIL* CTD stations 7, 27, 35 and 55. Abbreviations are given for Sub-Tropical Surface Water (STSW), Mode Water (MW), Sub-Antarctic Surface Water (SAASW), South Indian Central Water (SICW), Antarctic Intermediate Water (AAIW), North Atlantic Deep Water (NADW) and Antarctic Bottom Water (ABW).

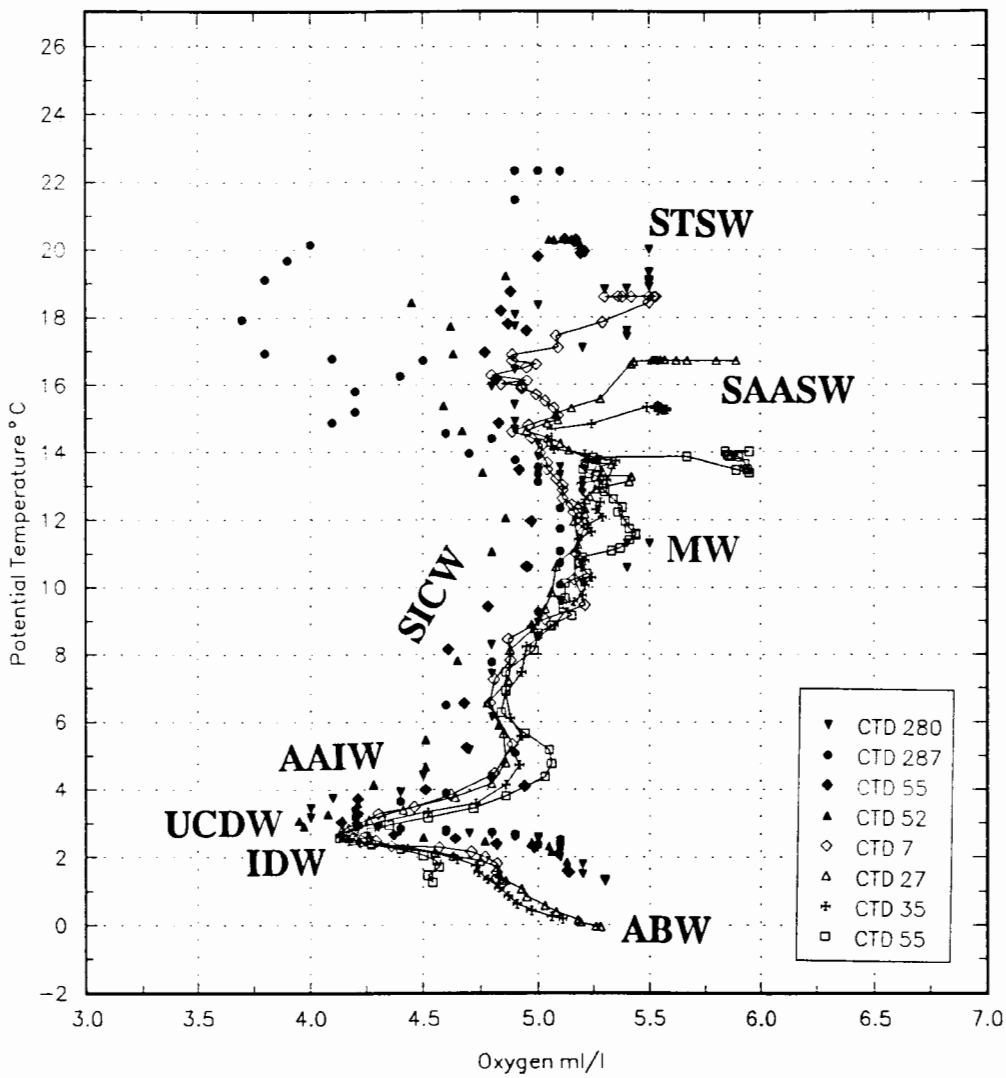


Figure 7.11b: $T/O_2$ plot comparing the Agulhas Return Current CTD stations; *ARC* 52 and 55 and *Marathon* 280 and 287 to the *SUZIL* CTD stations 7, 27, 35 and 55. Abbreviations are given for Sub-Tropical Surface Water (STSW), Sub-Antarctic Surface Water (SAASW), Mode Water (MW), South Indian Central Water (SICW), Antarctic Intermediate Water (AAIW), Indian Deep Water (IDW), Upper Circumpolar Deep Water (UCDW) and Antarctic Bottom Water (ABW).

Progressing eastward from 67°E to 76°E (CTD stations 35 and 55) the surface waters become fresher/colder and more oxygenated as a result of capping with SAASW, figures 7.11 a and b, resulting in a salinity maximum near the base of the pycnocline, at about 150 m depth (Park et al. 1993). It is possible that this "capping" is attributed to the equatorward flow of SAASW as a result of meandering northward branches. This agrees well with the geostrophics associated with the zonal section at 38°S, which shows a northward flow at 67°E, a similar as CTD station 37 (66°22'E).

*Mode Water*

Mode Water (MW) is formed by the deep winter convection in the area immediately north of the Antarctic Circumpolar Current and appears as a pycnostad beneath the seasonal thermocline, during the summer months. Mode waters are situated between 26,5$\sigma$t-26,7$\sigma$t and at a depth range of 200-600 m (Park et al. 1993). Associated with this pycnostad is a subsurface oxygen maximum centered at 300-500m.

Analysing the *SUZIL* data it can be seen that CTD stations 7, 27, 35 and 55 all display MW characteristics around 26,5$\sigma$t, with values ranging from 13,68°C 35,318 psu at CTD station 7 to 13,41°C 35,223 psu at CTD station 55. Mode water characteristics are dependent on the surroundings in which they form. Winter overturning of subtropical Agulhas origin water (CTD stations 7 and 27) will produce warmer and more saline water characteristics from one formed further downstream (Park et al. 1993).

*Central waters*

Comparing the thermoclines associated with CTD stations 7, 27, 35 and 55 it can be seen that there is a gradual freshening downstream (0,05 psu) as the Agulhas Return Current is slowly modified with the surrounding water masses. Comparing to the Central waters in the retroflection zone it can be seen that in the upper portion above 26,75 $\sigma$t of the thermocline T/S properties are very similar with a gradual freshening of 0,13 psu occurring

below 27$\sigma$t. A possible reason for this freshening may be due to the influence of more recent low salinity AAIW.

*Intermediate Water*

AAIW is best characterised by a deep salinity minimum centered around 27,25$\sigma$t. Further east (CTD station 55) the AAIW 4,28°C 34,34 psu is significantly cooler and fresher than in the western-most section (CTD station 7) 4,47°C, 34,39 psu, suggesting that a modification has occurred within the Crozet Basin. This modification can be seen by CTD station 35 which shows a tongue like protrusion of low salinity AAIW 4,135°C 34,37psu across the frontal zone. Data collected during *ANTARES-1* in 1993 reveals unprecedented strong cross-frontal injections of newly formed AAIW into the subtropical zone north of the Agulhas Return Current (Park and Gamberoni 1995).

It is possible that the northward recirculation of the Agulhas Return Current in the Crozet Basin (Park et al. 1993, Stramma and Lutjeharms 1995) is a major carrier of the injected AAIW within the subtropical gyre circulation of the Indian Ocean. This would also agree with Molinelli (1981) who suggests that the region near the Kerguelan Plateau is a source of AAIW entering the Indian Ocean.

# Chapter 8
# CONCLUSION

Past experiments using buoy trajectories (Stravopoulos and Duncan 1974, Gründlingh 1978, Luyten 1985), satellite imagery (Harris et al. 1978, Lutjeharms 1981a, Lutjeharms and Valentine 1988, Lutjeharms 1989, Meeuwis 1991), subsurface hydrographic measurements (Luyten 1985) and hydrographic datasets (*AJAX, SCARC, ARC, Marathon, Discovery #164, SUZIL, FIBEX, Marion 83* and *Gallieni*), have all revealed certain specific elements of the flow of the Agulhas Return Current, from the retroflection region to 76°E. However, no comparison has ever been made between these modern datasets and they have also never been combined to study the Agulhas Return Current as an entity. As a result physical modifications arising with distance downstream from the retroflection have never been accurately documented.

The purpose of this thesis therefore, is to establish a reliable hydrographic profile of the Agulhas Return Current from the above mentioned CTD and XBT datasets and in doing so to address the key research questions, outlined in **Knowledge Gaps on the Agulhas Return Current**.

***The geographic location of the Agulhas Return Current.***

The position of the Agulhas Return Current has been identified in each hydrographic section spanning the length of the Current from approximately 21°E to 76°E. It can be seen that the Agulhas Return Current first flows zonally between 20°-25°E at approximately 39°30'-40°30'S, before forming a planetary wave over the shallow Agulhas Plateau between 25°-28°E. This wave results in a northward shift of the Current to 37°S. Further eastward the Agulhas Return Current continues it's zonal flow more or less at 40°S across the South Indian Ocean to between 66°E and 70°E

***The geostrophic velocity and the volume transport of the Agulhas Return Current.***

Geostrophic speeds of the Agulhas Return Current show a gradual decrease from an average of 65 cm/s in the retroflection region to 17 cm/s at 76°E. Volume transports are similarly reduced from aa average of 60 Sv in the retroflection region, to 23 at 76°E. This gradual loss is caused by topographically induced meanders and the generation of eddies seen from the datasets at 40°E, 53°E, 59°E, 60°-67°E, 71°E and 76°E, which peel off Agulhas water equatorwards.

***The characteristic water properties associated with the Agulhas Return Current.***

Temperature-salinity properties show STSW water masses characteristic of the Agulhas Return Current, $>16$°C and $>35{,}3$ psu, to extend as far east as 61°E. Further downstream between 67°E and 76°E the surface waters become capped with fresher/colder and more oxygenated water masses. It is possible that this capping is attributed to the equatorward flow of SAASW as a result of meandering northward branches. A meridional transect carried out during *SUZIL* shows an upward tilt towards the east, west of 72°E confirming such a northward flow.

***The full geographic extent of the Agulhas Return Current.***

It is clear from the present study that the Agulhas Return Current extends across the full width of the south Indian Ocean, terminating between 66°E and 70°E. I therefore propose that the name "South Indian Ocean Current", given by Stramma (1992) for the flow just north of the Subtropical Convergence in the Indian Ocean, be retained for the flow east of 70°E only.

# REFERENCES

BANG, N. D. (1969). Major eddies and frontal structures in the Agulhas Current Retroflexion area in March 1969, Reprint from symposium on oceanography in South Africa 1970.

BANG, N. D (1970). Dynamic interpretation of a detailed surface temperature chart of the Agulhas Current retroflexion and fragmentation area, *South African Geographic Journal*, **52**, 67-76.

BELKIN, I. M. (1988b). Hydrological fronts of the Indian Subantarctic by data of the Japanese Antarctic Research Expeditions (JARE), P. P. Shirshov Institute of Oceanology, USSR Academy of Sciences, Moscow, pp 27.

BELKIN, I. M. (1989a). Thermohaline streucture, hydrological fronts and flux of the Antarctic Circumpolar Current in the central part of the Indian sector of the Southern Ocean, *The Antarctic, The Committee Reports*, **28**, 97-112.

BELKIN, I. M. (1989b). Alteration of the front distributions in the Southern Ocean near the Crozet Plateau, Transcript USSR Academy of Sciences, *Earth Scientific Sector*, **308**, 265-268.

BELKIN, I. M. and GORDON, A. L. (1994). Southern ocean fronts from the Greenwich meridian to Tasmania, *Manuscript*.

BELKIN, I. M. and GORDON, A. L. (1996). Southern ocean fronts from the Greenwich meridian to Tasmania, *Journal of Geophysical Research,* **101**, 3675-3696

BENNETT, S. L. (1988). Where three oceans meet: the Agulhas Retroflection region, *Ph.D. dissertation*, **WHOI-88-51**, Woods Hole Oceanographic Institute, Woods Hole, Massachusetts, pp 367.

BIGGS, R. B. and WETZEL, C. D. (1968). Concentration of particulate carbohydrate at the halocline in Chesapeake Bay, *Limnology and Oceanography*, **13**, 169-171.

CAMP, D. B., HAINES, W. E., HUBER, W. F., RENNIE, S. E. and GORDON, A. L. (1986). Agulhas retroflection cruise, *Hydrographic (CTD) data, Final technical report*, **LDGO-86-1**, Lamont-Doherty Geological Observatory of Columbia University Palisades, New York.

CHAPMAN, P., DUNCOMBE RAE, C. M. and ALLANSON, B. R. (1987). Nutrients, chlorophyll and oxygen relationships in the surface layers at the Agulhas retroflection, *Deep-Sea Research*, **34** (8a), 1,399-1,416.

CHAPMAN, P. (1988). On the occurrance of oxygen-depleted water south of Africa and it's implications for Agulhas-Atlantic mixing, *South African Journal of Marine Science*, **7**, 767-794.

CHENEY, R. E., MARSH, J. G. and BECKLEY, B. D. (1983). Global mesoscale variability from collimear tracks of SEASAT altimeter data, *Journal of Geophysical Research*, **88**, 4343-4354.

CLOWES, A. J. (1950). An introduction to the hydrology of South African waters. *Fish and Marine Biology Survey Union of South Africa, Investigational Report **12***, Department of Sea Fisheries.

DANIAULT, N. (1984). *Apport des techniques spatiales à la connaissance des courants de surface,* Application à l'Ocean Antarctique, Ph.D dissertation, University de Bretagne Occidentale.

DANIAULT, N, and MÉNARD, Y (1985). Eddy kinetic energy distribution in the Southern ocean from altimetry and FGGE drifting buoys, *Journal of Geophysical Research*, **90**, 11,877-11,889.

DARBYSHIRE, J. (1964). A hydrological investigation of the Agulhas Current area, *Deep-Sea Research*, **11**, 781 - 815.

DARBYSHIRE, M. (1966). The surface waters near the coasts of Southern Africa, *Deep-Sea Research,* **13**, 57 - 61.

DARBYSHIRE, J. (1972). The effect of bottom topography on the Agulhas Current, *Pure and Applied Geophysics,* **101**, 208 - 220.

DAVID, P. and GUERIN-ANCEY, O. (1990). Travaux d'hydrologie. Rapport preliminaire, in *Les Rapports des Compagnes a la Mer, Aux Iles Saint-Paul et Amsterdam, a bord du Marion Dufresne (MD 50/JASUS)*, **Pulication 86-04**, Mission de recherche des Terres Australes et Antartiques Francaises, Paris, 43-59.

DEACON, G. E. R. (1937). The hydrology of the Southern Ocean, *Discovery Report Number **15***, 125 - 152.

DIETRICH, G. (1935). Aufbau und Dynamik des Sudlichen Agulhas stromgebietes. *Veroff. Inst. Meeresk.* University of Berlin.

DUNCAN, C. P. (1970). *The Agulhas Current,* Ph.D dissertation, University of Hawaii, pp 76.

EMERY, W. J. and MEINCKE, J. (1986). Global water masses: Summary and review, *Oceanologia Acta*, **9**, 383-391.

FINE, R. A., WARNER, M. J. and WEISS, R. F. (1988). Water mass modification at the Agulhas retroflection: chlorofluromethane studies, *Deep-Sea Research*, **35**, 311-332.

GAMBERONI, L., GERONIMI, J. JEANNIN, F. and MURAIL, J.F (1982). Study of frontal zones in the Crozet-Kerguelen region, *Oceanology Acta*, **5**, 289-299.

GORDON, A. L (1981). South Atlantic thermocline ventilation, *Deep-Sea Research*, **28**, 1,239-1,264.

GORDON, A. L., MOLINELLI, E. and BAKER, T. (1982). *The Southern Ocean Atlas*, Columbia University Press, New York, pp 35.

GORDON, A. L. (1985). Indian-Atlantic transfer of thermocline water at the Agulhas Retroflection, *Science*, **227** : 1030 - 1033.

GORDON, A. L (1986). Inter-ocean exchange of thermocline water, *Journal of Geophysical Research*, **91**, 5,037-5,046.

GORDON, A. L., LUTJEHARMS, J. R. E. AND GRüNDLINGH, M. L. (1987). Stratification and circulation at the Agulhas retroflection, *Deep-Sea Research,* **34**, 565 - 599.

GORDON, A. L. and HAXBY, W. F. (1990). Agulhas eddies invade the south Atlantic - evidence from GEOSAT altimeter and shipboard conductivity - temperature - depth survey, *Journal of Geophysical Research*, **95**, 3117 - 3125.

GORDON, A. L., WEISS, R. F., SMETHIE, W. M. and WARNER, M. J. (1992). Thermocline and intermediate water communication between the South Atlantic and Indian Ocean, *Journal of Geophysical Research*, **97**, 7,223-7,240.

GOSCHEN, W. S. AND SCHUMANN, E. (1988). Ocean current and temperature structures in Algoa bay and beyond November 1986, *South African Journal of Marine Science,* **7**,18 - 20.

GRÜNDLINGH, M. L. (1977). Drift observations from Nimbus VI satellite-tracked buoys in the Southwestern Indian Ocean, *Deep-Sea Research,* **24**, 903 - 913.

GRÜNDLINGH, M. L. (1978). Drift of a satellite-tracked buoy in the Southern Agulhas Current and Agulhas Return Current, *Deep-Sea Research,* **25**, 1209 - 1224.

GRÜNDLINGH, M. L. (1980). On the volume transport of the Agulhas Current, *Deep-Sea Research*, **27**, 557 - 563.

GRÜNDLINGH, M. L. (1979). Observations of a large meander in the Agulhas Current, *Journal of Geophysical Research,* **84**, 3776 - 3778.

GRÜNDLINGH, M. L. AND LUTJEHARMS, J. R. E. (1979). Large scale flow patterns of the Agulhas Current System, *South African Journal of Science,* **75**, 269 - 270.

GRÜNDLINGH, M. L (1983). *Eddies in the southern Indian Ocean and Agulhas Current.* In: A.R. ROBINSON Editor, Eddies in Marine Science, Springer-Verlag, Berlin, pp 246 - 264.

GRÜNDLINGH, M. L. (1985). Occurance of Red Sea water in the southwestern Indian Ocean, *Journal of Physical Oceanography*, **15**, 207-212.

HARDER, W. (1968). Reactions of plankton organisms to water stratification, *Limnology and Oceanography*, **13**, 156-168.

HARRIS, T. (1970). Planetary type waves in the South West Indian Ocean, *Nature,* **227**, 1043 - 1044.

HARRIS, T. and BANG, N. D. (1974). Topographic rossby waves in the Agulhas Current, *South African Journal of Science,* **70**, 212 - 214.

HARRIS, T. AND VAN FOREEST, D. (1977). *The Agulhas Current System*, University of Cape Town.

HARRIS, T. F. W. LEGECKIS, R. AND VAN FOREEST, D. (1978). Satellite infra-red images in the Agulhas Current system, *Deep-Sea Research,* **25**, 543 - 548.

HOFFMAN, E. E. (1985). The large-scale horizontal structure of the Antarctic Circumpolar Current from FGGE drifters, *Journal of Geophysical Research*, **7**, 245-270.

HOLFORD, J. M. (1990). A description of the Agulhas retroflection zone, Institute of Oceanographic Sciences, Deacon Laboratory, *Internal Report Number **294***, pp 13.

JACOBS, S. S. and GEORGI, D. T. (1977). Observations on the southwest Indian/Antarctic Ocean. In: *A Voyage of Discovery*, M. ANGEL editor, George Deacon 70th Anniverary volume, supplement to *Deep-Sea Research*, 43-84.

KERHALLET, C. P. (1851). Considerations generales sur l'ocean Indien, *Annual Hydrography,* **1**, 233-243.

LE PICHON, X. (1960). The deep water circulation in the southwest Indian Ocean, *Journal of Geophysical Research,* **65**, 4061 - 4074.

LUTJEHARMS, J. R. E. (1972). *A guide to research done in the south west Indian Ocean.* University of Cape Town.

LUTJEHARMS, J. R. E. (1981). Features of the southern Agulhas Current circulation from satellite remote sensing, *South African Journal of Science,* **77**, 231 - 236.

LUTJEHARMS, J. R. E. and VALENTINE, H. R. (1984). Southern Ocean thermal fronts south of Africa, *Deep-Sea Research*, **31**, 1,461-1,475.

LUTJEHARMS, J. R. E. AND VAN BALLEGOOYEN, R. C. (1984). Topographic control in the Agulhas Current system, *Deep-Sea Research*, **31**, 1321 - 1337.

LUTJEHARMS, J. R. E. AND GORDON, A. L. (1987). Shedding of an Agulhas ring observed at sea, *Nature,* **325**, 138 - 140.

LUTJEHARMS, J. R. E. AND VAN BALLEGOOYEN, R. C. (1988a). The retroflection of the Agulhas Current, *Journal of Physical Oceanography*, **18**, 1570 - 1583.

LUTJEHARMS, J. R. E. AND VAN BALLEGOOYEN, R. C. (1988b). Anomalous upstream retroflection in the Agulhas Current, *Science*, **240**, 1770 - 1772.

LUTJEHARMS, J. R. E. and VALENTINE, H. R. (1988a). On mesoscale eddies at the Agulhas Plateau, *South African Journal of Science,* **84**, 194 - 200.

LUTJEHARMS, J. R. E. and VALENTINE, H. R. (1988b). Eddies at the Sub-Tropical Convergence South of Africa, *Journal of Physical Oceanography,* **18**, 761 - 774.

LUTJEHARMS, J. R. E and CONNELL, A. D. (1989). The Natal Pulse and inshore counter currents off the South African east coast, *South African Journal of Science*, **85**, 533 - 535.

LUTJEHARMS, J. R. E (1989). The role of mesoscale turbulence in the Agulhas Current system. In: J.C.J. NIHOUL and B.M.JAMART Editors, *Mesoscale/Synoptic Coherent Structures in Geophysical Turbulence*, Elsiever Oceanography Series, Amsterdam, pp 357 - 372.

LUTJEHARMS, J. R. E., VALENTINE, H. R. and VAN BALLEGOOYEN, R. C. (1993). On the Subtropical Convergence in the South Atlantic Ocean, *South African Journal of Science*, **89**, 552-559.

LUYTEN, J. R. (1985). Agulhas Current trajectory from new Argos drifter compared with simultaneous shipboard measurements, *Oceans '85, Ocean Engineering and the Environment,* **2**, 1165 - 1167.

MCCARTNEY, M. S. (1977). Subantarctic mode water. In: *A Voyage of Discovery*, M. ANGEL editor, New York, 103-119.

MEEUWIS, J. M. (1991). *Geographic characteristics of circulation patterns and features in the South Atlantic and South Indian oceans using satellite remore sensing,* D. Litt. et Phil, Rand Afrikaans University.

MEY, R. D. and WALKER, N. D. (1990). Surface heat fluxes and marine boundary layer modification in the Agulhas retroflection region, *Journal of Geophysical Research*, **95**, 15,997-16,015.

MOLINELLI, E. J. (1981). The antarctic influence on antarctic intermediate water, *Journal of Marine Research*, **39**, 267-293.

NASA (1992). The dynamic topography of Earth's oceans. The TOPEX/POSEIDON Global Ocean-monitoring Mission.

NIILER, P. P. AND ROBINSON, A. R. (1967). The theory of free inertial jets II. A numerical experiment for the path of the Gulf stream, *Tellus,* **19**, 601 - 618.

OLSEN, D. B. AND EVANS, R. H. (1986). Rings of the Agulhas Current, *Deep-Sea Research,* **33**, 27 - 42.

ORREN, M. J. (1963). Hydrological observations in the south west Indian Ocean, *Investigational Report Number* ***45***, Department of Sea Fisheries.

ORREN, M. J. (1966). Hydrology of the south west Indian Ocean. *Investigational Report of the Division of Sea Fisheries of South Africa Report Number* ***45***, 1-61.

PARK, Y. H., CHARRIAUD, E., GAMBERONI, L., LAMY, A., and SAINT-GUILY, B. (1989). Structure et variabilité du Courant Circumpolaire Antarctique dans la région Kerguelen-Amsterdam, *C. R. Académie Sciences Paris*, **308**, Serie II, 177-183.

PARK, Y. H., GAMBÉRONI, L., CHARRIAUD, E. (1991). Frontal structure and transport of the Antarctic Circumpolar Current in the south Indian Ocean sector, 40-80°E, *Marine Chemistry*, **35**, 45-62.

PARK, Y. H, and SAINT-GUILY, B, (1992). Sea level variability in the Crozet-Kerguelen-Amsterdam area from bottom pressure and Geosat altimetry,in *Sea Level changes: Determination and Effects.Geophysical Monograph,* **69**, edited by P. L. Woodworth et al., 117-131, American Geophysical Union, Washington. D. C.

PARK, Y, H., GAMBÉRONI, L., CHARRIAUD, E. (1993). Frontal structure, water masses and circulation in the Crozet Basin, *Journal of Geophysical Research*, **98**, 12,361-12,385.

Projet MARISONDE (1979). Bouées pour PEMG. Establissement d'Etudes et de Recherches Météorologiques.

PEARCE, A. (1977). Some features of the upper 500m of the Agulhas Current, *Journal of Marine Research,* **35**, 731 - 753.

PEARCE, A. (1980). Early observations and historical notes on the Agulhas Current circulation, *Transactions of the Royal Society of South Africa,* **44**, 205 - 212.
PEARCE, A. (1983). Adrift in the Agulhas Return Current, *Deep-Sea Research,* **30**, 343 - 347.

PETERMANN, A. (1865). Karte der Arktischen und Antarktischen Regimen zur Ubersicht des geographischen standpundtes im Jahre 1865, *Petermann's Mitteilungen,* 35 - 36.

PIOLA, A. R. and GEORGI, D. T. (1982). Circumpolar properties of Antarctic Intermmediate water and Subantarctic mode water, *Deep-Sea Research*, **29**, 687-711.

PIOLA, A. R. and GORDON, A. L. (1989). Intermediate waters in the southwest South Atlantic, *Deep-Sea Research*, **36**, 1-16.

POLLARD, R. T., READ, J. F. and SMITHERS, J. (1987). CTD sections across the southwest Indian ocean and antarctic circumpolar Current in southern summer 1986/7, *Institute of Oceanographic Sciences Deacon Laboratory Report Number 23*, pp 161.

POMEROY, A. S. (1975). Sea temperatures Cape-Marion-Kerguelen during February - April 1975, *Unpublished Report*, University of Cape Town.

READ, J. F. AND POLLARD, R. T. (1993). Structure and transport of the Antarctic Circumpolar Current and Agulhas Return Current at 40°E, *Journal of Geophysical Research,* **98**, 12,281 - 12,295.

RENNELL, J. (1778). *A Chart of the Bank of Lagullas and Southern Coast of Africa.*

RENNELL, J. (1832). *An Investigation of the Currents of the Atlantic Ocean and those which prevail between the Indian Ocean and the Atlantic.*

RIGG, G. M. (1995). *The Hydrography and dynamics of rings and eddies of the Agulhas retroflection,* MSc dissertation, Oceanography Department of the University of Cape Town, Cape Town, pp 270.

ROUAULT, M., LEE-THORP, A. M., ANSORGE, I. J. and LUTJEHARMS, J. R. E. (1995). The Agulhas Current Air Sea Interaction Experiment (ACASEX), *South African Journal of Science*, **91**, 493 - 496.

SHANNON, L. V. (1966). Hydrology of the south and west coasts of South Africa, *Investigational report of the Division of Sea Fisheries of South Africa Report Number* ***58***, pp 22.

SHANNON, L. V., LUTJEHARMS, J. R. E. and AGENBAG, J. J. (1989). Episodic input of Subantarctic water into the benguela region, *South African Journal of Science*, **85**, 317-322.

STAVROPOULOS, C.C. and DUNCAN, C. P. (1974). A satellite -tracked buoy in the Agulhas Current, *Journal of Geophysical Research,* **79**, 2744 - 2746.

STRAMMA, L. AND PETERSON, R. G. (1990). The South Atlantic Current, *Journal of Physical Oceanography,* **20**, 846 - 859.

STRAMMA, L. (1992). The South Indian Ocean Current, *Journal of Physical Oceanography,* **22**, 421 - 430.

STRAMMA, L. and LUTJEHARMS, J. R. E (1995). The flow field of the subtropical gyre in the South Indian Ocean, *Journal of Geophysical Research*, **submitted.**

SVERDRUP, D. P., JOHNSON, M. W. and FLEMING, R. H. (1942). *The Oceans: Their Physics, Chemistry, and general Biology*, Prentice-Hall, Englewood Cliffs, New Jersey, pp 1087.

UNESCO (1983). Algorithms for computation of fundamental properties of seawater. *UNESCO Technical Papers in Marine Science,* **44**, 53 pp.

VALENTINE, H. R., DUNCOMBE RAE, C. M., VAN BALLEGOOYEN, R. C. and LUTJEHARMS, J. R. E. (1988). *The Subtropical Convergence and Agulhas retroflection cruise (SCARC) data report*, CSIR Report, **T/SEA 8804**, pp 258.

VALENTINE, H. R. (1990). A fine-scale volumetric census of water masses of the Agulhas retroflection area, CSIR Report, **EMA-R 691**, pp 105.

VALENTINE, H. R., LUTJEHARMS, J. R. E. and BRUNDRIT, G. B. (1993). The water masses and volumetry of the southern Agulhas Current region, *Deep-Sea Research*, **40**, 1,285-1,305.

VAN BALLEGOOYEN, R. (1982). An investigation of topographic control in the Agulhas Current system: Using the Free Inertial Jet Model. University of Cape Town.

VAN FOREEST, D. (1977). *The Agulhas Current system above the intermediate level,* MSc dissertation, University of Cape Town.

VERONIS, G. (1973). Model of world circulation, 1, Wind driven two layer, *Journal of Marine Research,* **31**, 228 - 288.

VISSER, G. A. AND VAN NIEKERK, M. M. (1965). Ocean currents and water masses at 1 000, 1 500, and 3 000 metres in the south west Indian Ocean. *Investigational Report Number 52*, Department of Sea Fisheries.

WARREN, B. A. (1962). *Topographic influences on the path of the Gulf stream*, Ph.D dissertation, Massachusetts Institute of Technology, pp 106.

WARREN, B. A. (1981). Deep circulation of the world ocean. In: *Evolution of Physical Oceanography, Scientific surveys in honour of Henry Stommel.* Warren, B. A. and Wunsch C. (eds), Cambridge, Massachusetts Institute of Technology Press, Massachusetts.

WEBB, D. J., KILLWORTH, P. D., COWARD, A. C. AND THOMPSON, S. R. (1991). *The FRAM Atlas of the Southern Ocean*, National Environment Research Council, Archway Press, Oxford.

WEEKS, S. J. (1992). *Spatial and temporal variability of chlorophyll concentrations from Nimbus-7 Coastal Zone Colour Scanner data in the Benguela upwelling system and the Sub-Tropical Convergence region south of Africa,* MSc dissertation, University of Cape Town.

WHITWORTH, T. and NOWLIN, W. D. (1987). Water masses and currents of the Southern Ocean at the Greenwich Meridian, *Journal of Geophysical Research*, **92**, 462-6,476.

WYRTKI, K. (1971). *Oceanographic Atlas of the International Indian Ocean Expedition.* National Science Foundation, Washington.

ZILLMAN, J. W. (1970). Sea surface temperature gradients south of Australia, *Australian Meteorological Magazine,* **18**, 22 - 30.

# ADDENDA

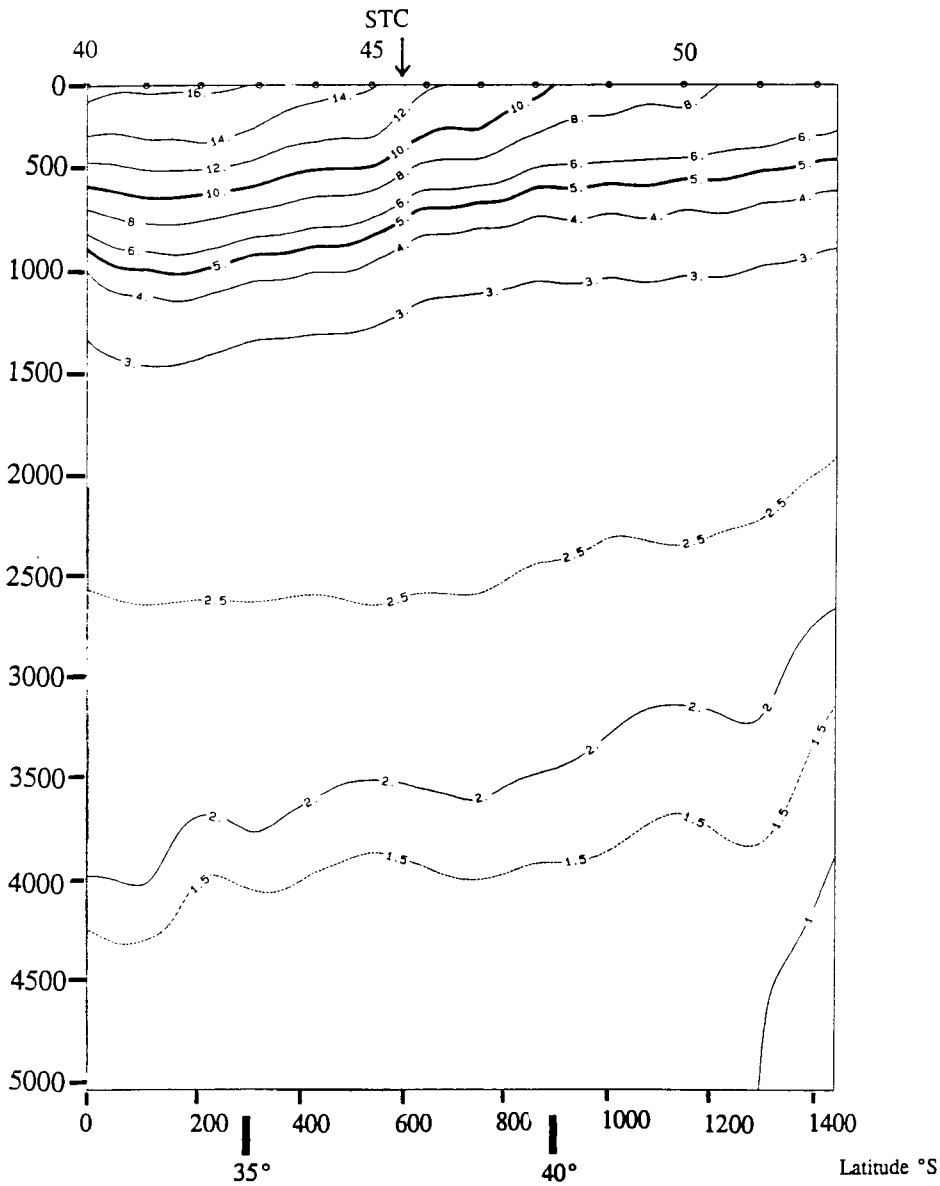


Figure A.1a: Potential temperature section between CTD stations 40-52 of *AJAX* for a total depth of 5 000 db. The position of the STC is evident between CTD station 45-46.

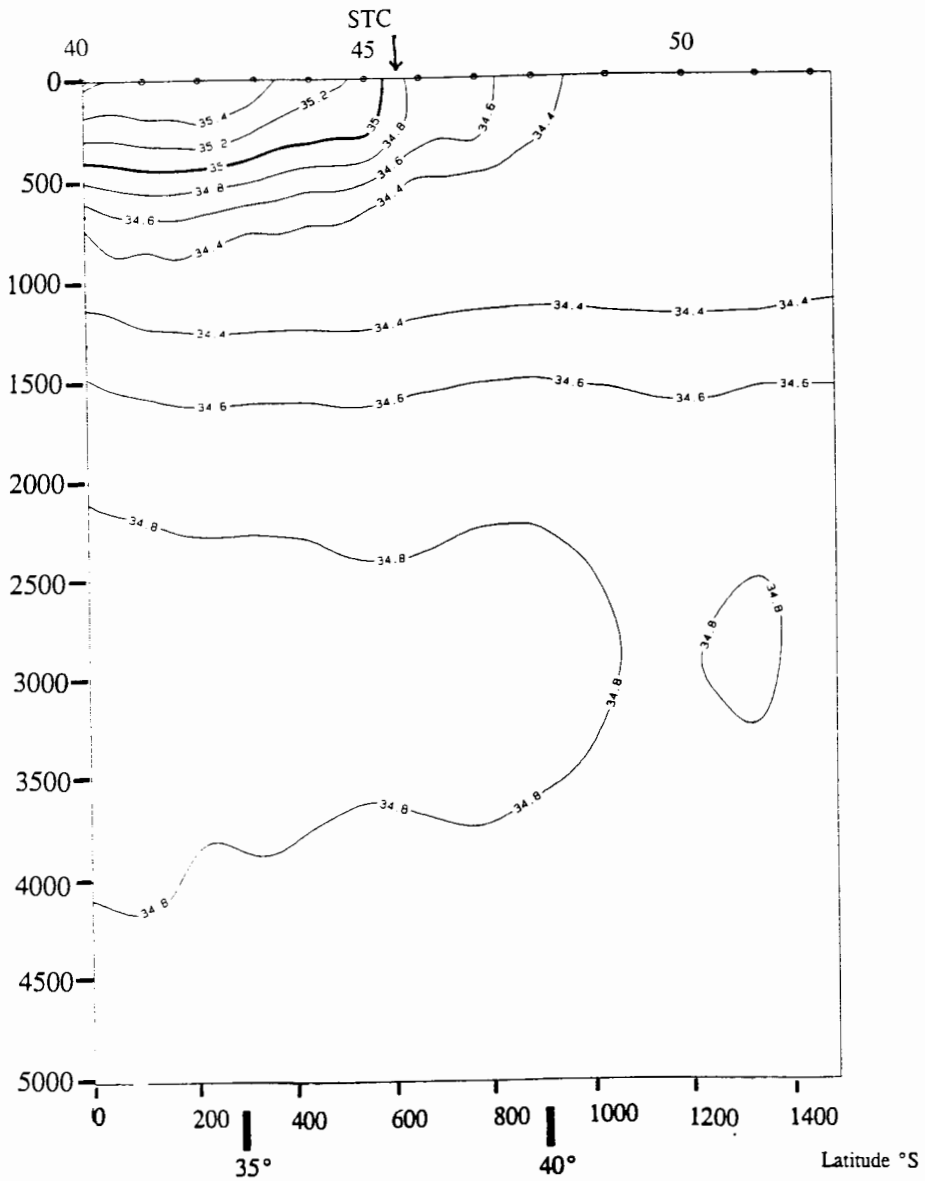


Figure A.1b: Salinity section between CTD stations 40-52 of *AJAX* for a total depth of 5 000 db. The position of the STC is evident between CTD station 45-46.

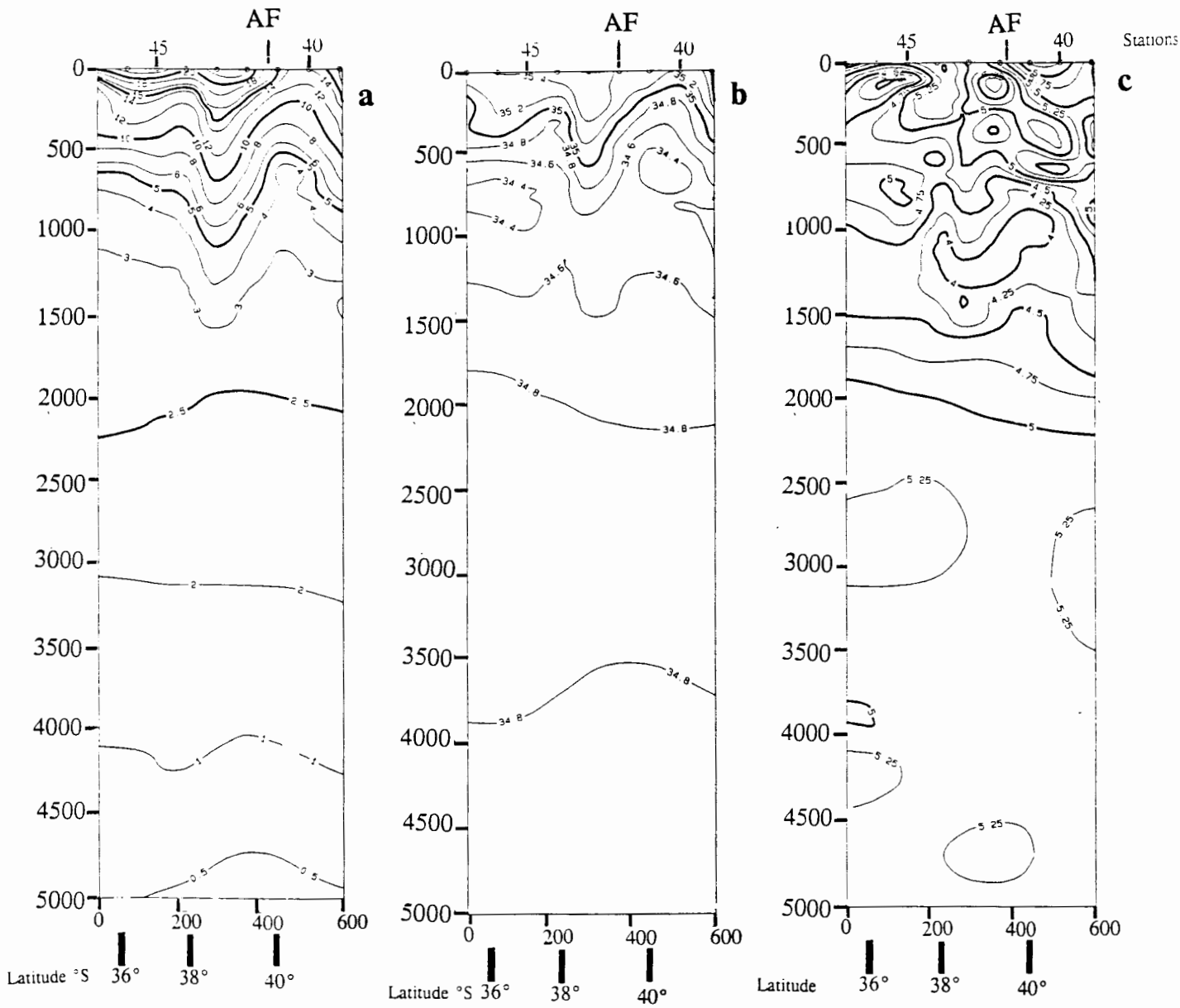


Figures A.2a, b and c: Potential temperature, salinity and oxygen section between CTD stations 39-47 of *ARC transect 1* for a total depth of 5 000 db. The position of the Agulhas Front; the southern boundary of the Agulhas Return Current is evident between CTD stations 41-42.

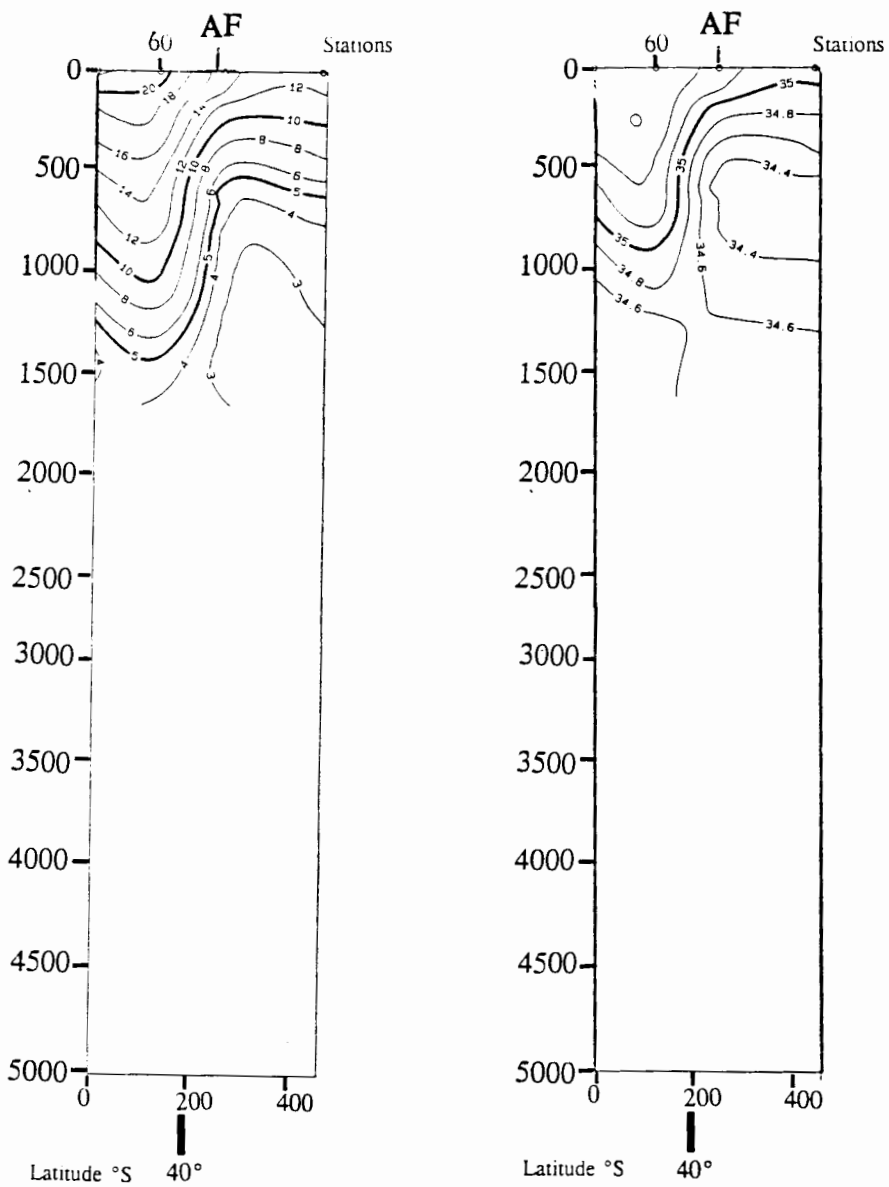


Figures A.3a and b: Potential temperature and salinity sections between CTD stations 58-61 of *ARC transect 2* for a total depth of 5 000 db. The position of the Agulhas Front; the southern boundary of the Agulhas Return Current is evident between CTD stations 59-60.

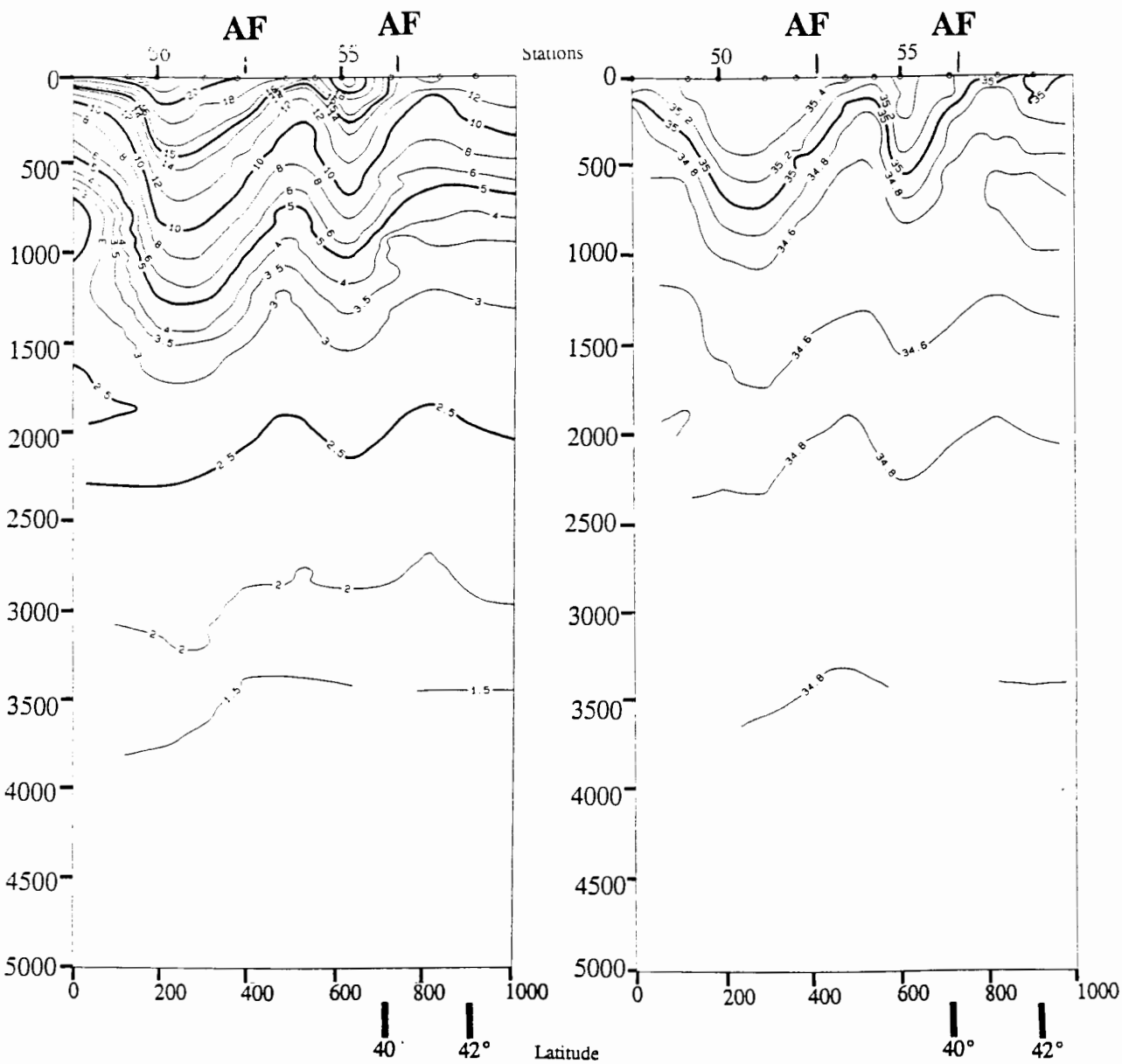


Figures A.4a and b: Potential temperature and salinity sections between CTD stations 48-58 of *ARC transect 3* for a total depth of 5 000 db. The position of the Agulhas Front; the southern boundary of the Agulhas Return Current is evident between CTD stations 55-56 and 52-53.

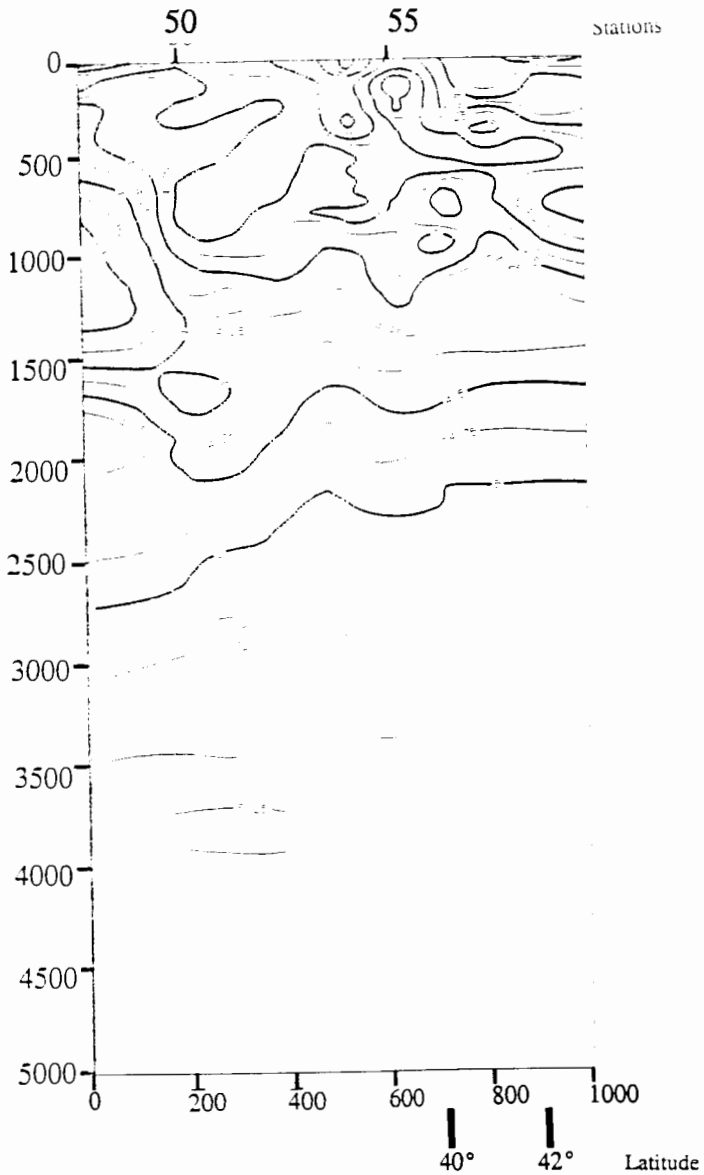


Figure A.4c: Oxygen section between CTD stations 48-58 of *ARC transect 3* for a total depth of 5 000 db. The position of the Agulhas Front; the southern boundary of the Agulhas Return Current is evident between CTD stations 55-56 and 52-53.

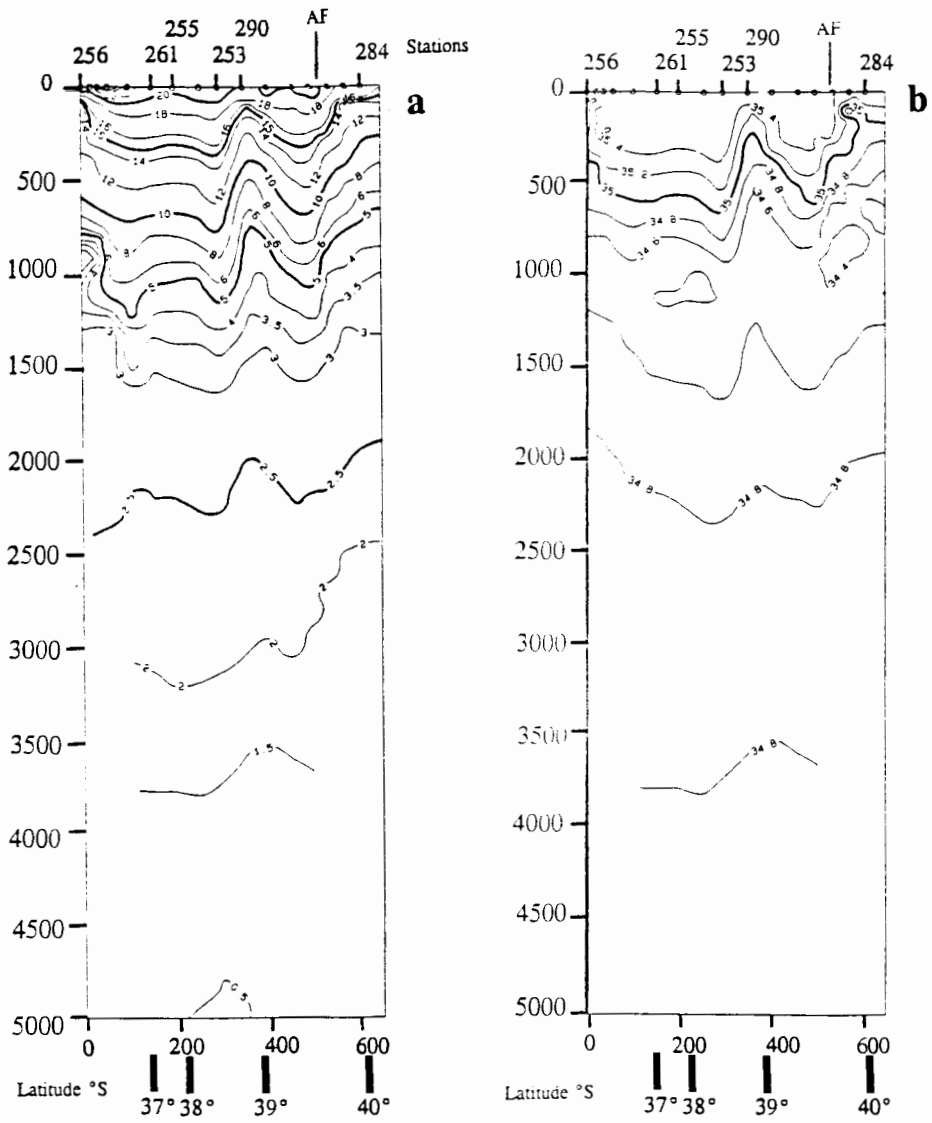


Figures A.5a and b: Potential temperature and salinity sections between CTD stations 256-284 of *Marathon transect 1* for a total depth of 5 000 db. The position of the Agulhas Front; the southern boundary of the Agulhas Return Current is evident between CTD stations 287-285.

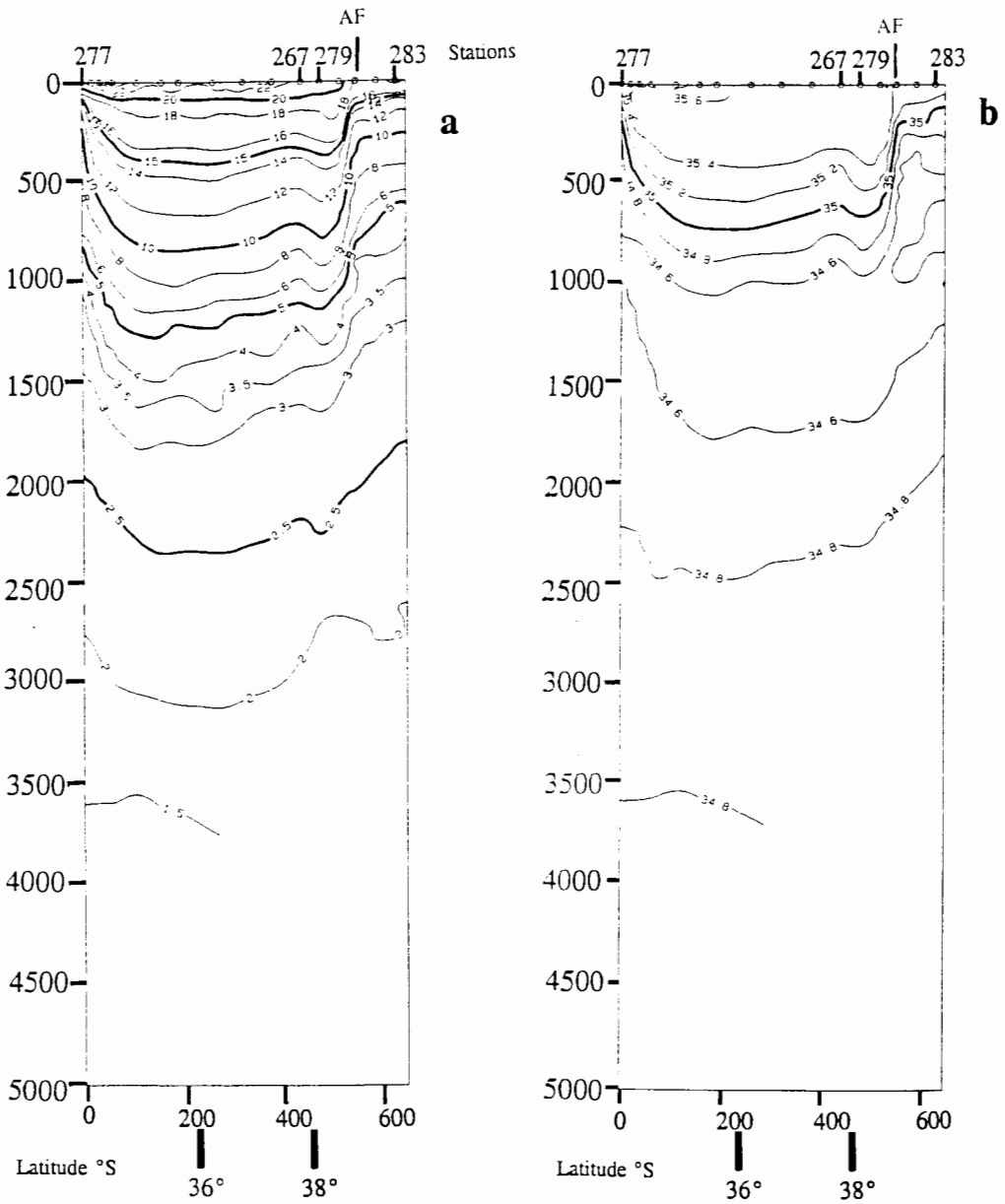


Figures A.6a and b: Potential temperature and salinity sections between CTD stations 277-283 of *Marathon transect 2* for a total depth of 5 000 db. The position of the Agulhas Front; the southern boundary of the Agulhas Return Current is evident between CTD stations 280-281.

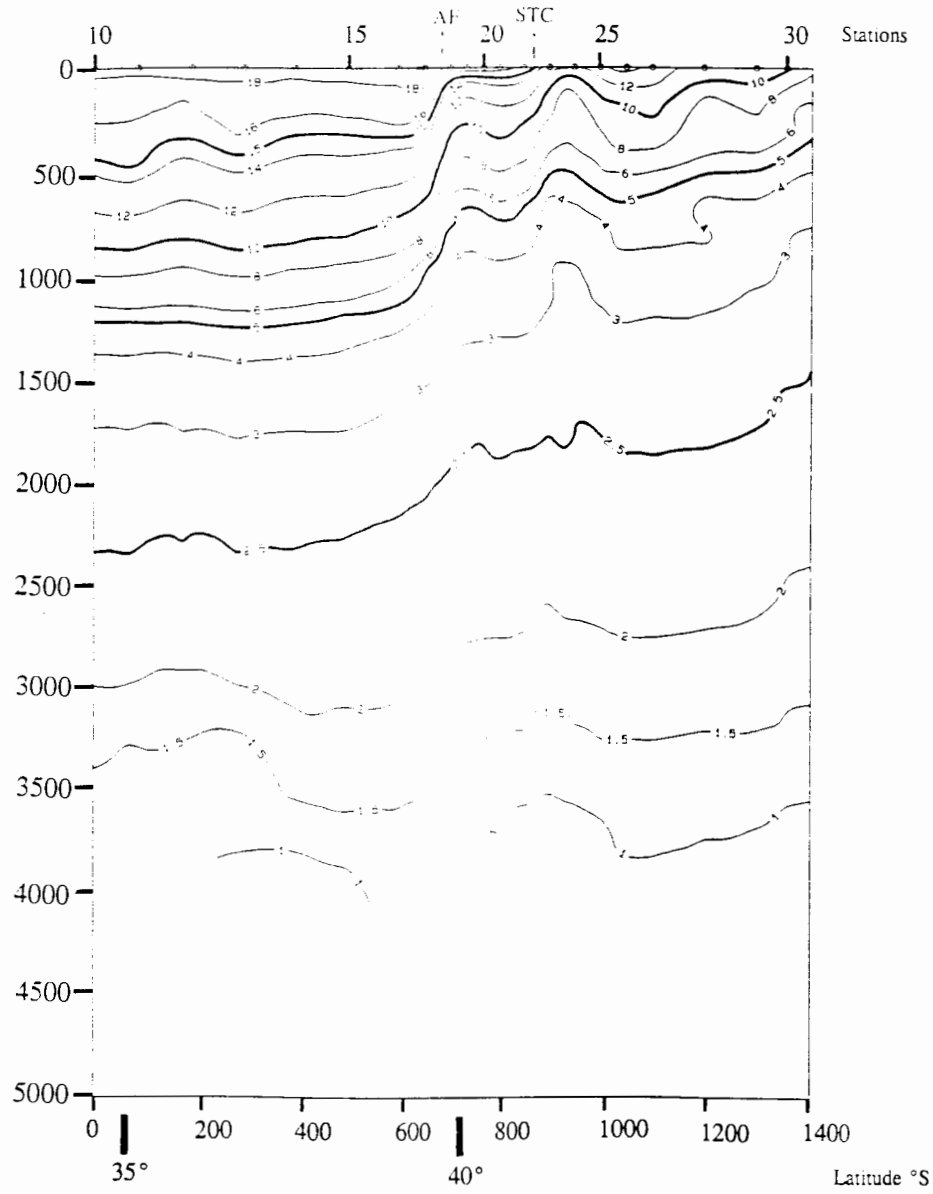


Figure A.7a: Potential temperature section between CTD stations 10-30 of *Discovery 164* for a total depth of 5 000 db. The position of the Agulhas Front; the southern boundary of the Agulhas Return Current is evident between CTD stations 17-18.

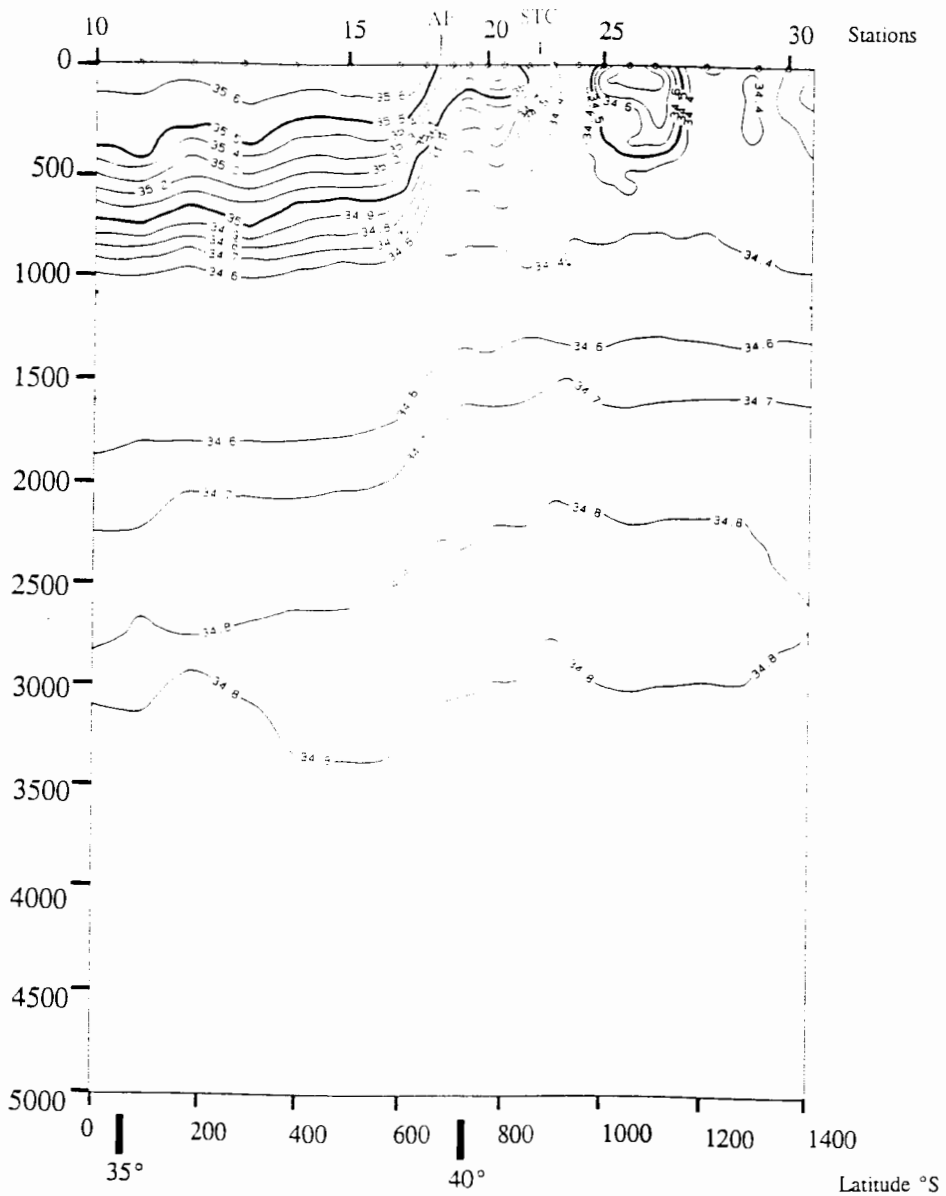


Figure A.7b: Salinity section between CTD stations 10-30 of *Discovery 164* for a total depth of 5 000 db. The position of the Agulhas Front; the southern boundary of the Agulhas Return Current is evident between CTD stations 17-18.

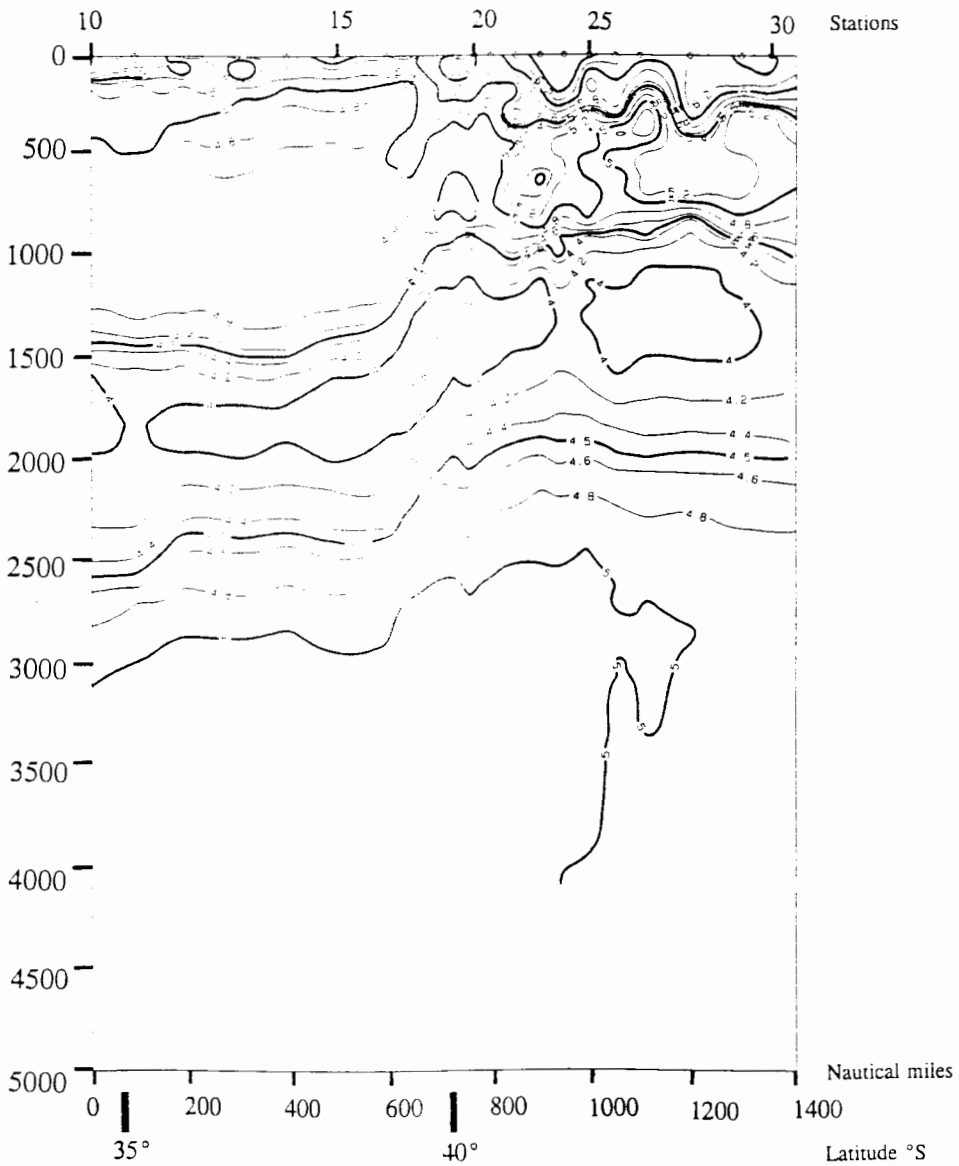


Figure A.7c: Oxygen section between CTD stations 10-30 of *Discovery 164* for a total depth of 5 000 db. The position of the Agulhas Front; the southern boundary of the Agulhas Return Current is evident between CTD stations 17-18.

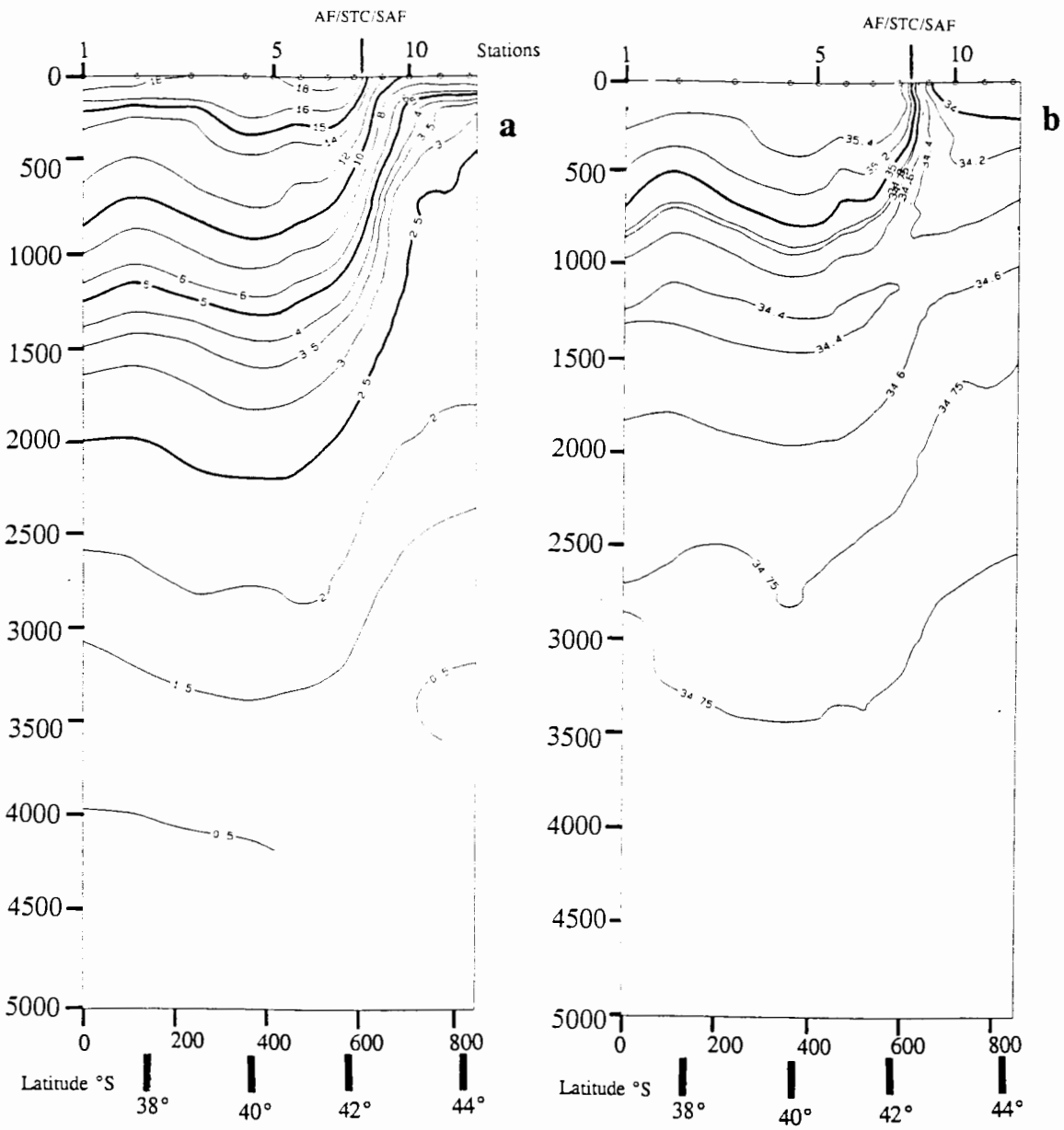


Figures A.8a and b: Potential temperature and salinity sections between CTD stations 1-12 of *SUZIL transect 1* for a total depth of 5 000 db. The position of the Agulhas Front; the southern boundary of the Agulhas Return Current is evident between CTD stations 7-8.

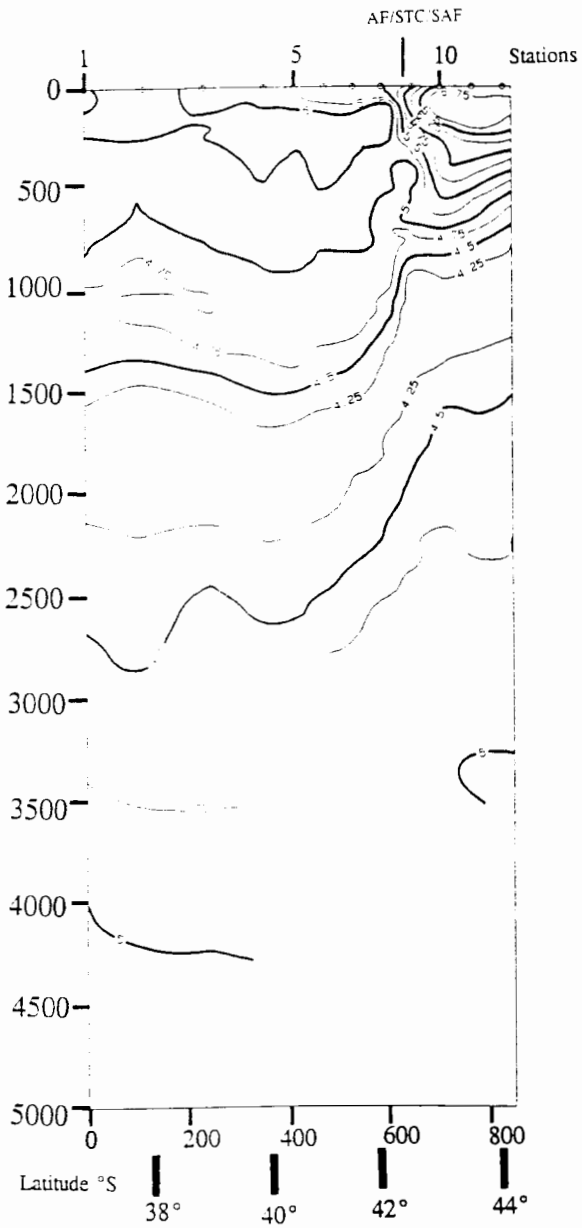


Figure A.8c: Oxygen section between CTD stations 1-12 of *SUZIL transect 1* for a total depth of 5 000 db. The position of the Agulhas Front; the southern boundary of the Agulhas Return Current is evident between CTD stations 7-8.